UNIVERSITY OF SOUTHAMPTON

School of Life Sciences
Centre for Biological Sciences

RING Finger Protein 17 (Rnf17) of Myc/Max/Mxd Network: Expression and Function during Mouse Reproduction and Development

by

Ayat Majed Sultan Bakheet

Thesis for the Degree of Doctor of Philosophy

September 2013

UNIVERSITY OF SOUTHAMPTON

ABSTRACT

SCHOOL OF LIFE SCIENCES, CENTRE FOR BIOILFGICAL SCIENCES

Doctor of Philosophy

RING Finger protein 17 (Rnf17) of Myc/Max/Mxd Network: Expression and Function during Mouse Reproduction and Development

By **Ayat Majed Sultan Bakheet**

The preimplantation mammalian embryo is sensitive to the environment in which they develop and grow, either *in vivo* or *in vitro*. Disturbance to embryo environmental conditions can affect embryo growth. Changes in gene expression is one of the embryo responses to such conditions that may influence developmental potential and phenotype during later gestation. The signalling network Myc/Max/Mxd function as a molecular switch that regulates cell growth, proliferation and differentiation by controlling a common set of genes. RING finger protein 17(Rnf17) enhance Myc activity by sequestering all four members of Mxd family and creating a "Mxd-null phenotype". The MXD family functions as MYC repressor proteins. Two isoforms were described for Rnf17, long (Rnf17L) and short (Rnf17S). Rnf17 is expressed in adult mouse testis and in the mouse preimplantation embryo. The Rnf17 proteins contain RING finger domain and varying copies of the Tudor repeat domain (Tdrd). The aim of my thesis was to study the potential for Rnf17 regulating the Myc/Max/Mxd network during preimplantation development on the phenotype of the blastocyst and foetal testes. First, F9 murine carcinoma cells were used to question whether Rnf17 can modulate Myc responses. Functional assays were developed for Rnf17 over-expression by expression plasmids or Rnf17 knockdown by RNAi construct. The specificity of Rnf17 E3 ligase was investigated by co-transfection of Flagg-tagged constructs for RNF17 and MXD1 in F9 cells. Second, expression of Rnf17 mRNA and subcellular localisation of RNF17 protein were examined in mouse preimplantation embryo and in E17.5 foetal testes under normal condition and in response to maternal protein diets (LPD; 9% casein, HPD; 30% casein and control NPD; 18% casein). Finally Rnf17 knockdown was performed in mouse embryo by siRNA microinjection to point out the role of Rnf17 in embryo development.

RNF17 was able to degrade MXD1 by ubiquitinylation pathway in co-transfected Cos-1 cells. Rnf17-SV40 expression construct significantly induced Luciferase activity of c-Myc reporter construct ($P \leq 0.05$) when over-expressed in F9 cells, and knockdown of Rnf17 using Rnf17-RNAi construct significantly reduced Luciferase activity of Rnf17-sensor construct ($P \leq 0.05$). Rnf17 mRNA is expressed through preimplantation development, in E17.5 foetal testes and in F9 cells. Members of Myc/Max/Mxd are expressed in mouse preimplantation embryo. The expression pattern of RNF17 in F9 cells and mouse embryos was predominantly nuclear and also presented in the cytoplasm. RNF17 was only expressed in the nuclei of Sertoli cells with faint signal in prospermatogonia in E17.5 foetal testes. Knockdown of Rnf17 in microinjected embryos using Rnf17_siRNA reduced expression of Rnf17S, delayed blastocyst formation, and reduced RNF17 protein signal. Maternal diet

differentially regulate expression of Rnf17 and c-Myc in mouse blastocyst and E17.5 testes.

In conclusion, over-expression of Rnf17 can amplify Myc response in F9 cells. MXD is a target protein for Rnf17 E3 ligase. Knockdown of Rnf17 in mouse embryo delayed blastocyst development. This study implicates that Rnf17 involved in regulating Myc/Max/Mxd signalling network and indicates a role for Rnf17 in blastocyst proliferation and growth. Changes in Rnf17 expression have the capacity to modulate early embryonic development and may contribute to phenotypic changes occurring later in life.

DECLARATION OF AUTHORSHIP

I, **Ayat Majed Sultan Bakheet**

declare that the thesis entitled

RING Finger Protein 17 (Rnf17) of Myc/Max/Mxd Network: Expression and Function during Mouse Reproduction and Development

and the work presented in the thesis are both my own, and have been generated by me as the result of my own original research. I confirm that:

- this work was done wholly or mainly while in candidature for a research degree at this University;
- where any part of this thesis has previously been submitted for a degree or any other qualification at this University or any other institution, this has been clearly stated;
- where I have consulted the published work of others, this is always clearly attributed;
- where I have quoted from the work of others, the source is always given. With the exception of such quotations, this thesis is entirely my own work;
- I have acknowledged all main sources of help;
- where the thesis is based on work done by myself jointly with others, I have made clear exactly what was done by others and what I have contributed myself;
- none of this work has been published before submission, **or** [delete as appropriate] parts of this work have been published as: [please list references]

Signed: ……..

Date:…….

Contents

List of Figures

List of Tables

Acknowledgements

I would like to express my sincere gratitude to Prof Tom Fleming and my supervisor Dr Howard Barton for continues support, for their patience, motivation, enthusiasm and guidance help in my PhD and research.

I would like to thank all members of Tom's group, for past and present, I had the pleasure to work alongside. In Particular, to Dr Emma Lucas for teaching me primer design and real-time PCR. To Dr Bhav Sheth for interesting work in embryo microinjection and for fruitful discussion. To Dr Andy Cox for teaching me embryo immunostaining and confocal microscopy, I could not have a great images and results without your help. To Steph Marfy-Smith for always being there and help me in real-time PCR. Finally, To Dr Miguel Velazquez, your scientific advice has been invaluable.

I am indebted to Kuwait Government, Ministry of Health for generously sponsored my PhD. To all members in IVF Centre, Maternity Hospital, Kuwait, for past and present, for encouraging and supporting me during my PhD.

Finally, to my Mum, my sisters and brothers thanks for endless support over the 4 years and for always believing in me. I could not have done any of this without your inspiration.

This Thesis is dedicated to my Father

I am incredibly proud of you. Your beliefs in me is the reason I believe in myself.

List of Abbreviations

APC/C	Anaphase Promoting Complex/Cyclosome
Amp	Ampicilin
ART	Assisted Reproduction Technology
bHLH	Basic helix-loop-helix
bHLHZip	Basic helix-loop-helix zipper
BRCA1	Breast cancer1, early onset
BSA	Bovine serum albumin
BubR1	Bub-related 1
CB	Chromatoid bodies
CDC5L	Cell division cycle 5-like
CHFR	Checkpoint with forkhead and RING finger protein
Ct	threshold Cycle
DMSO	Dimethyl sulfoxide
Dnmt	DNA methyltransferase
DOHaD	Developmental origins of health and disease
E1	Ubiquitin-activating enzyme
E2	Ubiquitin-conjugating enzyme
E3	Ubiquitin-ligase
FCS	Foetal calf serum
GFP	Green fluorescence protein
GST	Glutathione-S transferase
HAT	Histone acetyl transferase
hCG	Human chorionic gonadotrophin
HDAC	Histone deacetylase activity
H & E	Haematoxylin and Eosin
hnRNP-M	Heterogeneous nuclear ribonucleoprotein-M
HPD	High protein diet
IAP	Intracisternal A Particle
ICM	Inner cell mass

ICSI	Intra-cytoplasmic injection
IMC	Intermitochondrial cement
IPTG	Isopropylthio-β-galactoside
IVC	*In vitro* culture
IVF	*In vitro* fertilisation
LB	Luria Broth
Line-1	Long interspersed nuclear element 1
LOS	Large offspring syndrome
LPD	Low protein diet
LU	Luciferase
Mad2	Mitotic arrest deficient-Like 2
Max	MYC Associated Factor X
miRNA	microRNA
Mmip-2	Mad member interacting protein 2
Mxd	Max dimerisation protein
MudPIT	Multidimensional Protein Identification Technology
Myc	Myelocytomatosis oncogen
NES	Nuclear exporting signal
NLS	Nuclear localisation signal
NPD	Normal protein diets
PBS	Phosphate-buffered saline
PEI	polyethylinenimin
PFA	paraformaldehyde
PGC	Primordial germ cells
PGD	Prenatal genetic diagnosis
PLRG1	Pleiotropic regulator 1
PRMT5	Protein arginine methyltrasferase 5
RFPL4	Ret Finger protein-Like 4
RING	Realy interesting new gene
piRNAs	Piwi-interacting RNAs
PIWI	P-element induced wimpy testis

RNAi	RNA interference
Rnf17	RING finger protein 17
Rnf17L	Long Rnf17
Rnf17S	Short Rnf17
RSK	Ribosomal Kinase
RT	Reverse transcriptase
RT-qPCR	Quantitative real time PCR
SBP	Systolic blood pressure
sDMA	Symmetrical dimethyl arginine
siRNA	short interference
S6K	S6 Kinase
SMN	RNA Survival Motor Neuron
Sox9	SRY-box containing gene 9
TE	Trophectoderm
Ub	Ubiquitin
Y2H	Yeast two hybrid
ZGA	Zygotic gene activation

Chapter 1

1. General Introduction

The preimplantation period is a critical stage that needs optimum conditions to maintain high rates of proliferation, growth and differentiation. Compromised environmental conditions during embryo development may influence foetal growth and have adverse consequences on the future health of the offspring.

The Developmental Origins of Health and Disease (DOHaD) hypothesis, also known as the Barker hypothesis, has described the relationship between disturbance in environmental conditions in foetal life and long-term developmental and physiological changes in tissues or organ systems which may increase disease risk in adulthood. Maternal diets, either under nutrition or over nutrition, and Assisted Reproduction Technology (ART) have been reported to alter the environment of embryo growth and may lead to phenotypic and epigenetic changes.

This literature review will address the effects of maternal diets and culture conditions on gene expression at the preimplantation embryo stage as well as on embryo growth and phenotype that can influence future health. The mechanism of the signalling network- Myc/Max/Mxd will be outlined, which is associated with cell proliferation and differentiation and regulates gene expression. Finally, we will focus on the structure and function of the RING finger protein 17 (Rnf17). Rnf17 has been found to interact with Mxd, a member of the Myc/Max/Mxd network, and regulates its activity.

1.1 Environmental conditions and DOHaD hypothesis

The observations made by Professor David Barker and colleagues in the late 1980s identified the association between low birth weight in humans and the risk of cardiovascular disease (Barker & Osmond, 1986; Barker *et al, 2000*). On the basis of these observations, the effects of *in utero* developmental conditions on embryo growth and later adult health were explained by the

DOHaD hypothesis. The hypothesis is based on human and animal studies and suggests a relationship between early growth, nutrition and long-term risk of age-related diseases, such as chronic heart disease. Later studies have adapted the DOHaD hypothesis to investigate conditions related to preimplantation growth such as *in vitro* culture and also to study the mechanisms underlying the physiological and phenotypic changes to the foetus and adult later life (Langley-Evans, 2006).

1.1.1 Effect of maternal diets on embryo growth and adult health

Restricted maternal diet during periconception, preimplantation or gestation periods were reported to influence early embryo growth and long-term health and adult-onset diseases. For example, mothers fed a LPD of 9% protein content, but isocaloric with NPD exclusively during the mouse preimplantation stage produced offspring with increased weight at birth and throughout postnatal life (Watkins *et al,* 2008a). LPD offspring displayed raised SBP with reduced female heart size. LPD females offspring showed anxiety-related behaviour (rearing and jumping) in open field analysis. Female mice exposed to LPD of 9% isocaloric during one ovulatory cycle, and prior to natural mating, showed sensitivity of oocyte maturation to maternal diet, and their offspring were identified to be abnormal, with anxiety-related behaviour in open field activities (Watkins *et al*, 2008b). The study displayed elevated SBP in male offspring at all assay times, and in both sexes at 21 weeks, whereas female offspring exhibited smaller kidneys but increased nephron numbers at 28 weeks.

In a study by Kwong *et al* (2000), female rats were fed standard chow diet at pre-conception followed by normal protein diets (NPD) (18% casein) or LPD (9% casein) in the plug-positive to preimplantation period (0-4.25 day) and then the diet was switched to NPD for the reminder of gestation. Preimplantation maternal LPD did not affect the gestational length, litter size

or the sex ratio. Maternal LPD significantly caused reduction in the birth weight of female offspring up to 7 weeks after which an overcompensation to heavier weight gain than the control female offspring, and remained equivalent to the control NPD up to weeks 11-12. The male offspring displayed induced SBP at age 4 and 11 weeks with a disproportionate size of liver and kidney in relation to body weight at age 12 weeks.

Different species have shown that restricted maternal diets during preimplantation time may affect the cell numbers and differentiation in the blastocyst either at early or late stages. Kwong *et al* (2000) showed that no differences were seen in the cell lineage number at day 3 in morula or at day 4 in blastocysts of rats fed LPD or control NPD. However, a significant reduction in inner cell mass (ICM) was seen in early blastocysts at day 4 and at day 4.25 in expanded blastocysts with a smaller reduction within the trophectoderm (TE). The study revealed the effect of restricted maternal LPD (6% casein) to slow the rate of proliferation by reducing cell number when mitotic index was measured. However, no differences in implantation rate, in the size of the deciduum or enclosed visceral yolk-sac were observed.

Female mice were exposed at the periconception period to diets supplied with 7% total fat, 4.7% crude fibre, and between 15.5 and 16.5 MJ/kg of digestible energy, with a protein concentration of 21.7% for the high- protein diet (HPD), 12.7% for the medium-protein diet (MPD; control), and 8.4% for the low-protein diet (LPD). The study showed reduced ICM with significant reduction in the proportion of ICM:TE cells of females derived from HPD: 27.7% and LPD: 24.4% compared to MPD: 42.9% (Mitchell *et al*, 2009).

Not only do maternal LPD or HPD affect blastocyst development, but also maternal diet-induced obesity affects embryo development and growth. The development of the zygotes into blastocysts from female mice fed an obesogenic diet (10% simple sugars, 20% animal lard, 28% polysaccharide,

23% protein [w/w], supplemented with sweetened condensed milk and micronutrient mineral mix) failed in comparison with controls (Igosheva *et al,* 2010). The study also showed that the maternal diet-induced obesity led to a dramatic increase in inner mitochondrial membrane potential in oocytes (147%) and zygotes (74%) compared with those of lean females. Abnormal localisation of mitochondria was detected in the eggs of the obese females, which may have contributed to the failure of blastocyst development and the preimplantation embryo.

1.1.2 Effects of culture conditions on embryo growth and adult health

Several studies have considered the sensitivity of the embryo to its culture environment, particularly *in vitro* culture (IVC) or *in vitro* fertilisation (IVF), and the possible short- and long-term consequences.

A prospective follow-up study (Wisborg *et al*, 2010) showed a significantly increased risk of preterm delivery and considerable preterm delivery in women who conceived after IVF or intra-cytoplasmic injection (ICSI) compared with fertile women has been observed. No significant differences in the risk of preterm delivery and considerable preterm delivery were observed between fertile women, women who became pregnant after non-IVF assisted reproductive treatment or subfertile women. Compared with spontaneously delivered infants of infertile women, IVF/ICSI children were of the highest risk for low birth weight. Wisborg (2010) also showed that infants born after IVF or ICSI and after non-IVF treatment had a high risk of admission to a neonatal intensive care unit.

Low birth weight after ART conception is associated to increased rates of cardiovascular and metabolic diseases, e.g. Diabetes-2 in adulthood. Major birth defects were diagnosed by one year of age in infants born with the use of assisted conception by IVF/ICSI (Hansen *et al*, 2002). Infants conceived after IVF/ICSI had low birth weight, preterm birth and twice as high a risk of a

major birth defect as naturally conceived infants. About two thirds of the major defects were diagnosed during the first week of life and > 90% were diagnosed by six months of age. IVF children had a significantly greater prevalence of cardiovascular, urogenital, central nervous system and other defects, whereas ICSI recorded high rates for both the renal and the musculoskeletal defects, chromosomal and metabolic abnormalities. Overall, the study revealed that 1.6% of IVF and 2.0% of ICSI infants were significantly more likely to have multiple major defects than naturally conceived infants (0.5%) (Hansen *et al*, 2002).

Ceelen *et al* (2008) considered the postnatal growth and development in children from 8 to 18 years old born to subfertile parents who were either treated with IVF or conceived spontaneously (control). This study showed that children born after IVF were of lower birth weight and gestational age compared to the control. IVF-children displayed higher systolic and diastolic blood pressure, which may result in an increase the risk of developing cardiovascular disease independent of birth weight. The level of fasting glucose was higher in children born after IVF compared to those conceived spontaneously, but no significant differences were measured in fasting insulin concentration and insulin resistance.

ART media could be detrimental to development of the preimplantation embryo. In the Lane and Gardner (2003) study, a significant decrease was observed in total cell numbers of mouse blastocysts cultured in media of 37.5 µM ammonium. Increasing ammonium level to 150 or 300 µM significantly reduced total cell numbers, number of ICM cells, and the percentage of ICM cells. Embryos cultured in 300 µM ammonium increased the apoptotic cell index and significantly decreased percentage of implantation and foetal development. However, embryos that managed to implant were significantly delayed in their development by 1.5 days at day 15 of pregnancy. Blastocysts cultured in media with 300 µM ammonium concentration

increased the level of the expression of the imprinted gene *H19* compared to the control blastocysts cultured in media without ammonium.

Using Microarray assay (Rinauda *et al*, 2006), the gene expression profile of mouse embryos cultured in the presence of 5% O_2, as the physiological condition for tissue growth more closely approximated to *in vivo* embryos, compared to those developed in 20% O_2. Genes involved in cell growth were mis-regulated when cultured at 20% O_2 in media with or without the addition of amino acids (KSOM/AA or Whitten's, respectively). Embryos cultured in Whitten's showed a down regulation of genes involved in gastrulation which could compromise the developmental competence of the blastocysts. Rinauda's study showed increased cell numbers (ICM/TE) of the blastocysts cultured at 5% O_2 in KSOM/AA or Whitten's media. Blastocysts cultured in KSOM/AA were of 55% highest ICM cell number and percentage than those cultured in the Whitten's. Embryos cultured at 20% O_2 in both media had reduced birth weight.

Watkins *et al* (2007) reported that *in vitro* cultured mouse embryos had reduced blastocyst cell number compared to *in vivo* developed blastocysts at 96 hour post-human chorionic gonadotropin (hCG). Extended culture of the *in vitro* group for a further 20 hours showed a comparable cell number to those within *in vivo* embryos at 96-hours post-hCG. At 21 weeks, offspring derived from *in vitro* culture in T6 medium supplemented with protein source (BSA) and transferred to recipient (IVC-ET) displayed the highest mean SBP that was significantly higher than those derived from *in vivo.* Significant differences between female offspring derived from IVC-ET and IV-ET kidney and lung weights were observed at 27 weeks.

1.1.3 Effects of environmental conditions on gene expression in preimplantation embryo development

Gene expression is of major importance in early embryo development, in which expression of the imprinted genes contributes to normal gene

expression. Imprinted genes are expressed in a parent-of-origin-specific manner in which only one allele from the mother or father is expressed. For example, genes associated with growth, such as insulin-like growth factor 2 (*Igf2*), *Igf2* receptor gene (*Igf2R*), and *H19,* are imprinted during gametogenesis or preimplantation periods. *Igf2* is activated in the paternal genome, but is turned off in the maternal genome. *Igf2* is regulated by the active maternal gene *H19* that is turned off in the paternal genome. *Igf2R* is imprinted in the same way as of the *H19* (Wolpert *et al*, 1998). Loss of imprinting of one or a cluster of these genes has been shown to contribute to epigenetic and phenotypic changes.

Variations in foetal overgrowth have been investigated in sheep, human, mouse, and other species and are associated with altered expression of imprinted genes. Sheep reported for the large offspring syndrome (LOS) in which a significant increase in body weight and organ enlargements are associated with body growth and birth problems. LOS is related to the loss of imprinting and hypomethylation of a differentially methylated region (DMR) of the maternal *Igf2R* allele, which causes degradation of *Igf2*. Young *et al* (2001) showed a reduction of *Igf2R* expression in some sheep embryo tissues following *in vitro* culture of fertilised embryos for five days in a medium (co-cultured granulosa cells) supplemented with serum. Foetuses exhibiting LOS had a reduced expression of *Igf2R* by 30-60% relative to controls (medium without serum) with a reduction of IGF2R protein levels by 61% in muscle, 81% in liver and 67% in circulating form. Restriction analysis revealed a complete loss of methylation of IGF2R in DMR in 9 of 12 LOS individuals. As reduced IGF2R impaired IGF2 levels in the circulation, radioimmunoassay showed reduced levels of IGF2 in 125-day tissue samples.

In humans, studies revealed that ART manipulations are associated with epigenetic diseases, specifically Beckwith-Wiedemann syndrome (BWS) and Angelman syndrome (AS). BWS is one of the most common overgrowth

syndrome associated with genetic and epigenetic changes in an imprinting cluster including *IGF2* and various maternally expressed genes on chromosome 11p15. Loss of imprinting of paternal *IGF2* is responsible for abnormal methylation and silencing in the DMR (normally unmethylated) from *H19* activating and over-expressing the maternal *IGF2* contributing to foetus overgrowth (Reik and Maher, 1997). Maher *et al* (2003) assessed two cases out of six BWS children born after IVF/CSI had loss of methylation on the *KvDMR1* maternal allele (maternally methylated gene in somatic tissues). DeBaun *et al* (2003) tested imprinting alteration in six out of seven BWS children born after IVF/ICSI. Five of the six showed abnormal imprinting of maternal *LIT1* indicated by hypomethylation of the *LIT1* DMR, whereas only one BWS child exhibited abnormal imprinting of *H19* indicated by hypermethylation of the *H19* DMR.

Doherty *et al* (2000) revealed that culture media can dramatically affect the expression of the imprinted *H19*. Blastocysts cultured from 2-cell in Whitten's medium or KSOM containing amino acids (KSOM+AA) expressed both alleles (maternal and paternal) of *H19.* The normally silent paternal *H19* allele expressed in the blastocyst: 40% ± 6% of the total *H19* expressed in the Whitten's medium, compared to those cultured in KSOM+AA: 10% ± 3% of the paternal *H19.* Blastocysts cultured in Whitten's medium showed loss of methylation status of DNA at the *Hha*I site 5 (CpG dinucleotide located upstream from the start of *H19*), but methylation was detected for embryos cultured in KSOM+AA medium which confirmed the selective effect of the culture media on *H19*.

Giritharan *et al*, (2007) assessed the global pattern of gene expression in the mouse preimplantation period using Microarray technology. The Affymetrix 430 2.0 chip was used to compare mouse blastocysts produced by different fertilisation methods; *in vitro* fertilisation (IVF) or *in vitro* culture (IVC) compared to *in vivo*. Differential gene expression in the IVF blastocysts were detected in comparing to IVC and *in vivo* blastocysts. 29 genes were

changed by more than a 4-fold expression in the IVF embryos in relation to the *in vivo* and 3 genes in IVC.

Maternal diet may cause a gender–specific programming of imprinting gene expression. Maternal LPD reduced the level of *H19* (30%) in rat male blastocyst exposed to maternal LPD (9% casein) without affecting the relative expression of *β-actin, Igf2* and *Igf2R,* either in males or in females. The examined blastocyst either remained on LPD until day 20 or switched back to the control diet (18% casein) after implantation on day 4.25. On day 20, only the switched diet group showed a reduction in relative levels of *H19* (9.4%) and *Igf2* (10.9%) in male foetal liver. Reduced levels of growth regulating genes (*H19* and *Igf2*) have been suggested as affecting individual foetal growth in response to maternal LPD (Kwong *et al*, 2006).

Maternal methyl-supplemented diets (folic acid, vitamin B_{12}, betaine, and choline) provide substantially increased amounts of cofactors and methyl donors for methyl metabolism and Dnmt (DNA methyltransferase enzyme which catalyses the transfer of a methyl group to DNA) (Cooney *et al,* 2002). Such an example is the mutation of mouse *agouti* allele. The mouse *agouti* allele (wild-type) A^{w} regulates the alternative production of black (eumelanin) and yellow (pheomelanin) pigment in individual hair follicles. Insertion of intracisternal A particle (IAP) in the regulatory regions of the agouti locus controls the gene and yellow offspring are produced: viable yellow (A^{vy}), IAP yellow (A^{iapy}), or hypervariable yellow (A^{hvy}). The long terminal repeat (LTR) of the IAP expression is regulated by DNA methylation and causes hair follicle melanocytes to synthesise yellow instead of black pigment (Fig 1.1). DNA methylation as a result of maternal methyl diets are reported to change the LTR status and cause the epigenetic phenotype of A^{vy} that is also found to be maternally heritable (Wolff *et al*, 1998; Morgan *et al*, 1999).

Although epigenetic factors may change the phenotypes of the individual and affect later health, it is considered to be heritable, and passes through the

germ line in mammals. Morgan *et al* (1999) described that the inheritance of A^{vy} (as epigenetic changes) due to an epigenetic modification of the IAP at the agouti locus in mice may include DNA methylation. Thus, silencing of the IAP is the result of the epigenetic modification rather than maternal environment effect. The study also reported that yellow mice females (under standard conditions and diet) when mated with A^{vy}/a males ("*a"* is the *non-agouti* allele) were able to produce pseudoagouti offspring with more extensively methylated A^{vy} allele in pseudoagouti than in yellow mice.

A study by Waterland *et al* (2007) described that the A^{vy} hypermethylation is diet-induced. *A^{vy}/mice females* of two generations (F1 and F2) were weaned onto methyl-supplemented diet and then mated with *a/a* males. The effect of methyl diets was stable in the successive offspring (F1, F2 and third generation, F3) with fewer slightly mottled and more heavily mottled A^{vy}/a offspring. Waterland (2007) revealed that the acquired A^{vy} is passed to the offspring through the female germ line because of a supplemented diet rather than transgenerational modification at the locus.

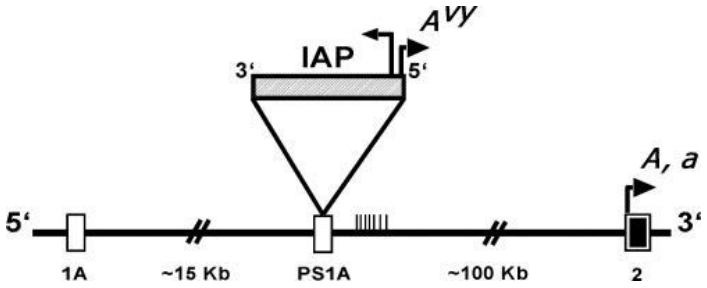

Fig 1.1: The mouse *A^{vy}* locus. The *A^{vy}* mutation was caused by insertion of retro-transposition IAP ~ 100 kb upstream of the first coding exon (the 4.5 kb IAP is not drawn to scale). The *agouti* (*A*) and *nonagouti* (*a*) transcripts originate at exon 2 (arrow head labelled *A, a*). The *A^{vy}* transcript originates from a cryptic promoter within the IAP (arrowhead labelled *Avy*) (Waterland *et al,* 2007).

Sinclair *et al* (2007) demonstrated that reductions in vitamin B_{12}, folate and methionine, from maternal diet around the time of ovine conception leads to epigenetic modifications to the genome affecting the DNA methylation in the offspring, with long-term implications for adult health. Using restriction landmark genome scanning (RLGS), these modifications were shown in 4% of 1,400 CpG islands in the liver of the sheep foetus for Methyl-deficient diet (MD) (reduced peripheral concentration of Vitamin B_{12}, folate, and methionine), of which 53% of the alteration was specific to males. Greater growth rates of ewe offspring for MD were observed than control offspring, and they became heavier by 22 months of age. Female offspring were fatter than males with less tolerance to infused glucose, but no differences in body fatness between treatment groups were observed. However, MD males were 25% fatter than control males. Females displayed greater resting heart rate than males, which displayed no differences in the treated

groups, and were within the normal range for non-stressed sheep. Blood pressure, systolic, diastolic and mean arterial pressure responses were increased only in MD male offspring.

1.2 Tight junctions and signalling

Whilst ART and *in vitro* culture aim to produce healthy and viable embryos, they may compromise embryo viability. Trophectoderm tight junctions have been found to be compromised in preimplantation embryos by affecting gene expression and cell differentiation in human ART (Ghassemifar *et al*, 2003; Eckert *et al*, 2007). The efficiency of para-cellular transport is regulated by the correct formation of intercellular junctions: zonular tight junction (TJ) and zonular adherens junction (AJ). The junctions also function as mediators of intercellular signalling between epithelial cells, of which TJ interruption could affect cell proliferation and gene expression (Sheth *et al*, 2008; Eckert and Fleming, 2008). Impaired junctions may be the result of reduced expression, or mislocalisation, of TJ proteins or disruption of gap junction communication or cellular energy status (Eckert and Fleming, 2008).

Eckert *et al*, 2007 has linked the mechanisms of metabolism and junction membrane assembly in the early developed embryo, such that amino acid turnover could predict TE differentiation. In this study, increased amino acid turnover during embryo developmental stages were related to an increased level of membrane assembly of junction components and protein synthesis, around the time of cavitation. This resulted in normal blastocysts with functional integrity of TE. In contrast, embryos failing to exhibit normal amino acid turnover could produce morphologically normal blastocysts but impaired TE differentiation. Membrane assembly of occludin and ZO-1α+ showed a significant relationship with amino acid turnover (Eckert *et al*, 2007).

Unbalanced embryo homeostasis is a state resulting from abnormal environmental conditions and may influence expression of various genes. For example, changing expression of metabolic and differentiation-related

genes in early developmental stages has been shown to alter expression levels of genes involved in trophectoderm differentiation and intracellular junction formation (Fleming *et al*, 2004). Thus, differentiation failure could be a consequence of junction assembly deficiency, as well as a cause of disturbed differentiation of the first epithelium during embryo development (Eckert and Fleming, 2008).

1.3 Myc/Max/Mxd network

Culture conditions or compromised maternal diets have been identified to affect preimplantation embryo growth, gene expression, signalling pathways and adult health. The Myc/Max/Mxd network is known to be expressed during embryo development, and has been suggested to function as a molecular switch that regulates cell growth and differentiation by controlling a common set of genes (Hultquist *et al,* 2004).

The Myc/Max/Mxd network (hereafter according to Mouse Genomic Informatics, the Mad1, Mxi1, Mad3 and Mad4 are referred to Mxd1, Mxd2, Mxd3 and Mxd4, respectively) comprises a group of transcription factors whose distinct interactions result in gene-specific transcriptional activation or repression (Grandori *et al*, 2000). Members of this network contain the basic helix-loop-helix zipper (bHLHZip) domain which facilitates dimerisation of Max with members of the Mxd family (Mxd1, Mxd2, Mxd3 and Mxd4) or Myc family (c-Myc, N-Myc, L-Myc). This domain is also required for DNA binding. The basic helix-loop-helix (bHLH) proteins act as transcriptional regulators and are involved with neurogenesis, myogenesis, cell proliferation, tissue differentiation, and other essential developmental processes (Morgenstern and Atchley, 1999).

Max can dimerise with itself, but these so-called homodimers are transcriptionally silent and may even have a dominant negative function (Grandori *et al*, 2000). Max can also forms heterodimers with Mnt and Mga proteins through the bHLHZip domain, but the activities of such complexes

are not as well studied, and are believed to exhibit inhibitory activities. Mxd proteins and Max complexes compete with Myc and Max complexes for binding to a specific-DNA-sequence (CACGTG), termed the E-box. Mxd and Max repress transcription from such a sequence whereas Myc and Max promote transcription (Grandori *et al*, 2000).

One mechanism by which the Myc-Max heterodimeric complex activates transcription is through the recruitment of a histone acetyltransferase (HAT) via TRRAP (Transformation/transcription domain-associated protein). Acetylation of surrounding histones and remodelling of the chromatin correlates with transcription and the ensuing phenotypic response of enhanced proliferation, cell cycle progression, growth, and, under certain conditions, apoptosis, although some studies suggest that the recruitment of Myc does not necessarily correlate with histone acetylation (Eberhardy *et al*, 2000). On the other hand, the heterodimers of Mxd-Max represses transcription by recruitment of a histone deacetylase activity (HDAC) via mSin3 co-repressor complex. This causes deacetylation of histone tails and the restoration of a repressive chromatin structure that prevents the transcription of the associated genes. In this way Mxd promotes growth arrest, and differentiation (Grandori *et al*, 2000) (Fig 1.2).

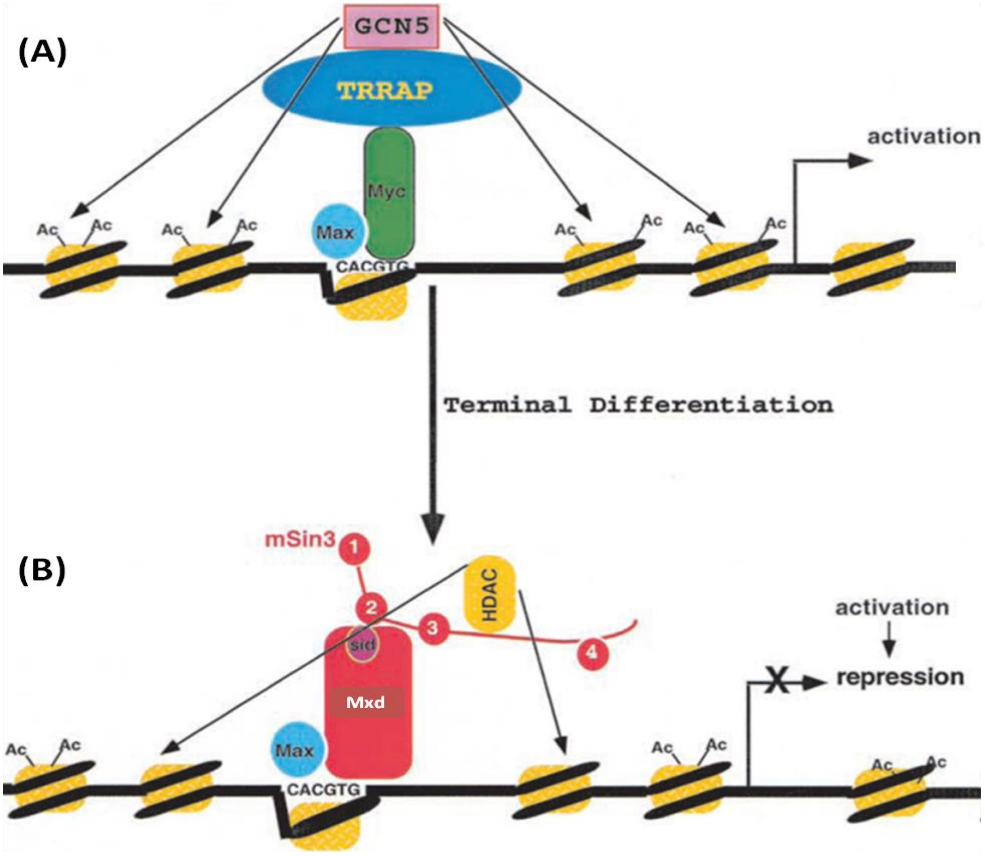

Fig 1.2: Myc and Mxd members of Myc/Max/Mxd network regulate the acetylation state of nucleosomal histone near E-box binding sites. (A) Myc-Max heterodimer bound to an E-box sequence near the promoter of a target gene and recruit the TRRAP co-activator and the HAT, GCN5 resulting in acetylation of nucleosomal histones and expression of the target gene. **(B)** During terminal differentiation, Myc is down regulated and release Max whereas Mxd is induced and heterodimer with Max. Mxd-Max heterodimer occupy the target gene E-box site and recruits the mSin3 co-repressor and HDACs leading to deacetylation and repression of target gene expression (modified from Eisenman, 2001).

In addition to the well-studied genes operating the Myc/Max/Mxd pathway, as described above, there are other genes that have not been examined to the same levels of molecular detail. These include Mga, Mnt, Mondo, Mlx, and some play an important role during early development. For example, Mga is expressed in early mouse embryonic stages, at E9.5, E10 and E10.5, and its expression overlaps with members of T-box, suggesting a role of Mga in regulatory pathways controlling mesoderm induction (Hurlin *et al*, 1999). Mga contains two domains, T-box and bHLHZip, which suggest a more complex transcriptional and biological activity of Mga than other members of bHLHZip and T-domain. The T-domain acts as a master regulator directing the transcription genes essential for a variety of embryonic inductive events (Hurlin *et al*, 1999; Rikin and Evans, 2010). Mga suppression of Myc activation is less potent than that caused by Mxd proteins and Mnt (Hurlin *et al*, 1999).

In zebrafish, Mga, is a T-box transcription factor required for embryogenesis, and regulates normal heart tube looping (Rikin and Evans, 2010). Blocking the function of Mga by injecting fertilized eggs of zebrafish with morpholinos generates phenotypes with increased cardiac oedema, with thin linear “heart-string”, similar to that caused by mutant *tbox5*, *tbox20* or *gata4*. Morphant Mga shows up-regulation of *c-myc, l-myc, mxd2* and *mxd4* and 2-fold enhanced transcripts of *tbox20, gata6* and *gata4* (Rikin and Evans, 2010).

Another bHLHZip Max-binding protein is Mnt, which co-expressed with Myc in a number of proliferating cell types. The complex Mnt/Max is similar to Mxd acting as a transcriptional repressor. Yeast two-hybrid screen revealed that Mnt also contains regions rich in proline residues that are similar to the activation domains of transcriptional factors, including Box I of the c-Myc activation domain. Mnt is similar to Mxd, and contains the SID that interacts with mSin3 co-repressor proteins, mediated through paired

amphipathic helix 2 (PAH2). The deletion of SID converts Mnt from transcriptional repressor to transcriptional activator (Hurlin *et al*, 1997).

In situ hybridization for mouse embryo showed that *mnt* is uniformly expressed at E9.5 and E10.5 and higher at later stages in neural structures. Expression of *mnt* at E10.5 appeared at the same time as c- and N-*myc* expression in proliferating cells, suggesting expression of *mn*t in both proliferating and differentiating cells. Immunoprecipitated Max from MCF-7 human breast carcinoma and HLF human neuroblastoma cell lines, using Mnt and Myc anti-sera, confirmed the presence of both Mnt/Max and Myc/Max hetero-complexes in proliferating cells (Hurlin *et al*, 1997).

1.4 Rnf17: RING finger protein

RING finger protein(*Rnf17*) is a germ cell specific gene that is expressed in the testis and required for male germ cell differentiation (Pan *et al*, 2005) and was identified by Yin *et al* 1999 and 2001, and originally termed Mmip-2 (**m**ad **m**ember **i**nteracting **p**rotein-**2**), following its isolation in a Y2H (yeast two hybrid) screen as a Mxd protein interactor. Rnf17 encodes a protein containing both RING finger and Tudor domains and is reported as a component of a novel nuage, a French term for a cloud, which displays a perinuclear location in male germ cells (Pan *et al*, 2005). Rnf17 is one of several novel spermatogonially expressed germ cell specific proteins and is involved in transcriptional or post-transcriptional regulation of gene expression (Wang *et al*, 2001). Microarray data showed that Rnf17 is also expressed in early embryo development (Giritharan *et al*, 2007); however, Rnf17 function has not been studied in the early embryo.

Hereafter, according to Mouse Genomic Informatics, the RING finger protein 17/Mmip2/Tdrd4 are referred to as Rnf17. Also small letters Rnf17 named mouse gene (mRNA) whereas capital letters RNF17 refers to the protein.

1.4.1 Structure and function of Rnf17

Pan *et al* (2005) identified two isoforms of mouse RNF17 that are longer than the ~300 residue protein previously reported as Mmip-2 (Yin *et al*, 1999). The short RNF17 (RNF17S) is 1130 amino acids (a.a) and the longer RNF17 (RNF17L) is 1640 a.a. Northern blot analysis of a panel of adult mouse tissues showed that Rnf17 is exclusively expressed in the testis, including the two *Rnf17* transcripts; *Rnf17L* (5.2 kb) and *Rnf17S* (3.5 kb) (Pan *et al,* 2005). The cDNA sequences of both Rnf17 were recorded in GenBank under the accession numbers: *Rnf17L,* AY864011; *Rnf17S*, AY854010 (Pan *et al*, 2005), and Mmip-2 is deposited with accession number: AF190166 (Yin *et al*, 1999).

The mouse Rnf17 proteins consist of a RING finger domain of a zinc-binding motif at the N-terminus with multiple Tudor domains at the C-terminus. Pan *et al (*2005) indicated 5 Tudor domains in the RNF17L and 3 in the RNF17S. However, AceView and UniProt annotated 4 Tudor domains in RNF17L and 2 in the RNF17S and they are named the maternal Tudor domain (Fig 1.3). AceView revealed that the *Rnf17* gene produces several proteins with no sequence overlap. The gene is well expressed with 9 spliced mRNAs, and they putatively encode proteins in which they have been experimentally expressed and annotated in the genome database (a, b, c, d, e, f, g, h, i) and the 2 unspliced mRNA variants appear not to encode good proteins which are expressed but not annotated in genome database (j, k) (Fig 1.4). Those encode good proteins containing 9 isoforms and some contain maternal Tudor domains (a, b, d, e), a second peroximal domain (a, i), a coiled coil stretch (a, b, c, g), a Leucine zipper domain (a, b, e, d) and as many as 3 nuclear localisation domains (a, b, c, g). However, the functional relevance of these domains is unclear at this point.

Comparing the transcript sequences with the mouse genomic sequence demonstrated alternative splicing. Rnf17 transcripts shared exons 1-25

(Pan exon nomenclature) and differed in their 3' terminal sequences. The short Rnf17 is AT rich in its last exon (exon 26) which contains a non-canonical polyadenylation signal (AATAA) and an in-frame translational termination codon. The long transcript of the Rnf17 lacks exon 26, but has 12 additional exons with a canonical polyadenylation site of (AATAAA) (Fig 1.5), which predicts alternative splicing. Exon 26 is not annotated in the mouse (www.ensembl.org), but is within the rat genome sequence. Surprisingly, the human sequence lacks this exon, but carries the two flanking exons that are well conserved in the mouse sequence.

It will be of significant interest to perform some evolutionary analysis to ascertain when this sequence was acquired by rodents, or lost by primates, and to examine Rnf17 genes within Laurasiatheria, a large group of placental mammals that includes shrews, hedgehogs, pangolins, bats, whales, most hoofed mammals and carnivorans, among others. Interestingly whilst the human genome does not carry the exon to produce the 2x Tudor domain protein, a related protein is expressed by humans that appears to originate by some distinct, but ill-defined mechanism. The last shared exon carried by both long and short murine transcripts is of 116bp and this size is conserved between mouse and human genes. Within genomic DNA in the mouse this exon is followed by a 6040bp intron that carries the novel exon 26. The 6040bp intron can be divided into a 5' intron of 2233bp, a 125bp exon (3' terminal short transcript) and a 3' intron of 3682bp. The human genome has a significantly smaller intron of 2283bp followed by exon of 290 (287bp in mouse), 164, 120, 81 and 57 (60bp in mouse). The novel rodent exon, if present in humans would reside with the 2283bp region. It is not clear why this intron is truncated compared to the mouse. In the rat, exon sizes for the 5 exons preceding and following the 3' terminal exon of the short transcript are absolutely conserved. The intron carrying the short transcript terminal exon is of 3812bp compared to 6040bp in the mouse. Other species that have an annotated Rnf17 gene are not at the level of completeness of

knowledge to ascertain whether the 3' terminal of the short murine transcript is a rodent peculiarity, or is found in other non-primates. Canis familaris displays extensive exon size conservation both 5' and 3' of the short cassette exon, but has a relatively short intron of 1131bp for putatively carrying the exon that gives rise to the short transcript and protein. Purely on size, one could argue that this would carry this exon. No species, other than the mouse and the rat, has the short transcript encoding only two Tudor domains annotated. However, as indicated above, the human genome does in fact express a related protein, with two Tudors, by another mechanism. It is of interest that this protein lacks the N-terminal RING finger domain and is expressed from transcript 203 (www.ensembl.org).

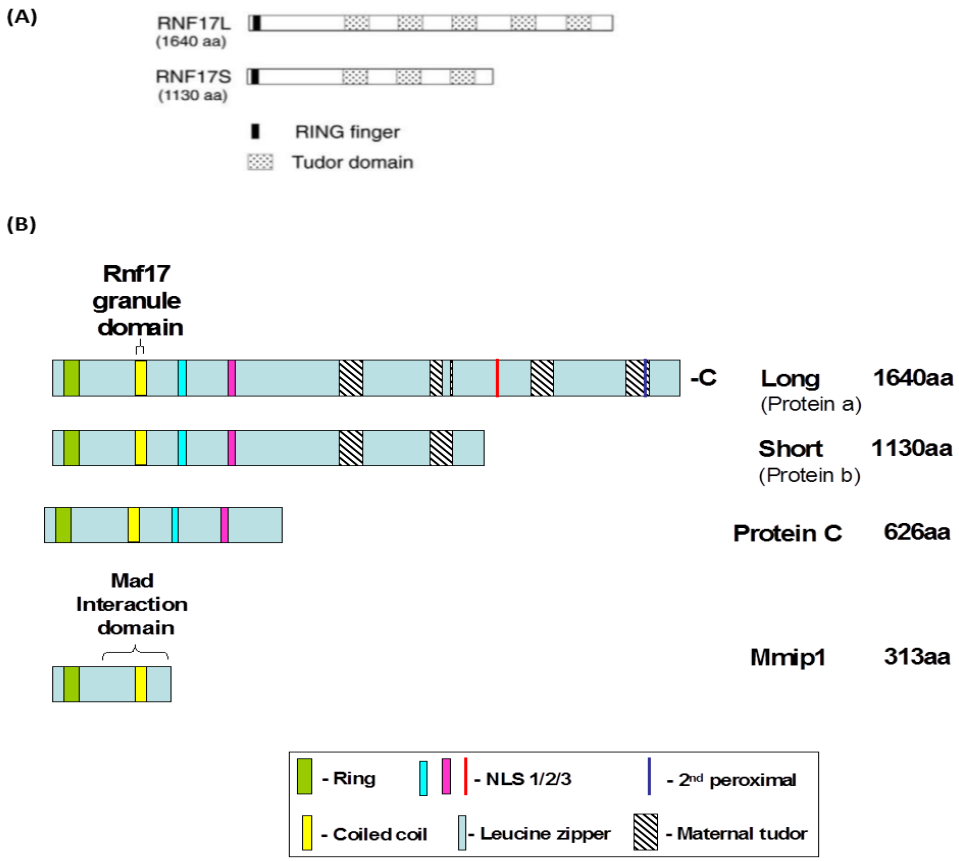

Fig 1.3: Structure of RNF17 transcripts. RNF17 contain a RING finger domain in the N-terminal and multiple Tudor domains in the C-terminal. **(A)** Two transcripts for RNF17 described by Pan *et al*, (2005) contain 5 Tudor domains in the RNF17L and three Tudor domains in the RNF17S. **(B)** Schematic diagram for RNF17 transcripts described by AceView shows four maternal Tudor domains are in the RNF17L (protein a) and two maternal Tudor domains in the RNF17S (protein b). No maternal Tudor domain is in RNF17 transcript C (protein C) or Mmip2.

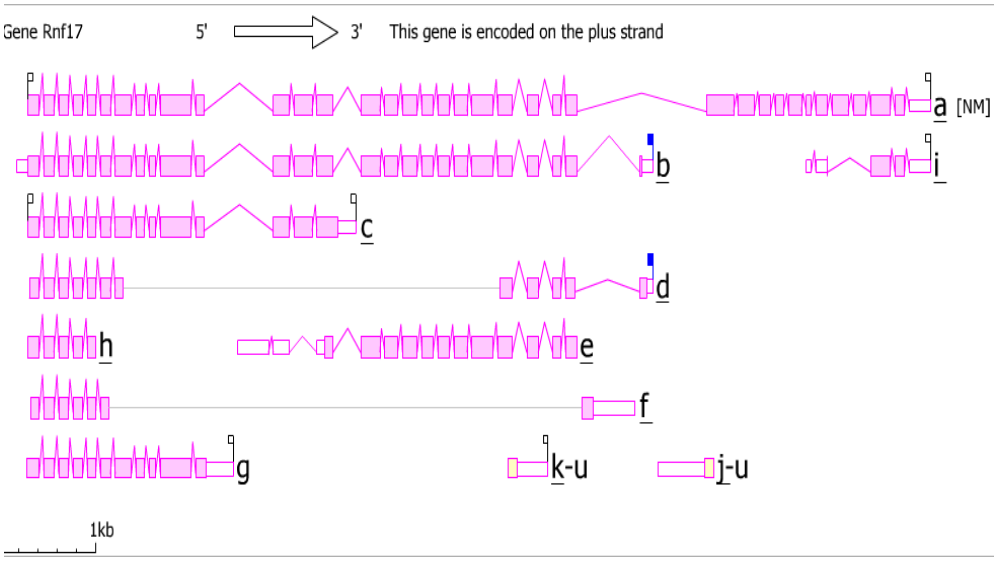

Fig 1.4: Alternative mRNAs aligned from 5' to3' on virtual genome as described in AceView. Nine spliced Rnf17 mRNA encode good proteins (a, b, c, d, e, f, g, h, i) and two unspliced Rnf17 mRNA appear not to encode good proteins (j, K). Underlined name/ending of transcript been supported by GenBank accession resulted from cDNA of testis, in vitro fertilised eggs, trophoblast stem cells, placenta, whole body, blastocyst, embryo and nine other tissues. Names not underlined result from cDNA concatenation in the coding region and should be experimentally checked.

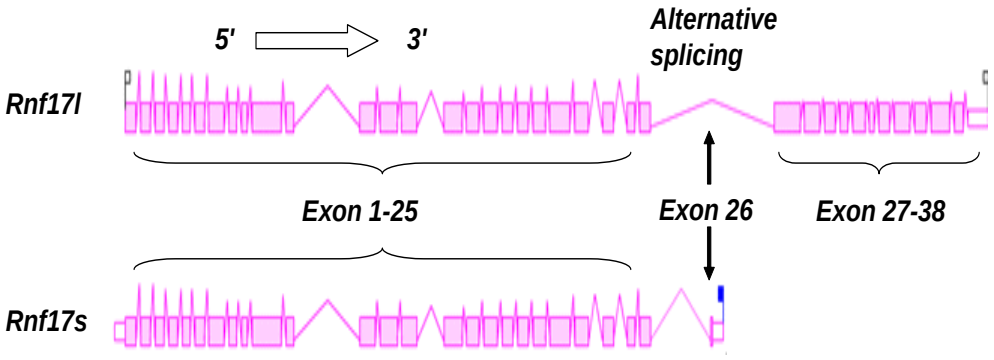

Fig 1.5: Schematic diagram of Rnf17 transcripts. Both the short Rnf17 (*Rnf17s*) and the long Rnf17 (*Rnf17l*) are shared exons 1 to 25. Exon 26 is last in *Rnf17s* and is lost in *Rnf17l* which predict alternative splicing of about 6040bp in the mouse and 2238bp in the human. *Rnf17l* has 12 additional exons (modified from AceView; Pan *et al*, 2005).

1.4.2 Rnf17 and alternative splicing complexes

Nuclear pre-mRNA splicing is the process of removing the primary transcript and joining the coding sequences to form mature mRNA that is transported to the cytoplasm for protein synthesis. Splicing is catalysed through several steps, mediated by a large RNA-protein complex, termed the spliceosome. The conserved cell division cycle 5-like protein (CDC5L) is required for the second catalytic step of pre-mRNA splicing, a step that is essential for spliceosome assembly and catalysis (Ajuh *et al,* 2000).

Human CDC5L interacts with human pleiotropic regulator 1 (PLRG1) and immuno-depletion of CDC5L from HeLa nuclear extract showed depletion of PRL1 (Ajuh *et a*l, 2000). The CDC5L/PLRG1 complex directly interacts *in vivo* with the heterogeneous nuclear ribonucleoprotein-M (hnRNP-M) and this interaction modulates both the 5' and the 3' alternative splicing process (Lleres *et al*, 2010). Loss of the CDC5L/PLRG1 interaction domain on the hnRNP-M correlated with a loss of ability to modulate alternative splice site selection in E1A mini-gene assay. Proteomic analysis of nuclear complexes of HeLa cells containing CDC5L antibody revealed an interaction between CDC5L (Q99459) and RNF17 (Swiss-PROT: Q9BXT8) (Lleres *et al*, 2010), suggesting some role for Rnf17 in the spliceosome complexes.

Cdc5l and Plrg1 are highly expressed in the mouse blastocyst in response to maternal NPD and LPD compared to Rnf17 (Fig 1.6), although no differential regulation observed in response to maternal diets (Papenbrock *et al*, unpublished data).

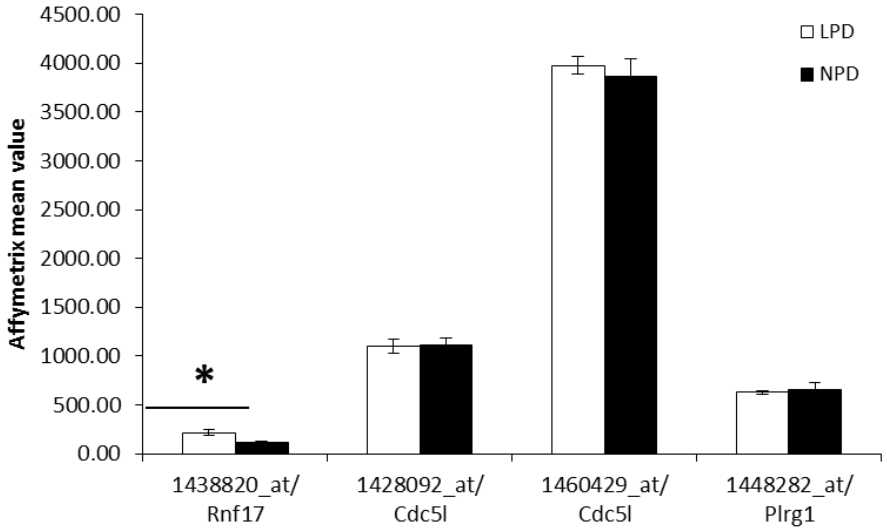

Fig 1.6: Microarray data show expression of Cdc5l and Plrg1 comparing to Rnf17 in mouse blastocysts in response to maternal LPD. Affymetrix 1438820_at for Rnf17 is significantly increased in mouse blastocysts in response to maternal LPD. No differential regulation was observed for Cdc5l and Plrg1 in mouse blastocysts; however, Affymetrix 1460429_at for Cdc5l showed 1.03 fold increases in response to maternal LPD (Papenbrock *et al,* unpublished data).

1.4.3 RING finger domain

A RING finger is a type of zinc finger that can be identified within protein sequences containing a cysteine and histidine amino acid motif of consensus sequence **C-X2-C-X[9-39]-C-X[1-3]-H-X[2-3]-C-X2-C-X[4-48]-C-X2-C**. The amino acid residues coordinate two zinc ions in a highly typical cross-brace structure and this domain may either bind DNA or be involved in protein-protein interactions (Fig 1.7). The RING domain in murine Rnf17 is at residues 30 to 75 of the full protein sequence and the sequence as shown in UniProt is:

CTRCGRKVSVASGDHHKFPCGHAFCELCLLAPQEYTTSKCTDCE

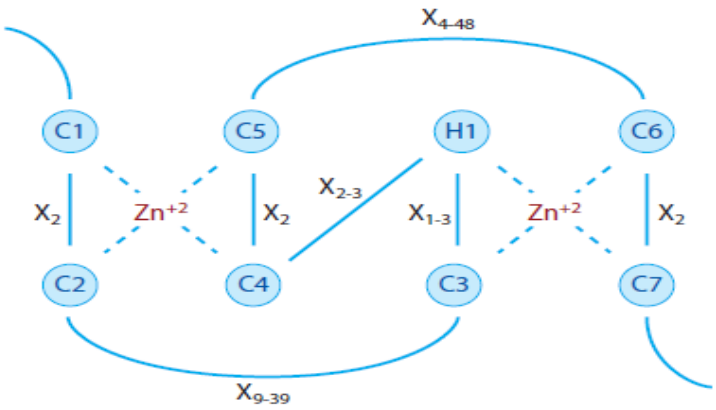

Fig 1.7: Schematic drawing of Zinc finger protein shows the cross-brace structure between amino acid residues and the two zinc ions. The first cysteine that coordinates zinc is labelled as C1, and so on. H1 denotes the histidine ligand. Xn refers to the number of amino acid residues in the spacer regions between the zinc ligands (modified from Deshaies and Joazeiro, 2009).

Many RING finger domains with their characteristic conserved pattern of His and Cys residues are observed to play a role in the tagging of proteins by ubiquitin that results in their degradation by the proteasome. RING domain proteins exert E3 ubiquitin ligase activity (Pickart, 2001).

The Ubiquitin system involves an ubiquitin-activating enzyme (E1), an ubiquitin-conjugating enzyme (E2) and ubiquitin-ligase (E3) and the system is particularly complex involving some 35 E2s and 250 E3s, although the genome only carries two E1s. E1 activates ubiquitin (Ub) that binds to the active-site cysteine of the E1. The activated Ub is transferred in a thioester linkage to the active-site cysteine of the E2 (E2~Ub). The E2~Ub interacts with E3 ligase via a RING domain and the E3 ligase catalyses the transfer of Ub from the E2 to a targeted substrate, the latter being degraded by proteasome 26S (Fig 1.8).

Van Wijk and colleagues, using the global Y2H screen described later, demonstrated that the human RNF17 RING domain was able to interact with the E2 protein, UBE2U. Expression of the putative Rnf17 E3 ligase enzyme during early development could implicate its role in modifying the proteome independently of the transcriptome, i.e. post-translationally, through changes to the half-lives of key target proteins, and this observation provides further support for the notion that transcriptomics alone cannot provide answers to key development issues.

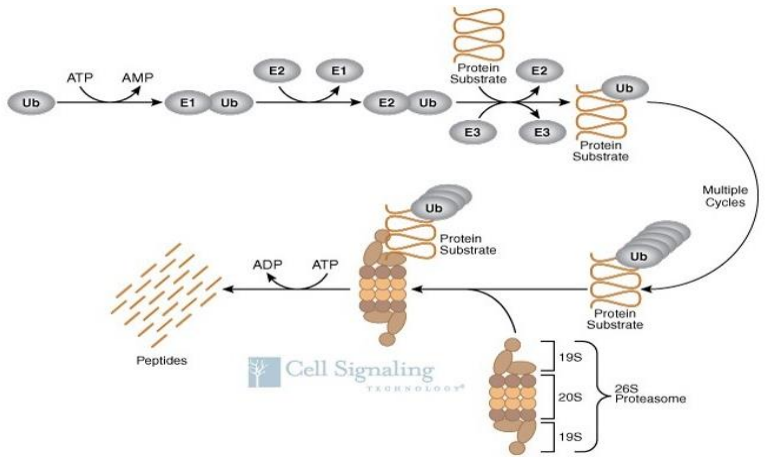

Fig 1.8: Schematic diagram shows the main steps of ubiquitin-proteasome system (www.ebi.ac.uk).

RING finger-containing proteins may modulate the Myc/Max/Mxd network by direct ubiquitinylation mediating degradation of target proteins. For example, c-IAP (isoform of IAps protein that acts as an inhibitor of apoptosis in human adult tissues) has been shown to degrade Mxd1 by ubiquitinylation, and increases the level of two of Myc-responsive genes (*ornithine decarboxylase-1* and *Cyclin D2*) and promotes cell proliferation and transformation (Xu *et al*, 2007).

Serum induction in cultured cells induced Mxd1 degradation by phosphorylation of Mxd1 at Ser 145 by RSK and S6K or PI3K/Akt pathways through ubiquitinylation (Zhu *et al*, 2008; Chou *et al*, 2009).

Taken together, questions that we could ask are:

- Whether Rnf17 as an E3 ubiquitin-ligase has a role in the degradation of the members of Mxd family?

- Does increased E3 ligase activity of Rnf17 promote cell proliferation by increasing c-Myc and enhancing c-Myc target genes?

1.4.4 Tudor domain

Tudor domains are small modules of amino acids mediating protein-protein interactions that are necessary for the assembly and regulation of germ granules. The Tudor domain is implicated in chromatin remodelling, RNA splicing and transport of mitochondrial RNA from mitochondria to polar granules (Thomas and Lasko, 2005; Chen *et al*, 2009; Arkov and Ramos, 2010). The founding member of this family is a germ cell specific protein Tudor with multiple Tudor domains form *Drosophila*. Related proteins in other organisms, including zebrafish and mouse are termed Tdrd (Tudor related domain) and have roles in germ cells (Pan *et al*, 2005; Chen *et al,* 2009). Microarray analysis, for the expression pattern of mammalian genes encoding Tudor domain proteins revealed a group whose expression is highly enriched in germ cells, such as Tdrd1, Tdrkh/Tdrd2, RNF17/Tdrd4, Tdrd5, Tdrd6, Tdrd7, Stk31/Tdrd8, Tdrd9, Tdrd10, Akap1 (Chen *et al,* 2009).

Tudor domain-containing proteins are localized together with PIWI proteins in cytoplasmic electron-dense structures known as chromatoid bodies (CB), intermitochondrial cement (IMC) or nuage. Interaction between Tudor domain-containing proteins and PIWI proteins, relatives of the Ago proteins that participate in RNA interference via the RISC, is mediated by symmetrical dimethyl arginine (sDMA). These modifications are brought about by a protein arginine N-methyltransferase such as Prmt5 and is pivotal to protein-protein interactions and to perform biological activities (Arkov and Ramos, 2010). Sites (RG/RA) and types (mono- or di-methyl, asymmetrical or symmetrical) of arginine methylation on PIWI proteins have been determined and identified to interact with Tudor domain aromatic cages via sDMA (Chen *et al*, 2009; Vagin *et al*, 2009). Double mutation of the TDRKH Tudor domain residues including D390, which is conserved across the TDRD family of

Tudor domains and F391, a component of the aromatic cage, completely abolished the binding of TDRKH to MIWI (Chen *et al*, 2009).

PIWI proteins are also associated with Piwi-interacting RNAs (piRNAs) and function in piRNA-mediated posttranscriptional silencing. PIWI proteins contain arginine-glycine and arginine-alanine (RG/RA)-rich clusters at their N-termini. Immunoprecipitates of endogenous MIWI and MILI from lysates of adult testes followed by mass spectrometry, revealed that Tudor domain proteins and proteins involved in piRNA pathways are associated with MIWI or MILI or with both complexes (Chen *et al*, 2009; Vagin *et al*, 2009). Chen (2009) determined the methylated sites of RG/RA-rich of MIWI and MILI and identified that 2 different arginines could be dimethylated simultaneously on a single peptide, suggesting a role of PIWI to recruit proteins with methyl arginine recognition models at the same time, such as Tudor domains and piRNA. By scanning the lower mass range of several DMA peptides' MS/MS fragments, Chen (2009) identified that the modifications on PIWI proteins (RG/RA) are symmetrically dimethylated (sDMA).

Both TDRD and their interaction partner MIWI, MILI or MIWI2 (mouse PIWI proteins) are localised in the cytoplasm in CB or nuage. Mutant TDRD proteins or PIWI proteins revealed disorganisation of CB or nuage and co-localisation of their components. For example, TDRD1 localised in MILI-containing nuage loses its localisation in *Mili*-deficient prospermatogonia and dispersed in the cytoplasm, whereas in *Tdrd1* mutant MILI is still localised in nuage. In contrast, MIWI2 that co-Immunoprecipitated with MILI and TDRD1 is not required for correct TDRD1 co-localisation. However, in *Tdrd1* mutant MIWI is lost from nuage and is diffuse in the cytoplasm (Vagin *et al*, 2009).

Endogenous MIWI and MILI complexes were recovered from mouse testis (3-6 months-old) using MIWI N2 or N3 and MILI N1 or N2 antibodies for Multidimensional Protein Identification Technology (MudPIT) analysis. MudPIT was followed by Immunoprecipitation for MIWI or MILI complexes

and showed that RNF17 interacts with MIWI but not MILI proteins (1.5-1.8%) (Vagin *et al*, 2009). The significance of this observation in early development is not clear as Microarray analysis revealed very low expression of MIWI and MIWI2, however MILI was highly expressed. In the same study (Vagin *et al*, 2009), proteomic analysis of 3xFlag-HA MILI, MIWI by MudPIT revealed a complex of proteins that interact with MILI and MIW including Tudor domain-containing proteins. The interaction showed that MIWI is associated with the greatest number of Tudor family proteins including RNF17 with a lesser degree of interaction (12 peptides, 8.7% coverage). Interactions identified by mass spectrometry were also confirmed by Western blotting.

In another study in zebrafish, Tdrd1 and the Piwi proteins, Zili and Ziwi, are localised in nuage-like structures in the cytoplasm in early stages of both oocyte and sperm development. Co-Immunoprecipitates using zebrafish Tdrd1-specific antibodies in testis showed interactions between Tdrd1 and Zili and Ziwi. Mass spectrometry on Tdrd1 Immunoprecipitates identified Ziwi and Zilli, Vasa and the Tudor domain-containing proteins Rnf17 (24 peptides in testis and 6 in ovary) and Tdrd5 (Huang *et al*, 2011) suggesting that Rnf17 and Zili zebrafish interact.

TDRD5 co-localised with MIWI in IMC, CBs, and Tudor/Piwi-containing nuclear bodies (T/PNBs). *Tdrd5* $^{-/-}$ mutants showed significant disorganisation of the IMCs and the CBs, co-localisation of MIWI and reduced expression of *Act* and CREM targets (Yabuta *et al* 2011). Yabuta (2011) revealed that the phenotype of *Rnf17*$^{-/-}$ mutants is similar to that of *Tdrd5* and *Miwi*$^{-/-}$ mutants, in which that RNF17 may function cooperatively with the IMCs and the CBs for the stabilization of the CREM target genes and other spermiogenic genes. The developed haploid genome and fertile offspring following injection of oocytes with round spermatids obtained from *Tdrd5*$^{-/-}$mice, raises the possibility that the mutants for *Rnf17*, *Tdrd6*, or *Miwi*, which show phenotypes similar to those of mutant *Tdrd5*, bear round spermatids with a functional haploid genome (Yabuta *et al*, 2011).

Arkov and Ramos (2010) reviewed that PRMT5 is the factor responsible for the sDMA modification and that it may control the subcellular localization of PIWI proteins in germ cells and is required for transposon silencing. Arginine methyltransferase 5 (Prmt5) is essential for early development as well as for the derivation and maintenance of pluripotent ES cells. It has a role in the establishment of unipotent primordial germ cells from embryonic stem cells (Tee *et al*, 2010; Nagamatsu *et al,* 2011). ICM outgrowths from ES cells showed predominant expression of PRMT5 in the cytoplasm of all ICM outgrowth cells, including Oct4-positive pluripotent cells, suggesting the involvement of PRMT5 in development and proliferation of the epiblast *in vivo* and *in vitro* (Tee *et al,* 2010). Microarray analysis of somatic cells reprogramming of MEFs with *prmt5, klf4* and *Oct3/4* and *Nanog-GF*P reporter gene showed that gene expression of these cells became ES cell-like. Induction in these cells was referred to *prmt5*, which is critical for germ cell specificity. RT-PCR for *prmt5 knockdown* revealed a reduction in the number of *Nanog-GFP* colonies. Results indicated that Prmt5 participates in the reprogramming process of somatic cells mediated by Sox2, *klf4, Oct3/4* and *c-Myc* (Nagamatsu *et al,* 2011). Prmt5 was highly expressed in our blastocyst array, indicating a possible arginine N-methyltransferase activity.

Immunoprecipitated 3xFlag-HA-MIWI complexes from adult testis were analysed by MudPIT represented associations of PRMT5 and its cofactor WDR77 with MIWI by 20 peptides (21% protein coverage) for PRMT5 and 14 peptides (18.4% protein coverage) for WDR77. Flag-HA-tagged MIWI2 or MILI Immunoprecipitated from embryonic testis also showed interaction between PRMT5/WDR77 and MIWI2 and MILI (Vagin *et al*, 2009). Myc-tagged MILI, MIWI or MIWI2 were co-expressed with Flag/HA-tagged PRMT5 or WDR77 in HEK 293 cells and showed interaction between PIWI proteins with WDR77 but not PRMT5, suggesting a role of WDR77 as interaction bridge between PIWIs and PRMT5 (Vagin *et al*, 2009).

WDR77 is uniformly distributed in the nucleus and cytoplasm of the embryonic gonocytes. At later stages WDR77 is localised to the CB of round spermatids (Vagin *et al*, 2009). PRMT5 is expressed in the early mouse embryo and at the early stages it is nuclear. At E4.5, Prmt5 is expressed in the nuclei of differentiated TE cells but is down-regulated transiently in the pluripotent ICM epiblast cells. However, at E6.5, Prmt5 was detected in the pluripotent epiblast cells of the post-implantation embryo, but predominantly in the cytoplasm (Tee *et al,* 2010). *Miwi* mutants have been shown to disturb WDR77 localization to CB, without affecting the uniform cytoplasmic localisation of PRMT5 (Vagin *et al*, 2009).

Prmt5 and Wdr77 are highly expressed in the mouse blastocyst in response to maternal diets compared to the significantly changed Rnf17. Affymetrix 1422844_a_at and 1434552_at are slightly increased in response to maternal LPD but failed to reach significance (Papenbrock *et al*, unpublished data) (Fig 1.9).

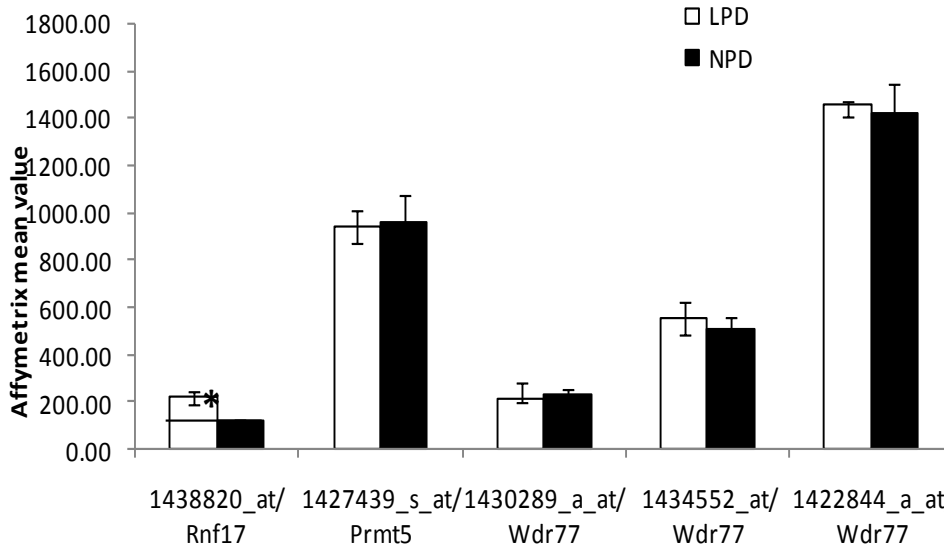

Fig 1.9: Microarray data show expression of prmt5 and Wdr77 comparing to Rnf17 in mouse blastocysts in response to maternal LPD. Affymetrix 1438820_at for Rnf17 is significantly increased in the mouse blastocysts in response to maternal LPD. No significant changes were observed in Prmt5 and Wdr77 in response to maternal LPD. Affymetrix 1427439_s_at for Prmt5 and 1430289_a_at for Wdr77 are down regulated in response to LPD of 0.98 and 0.93 respectively, whereas Affymetrix 1434552_at and 1422844_a_at for Wdr77 are up-regulated in response to LPD of 1.09 and 1.03 respectively (Papenbrock *et al*, unpublished data).

The crystal structure of a Tudor domain from the mammalian SURVIVAL MOTOR NEURON (SMN) protein revealed a β-barrel structure enclosing a pocket lined with aromatic amino acids (aromatic cage), that is required for the recognition of methylated lysine/arginine-containing ligands (Arkov and Ramos, 2010; Chen *et al*, 2009). The Tudor domain of SMN is needed for binding to methylated SmD1 and SmD3 (two SM proteins) by sDMA. Tudor domains have highly conserved amino acids and predicted structure, which suggests that the structure of the Tudor domain in SMN is likely to be very similar to those found in other Tudor domain containing proteins (Fig 1.10) (Thomson and Lasko, 2005).

Fig 1.10: Amino acid sequences of Tudor domain as described by Thomson and Lasko (2005) compare the Tudor domain of SMN (*Homo sapiens*) to 11 Tudor domains of TUD. Hydrophobic residues are highlighted in blue and negatively charged residues are highlighted in pink.

Mutagenesis of SND1 aromatic residues showed disturbances in the binding affinity to the sDMA peptides (Ke *et al*, 2010). SND1 carries a bifurcated Tudor, called the extended Tudor domain or the maternal Tudor domain that is essential for binding to sDMA. The SND1 extended Tudor domain contains three parts, the canonical tudor domain, the linker α-helix and the fifth SN-like domain. The Tudor domain module is embedded between two segments of the fifth SN-like domain, the N-terminal two β-strands and the C-terminal with three α-helices and three β-strands. The maternal Tudor domain sequence contains the canonical Tudor domain, the linker α-helix and the N-terminal two β-strands of the SN domain.

The UniProt database shows that Rnf17 contains four maternal Tudor domains in the long protein and two in the short protein, compared with 5 and 3 respectively in the work by Pan *et al* (2005). The alignment of Tudor domains of human RNF17 and human SND1 -Ke (2010)- showed that Tudor1 and Tudor4 for Rnf17 (row1 and 3) have the highly conserved aromatic side chains, as described above, whereas the aromatics of Tudors 2 and 3 are poorly conserved (row 4 and 5) and probably do not bind to sDMA.

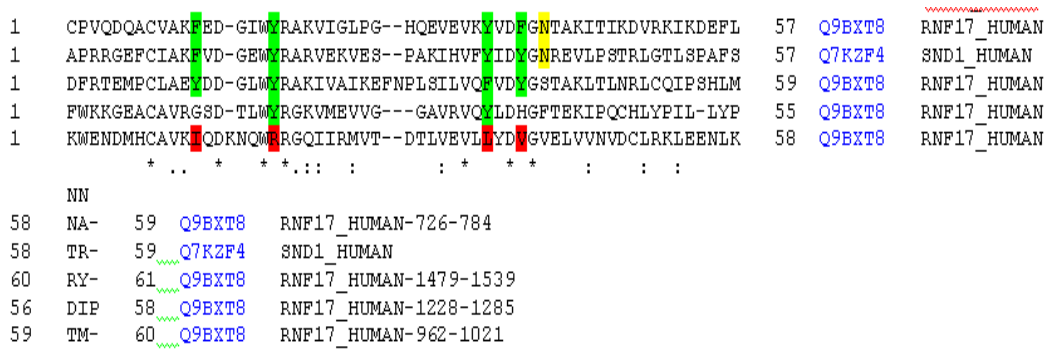

Taken together, Rnf17/Tdrd4 long and short proteins contain multiple Tudor domains, but each carries a consensus sequence for sDMA binding, however their function; specifically in the context of the other Rnf17 domains, has not yet been revealed by study. However, mouse knockout for Rnf17/Tdrd4 revealed crucial role or Rnf17 in spermatogenesis (Pan *et al*, 2005).

The structural analysis of Rnf17 raises several questions:

- Does interaction between RNF17 and MIWI family proteins have a role in localizing RNF17 to the nuage or a related structure? What are the implications of the nuage targeting elements on Mxd activity (Yin *et al*, 1999)?

- Are RNF17 and piRNAs found in the same complex that participates in transposon silencing?

- PRMT5/WDR77 interacts with MIWI, Is this interaction related to the RNF17/MIWI interaction and function in embryo growth?

- How are the different isoforms controlled spatially during embryo growth?

1.4.5 Expression of Rnf17 and members of Myc/Max/Mxd network in Microarray data

A number of Microarray datasets related to mouse early embryo development showed changes in the expression of key growth regulatory genes, specifically Rnf17, members of Myc/Max/Mxd network and genes' heterodimers with Max (Mga and Mnt). These data described the gene expression in the mouse preimplantation embryo.

Differential regulation of Rnf17 was observed in response to maternal diet (Papenbrock *et al,* unpublished data) and in a culture condition model (Giritharan *et al*, 2007). A set of Affymetrix probes are described to monitor Rnf17 expression in the mouse embryo, however: Affymetrix

probe1438820_at showed significant differences in maternal diet and culture condition studies. Rnf17 was increased 1.9 fold in mouse blastocyst in response to maternal LPD compared to maternal NPD (Table 1.1). In culture conditions, Rnf17 increased 1.81 and 1.86 fold in mouse blastocyst cultured *IVC* and *IVF* respectively, compared to those *in vivo*; however the differences were significant only in the *IVC* culture (*P*=0.01) (Table 1.2). The same Affymetrix probe, 1438820_at, showed that Rnf17 expression is increased during the preimplantation period (from oocyte to blastocyst) (Zeng *et al,* 2004; Fig 1.11).

In the same Microarray studies (Table 1.1 & 1.2) changes in expression levels of c-Myc were described using probe set 142492_a_at. Significant changes in mouse blastocyst for c-Myc (*P*=0.05) in response to maternal LPD showed 1.07 fold increase compared to maternal NPD. c-Myc showed decreased expression with *IVC* and *IVF* compared to the control (*in vivo*) by 0.4 and 0.74 fold respectively, but did not reach significance (*P*=0.23 and 0.66 respectively).

Members of Mxd family did not change expression in mouse blastocyst in response to maternal LPD (Table 1.1) as noticeably as in *IVC* or *IVF* culture conditions (Table 1.2). Expression of members of Mxd family differs through the preimplantation stage. Zeng *et al* (2004) showed in a longitudinal study using Microarray GEOD 1749 (www.ebi.ac.uk) that, after fertilisation, Mxd1 and Mxd4 are highly expressed at 1cell stage, followed by Mxd2 at 2cell and Mxd3 at 8 cell embryos (Fig 1.11).

The two poorly described Max family interactors, Mga and Mnt were differentially regulated. There was significant increase in Mga (1.34 fold) *IVC* compared with *in vivo* (*P*=0.05) and ~1.2 fold increase in mouse blastocysts in response to maternal LPD (*P*<0.05) using different probe sets. Mnt shows 1-2 fold increase *IVC* compared with *in vivo* but this did not reach statistical significance. However, Mnt was significantly increased (*P*<0.05) in

blastocyst in response to maternal LPD (1.2 fold) (Table 1.1& 1.2). Expression of Mga and Mnt also varied during different preimplantation stages, in the Microarray GEOD 1749.

The Dppa4 gene is expressed in ES cells in the same pattern as the pluripotency markers (such as *Oct3/4*, *Sox2* and *nanog*) and is down-regulated at the time of differentiation (Madan *et al* 2009; Masaki *et al*, 2007; Siegel *et al*, 2009). Dppa4 has the SAP domain (SAF (scaffold attachment factor), Acinus and PIAS (protein inhibitor of activated STAT)) that has an affinity for DNA and suggests a role of DPPa4 in modulating chromatin structure and in gene regulation (Masaki *et al*, 2010).

By Microarray analysis, Madan *et al* (2009) compared global gene expression in wild-type and Dppa4-defficient ES cells. This showed that 78 non-redundant genes were significantly altered. Two genes out of the 78 were up-regulated, whereas 76 were down-regulated. Genes required for ES cell pluripotency/self-renewal (*Oct3/4*, *Sox2, nanog,* Ronin or Myc*)* were not differentially regulated. 17 of the 67 down-regulated transcripts were more than 2-fold altered in *Dppa4*$^{-/-}$ ES cells. The 17 transcripts encode proteins which are suggested to function in germ cell development and fertility; such as Dazl, MVH/Ddx4, Rhox5 and Maelstrom.

Interestingly, the Rnf17 was one of the 17 transcript down-regulated genes in the Madan's study (Table 1.3). Although suppression of Dppa4 induces differentiation in ES cells and Rnf17 is expressed at terminal differentiation (Madan *et al*, 2009; Masaki *et al*, 2007; Siegel *et al*, 2009), the down regulation of Rnf17 in *Dppa4*$^{-/-}$ ES cells may reveal a role of Dppa4 in the regulation of the transcription of genes or influencing the stability of a specific transcript by modulating chromatin structure (Madan *et al*, 2009; Masaki *et al*, 2010).

Table 1.1: Affymetrix Microarray data and bioinformatics analysis (Papenbrock *et al*, unpublished data) show differential changes in expression of Rnf17 and Myc/Max/Mxd in mouse blastocyst in response to maternal LPD. Highlighted rows represent Affymetrix probes of significance differentially regulated ($P<0.05$).

gene	probe set	Accession	Description	LPD		NPD		P value	Fold change
				mean	St dev	mean	St dev		
Rnf17	1425708_at	AF285585	Mm.82895.1	50.35	6.09	45.66	6.75	0.35	1.10
Rnf17	1425709_at	AF285585	Mm.82895.1	111.57	7.75	114.74	3.48	0.53	0.97
Rnf17	1438820_at	AV225034	Mm.50751.1	216.92	30.48	116.43	11.24	**0.01**	1.86
Rnf17	1459275_at	BQ030930	Mm.217744.1	38.13	9.88	33.36	5.11	0.25	1.14
Mxd1	1455104_at	AV228517	Mm.40991.1	1.83	1.36	1.41	0.25	0.52	1.30
Mxd1	1422002_at	L38926	Mm.1329.1	1.16	0.20	2.44	2.19	0.29	0.48
Mxd1	1434830_at	AV228517	Mm.40991.1	62.79	6.45	49.27	8.21	0.15	1.27
Mxd2	1425732_a_at	D31824	Mm.2154.2	28.37	11.23	32.55	4.70	0.54	0.87
Mxd2	1425732_a_at	D31825	Mm.2154.1	161.98	19.36	159.26	22.10	0.77	1.02
Mxd3	1438847_at	BB836571	Mm.182471.4	243.02	47.03	265.51	24.02	0.46	0.92
Mxd3	1448878_at	NM_053213	Mm.206736.1	141.66	8.18	138.35	10.38	0.35	1.02
Mxd3	1422970_at	NM_016662	Mm.20350.1	24.63	8.37	25.88	3.77	0.83	0.95
Mxd4	1434378_a_at	BG868949	Mm.148395.2	12.47	4.23	10.78	6.27	0.58	1.16
Mxd4	1434379_at	BG868949	Mm.148395.2	1.00	0.00	2.07	2.14	0.39	0.48
Mxd4	1422574_at	BE291523	Mm.38795.1	35.97	6.84	37.75	10.51	0.72	0.95
Mxd4	1422575_at	BE291523	Mm.38795.1	78.53	9.10	78.99	6.88	0.94	0.99
Max	1423501_at	AA617392	Mm.3931.1	295.53	23.91	259.58	30.93	0.23	1.14
Myc	1424942_a_at	BC006728	Mm.2444.2	357.26	25.05	332.90	10.34	**0.05**	1.07
Mnt	1418192_at	NM_010813	Mm.3759.1	335.27	26.42	276.765	10.65	**0.03**	1.21
Mnt	1418193_at	NM_010813	Mm.3759.1	2.88	2.15	2.225	1.30	0.55	1.29
Mga	1431232_a_at	AK009477	Mm.87532.2	214.50	14.88	185.4	19.40	**0.03**	1.16
Mga	1433012_at	AK006636	Mm.195785.1	7.02	5.97	7.12	4.66	0.93	0.99
Mga	1434746_at	BG797579	Mm.56519.1	351.62	21.85	295.205	23.38	**0.01**	1.19
Mga	1442356_at	BB494975	Mm.216404.1	28.77	3.13	29.2675	4.97	0.90	0.98
Mga	1422646_at	BB315904	Mm.87532.1	44.96	6.40	39.215	3.12	0.18	1.15

Table 1.2: Affymetrix Microarray data and bioinformatic analysis by www.ebi.ac.uk and Giritharan *et al* (2007) show differential changes in expression of Rnf17 and members of Myc/Max/Mxd network in culture conditions.

Gene Symbol	Probe set	In vivo		IVC				IVF			
		mean	St dev	mean	St dev	P Value	Fold change	mean	St dev	P Value	Fold change
Rnf17‡	1438820_at	259.77	77.07	470.91	44.11	**0.01**	1.81	482.01	226.51	0.12	1.86
Rnf17‡*	1425709_at	78.01	15.41	70.93	35.97	0.70	0.91	67.12	25.27	0.30	0.86
Rnf17	1459275_at	37.12*	22.92	36.30*	25.30	0.94	0.98	81.00*†‡	62.44	0.32	2.18
Rnf17‡	1425708_at	122.17	57.04	149.86	26.14	0.31	1.23	172.57	68.63	0.23	1.41
Mxd2‡	1420376_a_at	5735.85	655.26	5368.79	362.70	0.23	0.94	5617.74	897.90	0.76	0.98
c-Myc	1424942_a_at	63.36*‡	65.11	24.95*	16.74	0.23	0.39	46.80*‡	27.10	0.66	0.74
Max‡	1423501_at	2534.70	359.70	2260.88	473.36	0.32	0.89	2426.20	545.76	0.80	0.96
Mga	1431232_a_at	52.32*†‡	13.00	43.33*†‡	16.38	0.46	0.83	35.16*‡	26.57	0.24	0.67
Mga	1422646_at	86.16‡	11.61	115.08‡	27.05	**0.05**	1.34	84.06*‡	24.12	0.81	0.98
Mnt	1431282_at	40.97*‡	27.78	70.22*‡	34.10	0.21	1.71	43.01*‡	44.08	0.95	1.05

Absent (*) Margin (†) Present (‡) represent the expression of the affymetrix probe examined in all replicates.

Table 1.3: Microarray analysis by Madan *et al* (2009) show down regulation of number of transcripts in Dppa4 knocked down ES cells. Those transcripts including Rnf17 are encoded proteins suggested functioning in germ cell development and fertility.

Gene Name	Probe set	p value	adj. p value
Rnf17	142508_at	6,82E-05	0,01923974
Rnf17	1438820_at	9,51E-05	0,02323373
Mael	1436837_at	6,02E-08	0,00026482
Dazl	1449502_at	2,42E-06	0,0020456
Dazl	1419542_at	3,19E-07	0,00054046
Rhox5	1423429_at	9,75E-06	0,00536097

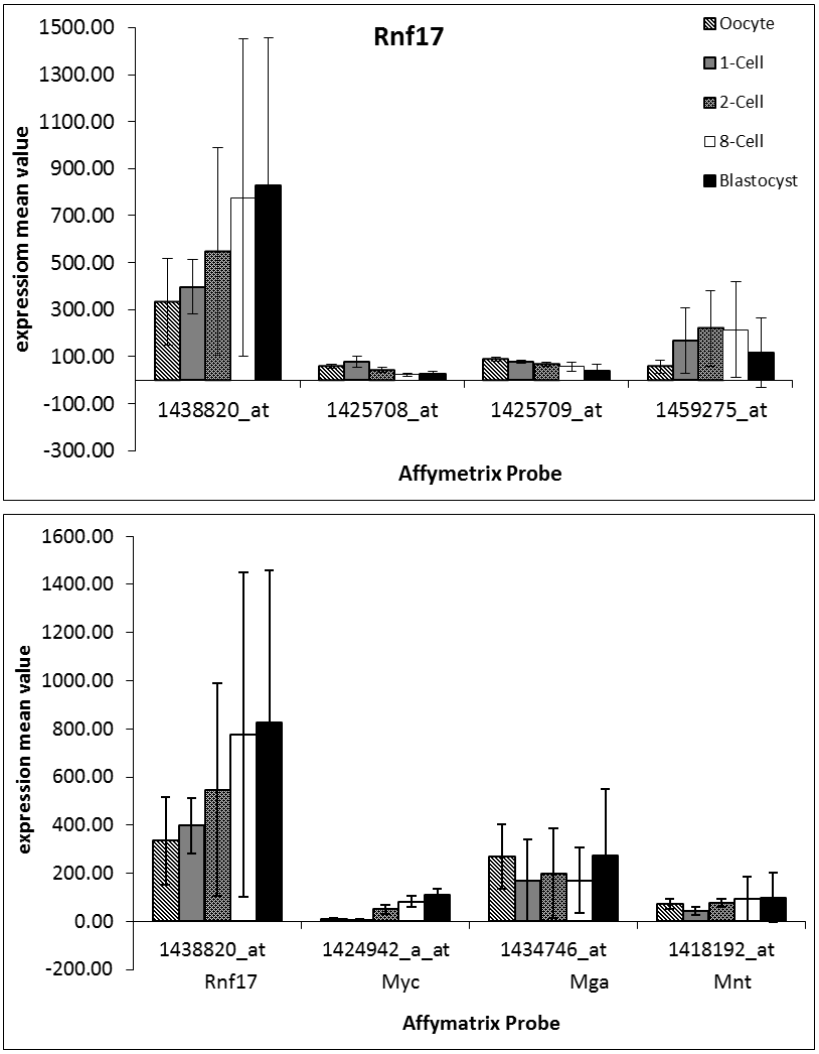

Fig 1.11: Microarray data show expression of genes involved in Myc/Max/Mxd throughout mouse preimplantation development. (A) Affymetrix probe 1438820_at for Rnf17 is highly expressed compared to different probes used for Rnf17. **(B)** The highly expressed Rnf17 Affymetrix probe shows high expression compared to differentially regulated genes that involved in Myc/Max/Mxd network (Myc, Mga and Mnt) (Papenbrock *et al,* unpublished data).

1.4.6 Rnf17 interaction with members of Myc/Max/Mxd network

Yin *et al,* (1999 and 2001) described the interaction between Rnf17 and the members of the Myc/Max/Mxd network using the yeast two-hybrid method (Y2H). The Y2H method is a system that provides a convenient assay for the study of protein-protein interactions and is used as a tool to identify proteins (genes) based on their ability to interact with other target proteins. As shown in Figure 1.12, initially a whole library of sequence is screened for interaction between the target-prey and candidate bait proteins (Stephens and Banting 2000).

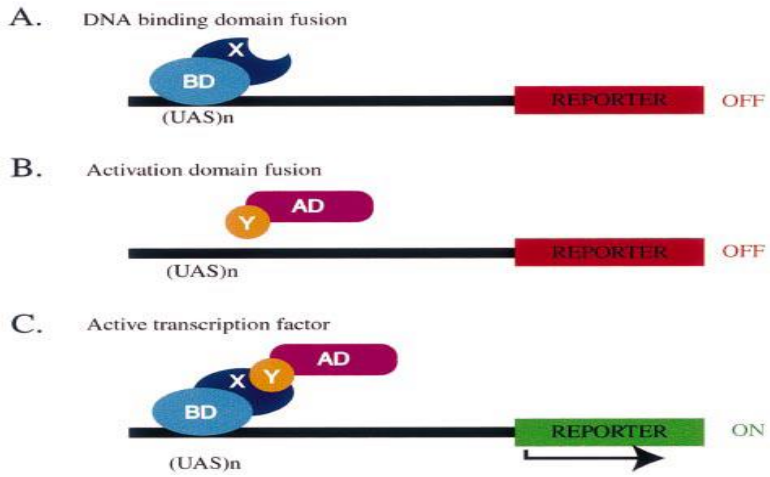

Fig 1.12: Yeast two-hybrid system. **(A)** in the absence of an activation domain (AD), the DNA binding domain (BD) that expressed as a fusion with protein X (called the bait) is capable of activating transcription. **(B)** The AD that expressed as a fusion with protein Y (the prey) is similarly incapable of activating transcription in the absence of a BD. **(C)** Interaction between the two fusion proteins by which interaction between X and Y results in reconstitution of an active transcription factor and subsequent transcription of a reporter gene such as *LacZ* providing a mean to assay the interaction between the two fusion proteins (Stephens and Banting, 2000).

In studies by Yin, a yeast expressing pGAD-RNF17 was transformed with pGBT9 vectors encoding c-MYC, MAX, MXD1, MXD2, MXD3 or MXD4. RNF17 showed a strong interaction with MXD1, MXD3 and MXD4, a weak interaction with MXD2, and a very weak interaction with c-MYC. No interaction was seen between RNF17 and MXD or unrelated bHLH proteins, ID1 (Inhibitor of DNA binding 1) or MyoD (Myoblast determination protein).

The interaction between MXD1 and RNF17 required only an intact ZIP domain of the MXD1 and at least two distinct regions for RNF17 (Yin *et al*, 1999). PGBT9-MXD1 incorporating a deleted first helix of the MXD1 HLH domain (delH1), interacted strongly with RNF17, but not with MAX. In contrast, pGBT9-MXD1 with a deleted ZIP domain (delZIP) failed to interact with RNF17. A deletion series of RNF17 from the amino (N-terminus) and carboxy (C-terminus) termini was expressed as fusion proteins in the pGAD10 vector and tested for interaction with the PGBT9-MXD1. Loss of 42 residues from the N-terminus enabled interaction with the MXD1 bait as strongly as the original construct because it retained a large segment of the RING finger. The removal of an additional 88 amino acids, the region between amino acids 44 ± 132, including all of the RING finger resulted in a considerable loss of interaction. A segment from RNF17 containing only the C-terminal 52 amino acids or further deletions from the C-terminal was entirely inactive and failed to interact with MXD1.

1.4.7 Expression of Rnf17 in tissues and cell models

Tissue expression of Rnf17 showed a signal of ca.4.5 kb transcript expressed in RNA from NIH 3T3 fibroblasts and Friend murine erythroleukemia cells. Also, RNA in mouse tissues of adult and embryos was tested for the endogenous distribution of Rnf17 and the adult testis showed the highest expression level compared to other tested tissues (Yin *et al,* 1999).

Bone marrow stem (BMS) cells that were transdifferentiated into male germ cells (BM-GC) expressed germ cell-specific genes including the Rnf17 (Nayernia *et al,* 2006). The Stra8-enhanced green fluorescence protein (eGFP) transgenic mouse line, expressing eGFP specifically in male germ cells, was used to derive male germ cells. Expression of Rnf17, germ-cell-specific genes (fragilis, stella, Mvh and Oct4), molecular markers of spermatogonia (Dazl, Piwil2, Stra8, Rbm, Hsp90a and c-kit) and the stem cells fraction (β1- and α6-integrins) were detected in BM-GC and testis tissues, but not in BMS cells.

Another study by Lavagnolli *et al*, 2009 suggested an *in vitro* model to study differentiation of GC in reprogrammed somatic cells. Lavagnolli's group revealed that near diploid ES-somatic cell hybrids (ES-SCH), resulting from the fusion of mouse ES and spleen cells (somatic cells), were able to differentiate *in vitro* into presumptive GC in the presence of retinoic acid through formation of embryoid bodies (EB). The resulting presumptive GC reacted positively with anti-EMA (epithelial membrane antigen), Vasa, Fragilis and Dazl antibodies and expressed GC-specific genes, including the Rnf17.

1.4.8 Subcellular localisation of Rnf17 and its relation to Myc and Mxd

Two studies of Yin *et al* (1999 & 2001) indicated that RNF17 and MXD family members can each influence the subcellular distribution of their binding partners when co-expressed in cultured cells. An RNF17-GFP fusion protein was shown to be expressed in the cytoplasm of NIH 3T3 fibroblasts, whereas a MXD3-GFP fusion protein showed nuclear localisation. Interaction between the two fusion proteins resulted in a shift of RNF17-GFP to the nucleus when MXD3-GFP was in excess, whereas increasing RNF17-GFP shifted the MXD3 to the cytoplasm (Yin *et al*, 1999). In the following study by Yin *et al* (2001), MXD2 was tested under conditions of stable expression with

non-GFP tagged proteins. MXD2 localised in the nucleus of control cells and in the cytoplasm of the pooled Rnf17 cells, whereas c-MYC and MAX were confined to the nucleus in both cells.

A series of terminal truncations of RNF17 encoded GFP fusion protein was expressed in NIH 3T3 cells to define the minimum requirement for the cytoplasmic RNF17-granule formation (Pan *et al*, 2005). A 45-a.a region of RNF17 (residues 243-287) allowed the formation of punctated GFP-RNF17 granules, whereas in those without this 45-a.a region the GFP-RNF17 was distributed diffusely. Immunoprecipitation and GST pull-down showed that RNF17L and RNF17S associate *in vivo* and that RNF17 (1-626) binds (homodimerises) to GST-RNF17 (1-287) but not control GST.

Pan *et al,* (2005) confirmed the previous observations that RNF17 is a cytoplasmic protein in male germ cells and identified two proteins, as predicted. Cytoplasmic and nuclear fractions of testicular extracts demonstrated that both RNF17 proteins were present in the cytoplasm; however, they were also detected in the nucleus but in much lower abundance.

In the Pan study (2005), it was the first time that Rnf17 was identified in a perinuclear dot-like structure which they termed the “Rnf17 granule”. Indirect immunofluorescence on testis sections using anti-serum 1774 (rabbit polyclonal antibodies raised against the N-terminal 100 residues of RNF17) confirmed the cytoplasmic localisation of the RNF17 in all germ cells; spermatogonia, spermatocytes and spermatids. In addition, double immunostaining of adult testis sections with anti-RNF17 and anti-SP10 antibodies to stain the acrosomes (SP-10 is an intra-acrosomal protein) then counterstained with DAPI the RNF17 granules appeared as large prominent dots in pachytene (VIII) and diplotene (XI) spermatocytes at late stages, as well as late stages of spermatids.

Pan *et al* (2005) distinguished the RNF17 granules as distinct organelles from CB and lysosomes in male germ cells. Double immunostaining of testis sections with anti-RNF17, anti-TDRD1, -TDRD6 (Tudor domain-containing proteins and components of CB) and anti-LAMP2 (lysosome component) revealed that RNF17 granules were distinct from the CB and lysosomes. Immuno-EM showed that RNF17 granules are spherical electron dense organelles, not surrounded by membranes, with diameter of 0.5 µm and smaller than CB (1- 2 µm).

1.4.9 Rnf17 is required for spermatogenesis

Rnf17-deficient (*Rnf17*$^{-/-}$) mice displayed normal development but were infertile (Pan *et al*, 2005). Pan *et al,* 2005 showed that testis and seminiferous tubules of 8-week-old *Rnf17*$^{-/-}$ mice were smaller than those of the wild-type and the epididymis contained apoptotic round spermatids, but no sperm. Also, adult *Rnf17*$^{-/-}$ testis, Leydig cells and Sertoli cells were normal in number, size and morphology. Germ cells developed into round spermatids, but failed to differentiate into elongating spermatids. Testes from *Rnf17*$^{-/-}$ mice at day 28 contained round spermatids but lacked elongating spermatids. *Rnf17*$^{-/-}$ mice displayed a reduction in the expression of genes that initiate transcription post-meiotically, but not those which transcribe in meiosis such as *Miwi, Pabpc3* (poly A-binding protein) and *Ldh3* (lactate dehydrogenase 3, C chain). No changes in expression of genes that regulate spermiogenesis were observed.

1.4.10 Rnf17 creates Mxd-null phenotype and may regulate some of c-Myc target genes

Yin *et al* (2001) showed that the over-expression of Rnf17 inhibited the function of the MXD protein creating a "*de facto* Mxd-null" or Mxd-attenuated phenotype. Analysis of the pooled Rnf17 cells with the neo-control cells (pooled G-418-resistant clones with empty pMSG-MT neo vector) revealed

that the pooled Rnf17 cells were more prone to apoptosis and showed equivalent sensitivity to apoptotic stimuli as c-Myc transfected cells.

Yin *et al* (2001) identified that the inactivation of Mxd by Rnf17 and ensuing de-repression of c-Myc would enable Rnf17 to regulate some of the c-Myc target genes. To confirm this notion, they examined expression of a c-Myc target gene, ornithine decarboxylase (ODC), which is positively regulated by c-Myc and antagonised by Mxd, and reported elevated levels of the ODC in response to Rnf17 expression.

1.5 Aim and hypothesis

Both maternal protein under nutrition *in vivo* and embryo culture *in vitro* can induce changes in cellular proliferation and gene expression in embryos and adulthood non-communicable diseases. One major objective of this project is to study the effect of maternal protein diets on cell proliferation and differentiation in mouse embryo in particular concerning Rnf17, which has been shown to interact with the Myc/Max/Mxd signalling network.

We hypothesise that Rnf17 induces cell proliferation in the preimplantation embryo by creating a Mxd-null phenotype, it can bind all MXD proteins and exclude them from participating in nuclear transcriptional repression, and thus, presumably, enhance cell proliferation. Our hypothesis will be examined under abnormal or stress preimplantation embryo environments, such as maternal diets. Previously, maternal LPD was shown to differentially regulate the expression of Rnf17 and members of Myc/Max/Mxd.

This project will aim:

1. To evaluate Rnf17 over-expression in F9 cells, as a model for preimplantation embryos, to address whether it could modulate Myc activity.

2. Using a microinjection technique, designed siRNA oligonucleotides targeting Rnf17 will be injected into mouse embryos to knockdown Rnf17 expression. From the resulting embryos the potential role of Rnf17 will be examined.

3. Using RT-qPCR the expression of Rnf17 (and members of the Myc/Max/Mxd family) will be examined in response to maternal low, high and control normal protein diets (LPD, HPD, NPD) in mouse blastocysts at E3.5 and in mouse foetal testes at E17.5.

4. Using immunostaining and confocal microscopy the expression pattern of RNF17 in preimplantation embryos and its subcellular localisation will be examined under normal conditions and in response to maternal LPD, HPD and control NPD mouse blastocysts at E3.5 and mouse foetal testes at E17.5.

These data should provide an overview of the expression of Rnf17 and the Myc/Max/Mxd network in preimplantation embryos, in changes that may occur in response to maternal dietary protein manipulation.

Chapter 2

2. Materials and Methods

2.1 Preparation of Rnf17 constructs

2.1.1 Amplification of target sequences TA cloning of 3´A overhangs PCR products

Rnf17 fragment was deposited as Mmip-2/Rnf17 according to Yin *et al*, 1999 with GenBank Accession no. AF190166.Rnf17 template was supplied from Jieyan Pan (University of Pennsylvania, USA).Primers for Mmip-2/Rnf17 fragment (951bp) were designed with restriction sites of *Hin*dIII at forward primer and *Xba*l at reverse primer:

F: 5′ AAGCTTCCACCATGGCGGCAGAGGCTTCG 3′

R: 5′ TCTGAGTCATTTTCTAGAGGGGTAACA 3′

Phusion® Hot Start "High-Fidelity DNA Polymerase" was used for PCR. 50µl of PCR reactions incubated for enzyme activation at 98˚C for 30 seconds. 35 cycles were run for denaturation at 98˚C for 10 seconds, primers annealing at 55˚C for 30 seconds and extension at 72˚C for 30 seconds.

PCR products (inserts) were scaled for 50µl on 1% agarose gel. Rnf17 band was cut, weight and solubilised in a ratio of 100mg insert: 300µl QXI Solubilisation Buffer (QIAE II Gel Extraction Kit). The solution centrifuged onto NucleoSpin Plasmid spin column and then washed with Wash Solution (NucleoSpin® Plasmid). The DNA eluted in 50µl autoclaved H_2O.The blunt-ended PCR products were modified by *Taq* polymerase to add an adenosine (A) residue to the 3′ ends of the product. Reactions were incubated at 74˚C for 30minutes.

pGEM®-T Easy vector system was used as a ready linearised vector plasmid with a single 3′-terminal Thymidine (T) overhang at each end. The treated insert with 3′ A-overhang was ligated to the pGEM®–T Easy vector to produce a PCR-TA clone. The ligation reactions incubated at 4˚C overnight. Negative control reaction was set with no insert (-insert).

2.1.2 Transformation of Rnf17-TA clone into *E. coli* SURE™ Competent cells

Rnf17 insert and TA (Rnf17-TA) clone was transformed into *E.coli* SURE™ strain. Frozen competent cells were thawed on ice before re-incubated with β-Mercaptoethanol on ice for 10 minutes with gentle swirl every 2 minutes. 1µl ligation reactions was added and kept into ice for 30 minutes. The cells were chemically transformed by heat shocked at 42˚C water bath for exactly 45 seconds. The cells placed on ice immediately for 2 minutes, then incubated at 37˚C with 450µl LB/Amp medium with shaking (250rpm) for 60 minutes. The cells/ligation mixture centrifuged at 13,000rpm for 5-10 minutes, the supernatant removed, and the cells re-suspend with fresh 100 µl LB/Amp medium. The suspension is plated onto LB/Amp agar and incubated at 37˚C overnight. Competent cells transformed without DNA was set as negative control (-ve control) and competent cells control DNA supplied with Competent cell kit was used as positive control (+ve control).Next day, the plates were checked for colonies growth. A number of colonies were picked and incubated with LB/Amp medium overnight on the shaking incubator at 37˚C.

2.1.3 Extraction of plasmid DNA of the PCR-TA clone

The DNA plasmid extracted using NucleoPlasmid kit following manufacturer instruction. Briefly, the overnight culture of plasmid transformed centrifuged and the bacterial pellet re-suspended with Re-suspension buffer and lysed by SDS/alkaline Lysis Buffer. The lysate cells incubated at room temperature for 10 minutes then neutralised with Neutralising Buffer then centrifuged. The column was washed with washing solution. The column was dried and DNA was eluted with 50µl autoclaved water. The extracted DNA of both PCR-TA clones was double cut with restriction enzymes.

2.1.4 Preparation of vectors and ligation to the prepared inserts

The pGL3-Control was modified for cloning Rnf17 by replacing the *luc*+ with a synthetic polylinker (HindIII_EcoRI_AgeI_SpeT_EcoRV_PstI_XbaI) via a *HindIII* and *Xba*I sites and double stranded link oligonucleotides was inserted incorporating a series of recognition sites for restriction endonucleases that single cutters within the vector:

F: 5' agcttgaattcaccggtactagtgatatcctgcagt 3'

R: 5' acttaagtggccatgatcactataggacgtcagatc 3'

In a total of 20µl the linker pGL3-Control were double cut with *Xba*I and *HindIII* followed with gel purification. 1µl Rnf17 insert ligated to 2.5µl pGL3-linker with 1µl 10X Ligation Buffer and 0.5µl T4 Ligase. The ligation reactions incubated at 4˚C overnight. Negative control reactions were set with no insert (-insert).

2.1.5 Transformation of constructs and plasmid extraction

Ligations of Rnf17-pGL3-linker was transformed into *E.coli* JM109 High Efficiency Competent Cells of $1x10^8$cfu/µg DNA, grown into LB/Amp medium and plated onto LB/Amp agar with X-gal and IPTG solutions. In the next day the plates were checked for colonies growth. A number of colonies were picked and incubated with LB/Amp media overnight on the shaking incubator at 37˚C. The plasmid extracted using NucleoPlasmid kit following manufacturer instruction.

2.1.6 Large scale of DNA extracting

The DNA plasmid extracted using GenElute™ Plasmid Miniprep Kit following manufacturer instruction. Briefly, the overnight culture of 100µl plasmid into 50ml LB growth media is centrifuged and the bacterial pellet re-suspended with Re-suspension buffer and the DNA lysate by SDS/alkaline Lysis Buffer. The lysated cells incubated at room temperature for 5 minutes then neutralised with Neutralising Solution followed by Binding solution to facilitate

DNA binding to the silica membrane of the column. The lysate is cleared with a Midiprep Filter Syringe. The GenElute Midiprep Binding Column is prepared and washed twice with Column Preparation Solution. Column was dried and DNA is eluted with 1ml Elute solution. The DNA was precipitated 1:10 volume of 3M Sodium Acetate pH 5.2, and 1:1 isopropanol. The mixture spin and the pellet washed with 1:1 of 70% Ethanol. The pellet was dried and the DNA diluted to with dH_2O and stored at -20˚C.

2.2 Myc responsive construct

Map sequence of commercial construct pMyc-TA-Luc (Clontech, UK) was deposited to design oligonucleotides for c-Myc reporter construct. Myc oligonucleotides were designed of double-stranded DNA including the TAT box as well as overhang nucleotides complementary to restriction sites; *Nhe*I and *Hin*dIII on both 5' (underlined):

5'<u>CTAGC</u>CACGTGCACGTGCACGTGCACGTGCACGTGCACGTGAGATC TGGGTATATAATGGA3'
3'GGTGCACGTGCACGTGCACGTGCACGTGCACGTGCACTCTAGACCC ATATATTACCT<u>TCGA</u>5'

Reverse and the forwards inserts were annealed at 65˚C and diluted to10ng/µl. In a total of 100µl, pGL3-Basic vector were double cut with *Nhe*I and *Hin*dIII and 10X Core Buffer followed with gel purification. In a total of 10µl ligation reaction, 1µl of diluted Myc inserts were ligated to 2µl of the linearised pGL3-Basic.

2.3 c-Myc expression plasmid

pEF-c-Myc expression vector is supplemented from Yongfeng Shang (Harvard Medical school, USA). The vector was designed to encode c-Myc cDNA downstream Elongation factor promoter (pEF) at *Eco*RI restriction site into pUC vector. The plasmid was cultured for large scale. pEF-c-Myc plasmid was diluted indH_2O and 1µl is transformed into *E.coli* JM109 High

Efficiency Competent Cells of 1X10^{7}cfu/µg DNA. Selected colonies were prep-culture and then single cut with *Eco*RI. Large DNA scale was set in 50µl LB/Amp growing media, followed by single cut with *Eco*RI.

2.4 Production of Rnf17-RNAi construct and Rnf17 sensor

2.4.1 Rnf17-RNAi oligonucleotides design and annealing

The RNA interference (RNAi) construct was designed following Ambion guideline for siRNA design (www.ambion.com). TheRnf17 target site for siRNA was selected to be down the length of Rnf17 sequence and immediately downstream AA dinucleotides. The selected target sequence (**AACTCAGATCTGCTCCTTCTC**) is located in position 722 in mmip-2 gene sequence (GenBank: AF190166, Yin *et al).*

The forward oligonucleotides consist of 19 nucleotide (nt) sense siRNA sequence followed by 9nt loop which linked the reverse complementary antisense siRNA sequence. Additional 5 T's were added to the 3'end of the oligonucleotide. To be cloned into the p*Silencer*™ 1.0 U6 vector, overhang nucleotides with complementary restriction sites; *Eco*RI at 5' and *Apa*I at 3' ends were added on the complementary reverse oligonucleotide.

Rnf17 wild type (Rnf17-RNAi-wt) was designed to induce RNAi of the target Rnf17-sensor. Rnf17 mutant (Rnf17-RNAi-mut) nucleotides was set as a non-targeting negative control RNAi with the same nucleotide composition as the Rnf17-RNAi-wt but lacks significant sequence homology to the genome (as shown below).

Rnf17-RNAi-wt

F:5 ′CTCAGATCTGCTCCTTCTCTTCAAGAGAGAAGGAGCAGATCTGAGTTTTTT 3′

R:5 ′AATTAAAAAACTCAGATCTGCTCCTTCTCTCTCTTGAAGAGAAGGAGCAGATCTGAGGGCC 3′

Rnf17-RNAi-mut

F:5′CTCAGATCACGAGGTTCTCTTCAAGAGAGAAGAACCTCGTGATCTG AGTTTTTT 3′

R:5′ATTAAAAAACTCAGATCACGAGGTTCTCTCTCTTGAAGAGAACCTC GTGATCTGAGGGCC 3′

The forward and the reverse oligonucleotides were dilute to 1µg/µl in dH_2O according to the manufacturer's instructions (Invitrogen™). 50µl annealing mixture was assembled for 2.5µl forward, 2.5µl reverse, and 5µl 5X *GoTaq* Buffer and 40µl dH_2O. The mixture was incubated in 80°C and cool down to RT. For ligation the annealed sense and antisense were diluted to 4ng/µl and 20ng/µl.

2.4.2 Preparation of *pSilencer*™ 1.0 U6 vector and insertion of the Rnf17-RNAi insert

The p*Silencer*™ 1.0 U6 vector was cultured in large scale. To insert the Rnf17oligonucleotides, 50µl p*Silencer*™ 1.0 U6 vector was linearised by sequential double cut with *Eco*RI then column purified, followed by *Apa*I cut and gel purification.

In a total of 10µl ligation reaction, 1µl of diluted Rnf17-RNAi inserts were ligated to 2µl of the linearised p*Silencer*™1.0-U6. 1µl of ligation reactions were transformation into *E.coli* JM109 High Efficiency Competent Cells of $1X10^8$cfu/µg DNA. The pellets of the cultured clones were re-suspended, lysat then neutralised and centrifuged to collect the DNA in the supernatant. DNA was precipitated and then re-suspended in 50µl dH_2O.

Extracted plasmid for Rnf17-RNAi expression vector was single cut with *Bam*HI and *Hin*dIII to confirm the insertion of siRNA template insert. The selected plasmids DNA were amplified by large DNA scale extraction.

2.4.3 Rnf17-Sensor oligonucleotides design and annealing

Rnf17-sensor was designed to insert a target sense sequence of Rnf17 between *PstI* and *Eco*RI of a pGL3-Control vector-containing polylinker. The

insertion of Rnf17-sensor sequence is targeting the antisense sequence of the Rnf17-RNAi. The designed forward and the reverse primers were annealed same as Rnf17-RNAi and diluted to 20ng/µl and 4ng/µl for ligation.

F: 5' AATTCTCAGATCTGCTCCTTCTCTGCA 3'

R: 5' GAGAAGGAGCAGATCTGAG 3'

2.4.4 Preparation of pGL3-Controlvector and insertion of the target sequence

The pGL3-Control was modified for cloning by insertion of a synthetic polylinker (HindIII_EcoRI_AgeI_SpeT_EcoRV_PstI_XbaI) downstream the *luc*+ by partial digestion with *Xba*II. In a total of 20µl reaction, pGL3-Control was double cut with *Eco*RI and *Pst*I followed by gel purification to remove the synthetic polylinker.

For ligation, 2µl of linearised plasmid were ligated to 1µl of the 20ng/µl diluted oligonucleotides and transformed. DNA extracted and single cut with *Eco*RI or *Eco*RV were set to ensure the replacement of the sensor template. The selected plasmids DNA were amplified by large DNA scale extraction.

2.4.5 Transfection of Rnf17-RNAi and Rnf17-sensors into F9 cells

F9 embryonal carcinoma cells or Raw 264.1 murine macrophage cells were transfected at densities of $0.5x10^6$ or $1x10^6$/ml/well. Transfection reaction and cell culture was set. A constant amount of Rnf17-Sensor was co-transfected together with doses of Rnf17-RNAi-wt or Rnf17-RNAi-mut expression plasmids, followed by Luciferase and Protein Assays.

2.5 Cell culture for transfection assay and Luciferase assay

F9 embryonal carcinoma cells and Raw 264.1 murine macrophage cells were used for transfection. Cells were thaw and washed with complete medium of DMEM. Cells were grown in a sterile and humidified atmosphere of 5% CO_2

for 48 hours. Nunclon flask of 80 cm^2 surface area was pre-coated with 0.2% gelatine for 30 minutes and washed twice with complete medium. Cells were cultured with 25ml complete medium and 250µl penicillin-streptomycin (1:100) in the gelatine pre-coated flask. Cells were examined daily for 48 hours using phase contrast of inverted microscope. When confluent, culture media is removed and cells were released from the surface of the flask with 6ml trypsin. De-attached cells were washed from trypsin and sub-culture for transfection and Luciferase assays.

For transfection assay and Luciferase assay, cells were counted using haemocytometer and plated out onto 8-well plate at a density of $1x10^5$ per2ml per well and incubated at 5%$CO_2$and 37˚C overnight. Before cells are plated, the 8-well dish was pre-coated with 0.2% gelatine for 30 minutes and washed two times with complete medium. Next day, the healthy adherent cells were washed two times with DMEM without FCS (DMEM-FCS) to remove the serum protein and incubated with 0.5ml DMEM-FCS up to time of transfection. Cells transfected in duplicate or replicate with 90µl transfection reactions. In a total of 200µl, tube A contained 1µg DNA and 100µl DMEM-FCS was incubated for 20minutes with tube B contained 3µl polyethylenimin (PEI) transfection reagent and 100µl DMEM-FCS. After the addition of the transfection DNA, cells incubated at 5%CO_2 and 37˚C for 4 hours, after which 1ml DMEM with 20% FCS was added to the cells and re-incubated overnight.

Next day, cells transfected for Luciferase assay were rinsed two times with 2ml of 1x PBS, lysed with 50µl of 5-fold dilution of 5x concentrate extraction buffer in dH_2O. Lysed cells were harvested, centrifuged and supernatant assayed for Luciferase activity. 5µl of supernatant added to 50µl of Luciferase assay reagent and luminescence of the sample is determined by luminometer (Turner Design TD-20/20 luminometer, DL-Ready™). Bio-Rad Assay (Bradford) was performed, following manufacturer's instructions, to normalise the reporter gene activities to amount of protein in the extract with bovine serum albumin (BSA) as a standard protein. 96 plates including the

BSA in one raw and samples in following raw were read in spectrophotometer to determine OD of all plate wells at 570nm.

Luciferase activity (LU) of transfected reporter constructs was measured and protein assay were normalised to a standard curve of BSA by dividing the LU by cell extracts (5µl) and then divided by protein concentration. The expressed value is LU/µg represent Luciferase activity per µg extracted protein. The transfection performed in triplicates and results represented by mean value and standard curve for LU/µg. Student's *t-test* was performed to evaluate the significance of LU/µg represented in *P* value of ≤ 0.05.

2.6 Endpoint PCR

2.6.1 Primer design

Primers for Rnf17 were designed for Rnf17S and Rnf17L as deposited in GenBank by Pan *et al*(2005)*,Rnf17S*; AY854010 and *Rnf17L*; AY854011.

2.6.2 RNA extraction and DNA synthesis

F9 cells were cultured at density of 5-10 $X10^6$. Once confluent, cells were trypsinised and washed with PBS. Total cellular RNA isolation was performed by TRI reagent (Sigma-Aldrich, UK) according to the manufacturer's procedure. Briefly, washed cells were lysed with 1 ml TRI Reagent. Proteins, DNA and RNA were separated into 3 phases by the addition of 0.2ml chloroform. The upper phase contained the RNA were precipitated in a clean tube with 0.5ml isopropanol and washed with 80% ethanol. The dried pellet of the RNA was suspending in 100µl DEPC-treated water.

RNA was treated with DNase I to purify from genomic contamination. The reaction was set for treated sample (+DNase I) and untreated sample (-DNase I) as a negative control and incubated at 37ºC for 30 minutes. All samples were purified with TRI reagent followed by chloroform separation, precipitated with isopropanol and washed with 80% ethanol.

For cDNA synthesis, 2µl of extracted RNA was eluted into 10µl DEPC-H_2O at 70ºC for 5 minutes. The Sensicript Reverse Transcript (RT) reaction was performed for the sample (+RT) and negative control without RT (-RT) and incubated for 60minutes at 42ºC.

2.6.3 PCR reaction and PCR cycle

PCR was performed using *Taq* polymerase enzyme. The reaction was set for the treated sample of +RT and +DNase I and for negative control of –RT and –DNase I for both the short and the long Rnf17. The PCR cycling conditions was run for 35 cycles started with enzyme activation at 95°C for 2 minutes followed by denaturation at 95°C for 30 seconds. Primers annealing was set at 54°C for 60 seconds and finally extension at 72°C for 30seconds.

2.7 Quantitative real-time PCR (RT-qPCR)

2.7.1 Animal procedures and sample collection

All animal procedures were performed in accordance with the Animals (Scientific Procedures) Act, 1986 under UK Home Office Project Licence. Virgin MF1 female mice (7–8.5 weeks) were mated naturally overnight with MF1 studs under standard rodent chow and tap water. On the morning after mating (E0.5), plug-positive females were randomly assigned to receive a control normal protein diet (18% casein; NPD), a low protein diet (9% casein; LPD) or a high protein diet (30% casein; HPD) until day of sample collection.

For blastocyst collection, pregnant female mice were killed at E3.5 by cervical dislocation and blastocysts were collected by flushing dissected uteri with pre-warmed H6 medium supplemented with 4mg/ml BSA (Sigma, St. Louis, MO; embryo culture tested; H6 BSA) from all diet groups. Each blastocyst was washed through three 5µl drops of nuclease-free PBS-PVA (1mg/ml) which had been exposed to UV at $3X10^3$ µJ/cm. Blastocysts transferred either individually or pooled into 5 into nuclease-free thin walled tubes (ThermoFisher scientific, UK) in a minimal volume (<1µl). Blastocysts were immediately snap-frozen on dry ice prior to storage at -70°C.

For foetal testes collection, pregnant female mice were killed at E17.5 by cervical dislocation and foetuses were collected into ice-cold phosphate-buffered saline (PBS). Testes were extracted from individual foetus and washed in cold-ice PBS before incubated with RNA Latter buffer at 4°C for 24 hours. Next day testes were stored at -80°C until time for RNA extraction.

2.7.2 RNA extraction from E3.5 blastocysts

Poly A^+ RNA was extracted from single blastocysts or 5 pooled blastocysts using the Dynabeads® mRNA DIRECT™ Kit (Invitrogen, UK) according to manufacturer procedure. Briefly, frozen stored embryos were lysed with lysis-binding buffer followed by incubation with prewashed Dynabeads® Oligo $(dT)_{25}$ at room temperature for 10 minutes on a roller. The beads with bound poly A^+ RNA were separated employing a Dynal MPC-P-12 magnet rack (Dynal Biotech). The supernatant was kept for DNA extraction for embryo sexing. After two washes with wash buffer A and three washes with wash buffer B, the poly A^+ RNA was eluted from Oligo $(dT)_{25}$ beads in 10ml nuclease-free water (Anachem, Luton, UK) by incubating at 65°C for 2 minutes.

2.7.3 RNA extraction from E17.5 foetal testes

Total RNA was extracted using the RNeasy Micro kit (QIAGEN) following the manufacturer's instructions, including the optional DNase I step. RNA quality and quantity was determined by spectroscopy at 230, 260 and 280nm using a Nanodrop (Nanodrop Technologies).

2.7.4 cDNA synthesis from extracted RNA

cDNA was synthesised using 8µl RNA eluted from E3.5 blastocysts or 2µg RNA eluted from E17.5 foetal testes. The RT Kit (QIAGEN, UK) was used for cDNA preparation, using a random priming strategy, according to the manufacturer's instructions. cDNA was synthesised in a total volume of 20 µl

reaction (+RT). A negative control (-RT) was prepared in the same reaction without addition of Sensicript enzyme.

2.7.5 Primers design and standard curve

Intron-spanning primers were designed using the Roche Applied Science Universal ProbeLibrary Assay Design Centre and synthesised by Invitrogen Custom Oligo service (Table 2.1).The designed primers were selected for the criteria of large intron-spanning assays and small amplicon size. Primers were designed to amplify the short or the long Rnf17 transcripts, c-Myc, Mxd3 and Line-1 in mouse E3.5 blastocysts or E17.5 foetal testes.

The short Rnf17 (Rnf17S) primers were designed to amplified 2230nt between exons 25 and 26 (alternative spliced), whereas primers for long Rnf17 (Rnf17L) were designed to amplify 1808nt between exons 29 and 30 (Fig 2.1).

All primers, except Mxd3, were tested for standard curve using F9 cells as a template. Mxd3 were tested for standard curve using foetal testes as a template. RNA were extracted and synthesised cDNA were amplified using the designed primers. The products were run into 2% agaross gel for gel extraction using QIAquick Gel Extraction Kit (QIAGEN, UK) following manufacturer's procedure. Quantitative analysis of the DNA were performed using Nanodrop and a series dilutions of 1:100 were set using a minimum 3 log range to calculate the Efficiency(E) according to the formula $E = 10^{1/\text{slope}}$.

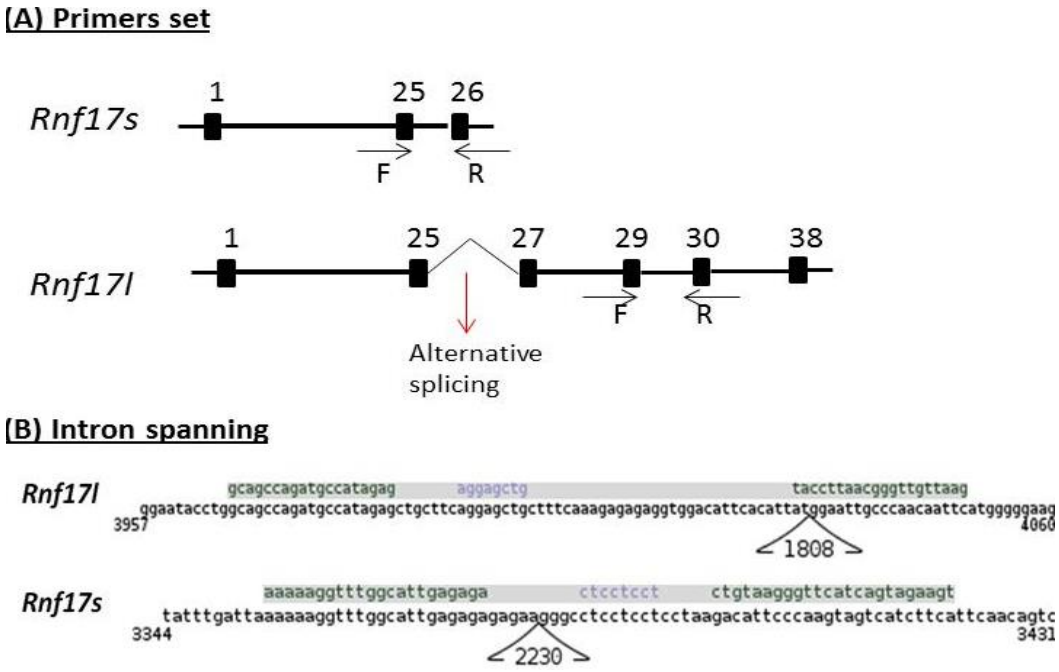

Fig 2.1: Schematic diagrams show primer design for Rnf17 for RT-qPCR. (A) Primers for Rnf17S set on exons 25 and 26 and primers for Rnf17L set on exon 29 as shown by arrows. **F**: Forward, **R**: Reverse. **(B)** Size of Intron spanning as designed by Roche Applied Science Universal Probelibrary Assay Design Centre for Rnf17S and Rnf17L.

Table 2.1: Primers designed for RT-qPCR.

Gene name	Gene symbol	Accession number	Forward primer 5'-3'	Reverse primer 5'-3'	Amplicon length (nt)	Effeciency
RING finger protein short transcript	Rnf17S	AY854010.1	aaaaaggtttggcattgagaga	tgaagatgactacttgggaatgtc	68	1.88
RING finger protein long transcript	Rnf17L	AY854011.1	gcagccagatgccatagag	gaattgttgggcaattccat	84	1.92
myelocytomatosis oncogene	c-Myc	NM_010849.4	tttgtctatttggggacagtgtt	catcgtcgtggctgtctg	128	1.83
MAX dimerisation protein 3	Mxd3	NM-01662.4	agctgaagcggtgcttagag	tcctgctcctccagcttct	124	1.87
Long interspersed element-1	LINE-1	U15647.1	cccaaaacatccaggaaatc	tgttcatgggcatctctttct	162	1.93
Peptidyl prolyl isomerise B*	Ppib	NM_011149	ttcttcataaccacagtcaagacc	accttccgtaccacatccat	92	1.95
Tubulin α-1*	Tuba1	NM_011653	ctggaacccacggtcatc	gtggccacgagcatagttatt	114	1.95
Mitogen-activated protein kinase 1*	Mapk1	NM_011949.3	ccttcagagcactccagaaagt	acaacaccaaaaaggcatcc	74	1.88
Calnexin*	Canx	NM_007597.2	ccacataggaggtctgacagc	caccaccagcattccttaaaa	66	1.85
Succinate dehydrogenase complex, subunit A*	Sdha	NM_023281	tgttcagttccaccccaca	tctccacgacacccttctgt	66	1.99
18S ribosomal RNA*	18S	NR_003278	ctcaacacgggaaacctcac	cgctccaccaactaagaacg	110	2.02
TATA box binding protein*	TbP	NM_013684	gggagaatcatggaccagaa	gatgggaattccaggagtca	90	1.94

* Reference genes used for data normalisation in RT-qPCR experiments

2.7.6 Quantitative real-time PCR (PCR-qPCR) cycle

RT-qPCR reactions were prepared using Precision Mastermix (Primerdesign, UK) containing SYBR Green, with a final concentration of 300 nM each of forward and reverse primers and 2µl cDNA in 20µl reaction volume. Each sample was analysed in duplicate, using clear 96-well plates (Axygen). Absence of contaminating genomic DNA was confirmed by analysis of negative control samples with no added RT (-RT). Duplicate reactions containing water in place of cDNA (no template controls; NTC) were also included for each assay as negative control. Thermal cycling and fluorescence detection were performed using a DNA Engine thermal cycler and Chromo4 Real-Time Detector (BioRad, UK) with Opticon Monitor v3.1 software. Thermal cycling conditions were 95°C 10minutes enzyme activation, then 50 cycles of 95°C for 15seconds followed by 60°C for 1minutes, with a final extension step of 10minutes at 72°C. For blastocysts, 50 cycles were performed due to the low starting material. Melting curves were produced for each sample by measuring fluorescence levels at 0.2°C steps from 60°C to 95°C and hold 15seconds, for confirmation of specific target amplification.

2.7.7 Determination of the most stable reference gens in E17.5 foetal testes

A panel of reference genes including *Tuba1, MapK1, Canx, Tbp, Sdha,* and *18S* were selected to test their level of expression stability in foetal testes under condition of maternal diets for RT-qPCR data normalisation. Primers were designed for 8 commonly used housekeeping genes (*Tuba1, MapK1, Canx, Tbp, Sdha,* and *18S)* using Rocha Approch as shown in Table 2.1.The expression levels of these genes was determined in 8 samples per diet group; LPD, NPD and HPD of foetal testes. Expression stability for each gene (termed *M* value) was calculated as the mean standard deviation of the log transformed expression ratios across samples for this gene relative to other reference genes remaining in the gene panel. Mean Ct values were

calculated on the basis of two replicates for each sample and converted to relative quantities using the comparative Ct methods (delta Ct). Reference gene stability was determined using the Visual Basic Application (VBA) applet for geNorm (Vandesompele *et al,* 2002; http://medgen.ugent.be/genorm/) and Normfinder (Andersen *et al*, 2004; www.mdl.dk).

2.7.8 Data analysis and statistical testing

Raw fluorescence readings were exported from Opticon Monitor software in term of threshold cycle (Ct). Ct values were converted to relative expression values using the delta Ct (dCt) method normalised to the most stable reference genes. The geometric mean of two selected reference gene for mouse E3.5 blastocysts (our lab data; Lucas *et al*, 2011) or mouse E17.5 foetal testes was calculated for each sample and used to normalise the expression of each tested gene for comparison between treatment groups and sexes. Results between dietary treatment groups were expressed as the mean expression value in relative to reference genes.

2.8 Embryo sexing

DNA collected through RNA extraction from E3.5 blastocysts were used for embryo sexing. DNA was precipitated 1:10 volume of 3M Sodium Acetate pH 5.2 and washed with 70% alcohol. The pellet was dried and the DNA diluted with nuclease-free water.

Sry and *Zfy* genes were amplified for the Y-specific target sequences and the *DXNds3*, a polymorphic microsatellite locus located on X chromosome was used as a control sequence. Primers and methods were applied as described in Kunieda *et al*, 1992. Briefly, for each primer two sets were designed for an inner and outer set (Table 2.2)

Two-step PCR using two pairs of primers was used by addition of *Taq* polymerase (QIAGEN). First PCR amplified the prepared DNA with outer primers and the PCR product was amplified in second PCR with the inner primers. PCR products were screened onto 2% agarose gel.

Table 2.2: Details of primers used for embryo sexing by two-step PCR (Kunieda *et al*, 1992)

Gene	Primers position (5'-3')	Position/PCR round	Size of target fragment
Sry2*	Forward: 5'TCTTAAACTCTGAAGAAGAGAC3'	Out/ First	404 bp
Sry4*	Reverse: 5'GTCTTGCCTGTATGTGATGG3'		
Sry1*	Forward: 5'GTGAGAGGCACAAGTTGGC3'	In/Second	147 bp
Sry3*	Reverse: 5'CTCTGTGTAGGATCTTCAATC3'		
Fzy3**	Forward: 5'AAGATAAGCTTACATAATCACATGGA3'	Out/ First	617 bp
Fzy4**	Reverse: 5'CCTATGAAATCCTTTGCTGCACATGT3'		
Fzy11**	Forward: 5'GTAGGAAGAATCTTTCTCATGCTGG3'	In/Second	217 bp
Fzy12**	Reverse: 5'TTTTTGAGTGCTGATGGGTGACGG3'		
Nds3***	Forward: 5'GAGTGCCTCATCTATACTTACAG3'	Out/ First	244 bp
Nds4***	Reverse: 5'TCTAGTTCATTGTTGATTAGTTGC3'		
Nds1***	Forward: 5'ATGCTTGGCCAGTGTACATAG3'	In/Second	111 bp
Nds2***	Reverse: 5'TCCGGAAAGCAGCCATTGGAGA3'		

*Sry: Sex Determination Region Y

**Fzy: Zing Finger Y-Chromosomal protein

***Nds: A polymorphic X chromosome microsatellite locus (DXNds-3)

2.9 Immunostaining

2.9.1 Production of RNF17 antibody (anti-RNF17)

Anti-RNF17 produced and affinity purified by Dr C.H. Barton. Briefly, A cDNA fragment from Rnf17 (long isoform supplied from Dr Jieyan Pan, University of Pennsylvania, USA) encoding 1-316 residues and was used to produce polyclonal anti-RNF17. Primers for Rnf17 fragment were designed containing restriction sites *BamH*I forward primer and *EcoR*I reverse primer as indicated by underlining:

F: 5′ATCGGATCCATGGCGGCAGAGGCTTCG3′:
R: 5′GTAGAATTCTCATTTTCTAGAGGGGTAACA 3′.

The amplified PCR product was gel purified and *Taq* tailed to be cloned into T-Easy. The construct was transformed into JM109X10^8cuf/µg competent cells and DNA was extracted from positive colonies. Single cut with *Eco*RI was performed to linearise the construct and cloned into pGEX-2TK expression vector (Amersham Pharmacia, UK). The protein was produced as a fusion protein with glutathione-S transferase (GST) (Sigma-Aldrich, UK) and the construct was transformed into *E.coli* cells. RNF17-GST fusion protein was purified by affinity chromatography using glutathione-Sepharose beads and used for production of rabbit polyclonal antibody (Pineda, Germany).

2.9.2 Preimplantation embryo immunolabelling

Embryos were collected from mothers fed chow or LPD, HPD or control NPD from E0.5 to E3.5. Embryos at different preimplantation stages were flushed in H6BSA either from the oviduct or from the uterus to collect zygote, 2-cell, 4-cell, 8-cell, morula and blastocysts. Flushed embryos were treated with acid tyrodes (AT) for zona pellucid removal and washed in H6BSA before fixed in 4% (V/W) paraformaldehyde (PFA) in PBS for 10 minutes. Embryos were permeablised in 1% Tween diluted in PBS (V/V; 1%PBS-T) at room temperature (RT), blocked in 5% goat serum in PBS (V/V) and labelled with

anti-RNF17 polyclonal antibody at a dilution of 1:1000 in 1%BSA in PBS (W/V) for 1 hour at RT or overnight at 4˚C. After three washes with 1%PBS-T, goat anti rabbit-Alexa 488 was added at a dilution of 1:300 in 1% BSA for 1 hour at RT followed with three washes with 1%PBS-T. Nuclei were stained with DAPI 1:500 in 1%PBS-T and embryos were rinsed twice in 1%PBS-T, mounted on polylysine slides in Vectashield (Vector Labs) and observed under Leica SP5 Confocal microscope.

Negative control was performed by incubating blastocysts with non-immunised or immunised rabbit sera (from the same rabbit used to antibody production) at the same dilution used for anti-RNF17 and same procedure. Negative controls for secondary antibody (goat anti rabbit Alexa fluor 488) was applied by incubating treated blastocysts with Alexa fluor 488 without the primary antibody.

2.9.3 Foetal testis immunofluorescence staining and histological analysis

Testes were collected from foetus derived from pregnant MF1 mice female fed LPD, HPD and control NPD from day of plug E0.5 up to day of dissection (E17.5). Foetus testes from each mother were embedded in O.C.T. embedding medium and snap freeze individually into dried ice before stored at -80ºC.Cryostat testes were sectioned for 6µm using microtom (Leica CM 1850 UV). Cryostat sections were attached to polylysine slides and left to dry at room temperature for at least 2 hours before stored in -80ºC or stained. Slides were washed with PBS and tissues fixed with 4%PFA, permeablised with 1%PBS-T. Sections were washed three times with 1%PBS-T before stained with anti-RNF17 diluted for 1:1000 in 1%BSA in PBS for 1hour or overnight. The slides washed with PBS and stained with secondary antibody Alexa fluor 488 diluted 1:300 in 1%BSA in PBS for 1hour at room temperature. Sections were washed with PBS and the nuclei were stained with DAPI followed by another wash before mounted in Vectashield (Vector Labs) and observed under Leica SP5 Confocal microscope.

For morphological analysis Haematoxylin and Eosin (H&E) staining was performed. Briefly, frozen sections were rinsed with distilled water and nuclei stained with haematoxylin, differentiate with 0.3% acid alcohol and cytoplasm stained with eosin (H&E; Sigma-Aldrich). All sections were then mounted with Pertex.

2.9.4 Immunostaining for cultured cells

F9 cells or Cos-1 cells were immunolabelled with anti-RNF17 after treated with experimental conditions. Cells were cultured on coverslip within 9- or 6-well dishes and treated with experimental condition. For immunostaining, cells were washed with ice cold PBS for three times before fixed with 4% PFA and washed again with PBS. Cells were permeablised with 1%BS-T, blocked with 1%FCS diluted in PBS and washed with 1%PBS-T. Anti-RNF17 were diluted for 1:1000 in 1%PBS-T and applied for 1 hour or overnight. Stained cells were washed with 1%BS-T before addition of 1: 300 Alexa fluor 488 in 1%PBS-T and rewashed again. Nuclei were stained with DAPI 1:500 diluted in 1% PBS-T, cells washed with 1%PBS-T and coverslip were mounted on polylysine slides with Vectasheid.

2.9.5 Fluorescence confocal microscopy and quantification of fluorescence intensity

Immunolabelled samples were examined by a X63 glycerol-immersion objective on a converted Leica SP5 confocal microscopy (Leica, German) with excitation source of a 488 nm wavelength argon laser. Detected fluorescence signals for Rnf17 density by SP5 confocal microscopy was quantified for stained embryos E3.5 blastocysts and E17.5 foetal testes using Volocity® v6.0.1 software (PerkinElmer's). The software detects the voxel number which makes up an object 3D dataset equivalent of a pixel. The software counts the voxel number and calculates the voxel volume as voxel intensity per area (μm^3) through z-axis.

Anti-RNF17 stain was measured by using Volocity® v6.0.1 software for intensity level in nucleus or cytoplasm. RNF17 foci number were counted within each nuclei per embryo (E3.5 or 17.5) at different stages for E3.5 and different diet groups for both E3.5 and E17.5. The intensity levels of counted RNF17 foci were measured at the same time. Mean average of foci number and foci intensity level for ach nuclei were calculated per embryos and used to compare between stages and between different diet groups.

2.10 Western blotting

F9 cells or Cos-1 cells were culture under experimental conditions and proteins were extracted using 5x fold diluted reporter lysis buffer (Promega). Lysate fractions for supernatant and pellet were collected and used for western blotting. Protein level from both fractions was measured by BCA Assay (Thermo Scientific) with addition of 0.1%SDS solution.

Cell extracts were boiled with 5X SDS loaded buffer and about 10µg/µl of protein was separated by SDS-PAGE (8% acrylamide) and transferred to nitrocellulose (PVDF) membrane (Schleicher & Schuell BA 85). After blocking with 10% (W/V) skimmed-milk powder in 0.1% PBS-T for 1 hour, the blots were incubated overnight at 4˚C with anti-RNF17 diluted to 1:1000 in 5% blocking solution. After three washes in 0.1% PBS-T, the membrane was incubated for 1 hour at RT with goat anti mouse secondary antibody diluted to 1:2000 in 5% blocking solution. Stained membrane was washed for three times and antibody detection was visualised by Odyssey (LICOR).

2.11 Microinjection of Rnf17_siRNA

Female FVB/N mice were superovulated by interperitoneal injection of pregnant mares serum (PMS, 5 i.u; Folligon, intervet) and human chorionic gonadotropin (hCG, 5 i.u; Chorulon, Intervet) at an interval of 48 hours. Embryos were collected at zygote stage from oviduct or swollen ampullae of pregnant female mice and cumulus cells were removed by hyaluronidase.

Embryos were cultured in KSOM at 37°C in an atmosphere of 5%CO2 before microinjection or up to 2-cell stage.

Short interference (siRNA) sequences were microinjected to knockdown Rnf17 in mouse embryos. Four oligonucleotide sequences for Rnf17 (Rnf17_siRNA) and a negative control siRNA sequence (AllStar_siRNA) were designed and sense and antisense sequences were annealed by manufacturer (QIAGEN, UK) (Table 2.3). According to manufacturer protocol, siRNA oligonucleotides were diluted in RNase-free water to obtain 10µM solution and stored at -20˚C until time of microinjection. Each Rnf17_siRNA was microinjected individually into the cytoplasm of zygote stage 2-cell stage. Microinjection needles were back filled with approximately 20µM siRNA dilution and delivered into each embryo. The injected embryos were in vitro cultured in groups in KSOM medium and overlaid with mineral oil at 37˚C in an atmosphere of 5% CO2 for three days for immunostaining or freezing for RT-qPCR. Embryo development was assessed by phase contrast microscopy (X 200).

Table 2.3: Details of designed siRNA sequences by Qiagen for Rnf17 knockdown.

siRNA ID	Oligonucleotid 5'-3'	target sequence
Rnf17 _siRNA_1	5'CAGCTAATTAATGATTTAGAA 3'	356-376
Rnf17_siRNA_2	5'GACCCAGCTAATTAATGATTTA3'	353-372
Rnf17_siRNA_3	5'CACCTCAAGAATATACCACAA 3'	183-203
Rnf17_siRNA_4	5'CAAGAATATACCACAAGTAAA 3'	188-208

2.12 Statistical analysis

All data were analysed by using SPSS for Windows (IBM SPSS, version 21). The distribution of collected data for each experiment were checked using histograms using SPSS. Statistical significance was assumed with a value of $P \leq 0.05$.

Data collected in Chapter 3 and Chapter 4 to compare between the level of RNF17 in the cytoplasm and the nucleus (in F9 cells and mouse embryo) were not normally distributed. Data were analysed using a Mann- Whitney U-test and data were expressed as mean with standard deviation representing error bar.

For the effect of maternal diets on gene expression, data were normalised using a random effects regression model that allows for variability within dam across-offspring and across-dam (Kwong *et al*, 2004). Data were analysed with one-way ANOVA for significant variances among the dietary groups, and post-hoc tests was applied using the Tukey HSD test indicating the mean score for diet groups and are shown in representative figures. To compare the main effects of diet and sex with unequal (n) variance (Chapter 5), a two-way ANOVA was used to detect significant differences between treated groups. The data were expressed as mean with their standard errors (mean ± SE) of 10 to 11 examined samples (n= 10 to 11). Data collected from each examined sample as mean of two biological replicates.

Data collected from expression plasmids represent the Luciferase activity of expression plasmid used in the experiment. In Chapter 3, data were analysed with one-way ANOVA for significant variances among the dose-dependent groups, and post-hoc tests was applied using the Tukey HSD test. In Chapter 6, data were analysed using Student's *t*-test. All data were expressed as mean with their standard deviation representing error bars for three replicates**.** The experiments were repeated for five times.

Chapter 3

3. A Cell Culture Model of RNF17 Expression and Function

3.1 Introduction

Rnf17 is a germ cell-specific gene which is expressed in early mouse embryo development (Giritharan *et al*, 2007) and in mouse adult testis and is required for male germ cell differentiation (Pan *et al*, 2005). Rnf17 was identified as Mmip2 by Yin *et al* (1999 and 2001), following its isolation in a Y2H screen as an MXD protein interactor. Pan *et al* (2005) described Rnf17 encodes a protein containing both RING finger and Tudor domains and is a component of a novel nuage that displays a perinuclear location in male germ cells.

RNF17 interaction with members of the Myc/Max/Mxd network has been described using the Y2H. Yin *et al* (1999) showed that RNF17 interacts with members of the MXD family. Interaction of Rnf17 with all four members of MXD family modulates the activity of c-MYC, as RNF17 recruits MXD proteins from the nucleus, where they antagonise Myc, to the cytoplasm (Yin *et al*, 2001). This activates the transcription of Myc-responsive genes by increasing the levels of Myc-Max dimers and facilitating Myc activities, including cell proliferation, and reducing the activity of Mxd i.e. terminal differentiation. In the Yin *et al* (1999) study, GFP expression plasmids encoded RNF17 or MXD3 were co-transfected in NIH3T3 fibroblasts in different molar ratios and the localisation and expression of the different GFPs were examined by epifluorescence microscopy. At equal molar ratios of transfection, MXD3 was detected in the nucleus, whereas RNF17 was localised in cytoplasmic foci. Over-expression of MXD3 allowed RNF17 to enter the nucleus whereas over-expression of RNF17 co-localised MXD3 into RNF17 foci in the cytoplasm.

RING domain-containing proteins exert E3 ubiquitin ligase activity (van Wijk *et al*, 2009) which results in degradation of their target protein by the

proteasome. Van Wijk (2009) demonstrated that the human RNF17 RING domain was able to interact with the E2 protein, UBE2U. Cano *et al* (2010) found a group of 15 E3 ligases coupled to RNA-binding domains (KH domains) provided them with a unique mRNA stability regulating activity. RNF17, described in this study is an E3 ligase based on the presence of a RING domain and carries multiple Tudor domains for interaction with dimethylated arginines on target proteins such as PIWI suggesting that it has additional as yet not described activities.

MXD1 is a target protein for Rnf17 in the ubiquitinylation process. Phosphorylation of MXD1 at Ser 145, by RSK and S6K or PI3/Akt pathways, is necessary for proteasome degradation of MXD1 through the ubiquitinylation pathway (Zhu *et al,* 2008; Chou *et al*, 2009).

3.1.1 Aim of experiment

The aim of this experiment is to investigate whether Rnf17 modulates c-Myc function by developing a functional assay for Rnf17 over-expression and co-transfection with a c-Myc responsive construct in F9 cells.

The second aim is to find out whether RNF17 functionally interacts with MXD through the ubiquitin-proteasome pathway. Flag-tagged expression plasmids for RNF17 and MXD1 will be co-transfected into Cos1 cells treated with proteasome inhibitor MG132.

3.2 Methods

3.2.1. Production of Rnf17-SV40construct and transfection efficiency into F9 cells

CMV promoter has been found to be poorly expressed in embryonic stem cells and F9 cells (Dr Neil Smyth, unpublished observation). Therefore, in this experiment the SV40 early promoter and enhancer system was used based upon the efficient expression of the pGL3-Control plasmid Luciferase in a transient transfection experiment. This plasmid was modified firstly to remove the Luc cassette via a *Hin*dIII and *Xba*I digest and then double stranded link oligonucleotides were inserted, incorporating a series of recognition sites for restriction endonucleases that only cut once within the vector.

The Rnf17-SV40 construct was designed to position the SV40 promoter upstream of the Rnf17 gene fragment. Initially, the pGL3-Control vector was tested in F9 cells to examine the transfection efficiency of the SV40 promoter in F9 cells (Dr C.H. Barton). 1 µg DNA of empty vector SV40-pGL3-control was transfected into F9 cells without (0.0 µg) or with (3.0 µg) transfecting agent, PEI. Transfection activity was measured by the induction of Luciferase activity in the SV40-pGL3-control. As shown in Fig 3.1 (data from Dr C.H. Barton), SV40-pGL3 is significantly delivered into cells using 3.0 µg of PEI ($P \leq 0.05$).

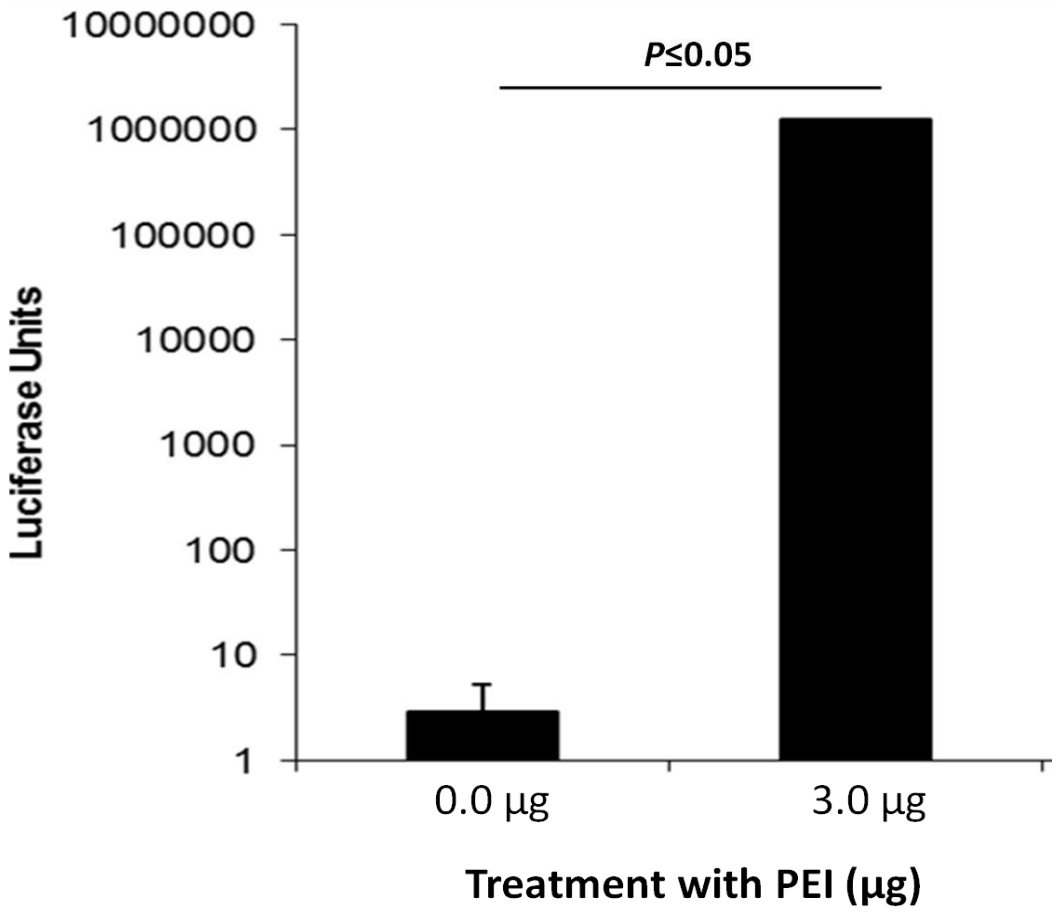

Fi**g 3.1: Induction of Luciferase activity in SV40-pGL3-control in F9 cells using transfecting agent (PEI).** Luciferase activity of 1.0 µg of SV40-pGL3-control is significantly increased using 3.0 µg PEI for transfection compared to control (0.0 µg PEI). Bar graphs are the mean of Luciferase activity of three replicates and error bars represent standard deviation.

To generate the Rnf17-SV40 construct, Rnf17 fragment was amplified by endpoint PCR (Fig 3.2A) followed by gel purification. The blunt-ended PCR product was modified by *Taq* polymerase to add the 3′ A-overhang and then ligated to pGEM®-T Easy vector (Fig 3.2B). The TA product was transformed into *E.coli* SURE™ strain and white/blue screening assay was recorded as shown in Table 3.1. The DNA plasmid was extracted from 4 white colonies (Fig 3.3A). A single cut of the extracted plasmid DNA with *Eco*RI dropped out 951bp of the Rnf17 insert (Fig 3.3B). This indicates that the selected colonies carried the target product. A double cut with *Xba*I and *Hin*dIII was performed on a selected colony of the Rnf17-pGEM®-T Easy and this dropped out the Rnf17 insert, 951bp (Fig 3.4A).

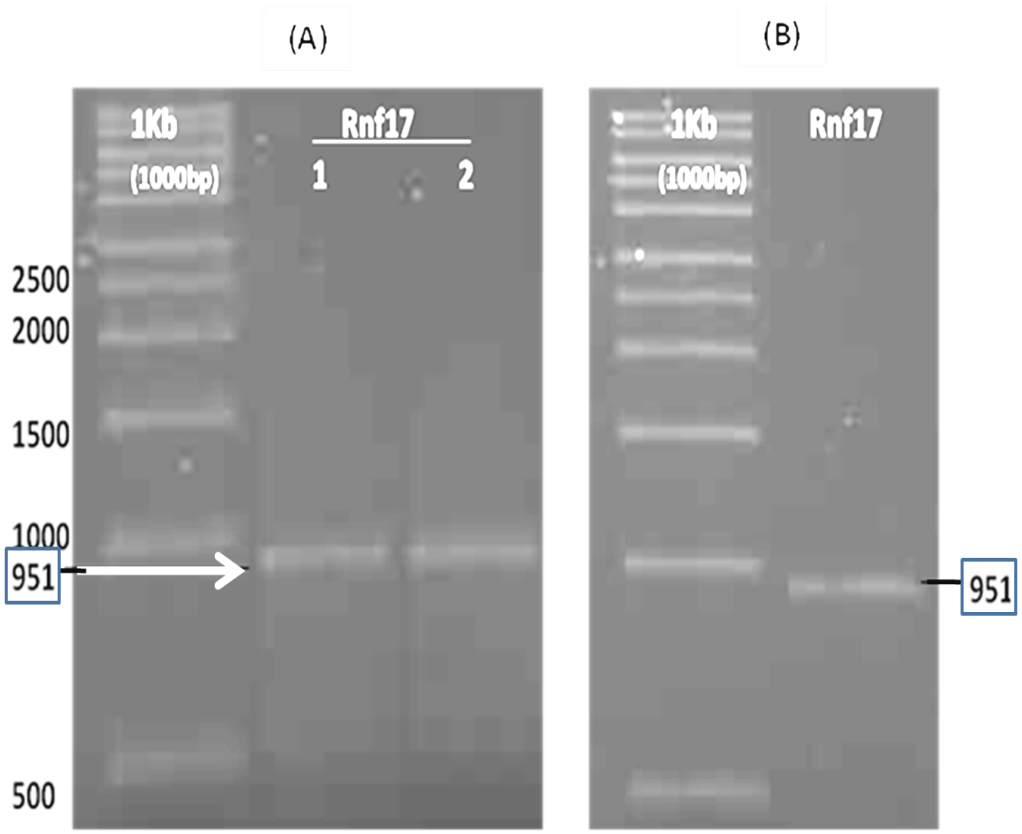

Fig 3.2: Amplification of 951bp Rnf17 fragments by PCR endpoint using Phusion® Hot Start High-Fidelity DNA Polymerase. **(A)** The PCR product run in duplicate; 1 & 2 with both being the correct size of Rnf17 fragment (951bp). **(B)** PCR products were gel purified followed by *Taq* treatment and revealed the same size for amplified Rnf17 fragment (951bp).

- **Lane 1 and 2 (A)**: duplicate for PCR product
- **1Kb**, Invitrogen DNA ladder.

Table 3.1: Number of colonies resulted from transformed Rnf17-pGEM®-T Easy vector into E.*coli* SURE™ strain competent cells with LB/Amp.
White colonies represent positive colonies with insert (+insert). Blue colonies represent those without insert (-insert).

Ligation	White colony (+insert)	Blue colony (-insert)
Rnf17-pGEM-T Easy vector	94	1
Ligation with no insert (negative control	0	10
Only competent cells (positive control)	0	235

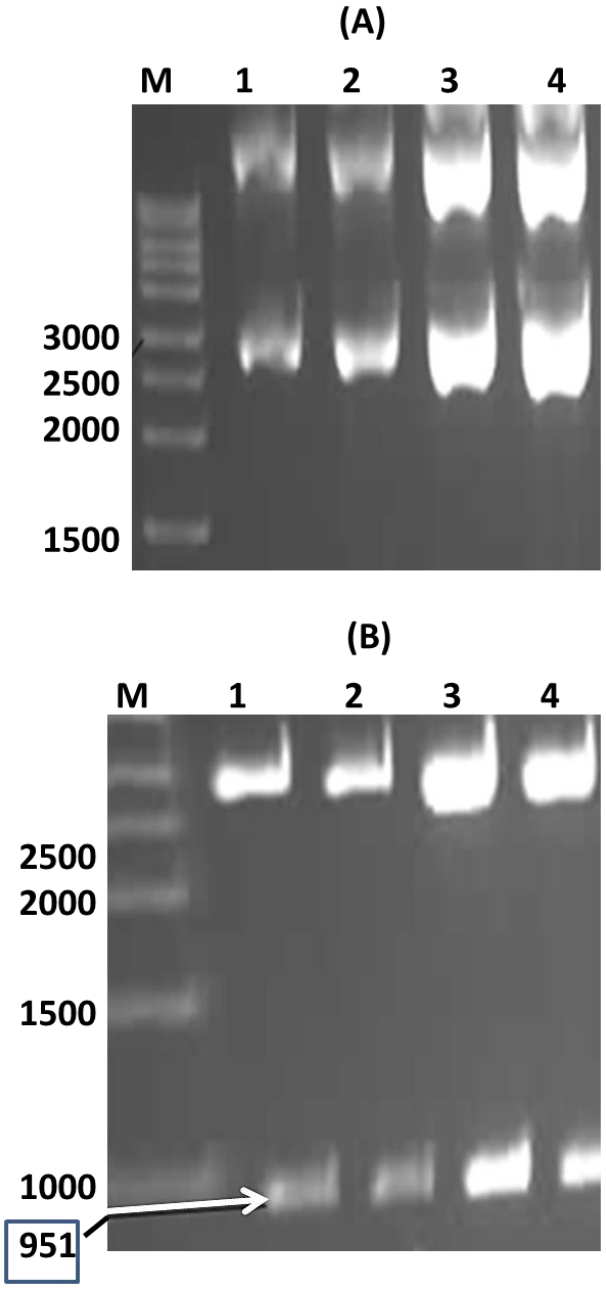

Fig 3.3 *(continued)*

Fig 3.3: DNA plasmid extracted from PCR-pGEM®-T Easy clone of Rnf17. PCR product for Rnf17 was ligated into pGEM®-T Easy and transformed into *E.coli* SURE™ strain. White/ blue screening was applied by Xgal/IPTG and white colonies were selected for DNA plasmid extraction (Lane 1 to 4). **(A)** Uncut DNA plasmid **(B)** Restricted DNA plasmid with *Eco*RI reduced the size of Rnf17 insert to 951bp from the pGEM®-T Easy.

- **Lanes 1 to 4 (A):** Uncut DNA plasmids
- **Lanes 1 to 4 (B):** Cut DNA plasmids with *Eco*RI
- **M**: Invitrogen DNA ladder

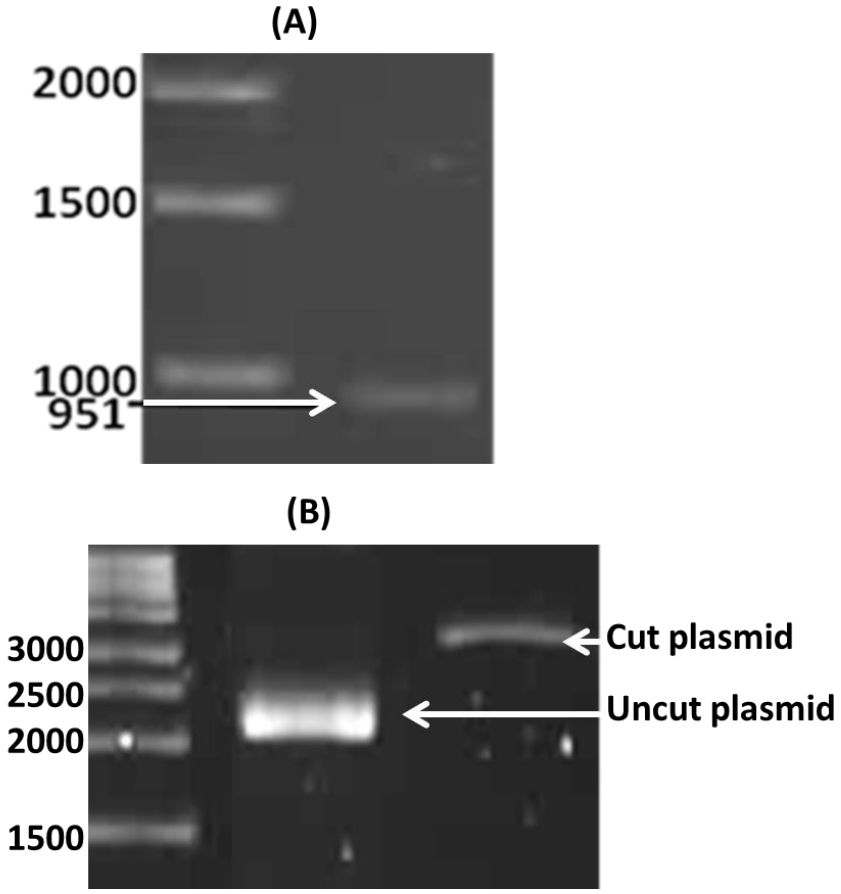

Fig 3.4: Preparation of Rnf17 insert and pGL3-linker for ligation. (A) PCR-pGEM®-T Easy of Rnf17 clone was double cut with *Xba*I and *Hin*dIII and gel purified. **(B)** The uncut and double cut pGL3-linker. The pGL3-link plasmid was linearised by double cut with *Xba*I and *Hind*III and gel purified.

pGL3-Control had been modified for cloning by replacing the *luc*+ with a synthetic polylinker (pGL3-linker), and the pGL3-linker was double cut with *Xba*I and *Hin*dIII restriction endonucleases and gel purification conducted to remove the polylinker (Fig 3.4B). The Rnf17 insert was ligated to the pGL3-link plasmid and transformed into the *E.coli* JM109 high efficiency competent cells of $1X10^8$ cfu/µg DNA. The pGL3 link plasmid does not contain Lac-Z gene, thus no x-gal and PTG were used for blue/white screening. X-gal and PTG was only used for blue/white screening with positive control (Table 3.2). 6 colonies for Rnf17-pGL3-link were selected for DNA extraction. The extracted DNA plasmids were cut with *Bam*HI and *Hin*dIII, this included extra nucleotides between the *Xba*I (1943 bp) and the *Bam*HI (2442 bp) of about 508 bp. As shown in Fig 3.5, the size of the dropped out band from the pGL3-link was 1459 bp, the 508 bp between the *Xba*I and the *Bam*HI plus the 951 bp of the Rnf17 insert.

Table 3.2: Number of colonies resulted from transformed Rnf17-pGL3-Link plasmid into E.*coli* JM109 high efficiency competent cells with LB/Amp. X-gal and PTG was only used for blue/white screening with positive control.

Ligation	**White colony (+insert)**	**Blue colony (-insert)**
Rnf17-pGL3-link	131	0
Ligation with no insert (negative control)	5	0
Only competent cells (positive control)	0	>300

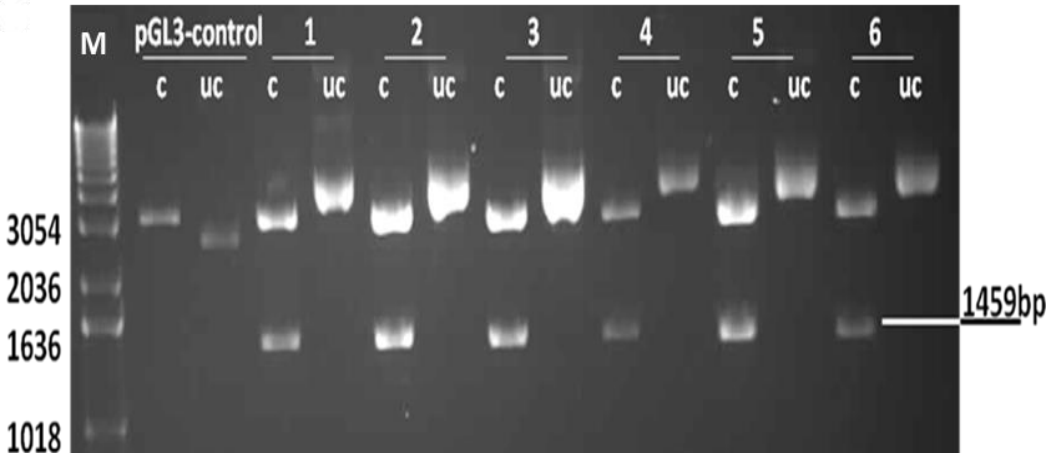

Fig 3.5: Preparation of Rnf17-SV40. (A) 6 (1-6) colonies of the transformed Rnf17-pGL3 ligation were selected for plasmid extraction. Double cut with *Bam*HI and *Hin*dIII was performed and the gel shows the cut (c) and the uncut (uc) plasmids compared to cut and uncut pGL3-control vector. The cut plasmids dropped out 1459 bp including the 951 bp of Rnf17 and the 508 bp -extra nucleotides- between *Xba*I and *Bam*HI**. M:** Invitrogen DNA ladder

3.2.2 c-Myc Luciferase Reporter gene constructs

To measure the activation pathway of the Rnf17 and c-Myc in F9 cells, a sensor construct for c-Myc was developed to encode five tandem copies of the E-box consensus sequence, located upstream of a minimal promoter that contained a TATA box, with a Luciferase reporter gene downstream. The construct was designed to measure the Luciferase activity in response to the binding of the transcription factor (c-Myc) to the E-box, which activates the transcription of Luciferase. The construct oligonucleotides for c-Myc were annealed and ligated into the pGL3-Basic vector between *Nhe*I and *Hin*dIII restriction sites (Fig 3.6).

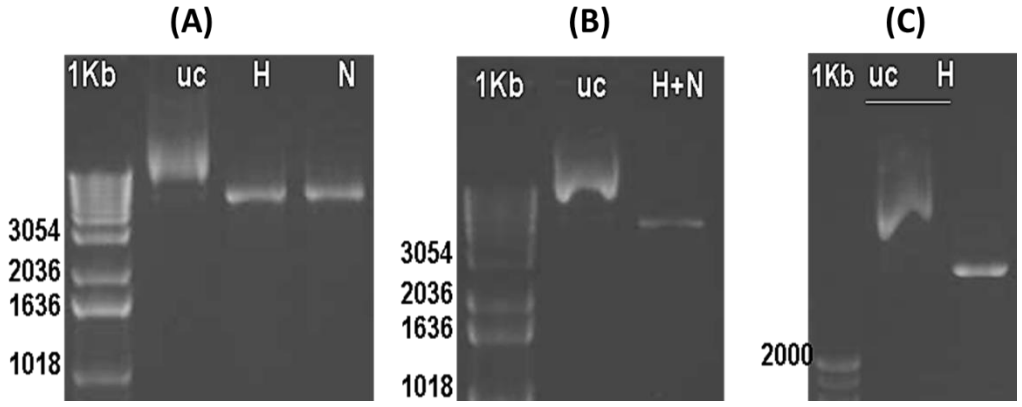

Fig 3.6: c-Myc Luciferase Reporter gene constructs. **(A)** The designed construct amplified by transformation followed by single cut with *Nhe*I (N) and *Hin*dIII (H) to confirm that both enzymes can cut at the designed sites. **(B)** The construct was double cut with *Nhe*I and *Hin*dIII to confirm that the selected clone contained the target insert. Comparing the size of the cut DNA plasmid with the uncut one (uc) and with the single cut in (A) indicated that the c-Myc oligonucleotides of 60bp was dropped out. **(C)** The c-Myc reporter gene construct was amplified for large DNA extract and the plasmid is confirmed to have the right insert by *Hind*III cut. The cut plasmids were compared to uncut (uc) one.

3.2.3 Cell transfection for RNF17 expression and proteasome inhibition by MG132

Cos1 cells were transfected with RNF17 expression plasmids and/or MXD1 plasmids, using Fugene as transfection agent. Transfected Cos-1 cells or F9 cells were treated for 24 hours with MG132 (1:1000 µM) dissolved in DMSO as a vehicle control. Transfected cell extracts were examined by Western blotting and cells were cultured on a cover slip for immunostaining.

3.2.4 Testing of RNF17 antibody (anti-RNF17)

The negative control for immunostaining was applied by staining cultured F9 cells or Cos1 cells. F9 cells were stained with secondary antibody only under the same conditions for anti-RNF17 staining. Alexa fluor staining did not detect nonspecific proteins in F9 cells (Fig 3.7A).

Untransfected Cos1 cells were stained with anti-RNF17 to confirm that endogenous RNF17 was not expressed in Cos1 cells and also to test that anti-RNF17 was not detecting nonspecific proteins as shown in (Fig 3.7B).

3.2.5 Production of RNF17-expression constructs.

Protein expression constructs were produced for short RNF17 (Flag-tagged RNF17S) and RNF17 protein C (Flag-tagged RNF17C) by a third year undergraduate student -Laura Cross- and Dr C.H. Barton.

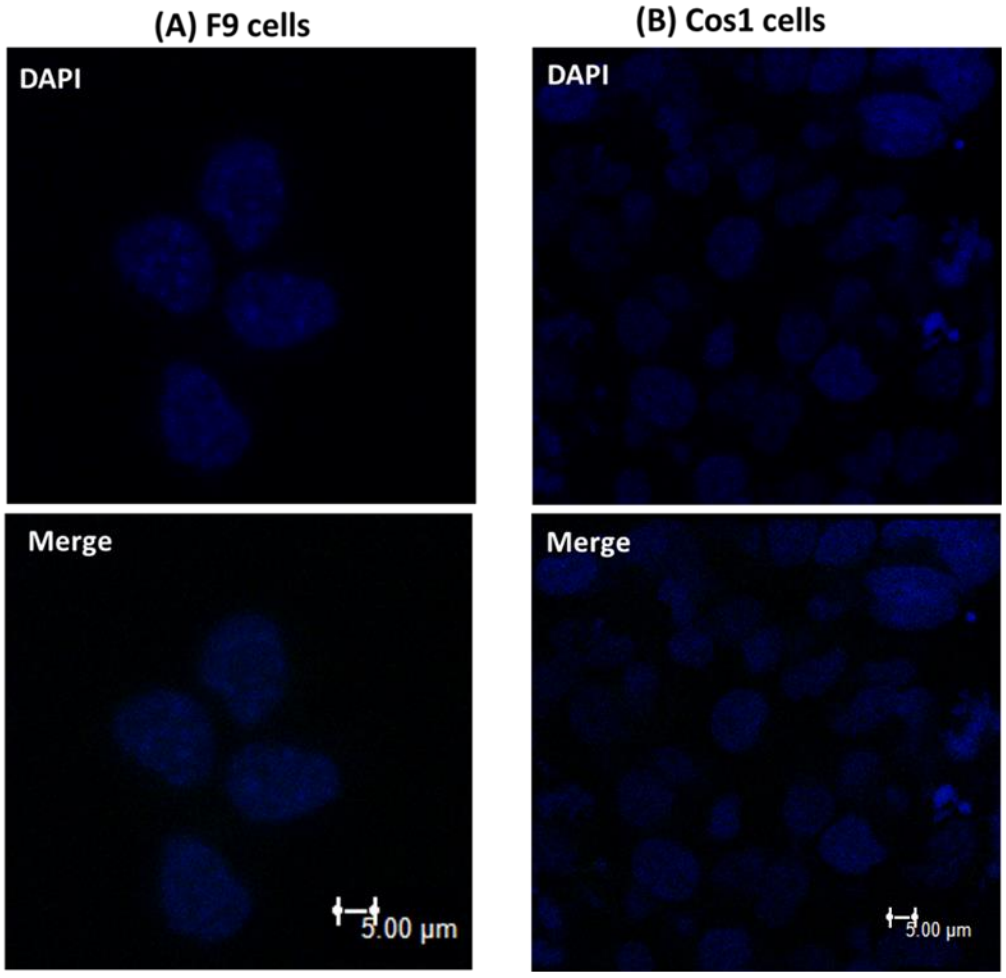

Fig 3.7: Negative control for anti-RNF17 immunostaining of culture cells. **(A)** Cultured F9 cells were stained with secondary antibody Alexa fluor 488 in 1%PBS-T. **(B)** Un-transfected Cos1 cells were stained with anti-RNf17 in 1%PBS-T. Nuclei were stained with DAPI and cells were visualised by confocal microscopy under emission of 488 and 550 nm. DAPI and merge images show that anti-RNF17 is not detecting nonspecific proteins.

3.3 Results

3.3.1 Expression of endogenous Rnf17 in F9 cells by endpoint PCR and RT-PCR

Since there are multiple isoforms of Rnf17, it was important to evaluate which transcripts were expressed in F9 cells, using the endpoint PCR approach. F9 cells were cultured to semi-confluence, harvested, RNA extracted and cDNA prepared. Rnf17 primers were designed to amplify specific diagnostic fragments from the short Rnf17 and the long Rnf17 transcripts. As shown in Fig 3.8, Rnf17S of 471 bp and Rnf17L of 568 bp were expressed in F9 cells, compared to the negative controls not containing reverse transcriptase enzyme (-RT) or not treated with DNaseI. An uncharacterised band of about 150 bp was amplified using primers for Rnf17S (red arrow in Fig 3.8) and the RT treated with DNaseI confirmed that the 150 bp was not associated with genomic DNA contamination.

This experiment clearly established that the long and short Rnf17 transcripts were expressed in F9 cells and as such made it a suitable model system for functional studies. The origin of the 150 bp product is not clear, although other transcripts have been described for this gene in AceView.

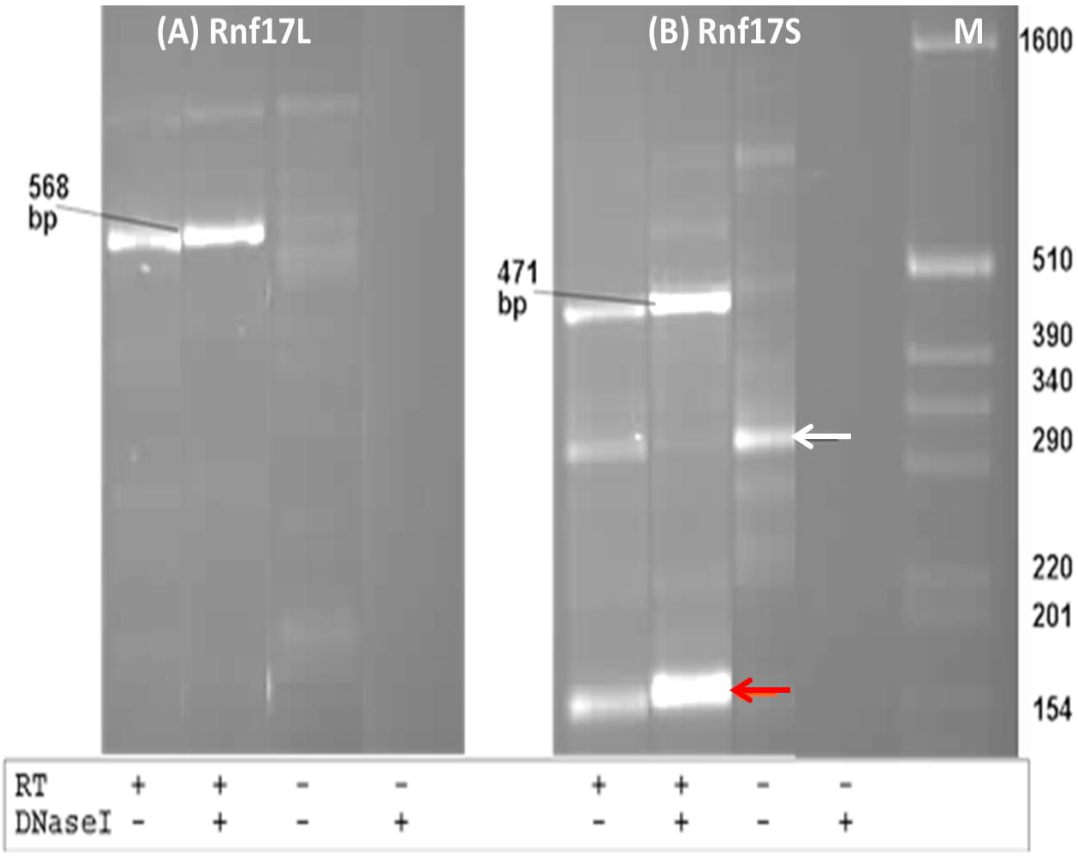

Fig 3.8: Expression of Rnf17 in F9 cells by endpoint PCR. Rnf17L and Rnf17S were set as deposited by Pan *et al*, (2005) in GenBank to amplify 568 bp for **(A)** Rnf17L and **(B)** 471 bp for Rnf17S**.** Red arrow in **(B)** shows uncharacterised band of about 150 bp that amplified using the Rnf17S primers and the white arrow is genomic DNA-derived product. RNA extracted from F9 cells and synthesised cDNA was treated with (+) or without (-) reverse transcriptase (RT) and DNaseI.

3.3.2 Cellular localisation of RNF17 in F9 cells

F9 cell extracts were separated into soluble and insoluble fractions and each was blotted in three replicates on SDS-PAGE. RNF17 was expressed in the insoluble fraction with bands corresponding to the expected size of long RNF17 and short RNF17 (Fig 3.9).

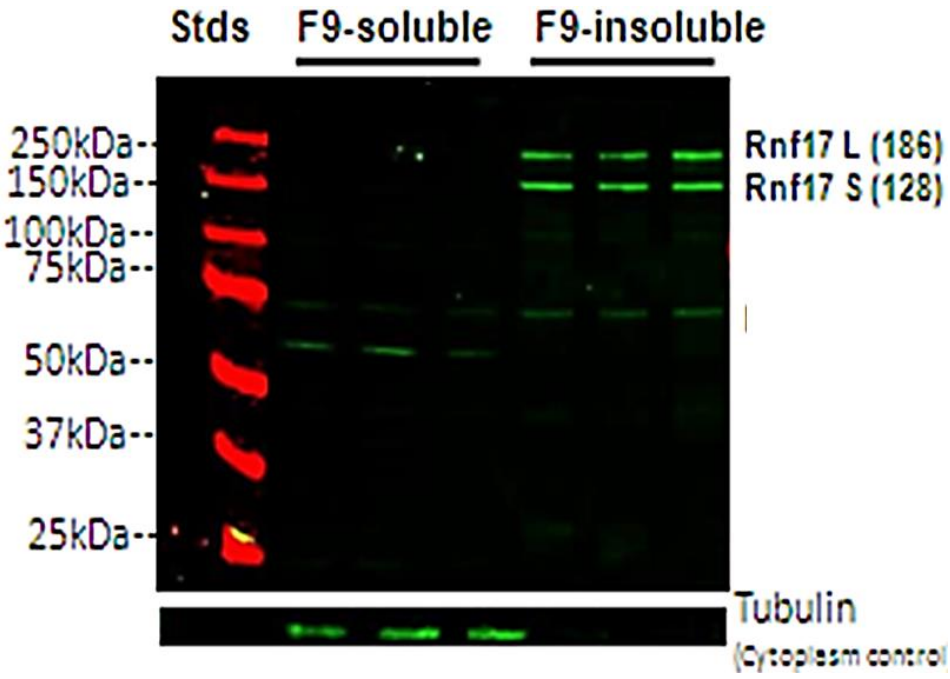

Fig 3.9: Expression of endogenous RNF17 in F9 cells by Western blotting. F9 cell extracts of soluble and insoluble fractions were blotted on SDS-PAGE in three replicates. Two isoforms for RNF17 long (RNF17L) and RNF17 short (RNF17S) were detected in insoluble fraction of F9 cells. Tubulin was used as a control for cytoplasmic (soluble) protein.

F9 cells were cultured on a coverslip for immunostaining and stained for RNF17. The expression of RNF17 was visualised by confocal microscopy and the level of RNF17 intensity was measured by Volocity software. RNF17 was found predominantly in the nucleus and excluded from the nucleolus. RNF17 also displayed appearance as foci in the cytoplasm. RNF17 was not expressed in mitotic cells (Fig 3.10 arrow A). It was noted that the cytoplasmic RNF17 foci were located close to the nuclear membrane and very few were scattered in the cytoplasm (Fig 3.10 arrow B).

Using Volocity software, voxel number and level of fluorescence intensity for RNF17, foci were counted in the nuclei or the cytoplasm in 64 cells at different staining times. Voxel number of RNF17 in the nucleus was higher than in the cytoplasm per cell (24-fold) (Fig 3.11A). No significance differences were seen within fluorescence intensity level for RNF17 in the nucleus than in the cytoplasm, although the difference was about 10% (Fig 3.11B).

The results indicated that the level of RNF17 was equally distributed between the cytoplasm and the nucleus. However, the accumulation of RNF17 foci around the nuclear membrane may reflect the reduced voxel count in the cytoplasm compared with that in the nucleus.

It is noted here that the error bar was too large, which may indicate artificial counting of the voxels. Additionally, some of F9 cells displayed variable foci sizes which indicated aggregation of foci expression. This was counted as one foci by the software and represented in the error bar.

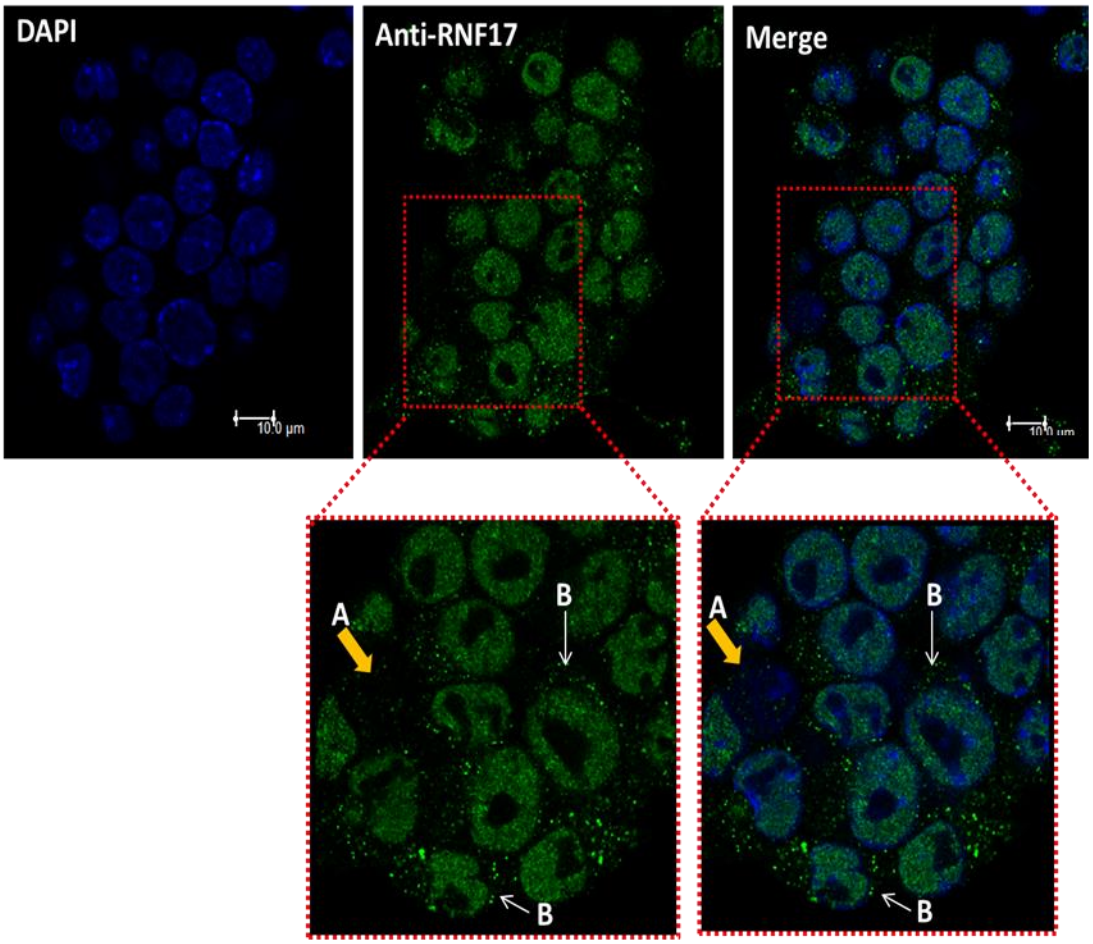

Fig 3.10: Cellular localisation of RNF17 in F9 cells. F9 cells were cultured on coverslip and immunostained with anti-RNF17 (middle panel), nuclei were stained with DAPI (left panel), merge images shown in right panel and cells were screened by confocal microscopy. RNF17 is predominantly inside the nucleus with foci appearance in the cytoplasm of F9 cells. RNF17 was not expressed in mitotic cells (**A;** yellow arrow). Cytoplasmic RNF17 foci were close to the nuclear membrane (**B;** white arrow).

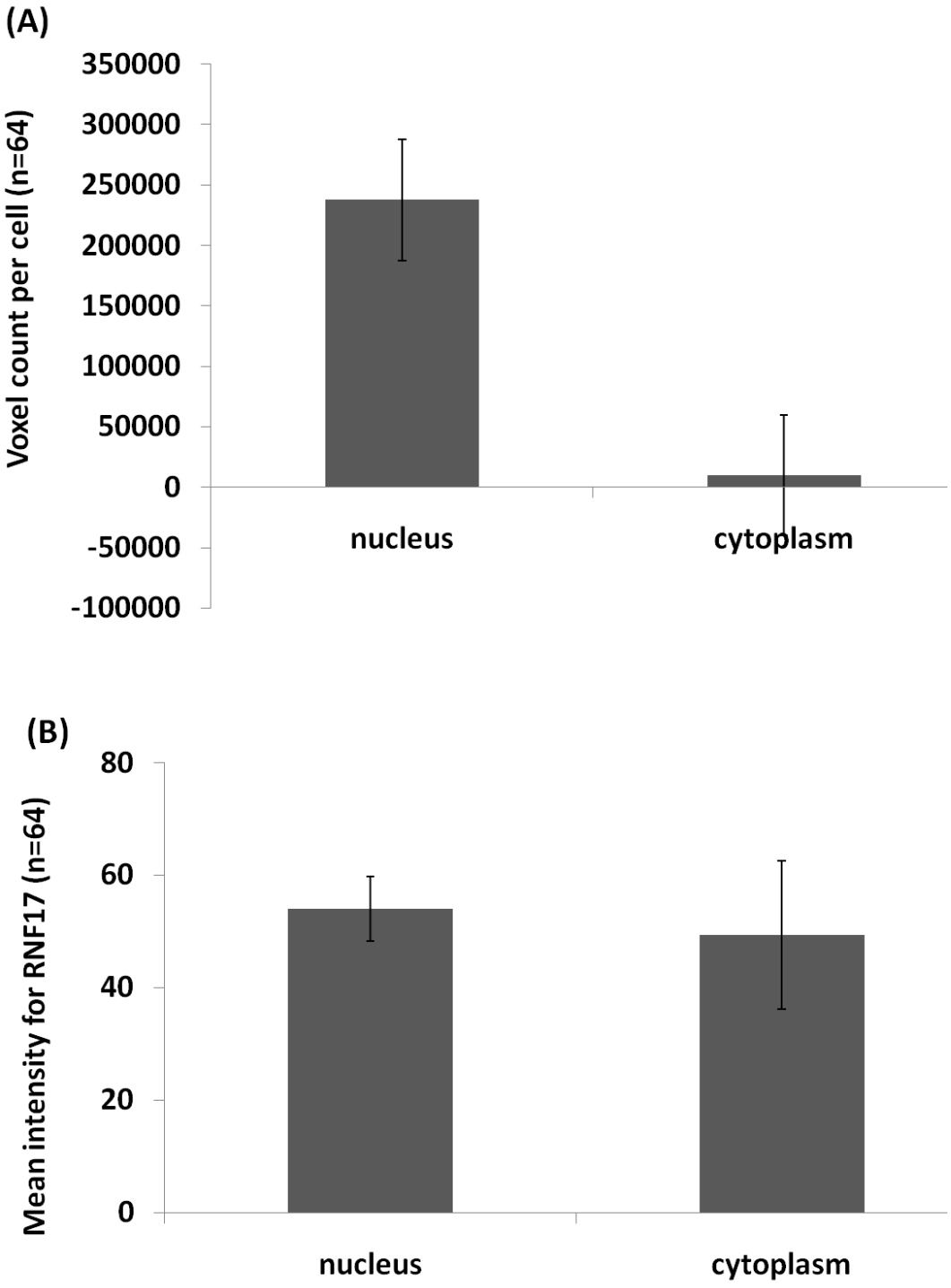

Fig 3.11 *(continued)*

Fig 3.11: Expression level of endogenous RNF17 in F9 cells. Cultured F9 cells were immunostained with anti-RNF17 and numbers of voxel or intensity level of RNF17 were measured in the cytoplasm or nucleus per cell using Volocity software. **(A)** Voxel number of RNF17 in the nuclei and in the cytoplasm per cells. **(B)** Mean level of fluorescence intensity of RNF17 in the nucleus and the in the cytoplasm of F9 cells. Bar graphs show the mean of examined cells (n=64), and error bars represent standard deviation.

3.3.3 Over-expression of Rnf17 induces c-Myc Luciferase activity

A constant amount of a c-Myc Luciferase reporter gene construct (1µg) was co-transfected into F9 cells with either pEF-c-Myc expression vector (control) or the Rnf17 expression vector. In all transfections, the level of total DNA was normalised with pUC plasmid. Transfecting the pEF-c-Myc expression plasmid into F9 cells (0.25 µg) significantly increased the Luciferase activity of the c-Myc reporter construct ($P \leq 0.05$) about 29-fold, compared to the control with the c-Myc Luciferase reporter gene construct. Further increases in the amount of pEF-c-Myc expression plasmid decreased the Luciferase response (Fig 3.12A) and this may have been due to the inhibition or squelching of the transcription of c-Myc (Cahill *et al*, 1994).

The Rnf17 expression vector increased the c-Myc-responsive Luciferase activity at 0.5 µg by 2-fold (Fig 3.12B) compared to Rnf17-untreated controls, but did not reached significance. Although the induction of c-Myc Luciferase activity was not significant, this may suggest that over-expression of Rnf17 recruits Mxd out of the nucleus to the cytoplasm releasing Max (Yin *et al*, 1999). The released Max can then interact with c-Myc, inducing transcription via binding to the E-box of the c-Myc Luciferase reporter gene construct.

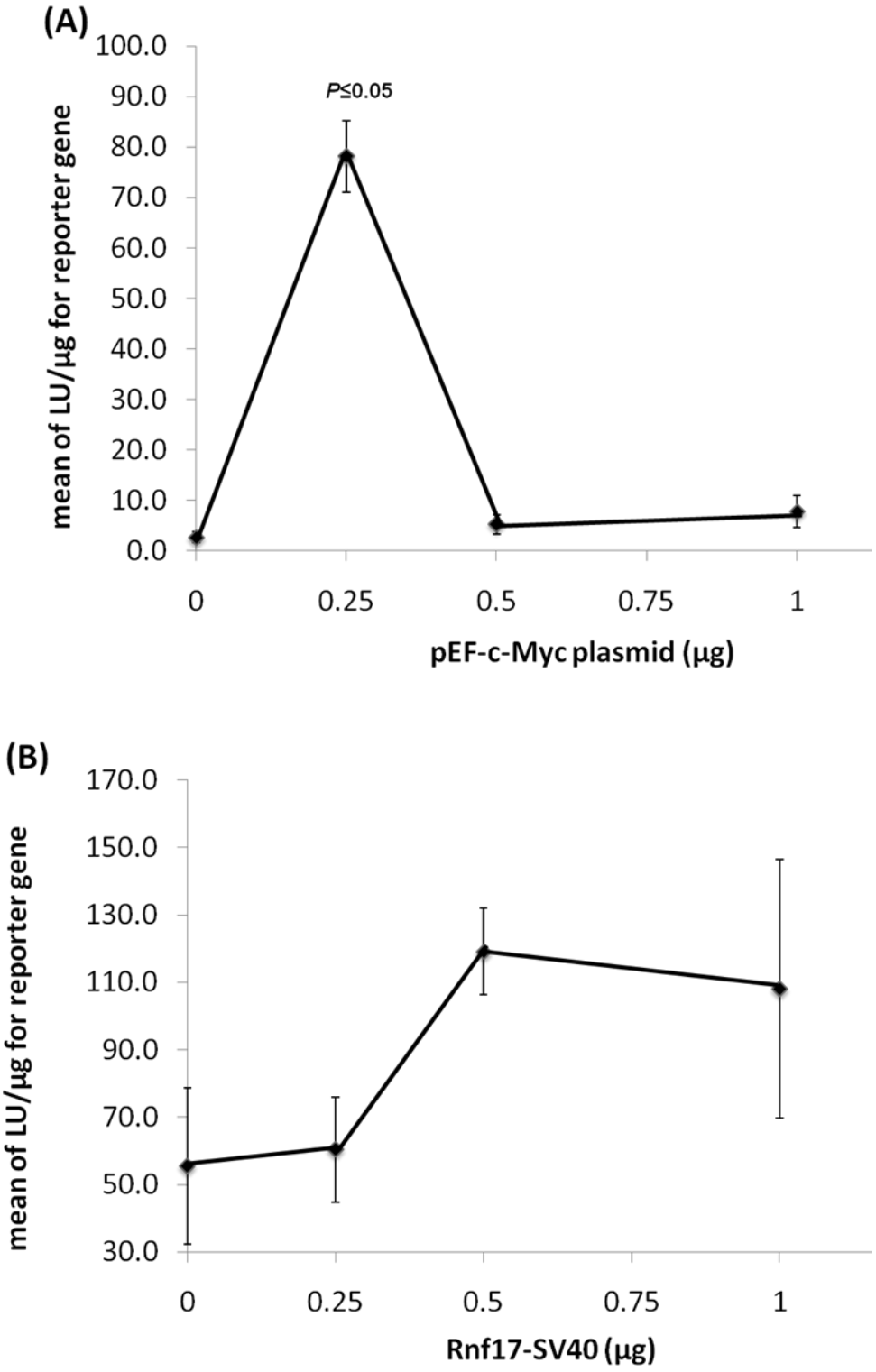

Fig 3.12 *(continued)*

Fig 3.12: Induction of c-Myc Luciferase reporter gene in response to c-Myc and Rnf17 in F9 cells. F9 cells were co-transfected with constant amount of 1.0 µg of c-Myc Luciferase reporter gene construct and increasing amounts (0.0, 0.25, 0.5, 0.27 µg) of either **(A)** pEF-c-Myc expression plasmid or **(B)** Rnf17-SV40. DNA concentrations were normalised using pUC18 empty vector. Bar graphs show mean of three replicates, and error bars represent standard deviation.

3.3.4 RNF17 induced degradation of MXD1 by ubiquitination mechanism

To test whether MXD is a target protein for the E3 ligase activity of the RING domain within RNF17, Flag-tagged expression plasmids for MXD, RNF17S and RNF17C (Protein C isoform) were used. A constant amount of Flag-tagged RNF17S or RNF17C (1 µg) was co-transfected into Cos1 cells with Flag-tagged MXD, or without Flag-tagged MXD as a control. Transfected cells were treated with proteasome inhibitor MG132 (1:1000 µM), control cells were treated with an equivalent dose of DMSO alone for 24 hours. Cell extracts of soluble and insoluble proteins were analysed with anti-Flag by Western blotting.

RNF17C and RNF17S were expressed in the soluble and insoluble extracts (Fig 3.13 lane 1 & 7). RNF17C completely disappeared from the soluble fraction following treatment with MG132 and accumulated into the insoluble fraction (Fig 3.13 lane 2). Addition of MG132 induced the appearance of RNF17S into the insoluble fraction and some loss from the soluble fraction (Fig 3.13 lane 8).

MXD1 was exclusively localised in the insoluble fraction with molecular weight 26kDa as expected (Fig 3.13 lane 5). MG132-treatment promoted the accumulation of higher molecular weight forms of MXD1 and these probably were ubiquitinylated forms. Ubiquitin of molecular weight 8.5 kDa is known to conjugate to the target proteins and form a polyubiquitin chain. The ubiquitin-tagged proteins, MXD1, could be seen on the gel of the insoluble fraction as a ladder of higher molecular weight of about 34.5, 43.0, 51.5 and 60.0 kDa; these were more distinct in the transfection with RNF17C (Fig 3.13B lane 6).

Co-transfection of Flag-tagged MXD1 with Flag-tagged RNF17C or Flag-tagged RNF17S reduced the expression of MXD1 and levels of RNF17C or RNf17S in the insoluble fraction (Fig 3.13B lane 3 & 9). Inhibition of

proteasomal activity with MG132 enabled the accumulation of MXD1 in the insoluble fraction and induced the appearance of RNF17C, but not RNF17S (Fig 3.13B lane 4 & 10).

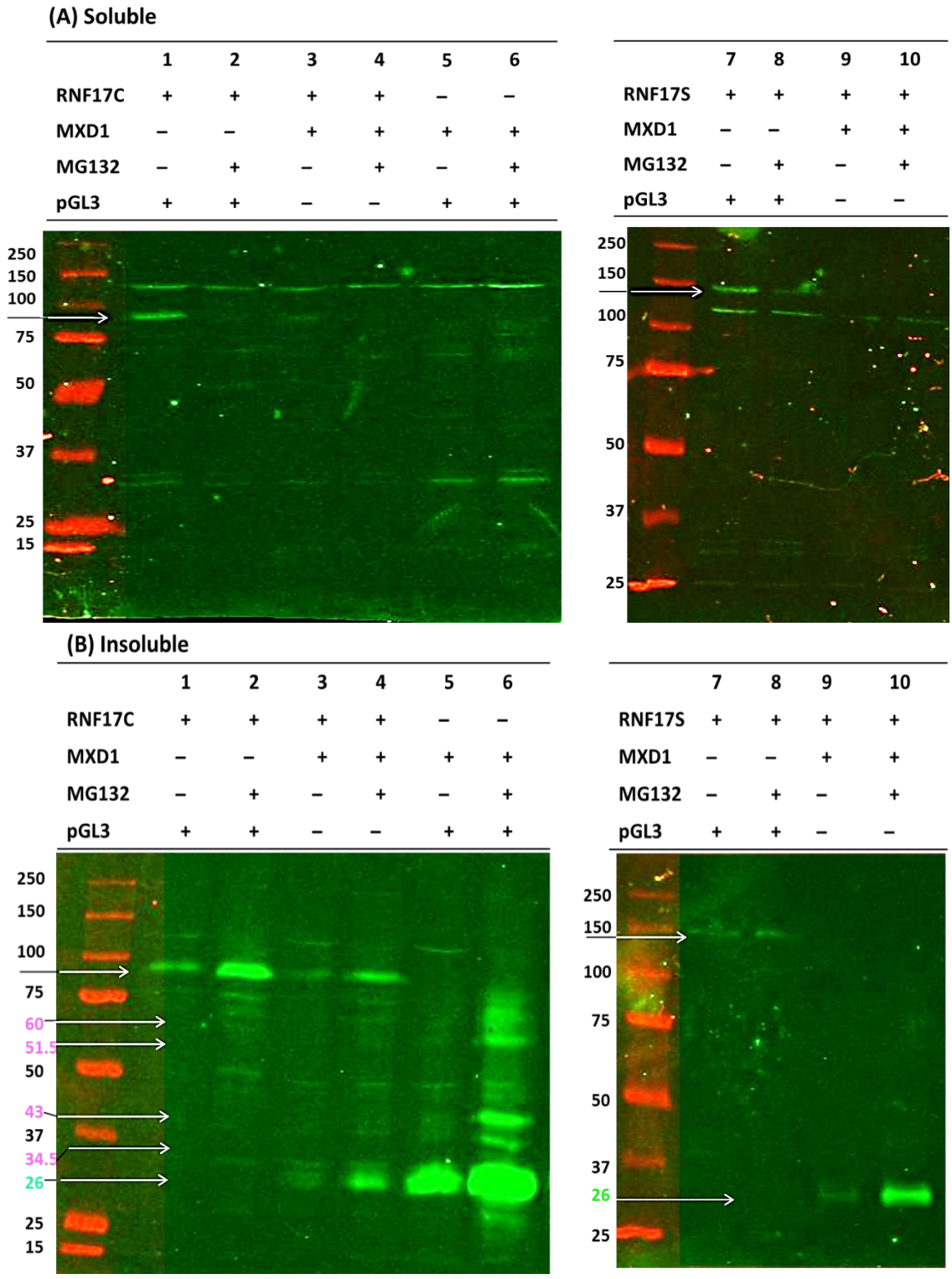

Fig 3.13 *(Continued)*

Fig 3.13: RNF17 induced MXD1 degradation in the presence of proteasomal inhibitor MG132 in transfected Cos1 cells. Cultured Cos1 cells were co-transfected with Flag-tagged-RNF17S or -RNF17C plasmids and/or Flag-tagged-MXD1 construct. Transfected cells were treated with MG132 or control cells treated with DMSO for 24 hours. **(A)** Soluble and **(B)** insoluble fractions from harvested cells were blotted on western blot gel. Co-transfection of RNF17 with MXD1 degraded MXD1 in the absence of MG132 **(B: Lane 3 & 9)** whereas MXD1 accumulated in the presence of MG132 **(B: Lane 4 & 10).** Transfection of MXD1 alone forms polyubiquitin chain in presence of MG132 **(B: Lane 6)** represented in a ladder of higher molecular weight bands of about 34.5, 43.0, 51.5 and 60.0 kDa compared to DMSO-treated cells **(B: Lane 5).**

3.3.5 Expression and subcellular localisation of RNF17 in MG132-treated cells

Cultured F9 cells were incubated with or without the proteasome inhibitor MG132 for 4 hours or 24 hours. Cells were immunostained with anti-RNF17 and expression was visualised by confocal microscopy. Compared to the endogenous expression pattern of RNF17 in F9 cells, RNF17 had lost the nuclear-punctated-structure and had become diffused in the nuclei of MG132-treated cells or control cells (DMSO treated) (Fig 3.14). RNF17 was completely absent from the cytoplasm.

In transfected Cos1 cells, RNF17C and RNF17S displayed a punctated appearance in the cytoplasm of DMSO-treated Cos1 cells (control) and accumulated in the peri-nuclear vicinity. In MG132-treated cells, RNF17C had diffused in the nuclei, whereas RNF17S displayed punctated appearance in the nuclei (Fig 3.15).

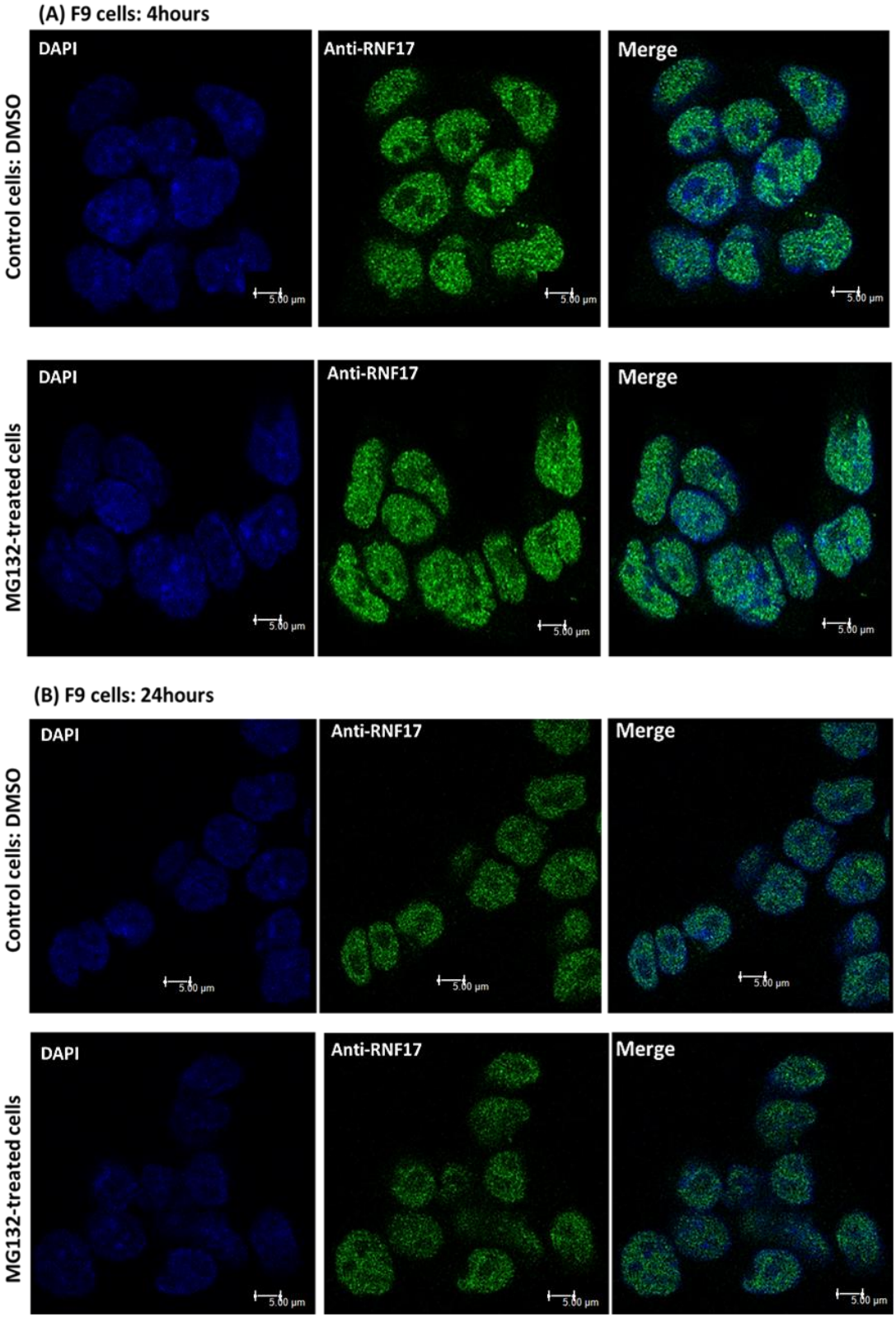

Fig 3.14 *(Continued)*

Fig 3.14: Effects of proteasome inhibitor MG132 on endogenous RNF17 expression and cellular localisation in F9 cells. Cultured F9 cells were treated with MG132 for **(A)** 4 hours or **(B)** 24 hours and immunostained with anti-RNF17 (middle panel). Nuclei were stained with DAPI (left panel), cells screened by confocal microscopy and merged images shown in right panel. Control cells were treated with DMSO. RNF17 lost its foci structure and disappeared from the cytoplasm but diffused into the nucleus.

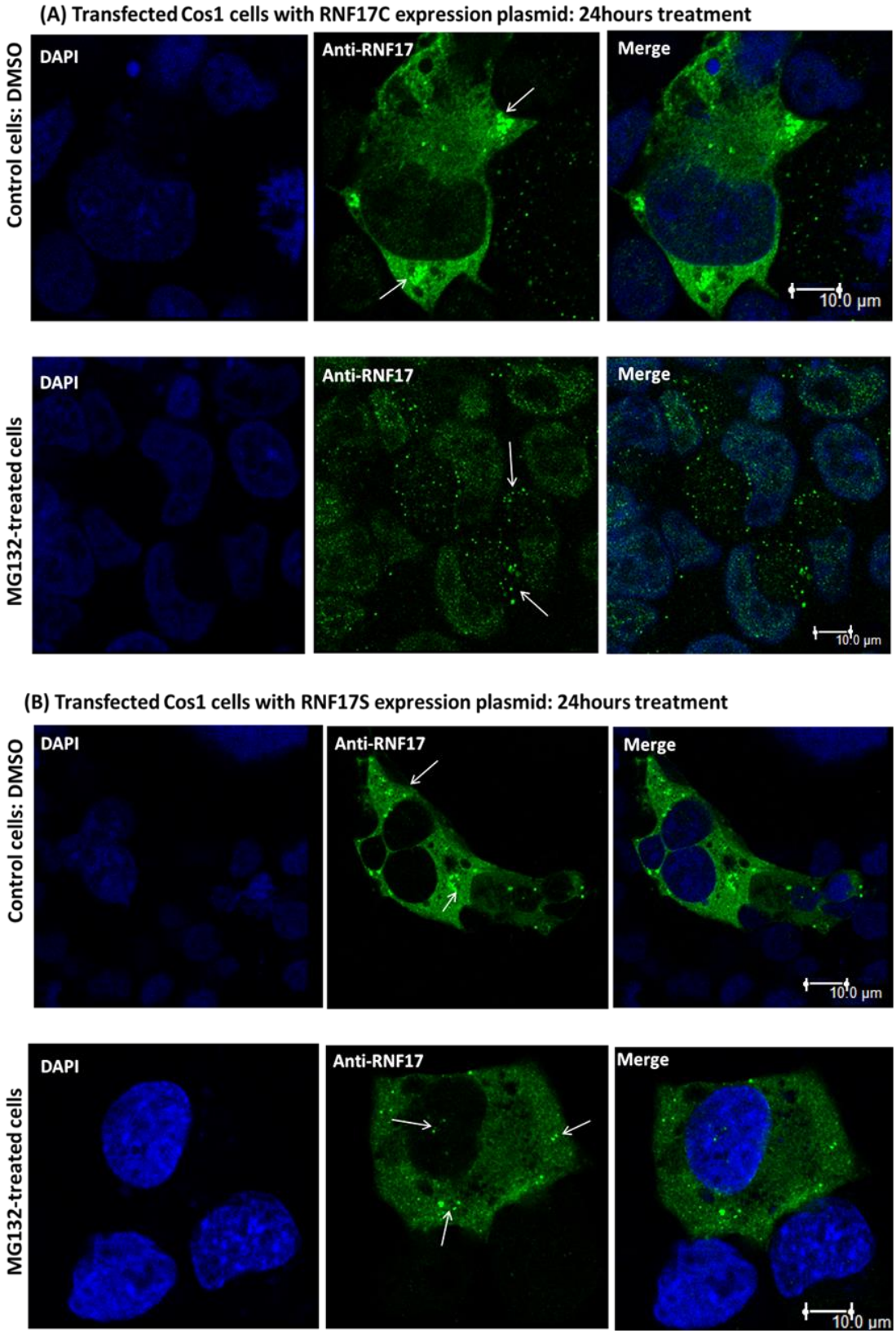

Fig 3.15 *(Continued)*

Fig 3.15: Effects of proteasome inhibitor MG132 on expression and cellular localisation of RNF17 expression plasmids transfected into Cos1 cells. Cultured Cos1 cells were transfected with **(A)** expression plasmids for RNF17C or **(B)** RNF17S for 24 hours. Transfected cells were treated with MG132 and control cells were treated with DMSO for 24 hours and stained with anti-RNF17 (middle panel). Nuclei were stained in DAPI (left panel), cells screened by confocal microscopy and merged images shown in right panel. RNF17C was diffused in the nucleus and in the cytoplasm of MG132-treated cells compared to control cells (arrows). RNF17S entered the nucleus and cytoplasmic foci reduced their number and accumulation in MG132-treated cells compared to control DMSO-treated cells (arrows).

3.4 Discussion

Four isoforms for Rnf17 have been annotated in Uniprot, and two of them, the Rnf17S (3.5 kb) and the Rnf17L (5.2 kb), were identified by Pan *et al* (2005). Using endpoint PCR, the expression of Rnf17 in F9 cells was detected. Results in Fig 3.8 show expression of Rnf17S and Rnf17L transcripts and an uncharacterised band of about 150 bp using the short Rnf17 primers was identified. Whether this undefined band is expressed in early embryos, needs further validation. In addition, it was unclear, given the known exons annotated for Rnf17 in Ensemble and AceView, which exons could encode this transcript or its coding potential. However, the product is RNA-derived, as it was not amplified in RT-negative controls and did not disappear from DNaseI treatment of the RNA, unlike the detected band of 290 bp detected from DNaseI untreated RNA. This indicates that it was not a product of genomic DNA contaminant.

To test the endogenous localisation of RNF17 in F9 cells, and anti-RNF17 rabbit polyclonal antibody was generated. Western blotting showed that the anti-RNF17 sera specifically recognised the short and long RNF17 isoforms (Uniprot). Using the generated anti-RNF17, RNF17 isoforms were detected by Western blot (Fig 3.9). The subcellular localisation of endogenous RNF17 in F9 cells was determined by immunostaining. RNF17 was expressed in the nucleus and localised in cytoplasmic foci located close, specifically surrounding, the nuclear membrane (Fig 3.10) and this was consistent with RNF17 immunoreactivity being identified in the insoluble fraction. This is distinct from the immunoreactivity of Tubulin which segregated in the soluble fraction. The database shows a consensus sequence for a bipartite NLS stretch amino acids within RNF17 with two stretches of K/R residues conforming to the consensus {(K/R)-X10-12-(K/R)(K/R) where X represents any amino acid residues} (AceView). Two bipartite NLS spanning residues 326-342 (**RK**ELCCDVYSSLE**KKK**V) and residues 458-474

(**RK**YSQIKDATILEKKM**K**) of RNF17 isoforms: Long, short and protein C, revealed the ability of RNF17 to enter the nucleus.

Increased expression of the c-Myc protein *in vitro* enables increased binding to the E-box sequences of the c-Myc reporter construct, and a direct output to this binding is the activation of transcription of Luciferase which can be readily measured in extracts from cells. c-Myc over-expression in F9 cells was tested-as a control experiment- and the results showed a significant induction of the Luciferase reporter construct. Higher levels of c-Myc expression caused "squelching" which has been described previously for over-expression of transfection factors and has been related to the removal of a limiting pool of co-activators into non-functional complexes not bound to DNA (Cahill *et al*, 1994). Interestingly, the over-expression of Rnf17 did not cause this squelching and Rnf17 is believed not to bind co-activators and thus is consistent with the proposed mechanism for Rnf17 in creating a MXD-null phenotype (Yin *et al,* 1999).

Co-transfection of Rnf17 and c-Myc expression plasmids had shown that Rnf17 induced c-Myc activity in F9 cells. One possibility is that this may be achieved by interacting with Mxd (Yin *et al*, 1999). However, it is possible that Rnf17 alters Mxd stability via acting as ubiquitin ligase (Pickart, 2001; van Wijk *et al*, 2009).

Comparing the intensity of the band for MXD1 in the absence of RNF17 in MG132-treated or untreated cells in Western blot experiments revealed a regulatory role for proteasome in MXD1 degradation by another E3 ligase. MXD1 was found exclusively in the insoluble fraction, whereas RNF17 can be seen in the soluble and insoluble fractions. The insoluble fraction contained nuclear and insoluble proteins whereas the soluble fraction contained cytosolic proteins. The strong band for RNF17C in the insoluble fraction probably reflected the immunostaining signals in the nucleus and in

the cytoplasmic foci. The weak band for RNF17S in the insoluble fraction of Western blotting probably indicated the cytoplasmic foci localisation of RNF17S.

The results in Fig 3.13 may indicate that different isoforms of RNF17 exhibit certain preferences in their substrate specificity. For example, the oncogene c-IAP contains a RING motif and has the properties of ubiquitin E3 ligase targeting MXD1 and promotes cell proliferation via cooperation with Myc (Xu *et al,* 2007). The c-IAP1 mediates the ubiquitinylation of TRAF2 (li *et al*, 2002 from Xu *et al,* 2007), whereas c-IAP2 degrades TRAF1 (Lee *et al*, 2004 from Xu *et al,* 2007). Yin (1999 and 2001) found that RNF17 is strongly interacts with MXD1, MXD3 and MXD4 but weakly interacts with MXD2. It would be interesting to test whether RNF17S or RNF17C have the specificity of ubiquitin-degradation for the members of the MXD family.

Changing ratios of RNF17:MXD has been shown to change their cellular localisation (Yin *et al* 1999). MG132 had inhibited proteasomal activity and blocked degradation of MXD1 which suggests the possibility of holding RNF17 in the nucleus. Immunostaining results showed that treated Cos1 cells with MG132 induced movement of the RNF17 construct into the nucleus, suggesting a target protein for RNF17 localised in the nucleus.

From the subcellular localisation experiments, the distribution of protein from transfected plasmids of RNF17S was found exclusively in the cytoplasm, while RNF17C was in both the nucleus and the cytoplasm. Treating cells with MG132 induced more RNF17C to enter the nucleus and reduced the number of clusters of cytoplasmic RNF17S. The localisation of both RNF17 proteins mirrored the band intensity in the Western blot experiments with or without MG132-treatment. It is not clear how this differential localisation is controlled, however it could involve the Tudor domains that are present in the

RNF17S protein which are lacking the protein C isoform (Uniprot). Thus, Tudor domains could impair the activity of the NLS.

Based on the subcellular localisation and Western blot results, a conclusion that RNF17 is shuttled between the nucleus and the cytoplasm in response to proteasomal activity, and acts as E3 ligase to degrade MXD via ubiquitinylation is reached. It is possible that Rnf17 functions to create a Mxd-null phenotype by ubiquitinylation. Rnf17 could modulate c-Myc in early development, such that changes in Rnf17's expression could bring about changes in the relative levels of cell populations within the developing embryo and have effects on developmental outcomes.

Chapter 4

4. Expression Patterns of Rnf17 during Mouse Preimplantation Embryo Development

4.1 Introduction

Preimplantation development is the period from fertilisation to implantation that varies in stage and duration from species to species. Growing oocytes accumulate RNAs and proteins that constitute the maternal contribution to early development (Hamatani *et al*, 2004; Zeng and Schultz, 2005). After fertilization, subsequent cleavage division occurs with the first mitotic division to produce the 2-cell embryo and continues to form a blastocyst. In the mouse, there are two major transcriptional waves throughout preimplantation development. Each transcriptional wave is combined with maternal transcript degradation and new zygotic gene activation (ZGA) at each developmental stage (Hamatani *et al,* 2004; Schultz, 2002). A minor zygotic genome activation starts after fertilisation and is characterised by maternal transcript degradation and new zygotic transcription synthesis and mRNA expression. This is followed by a major ZGA that contributes to a dramatic synthesis of zygotic transcripts at 2-cell up to blastocyst stages. Another gene reprogramming occurs during the 4-cell and 8-cell stages and distinctively separates the 8-cell from the 2-cell embryo (Zeng *et al*, 2004; Hamatani *et al*, 2004).

MAX expressed in mouse oocyte and cleavage embryos was found continually in all embryonic and extra-embryonic structures of the early post-implantation embryos (Domashenko *et al,* 1997; Shen-Li *et al*, 2000). The c-Myc mRNA was detected at the late 2-cell and 4-cell stages and reached a maximum at the morula stage before declining upon blastocyst formation (Domashenko *et al*, 1997). Following *IVF* or *IVC*, c-MYC displayed a strong signal from 1-cell up to 4-cell, before the signal decreased in morulae and was not detected in blastocysts (Suzuki *et al*, 2009). Microarray analysis revealed that Mxd2 is expressed between the 4-cell and 8-cell stages,

followed by an immediate decrease from the 8-cell to morula stage (Hamatani *et al,* 2004).

Two transcripts for Rnf17 are described in adult mouse testis; Long Rnf17 (Rnf17L) and Short Rnf17 (Rnf17S) and RNF17 is located in a perinuclear nuage in male germ cells (Pan *et al,* 2005). Microarray data showed that Rnf17 is also expressed in early embryo development. Affymetrix probe, 1438820_at, showed that Rnf17 expression is increased through the preimplantation period (from oocyte to blastocyst) (Zeng *et al,* 2004). The same Affymetrix probe showed that Rnf17 is significantly increased in the mouse blastocyst in response to maternal LPD (Papenbrock *et al,* unpublished data) and following blastocyst cultured *IVC* or *IVF* (Giritharan *et al*, 2007) using Affymetrix probe1438820_at.

4.1.1 Aim of experiment

The aim of this experiment is to investigate the expression of Rnf17 mRNA in mouse cleavage stages. Members of the Myc/Max/Mxd network and the transposon element (Long interspersed element 1; line-1) were examined at the same stages. The expression of mRNA of examined genes was detected by RT-qPCR using extracted RNA from single embryos at different preimplantation stages.

The second aim is to detect subcellular localisation of RNF17 protein during preimplantation development and compare this to the adult mouse testis. In this experiment, rabbit polyclonal anti-RNF17 generated in our laboratory was exploited and using confocal microscopy.

4.2 Methods

4.2.1 Creating standard curve for data normalization

Primers designed for Rnf17, c-Myc, Mxd3 and Line-1 were tested using synthesized cDNA of F9 cells. For RT-PCR reactions, three replicates of all samples were performed and data were exported from the Opticon Monitor Analysis Software, following Opticon Monitor v3.1 software guidelines. Figure 4.1 shows expression of Rnf17S, Rnf17L, c-Myc, Mxd3 and Line-1 and control Tubulin α-1.

The amplified PCR products for Rnf17S, Rnf17L, c-Myc and Line-1 were visualized by gel electrophoresis on a 2% agarose gel, whereas no band was detected for Mxd3 (Fig 4.2). Thus, the Mxd3 reaction was tested on cDNA prepared from foetal testis (E17.5). Mxd3 was expressed in foetal testis and a band for Mxd3 PCR product was detected on 2% gel (Fig 4.3).

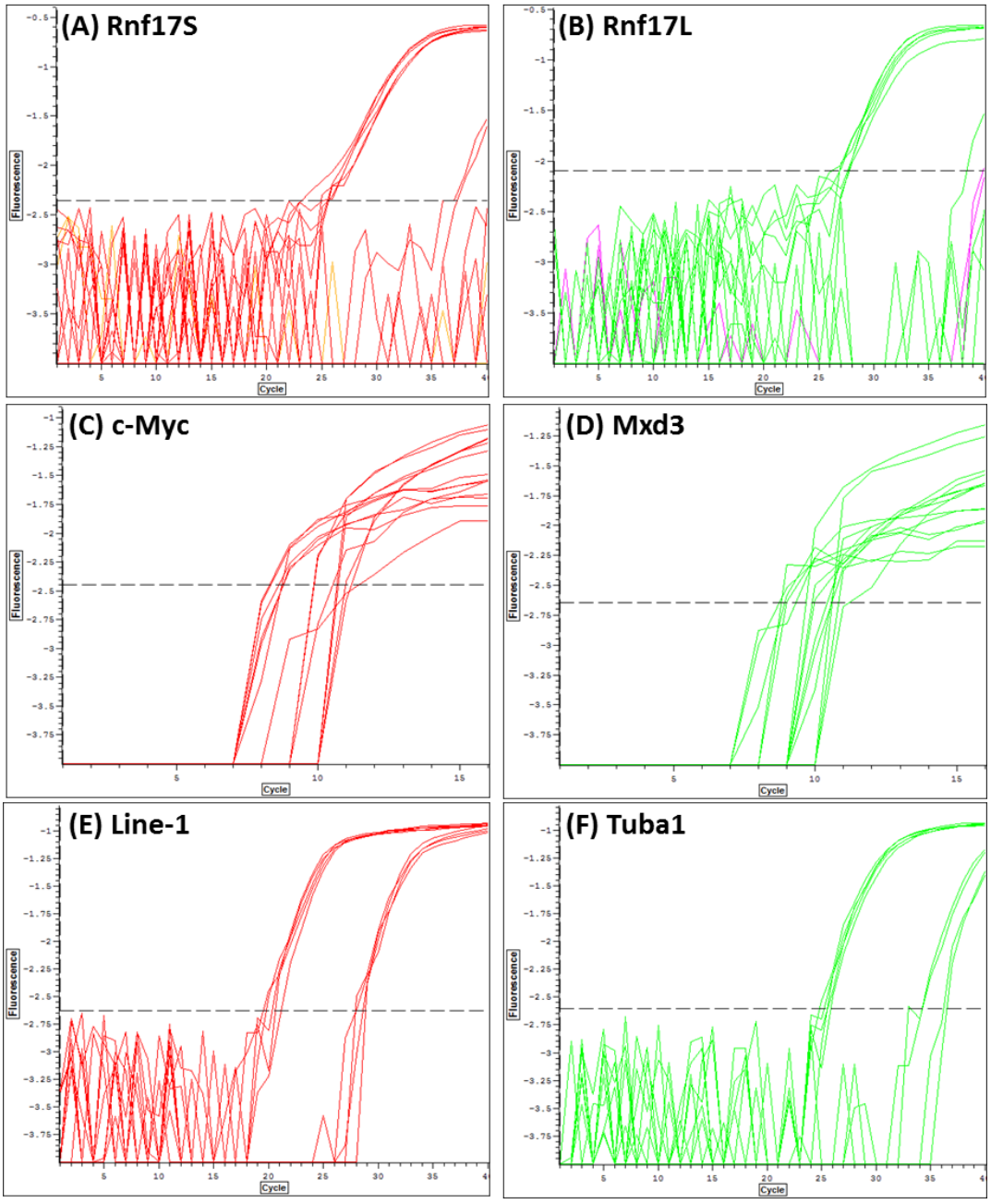

Fig 4.1: Expression of designed primers for RT-PCR. Specificity of designed primers was tested to detect expression of **(A)** Rnf17S, **(B)** Rnf17L, **(C)** c-Myc, **(D)** Mxd3 and **(E)** Line-1 using cDNA prepared from cultured F9 cells. **(F)** Tubulin α-1 (Tuba1) was used as a control. Expression of tested genes is displayed by threshold cycle (Ct) in all graphs exported from Optical Monitor Microsoft.

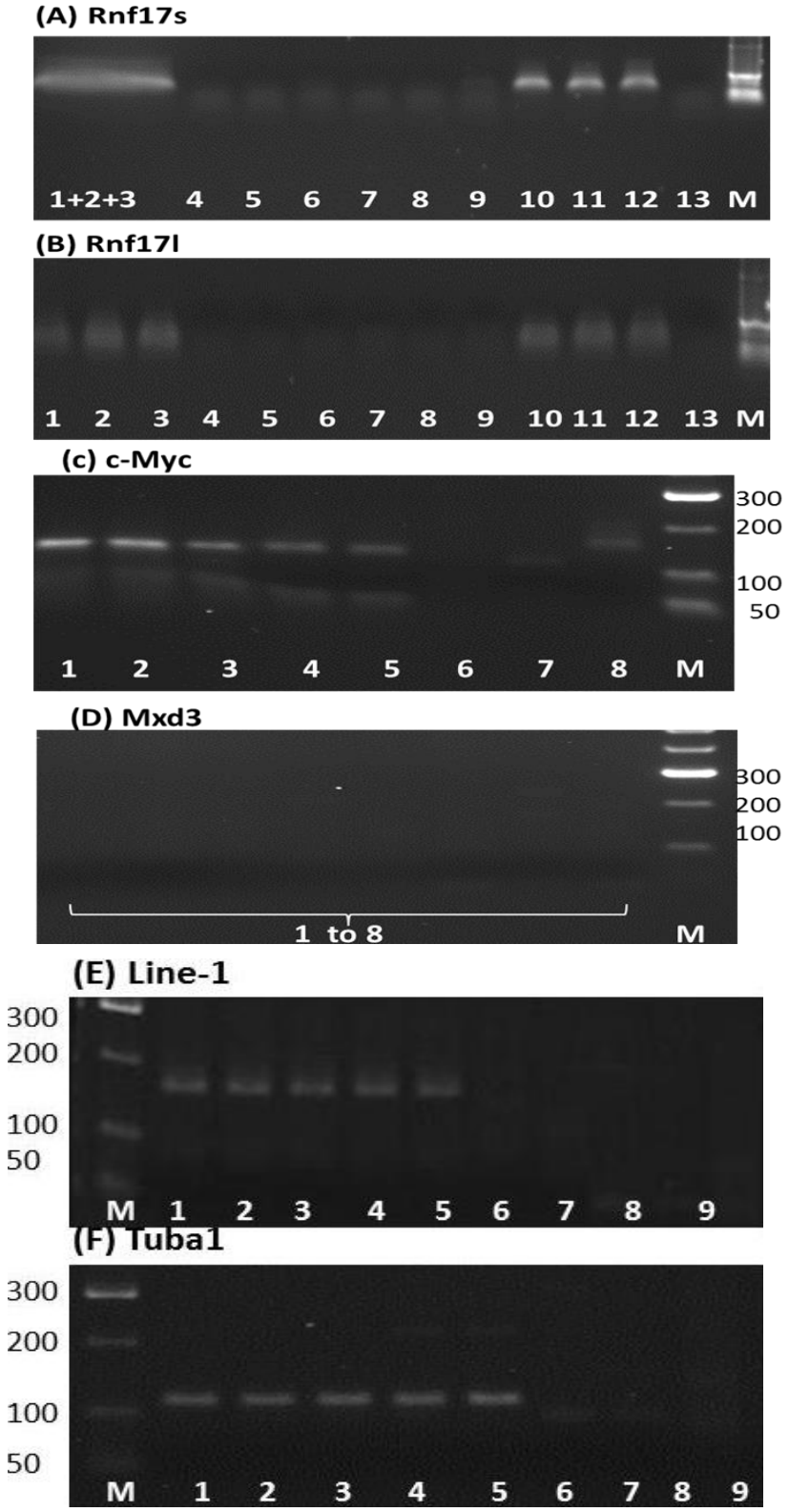

Fig 4.2 *(Continued)*

Fig 4.2: Electrophoresis of RT-qPCR products on a 2% agarose gel. F9 cells were used as template to test designed primers for candidate genes. **(A)** Rnf17S, Lanes 1, 2 and 3 were merged for gel extraction. **(B)** Rnf17L. **(C)** c-Myc. **(D)** Mxd3; no PCR products can be seen for Mxd3. **(E)** Line-1. **(F)** Tubulin α-1 (Tuba1)

- **Lanes 1, 2 & 3 for A, B, C, D, E & F**: +DNase//+RT.
- **Lanes 4, 5 & 6 for A, B, C & D**: +DNase//-RT.
- **Lanes 7, 8 & 9 for A, B, C & D**: -DNase//-RT.
- **Lanes 10, 11, 12 for A, B, C & D**: -DNase//+RT.
- **Lane 13 for A, B, C & D**: no template control (NTC).
- **Lanes 4 & 5 for E & F:** -DNase//+RT
- **Lanes 6 & 7 for E & F:** +DNase//-RT.
- **Lanes 8 & 9 for E & F:** no templatecontrol (NTC)
- **M**: DNA marker (HyperLadder II).

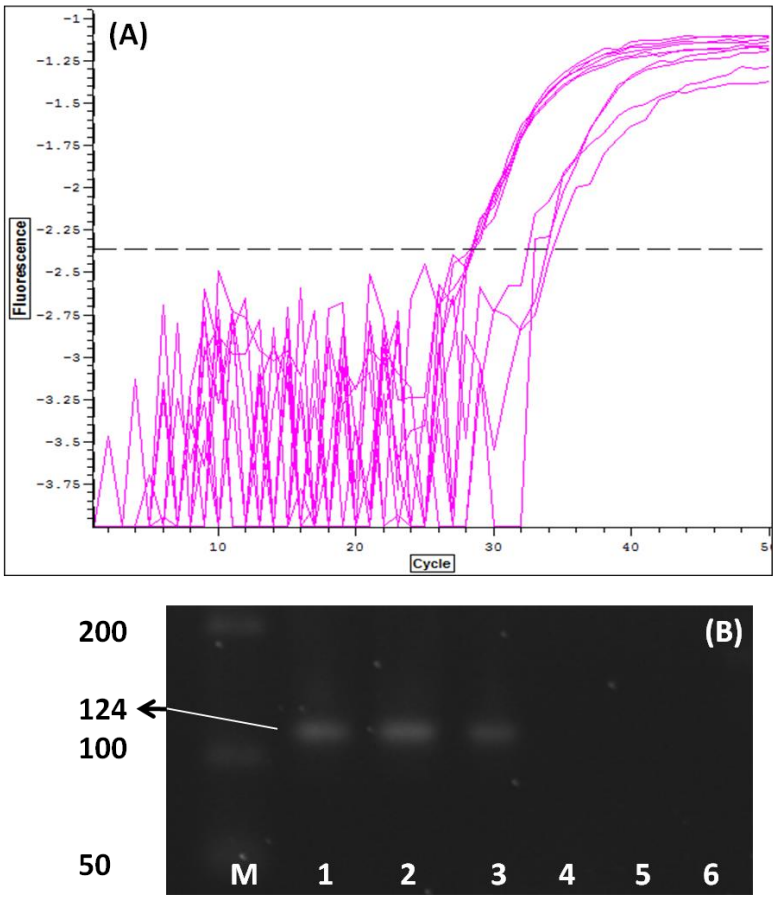

Fig 4.3: Expression of Mxd3 in foetal testis. Specificity of designed primers was tested to detect expression of Mxd3 using cDNA prepared from foetal testis E17.5. **(A)** Expression of Mxd3 is displayed by threshold cycle (Ct) in a graph exported from Optical Monitor Microsoft. **(B)** PCR product for Mxd3 is screened on 2% agarose gel.

- **Lanes 1, 2 & 3:** prepared cDNA with addition of reverse transcriptase (+RT).
- **Lanes 4 & 5:** prepared cDNA without addition of reverse transcriptase (-RT).
- **Lane 6:** no template control (NTC).
- **M:** DNA marker (HyperLadder II).

Serial dilutions were set up from 100 pg/µl to 1 ag/µl (Fig 4.4). All samples were run in replicate, and mean Ct values for each dilution were calculated to plot standard curves for each primer pair. Primer Efficiency (E) was calculated from the formula $E = 10^{1/slope}$ as shown in Figure 4.5.

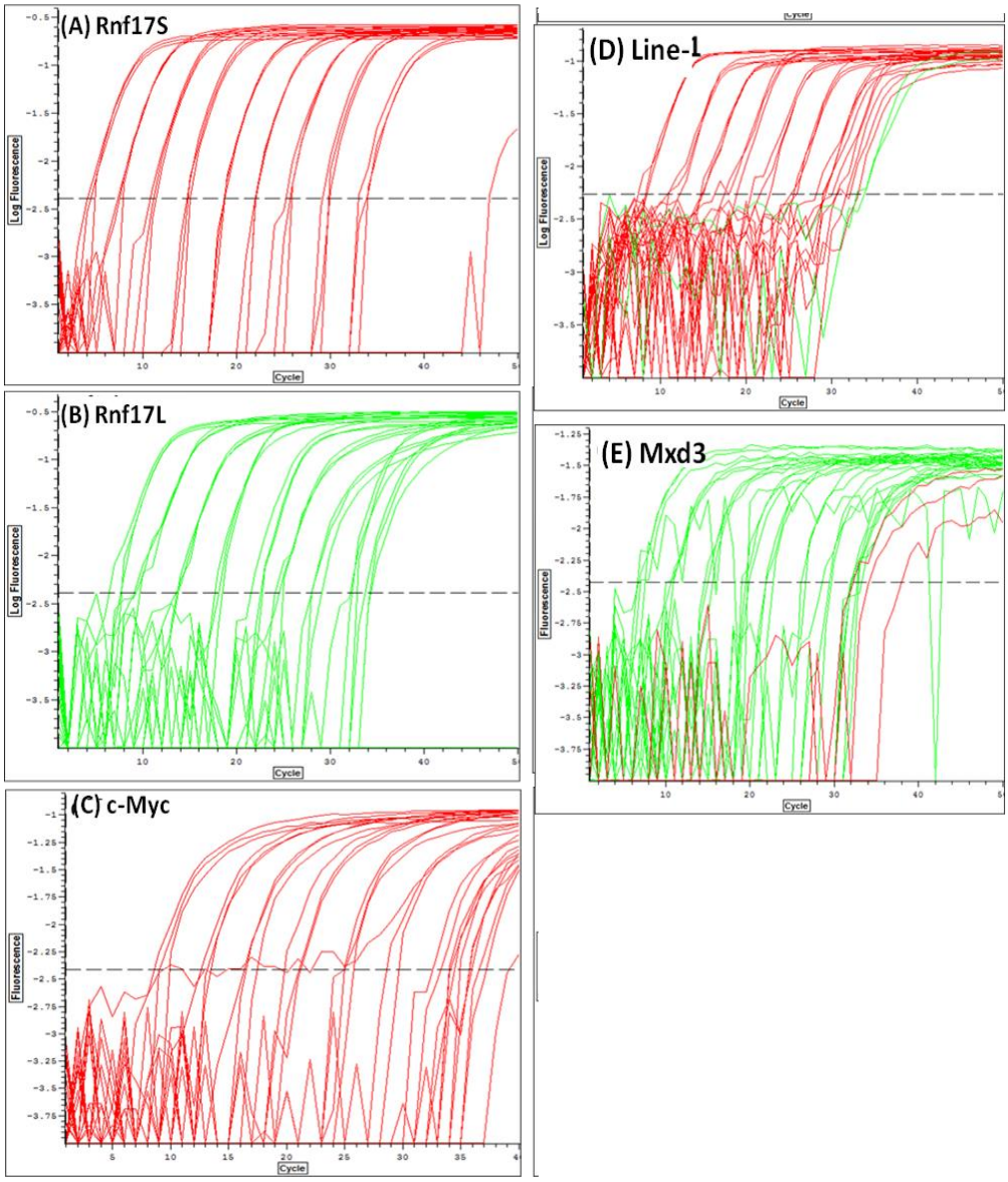

Fig 4.4: Amplification of RT-qPCR product for standard curve. Graphs exported from Opticon Monitor software represent serial dilutions generated from F9 cells template for **(A)** Rnf17S, **(B)** Rnf17L, **(C)** c-Myc and**(D)** Line-1, whereas those for **(E)** Mxd3 were generated from foetal testis E17.5. Dilutions were set up from 100 pg/µl to 1 ag/µl.

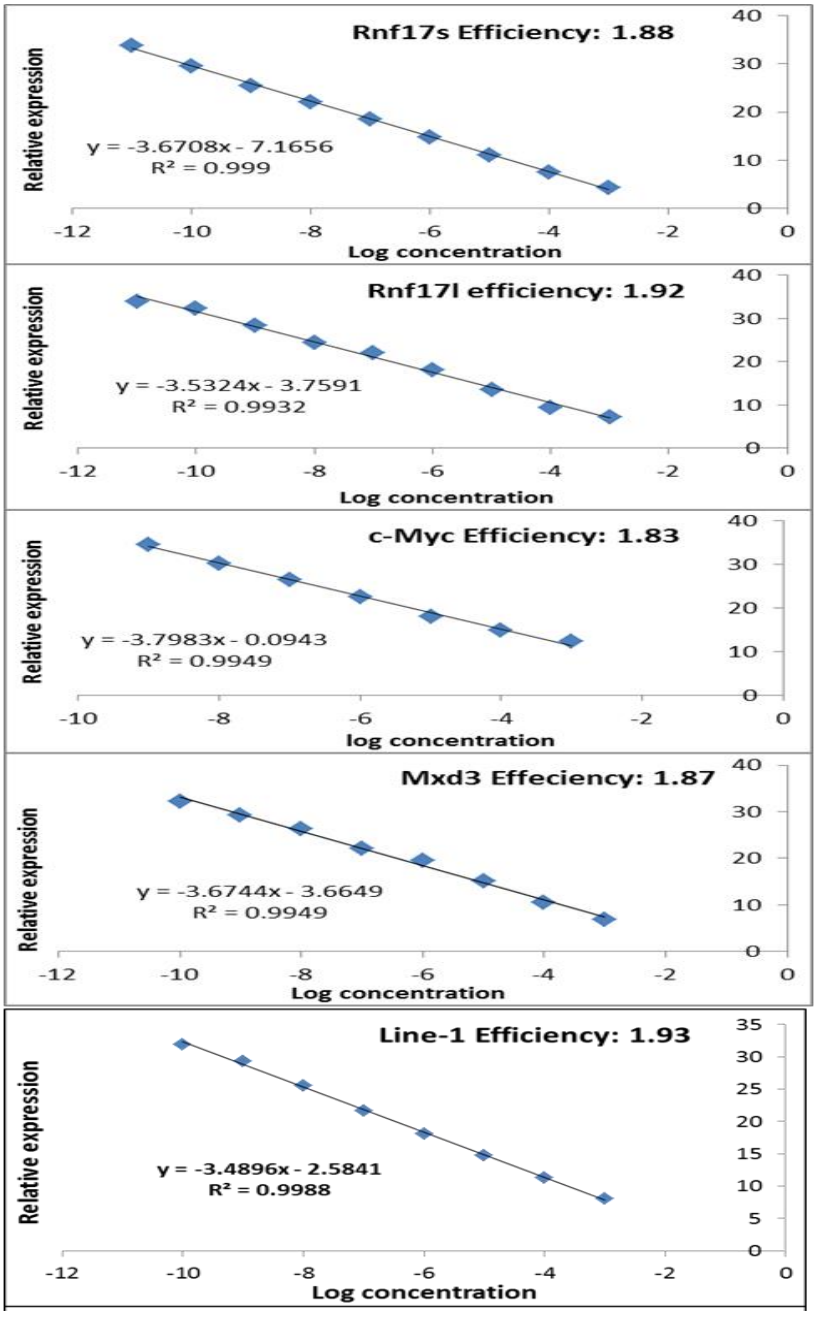

Fig 4.5: Standard curve generated from serial dilutions and calculated Efficiency of primers used in RT-qPCR. Mean Ct values was calculated for primer Efficiency and graphing the log of the serially diluted DNA samples from 100 pg/µl to 1 ag/µl vs. Ct value for each dilution.

4.3 Results

4.3.1 Expression of Rnf17, Myc, Mxd3 and Line-1 during preimplantation mouse embryo development

Expression of Rnf17, c-Myc, Mxd3 and Line-1 were examined in 2-cell, 4-cell, 8-cell, morula and blastocyst stages by RT-qPCR. Embryos were collected from mothers fed chow from the day of plug up to the date of embryo collection and cDNA was synthesised.

Rnf17S, Rnf17L, c-Myc, Mxd3 and Line-1 were expressed in all examined embryo stages and PCR products were visualised on 2% agarose gel electrophoresis (Fig 4.6). Primary data for the expression of examined genes and control Tuba were represented in the mean Ct values of the two replicates at one RT-qPCR cycle, and are shown in Table 4.1. Expression of Rnf17S and c-Myc were increased in parallel with the control Tuba1 in embryos developing from 2-cell up to blastocyst stages and the increased expression was associated with a reduction in Ct values of 6.48, 8.75 and 4.95, respectively. Expression of Rnf17L and Mxd3 displayed little change from the 2-cell to the blastocyst changes of 1.97, 0.74 in Ct, respectively.

PCR products were analysed by generating a melting curve in Figure 4.7 (bottom panel). The melting curve of a product is sequence specific: thus it distinguishes between specific and nonspecific PCR products. Figure 4.7 shows that the melting curve peak for Rnf17S (76.2ºC), Rnf17L (77.98ºC) and c-Myc (83.4ºC) are all amplified through all embryo stages. However, the melting curve peak for Mxd3 (85ºC) is amplified only at 8-cell, morula and blastocyst.

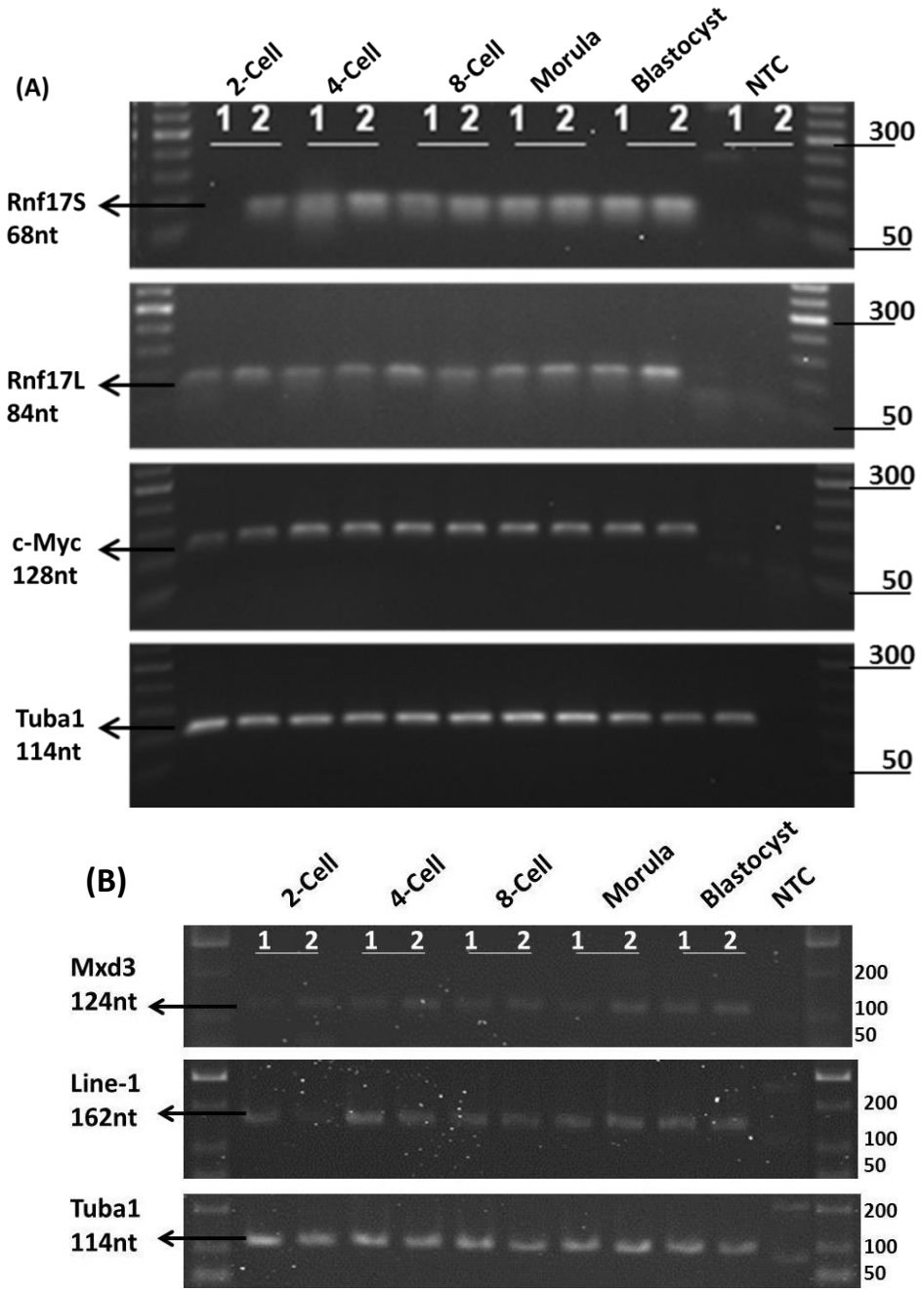

Fig 4.6: Expression of Rnf17S, Rnf17L, c-Myc, Mxd3 and Line-1 during mouse preimplantation development. RT-qPCR reaction was run in duplicate and PCR product size and expression were compared to positive control; Tuba1. **NTC**: no template control used as negative control. One replicate of 2-cell is missing from Rnf17S (Lane1).

Table 4.1: Ct values of Rnf17S, Rnf17L, c-Myc and Mxd3 compared to control Tuba1 during mouse preimplantation development. Data represented in mean value of two biological replicates.

	Rnf17S	**Rnf17L**	**c-Myc**	**Mxd3**	**Tuba1**
2-cell	35.47*****	34.61	35.69	34.71	26.63
4-cell	32.48	34.20	29.25	34.32	27.22
8-cell	31.81	34.06	29.04	33.94	24.95
Morula	29.78	33.96	28.04	33.92	22.16
blastocyst	28.99	32.64	26.94	33.97	21.68

*****One replicate

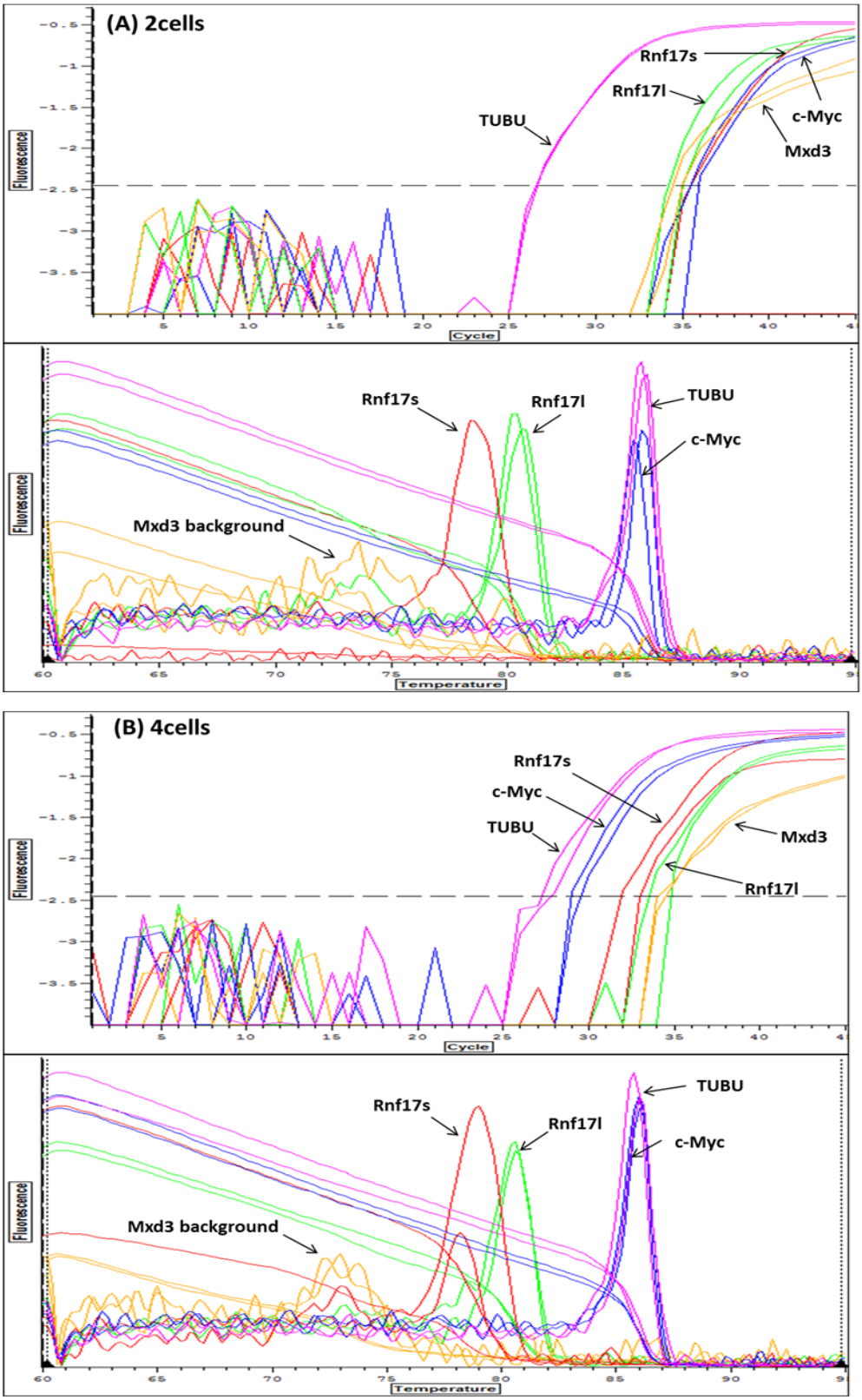

Fig 4.7 *(Continued)*

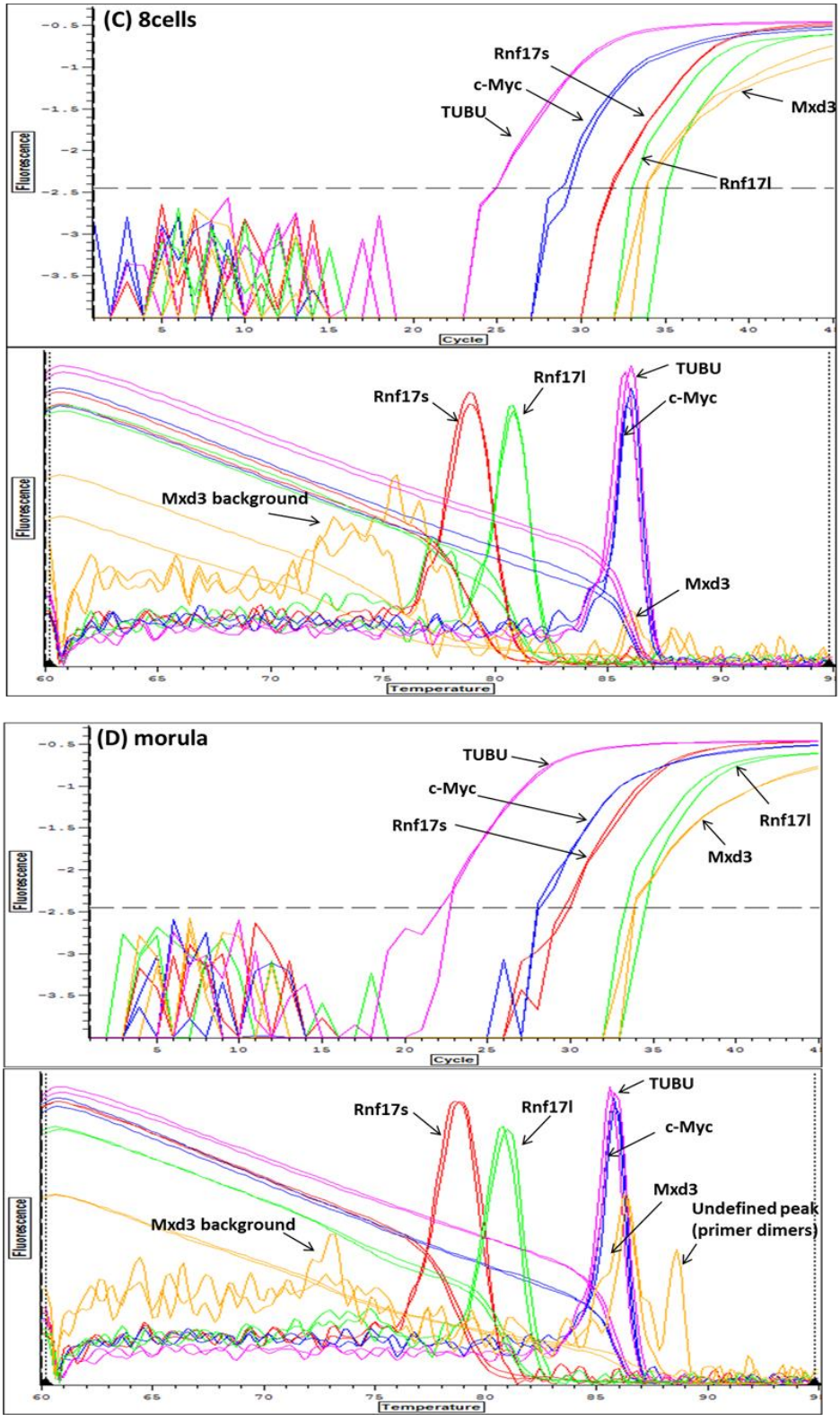

Fig 4.7 *(Continued)*

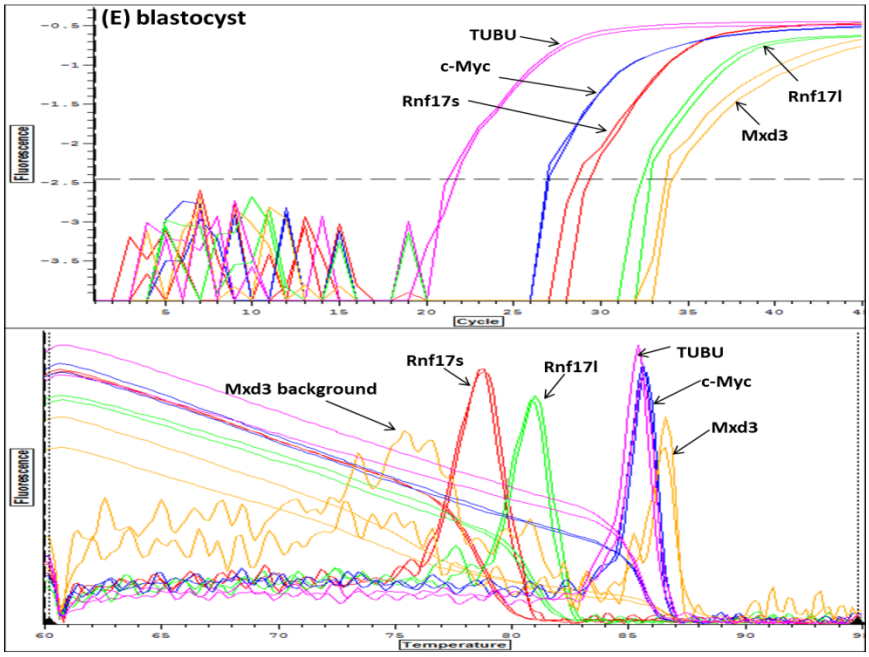

Fig 4.7: Expression of Rnf17, c-Myc and Mxd3 through preimplantation development using RT-PCR. Data graph for Log scale (top) and melting curve (bottom) exported from Opticon Monitor Microsoft for Rnf17S, Rnf17L, c-Myc and Mxd3 compared to control Tuba1. **(A)** 2-cell, **(B)** 4-cell, **(C)** 8-cell, **(D)** morula, **(E)** blastocyst. Melting curve peaks for Rnf17S, Rnf17L and c-Myc were amplified at all stages of the developed mouse embryo. Melting curve for Mxd3 (yellow) amplified at 8-cell, morula and blastocyst stages.

4.3.2 Subcellular localisation of RNF17 throughout preimplantation development

For negative control experiments, blastocysts were collected from mothers fed chow and incubated with pre-immune or immunised sera diluted 1:1000 in 1% BSA followed by secondary anti-goat/anti-rabbit conjugated with Alexa fluor 488. Diffuse and non-specific staining was seen with pre-immune and immune sera (Fig 4.8 A & B), probably reactions of non-specific proteins because what is eliminated following purification and a distinctive reaction with expected RNF17 was seen as shown below.

The second negative control was run by incubating blastocysts with the secondary antibody Alexa fluor 488. No fluorescence signal was detected in embryos incubated with secondary antibody indicating that no reaction with non-specific proteins has taken place (Fig 4.8C).

Mouse embryos were collected at different preimplantation stages and immunostained with anti-RNF17 and nuclei were labelled with DAPI. Embryos were examined by fluorescence microscopy. The data from examined embryos is shown in Table 4.2.

Table 4.2: Number for embryo stained with anti-RNF17. Embryos were collected at different cleavage stages from mothers fed chow from day of plug (E0.5) up to day of embryo collection.

Embryos stages	Number of examined embryos
Zygotes	**2 embryos from 1mother**
2-cell	**8 embryos from 3 mothers**
4-cell	**9 embryos from 3 mothers**
8-cell	**14 embryos from 4 mothers**
Morula	**17 embryos from 6 mothers**
Blastocyst	**17 embryos from 5 mothers**

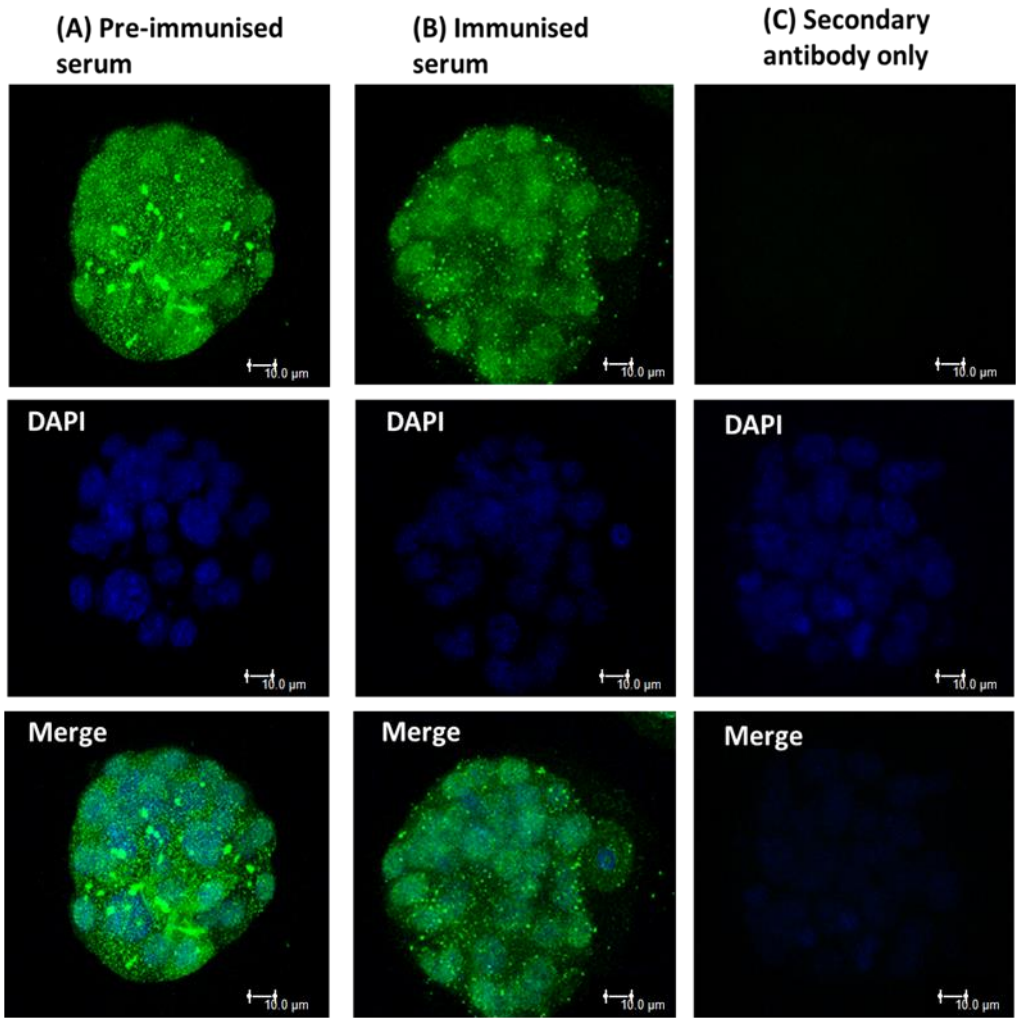

Fig 4.8: Negative control experiments for anti-RNF17 validation and protein detection in mouse blastocyst. Mouse blastocysts were immunostained with **(A)** pre-immune- or **(B)** immune-sera collected from immunised rabbits with the RNF17-fusion protein showed diffused and indistinctive staining of non-specific proteins. **(C)** Mouse blastocyst stained only with secondary antibody Alexa fluor 488 display no fluorescence signal indicating no cross-reaction with non-specific proteins. Nuclei were stained with DAPI, and embryos visualised by confocal microscopy.

RNF17 displayed distinct subcellular patterns during preimplantation development. RNF17 was deposited abundantly in the nucleus, and excluded from the nucleolus. RNF17 was also diffuse in the cytoplasm of early and late stages and displayed different patterns of subcellular expression at 4-cell and 8-cell (Fig 4.9).

The nuclear pattern of RNF17 was diffuse in the nuclei of zygote, 2-cell, morula and blastocysts (Fig 4.9 A, B, E & F), but was punctated in the nuclei of 4- and 8-cell embryos (Fig 4.9 C & D). RNF17 was diffuse in the cytoplasm of the zygote and 2-cell before the fluorescent signal became weaker at 4-cell and partially disappeared from the cytoplasm at 8-cell. RNF17 gradually increased in the cytoplasm of the morula with foci-like expression, and, thereafter, disappeared in the late blastocyst.

Using Volocity software, the intensity level for RNF17 in the nuclei was shown to increase relative to that in the cytoplasm by about 78% to 90% through the different preimplantation stages. The highest level was at 4-cell (90%) and 8-cell (91%), reflecting the disappearance of RNF17 from the cytoplasm of the 4-cell and 8-cell stages. The intensity level of RNF17 between the nuclei and the cytoplasm of blastocysts was the lowest throughout all the preimplantation stages (78%) (Fig 4.10). The mean number of RNF17 foci was increased at the 8-cell stage (Fig 4.11).

RNF17 was not expressed in the nucleus of mitotically divided cells. This was observed in cleaved embryos, morulae and blastocysts (Fig 4.12).

RNF17 was detected in the polar body of 2-cell stage before it became weaker at the 4-cell, then not detected in the following stages; 8-cell, morula and blastocyst (Fig 4.13).

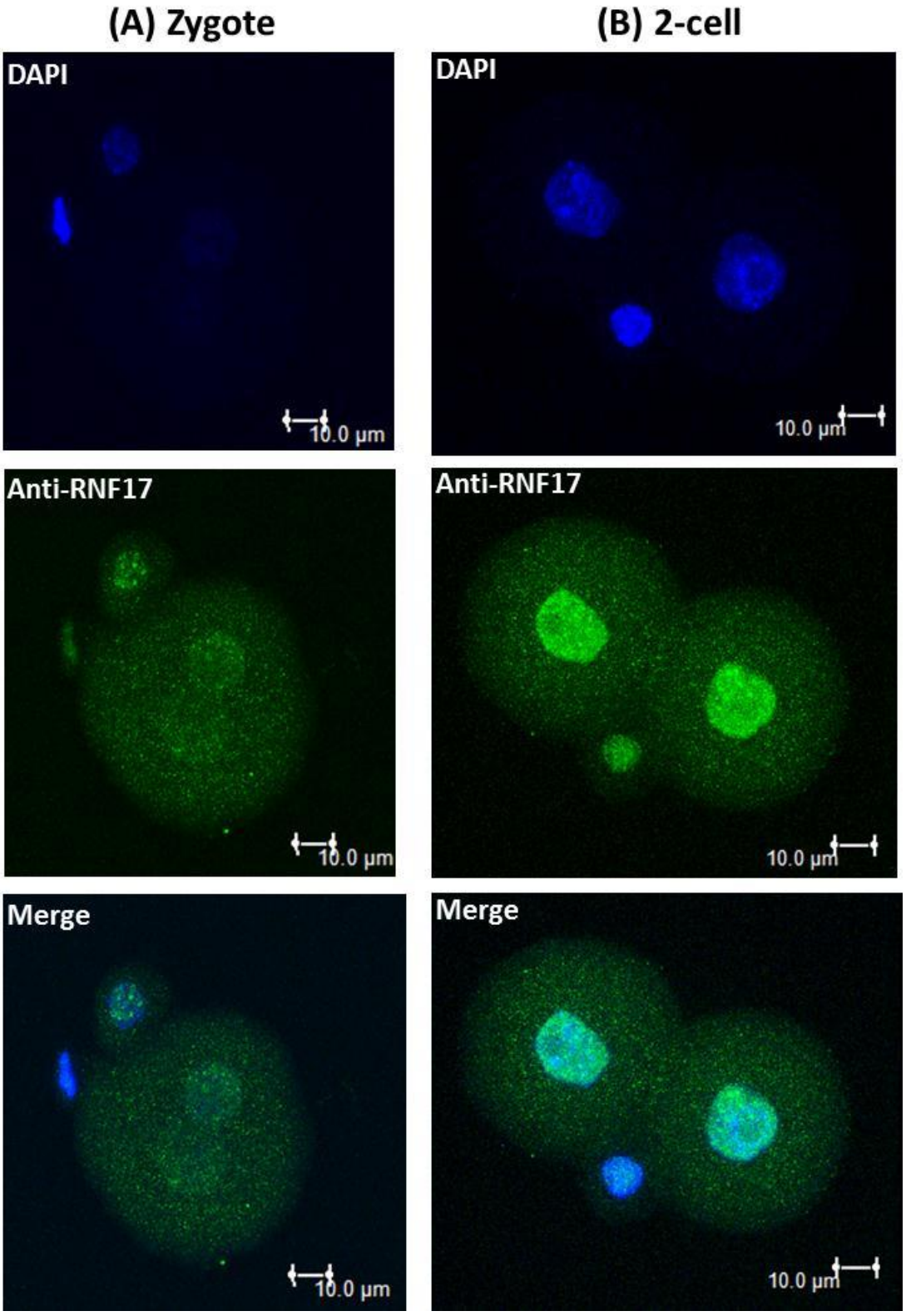

Fig 4.9 *(Continued)*

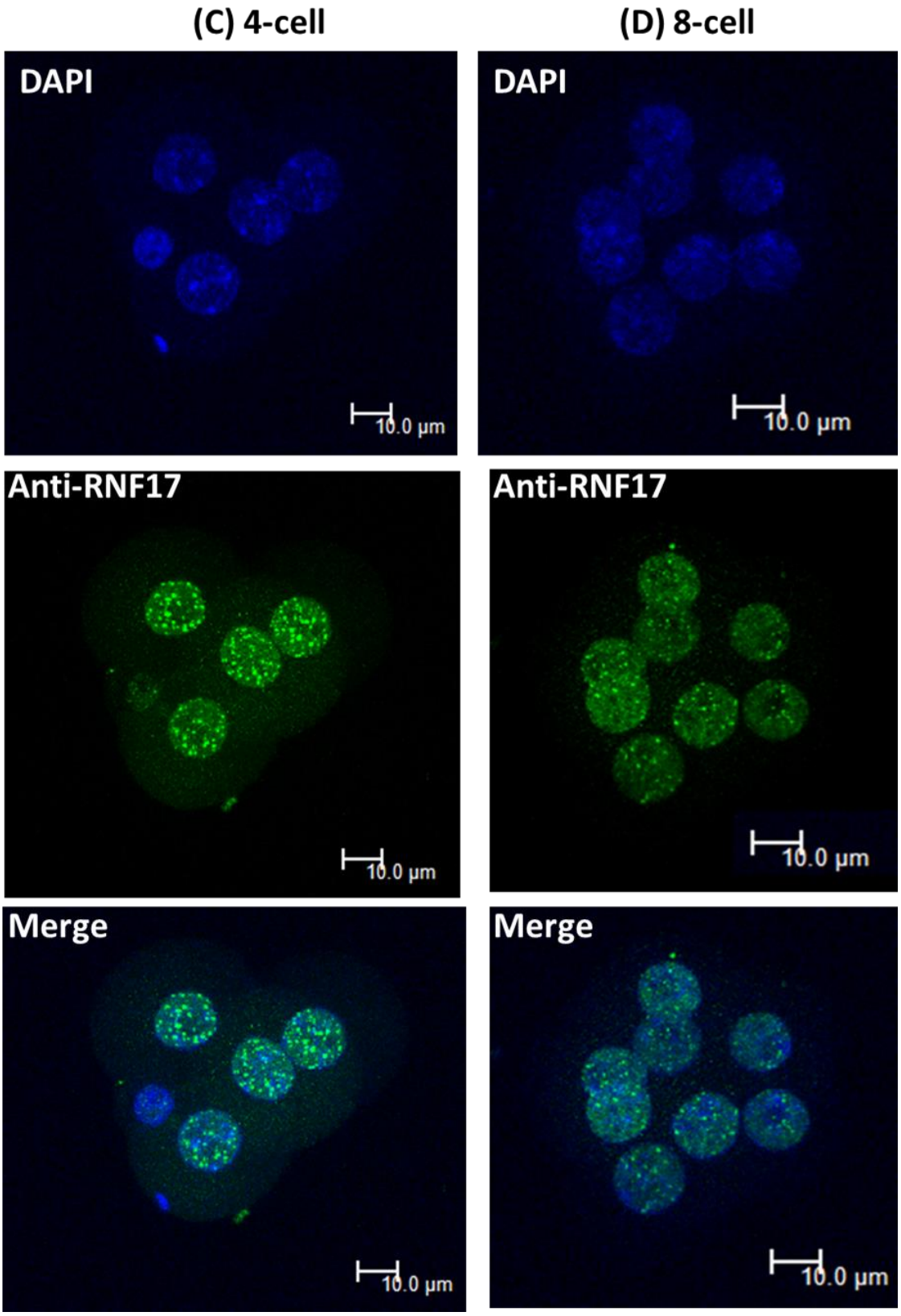

Fig 4.9 *(Continued)*

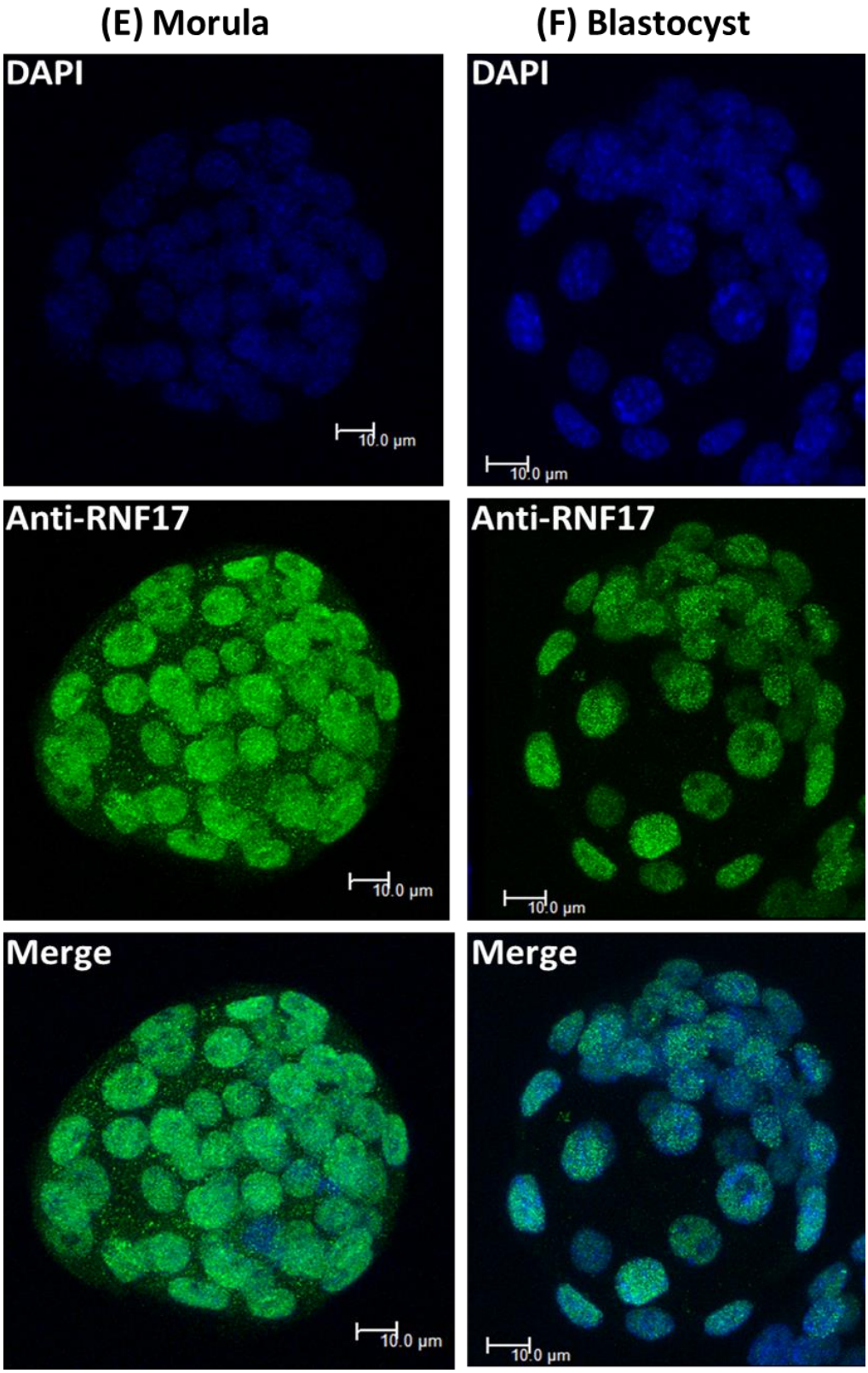

Fig 4.9 *(Continued)*

Fig 4.9: Subcellular localisation of RNF17 during preimplantation development. Mouse embryos from mothers fed chow were collected at different cleavage stages; **(A)** zygote, **(B)** 2-cell, **(C)** 4-cell, **(D)** 8-cell, **(E)** morula and **(F)** blastocyst. Embryos were immuno-labelled with affinity purified anti-RNAf17 and nuclei stained with DAPI. RNF17 is predominantly within the nuclei and diffuse in the cytoplasm of early (zygote and 2-cell) and late (morula and blastocyst) stages. RNF17 shows a punctuate distribution in the nuclei of 4- and 8-cell stages

- **Top panels:** staining of the nuclei with DAPI
- **Middle panels:** RNF17 signal
- **Bottom panels:** overlays (merge) of the two signals

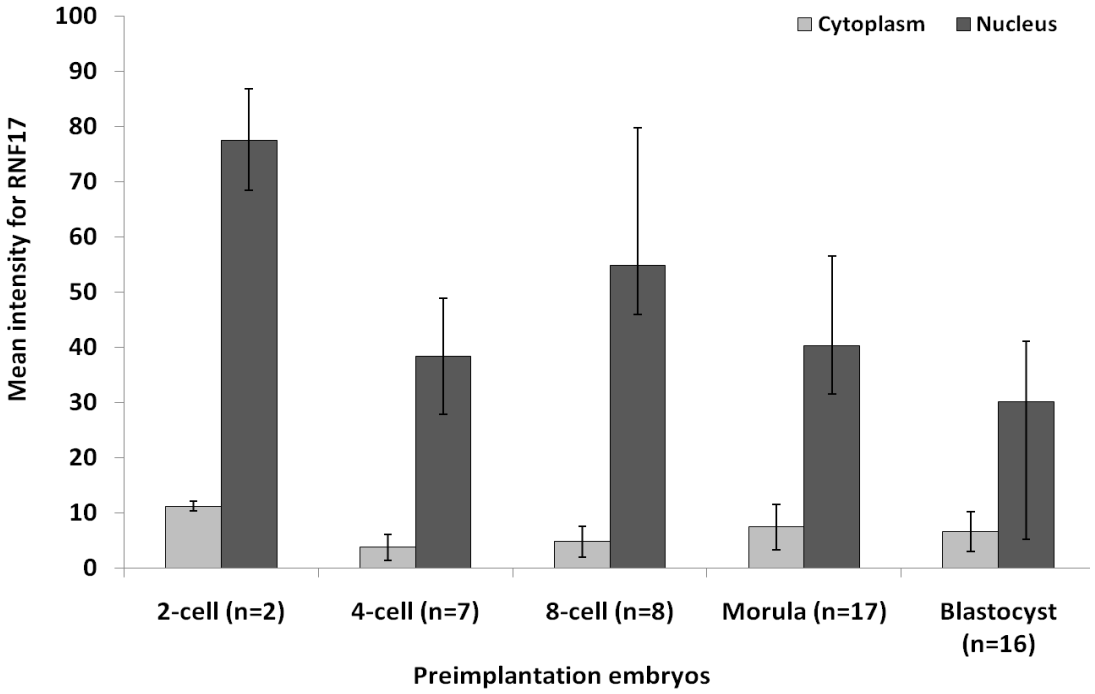

Fig 4.10: Mean intensity level for RNF17 in the nucleus and the cytoplasm throughout preimplantation stages. Mouse embryos were collected at different cleavage stages from mothers fed chow from day of plug (E0.5) up to day of embryo collection. Collected embryos were stained with anti-RNF17 and the level of fluorescence intensity was visualised by Leica SP5 confocal microscopy and measured using Volocity software. The intensity level of RNF17 was first determined in the nuclei then subtracted from total level of the embryo to calculate intensity level for RNF17 in the cytoplasm. Bar graphs show mean of examined embryos (n at each stage) and error bars represent standard deviation.

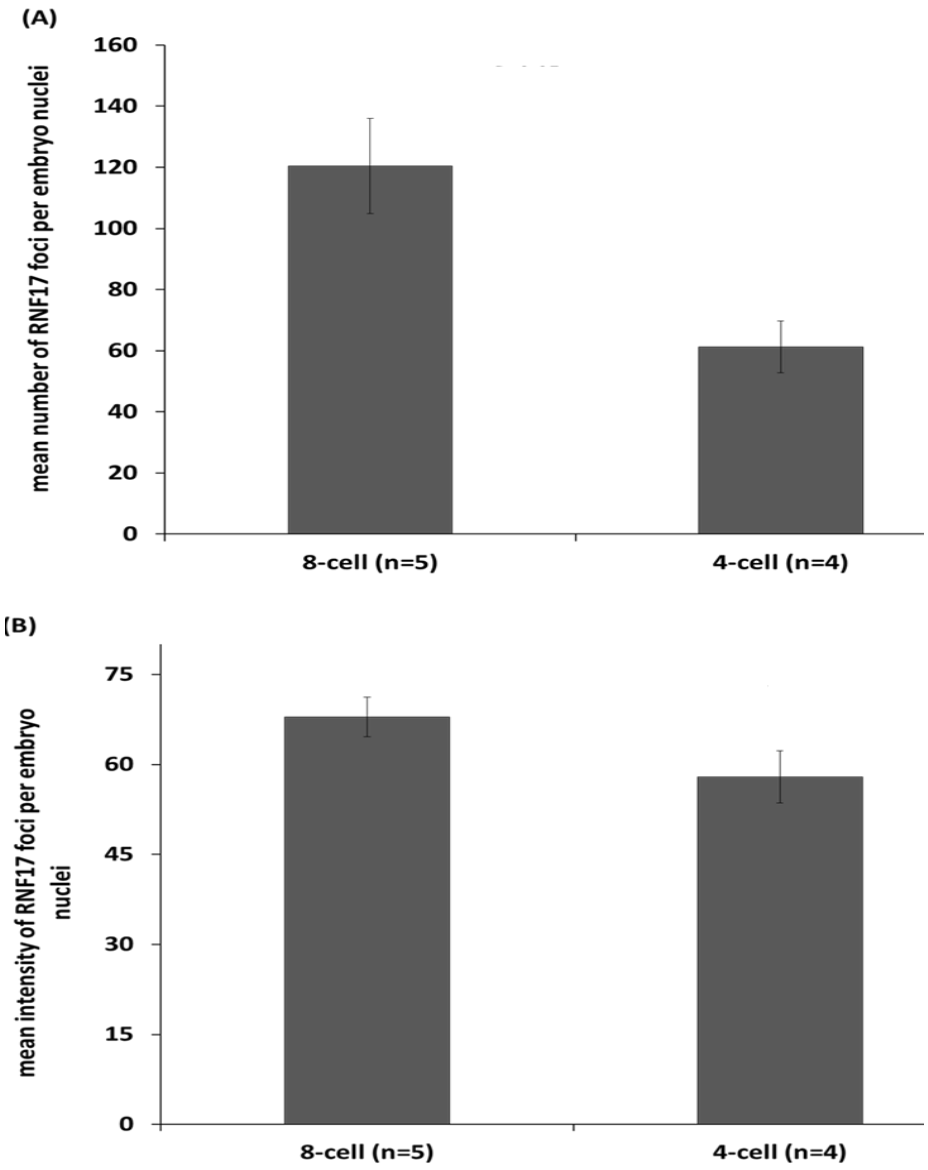

Fig 4.11: Number of RNF17 foci and mean intensity level of RNF17 foci in the nuclei of 4-cell and 8-cell embryos. Mouse embryos at 4-cell and 8-cell stages were collected from mothers fed chow and immunolabelled with anti-RNF17. Using Volocity software the number and intensity of RNF17 foci in the nuclei was calculated. Bar graphs show mean of examined embryos (n at each stage) and error bars represent standard deviation.

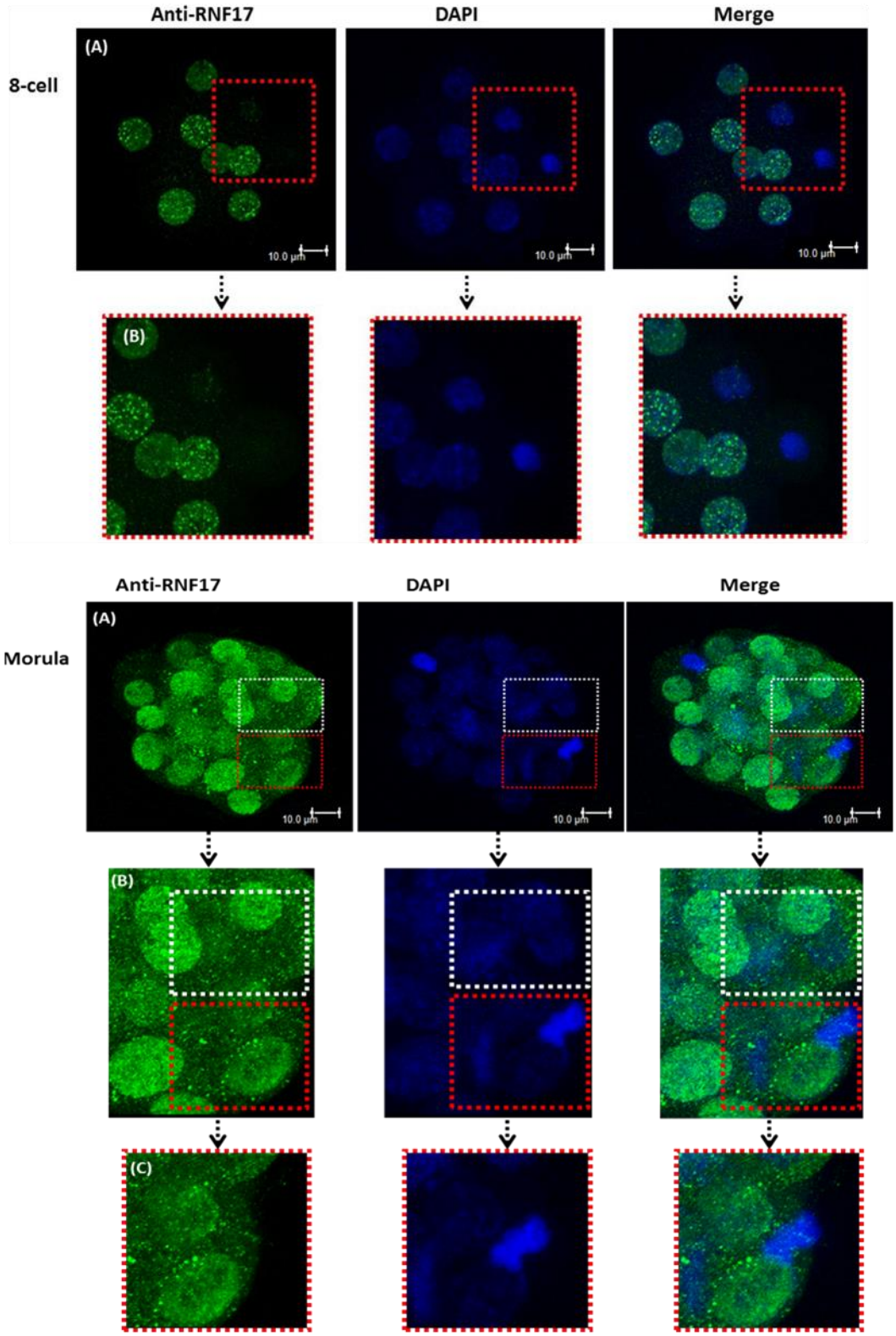

Fig 4.12*(continued)*

Fig 4.12: Expression of RNF17 in embryos during preimplantation development. (A) Embryos were immuno-labelled with anti-RNAf17 and nuclei stained with DAPI; dotted areas show blastomeres during mitosis**. (B)** Highly magnified cells show that anti-RNF17 is not detected in mitotic blastomeres at 8-cell and morula stages.

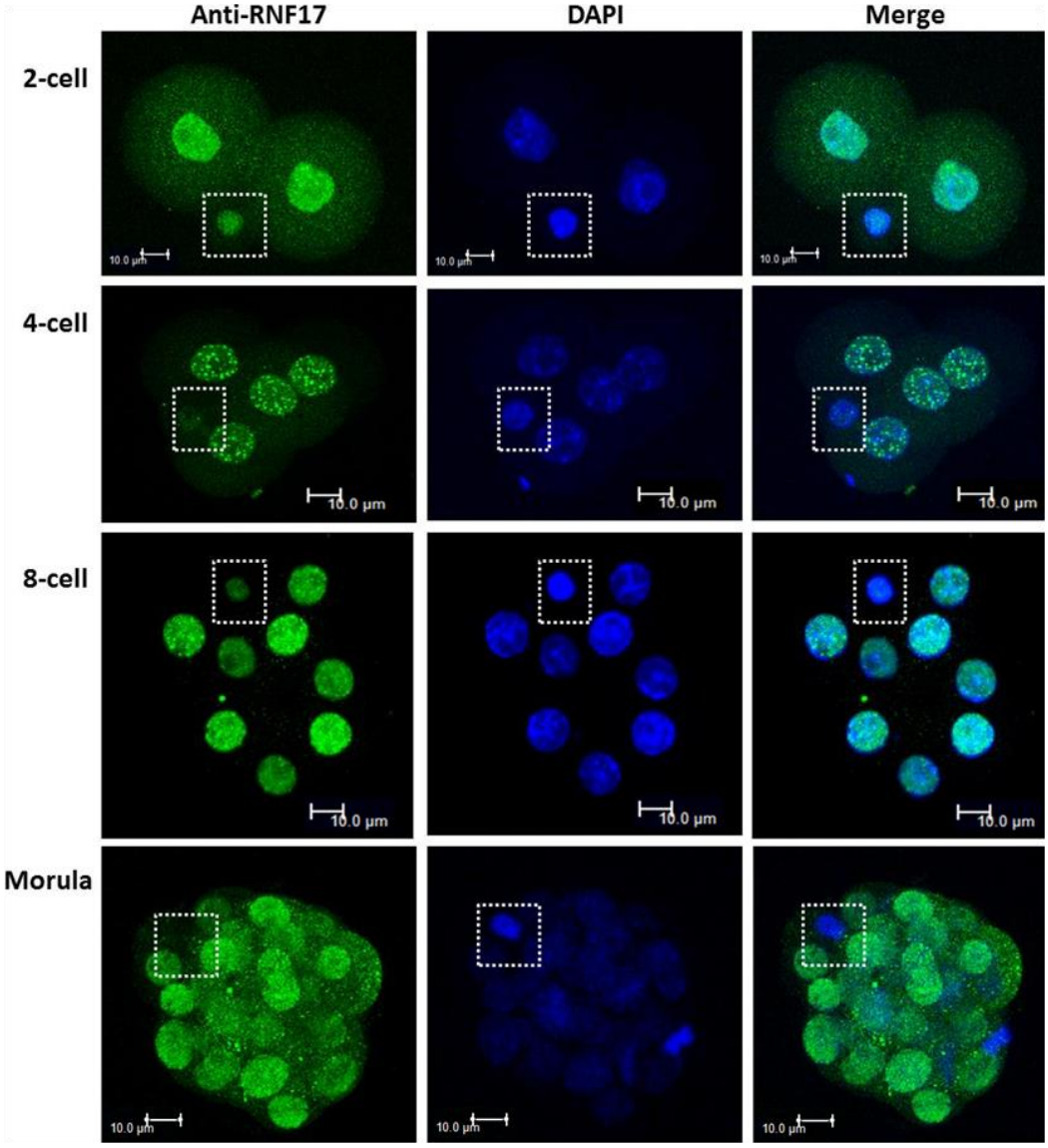

Fig 4.13: Expression of RNF17 in polar bodies during preimplantation development. Mouse embryos collected at different cleavage stages were immunolabelled with anti-RNF17 and nuclei stained with DAPI. RNF17 was detected in the polar body at 2-cell stage and gradually the signal reduced from 4-cell to 8-cell. No signal was detected for RNF17 at morula stage.

4.4 Discussion

In this chapter it is the first time that the expression of Rnf17 mRNA by RT-qPCR and the subcellular localisation of RNF17 protein were detected using confocal microscopy throughout the early embryo cleavage stages. Raw data for Ct values in RT-qPCR experiments showed that the expression of mRNA for Rnf17S and c-Myc increased throughout preimplantation development; i.e. between the 2-cell stage (E1.5) and blastocyst (E3.5). Rnf17S was highly expressed during preimplantation compared to Rnf17L.

Our results showed that expression of Rnf17 mRNA and RNF17 protein in the preimplantation embryo were consistent with Microarray data (E-GEOD-1749), as annotated by European Bioinformatics Institute (www.ebci.ac.uk) for the expression of Rnf17 mRNA in mouse oocyte and cleavage stages. The expression of RNF17 protein in the zygote may suggest a ubiquitination role of maternal RNF17 in degrading maternal proteins. Proteins involved in the ubiquitinylation pathway are up-regulated in the zygote, where they have been suggested to contribute to maternal proteins degradation (Wang *et al,* 2010; Hamatani *et al,* 2004). For example, a RING-finger containing protein, Ret Finger Protein-Like 4 (RFPL4) is an E3 ubiquitin ligase expressed in oocyte and is involved in degrading maternal transcripts (Suzumori *et al*, 2003). At the 2-cell stage, ZGA transition allows the degradation of maternal transcripts and initiates the expression of zygotic transcripts (Schultz, 2002). Expression of nuclear RNF17 protein at the 2-cell stage may suggest a changed distribution for RNF17, with enhanced nuclear localisation, and reveals that RNF17 is functioning as a transcriptional factor at time of ZGA.

Immunostaining results showed that RNF17 protein was punctated in the nuclei of the 4- and 8-cell embryos, whereas it started to disappear from the cytoplasm. Epigenetic chromatin remodelling occurs at ZGA and involves post-transcriptional modifications of nucleosomal histones, either repressive or activating. Several protein domains were found in chromatin-associated

proteins, such as Chromo, MBT and Tudor domains (Kim *et al,* 2006). A chromatin-associated domain array (CADOR) chip which reads the interaction of protein-domains with methylated histone tails, examined the binding of histone peptides with Tudor domain-containing proteins including RNF17 (Kim *et al,* 2006). This study used a human cDNA library and showed that Tudor domains of JMJD2 were bound to di- and tri- methylated H4K20 and to H3K4me3 and H3K9me3 (Kim *et al,* 2006; Huang et al, 2006) whereas Tudor domains of TDRD3 were bound with a symmetrically arginine-methylated (sDMA) peptide from the splicing factor SmD3 (SmD3-Rme2s) (Kim *et al,* 2006). SmD1 and SmD3 have been described to bind to the Tudor domain of SMN by sDMA (Ke *et al*, 2010). The highly conserved amino acids for Tudor domain-containing proteins (Thomson and Lasko, 2005) suggest a similar binding behaviour to that of TDRD3 or that of JMJD2. These findings may explain the punctated nuclear localisation of RNF17 that suggests the binding of RNF17 Tudor domains to histone tails, or SmD via sDMA for post-transcriptional modifications.

Rnf17 interacts with members of the Mxd family. In this chapter, expression of Mxd3 throughout early cleavage stages was detected in order to investigate the role of the interaction between Rnf17 and Mxd in the preimplantation embryo. Our results showed that Mxd3 mRNA, a member of the Mxd family, is first expressed at 8-cell and continued to blastocysts. Microarray analysis showed that Mxd2 increases in expression from the 4- to 8-cell stage (Hamatani *et al,* 2004). This indicates variability of the expression level of Mxd family at different cleavage stages. However, yeast two-hybrid screening and GST pull-down experiments showed that the interaction between RNF17 and MXD2 is the weakest of all the Mxd family members (Yin *et al,* 1999). Using electrophoresis mobility shift assays also revealed that RNF17 was less effective in reversing the effect of MXD2 than other Mxd members (Yin *el al*, 1999). This indicates that a strong interaction between Rnf17 and Mxd3 may reduce the expression level of Mxd3 in the

embryo. Another possibility is that immunostaining showed that RNF17 is exclusively expressed in the nucleus of 4- and 8- cell embryos, which may suggest interaction between RNF17 and MXD at this stage to increase Myc expression and induce cell proliferation.

PIWI proteins regulate the silencing of transposable elements via RNA-dependent DNA methylation in a process involving the interaction of PIWI with piRNA via Tudor domain-containing proteins (Seto *et al*, 2007; Hawkins *et al,* 2011). In Hamatani *et al* (2004) Microarray analysis showed that PIWI2 peaked at the 4-cell. Studies showed a functional link between retro-transposable activity and early embryo development. For example, murine ERV-L (MuERV-L) revealed the high contribution of transposable elements in 2-cell stage embryos and increased at 8- to 16-cell compared to LINE which was the highest fraction of transposons in growing oocytes (Ohnishi *et al*, 2010; Peaston *et al*, 2004). Using RT-qPCR, expression of Line-1 throughout preimplantation development was detected, and together with expression of RNF17 this may suggest a functional role for RNF17 in Piwi-piRNA interaction and transposable element silencing.

Immunostaining experiments showed that RNF17 protein disappears from mitotically divided cells in preimplantation embryos (Fig 4.12), and in F9 cells in Chapter 3 (Fig 3.11), which may indicate a role of RNF17 in mitosis cell entry or exit. Mitosis is a highly regulated process that ensures segregation of chromosomes into two daughter cells, and this is achieved by maintaining careful coordination of the protein levels of many mitotic regulators including RING-containing proteins (reviewed by Nigg, 2001). For example, the Bub1-related 1 (BubR1) and Mitotic Arrest Deficient-Like 2 (Mad2) gene are essential components of the mitotic checkpoint pathways. They inhibit the ubiquitin ligase activity of the Anaphase Promoting Complex/ Cyclosome (APC/C) during mitosis by binding and sequestering Cdc20, an APC/C activator. This property of the BubR1 and Mad2 is important to ensure cells

with unaligned chromosomes do not prematurely enter anaphase (Chan and Yen, 2003; Fang *et al*, 1998; Guo *et al,* 2012). In contrast, the expression of other RING-containing proteins is essential for mitosis entry. For example, the Checkpoint with forkhead and RING finger (CHFR) protein is a ubiquitin ligase and exhibits RING domain-dependent auto-ubiquitinylation activity *in vivo* that makes it capable of catalyzing its own ubiquitinylation (Privette and Petty, 2008). CHFR protein plays an important role in regulating mitosis at early to mid-prophase (by regulating the G2–M transition), and might have further roles in spindle formation, centrosome separation and chromosome segregation (Chaturvedi *et al,* 2002; Privette and Petty, 2008; Castiel *et al,* 2011). CHFR also plays a role via ubiquitinylation, in mediating the function of Still protein in centrosome organization, entry into mitosis and cell proliferation. Still (Sil, SCL/TAL1 interrupting locus) is a cytosolic and centrosomal protein expressed in proliferating cells and accumulates in a cell-cycle-dependent manner, reaching peak levels at the G2–M boundary (Castiel *et al,* 2011). Taken together, it is possible that the disappearance of RNF17 protein in mitotically divided cells is required for mitosis cell entry. RNF17 is bound to itself in GST pull-down assay and both isoforms (RNF17L and RNF17S) were co-Immunoprecipitated from adult mouse testis suggesting a possible heterodimer complex (Pan *et al,* 2005). This may raise the possibility that RNF17 possess auto-ubiquitinylation activity that allows it to catalyse its own ubiquitinylation at the time of cell cycle entry and to enhance the disappearance of RNF17 from mitotic cells. Clearly, the inhibition of ubiquitin ligase activity of RNF17 via mitotic checkpoint pathways is important to ensuring a correct chromosomal alignment during the mitosis phase and the correct segregation of chromosomes into two daughter cells.

RNF17 is detectable in first and second polar bodies and this was seen in zygote and 2-cell stages, and weakly in 4-cell (Fig 4.13), however our results had not discriminated between the first or the second polar bodies at these different stages. First and/or second polar bodies chromosome analysis is

now used extensively in preconception or prenatal genetic diagnosis (PGD) in ART clinics. PGD studies revealed that chromosomes extruded into the first and second polar bodies mirror the genetic and reproductive potentials for those remaining in the oocyte following meiosis resumption or second meiotic division of the fertilised oocyte (Evsikov and Evsikov, 1994; Wakayama and Yanagimachi, 1998; Durban *et al* 1998; Geraedts *et al,* 2011). Thus it is possible that the RNF17 signal that is observed in the polar body is because the polar bodies contain the counterparts of the chromosomes expressing RNF17. This signal was observed to remain until the polar bodies degenerated in the apoptotic-like process.

To summarise, Rnf17 mRNA is expressed in preimplantation embryos predicting a role in embryo growth and development. Expression of RNF17 protein at the zygote stage revealed that further expression of RNF17 is transcribed from maternal RNF17. The expression of RNF17 protein in the nuclei of the cleaved embryo suggested a transcriptional function for RNF17 proteins. It is suggested that RNF17 may bind to histone H3 and/or H4 tails and is involved in post-transcriptional modifications that are required for embryo growth and development.

Chapter 5

5. Effect of Maternal Diet on Expression of Rnf17 in Mouse Blastocysts and Foetal Testis

5.1 Introduction

Maternal dietary protein restriction during preimplantation development is associated with embryo development, specifically blastocyst proliferation. LPD (9% casein) has been shown to influence embryo proliferation by increasing the blastocyst number and inducing blastocyst TE proliferation (Eckert *et al*, 2012). Although Rnf17 function has not been studied in the early embryo, Affymetrix Microarray and bioinformatics analysis performed by our laboratory (Papenbrock *et al*, unpublished data) revealed differential regulation of c-Myc and Rnf17 expression in blastocysts in response to maternal LPD compared to control NPD. No data were reported for long-term effects of differential regulation of Rnf17 or members of the Myc/Max/Mxd network on embryo development in response to maternal diets.

Maternal diets have also been shown to affect the level of gene expression by inducing or modifying DNA methylation and epigenetic changes (Cooney *et al,* 2002; Wolff *et al*, 1998; Morgan *et al*, 1999; Sinclair *et al*, 2007). DNA methylation is required to silence the expression of transposable elements which is important for genomic integrity and germ cell development (De Fazio *et al*, 2011). No data has been reported on the effects of maternal LPD or HPD on the expression or silencing of transposable elements in the preimplantation embryo or in developed germ cells. DNA methylation-mediated silencing of transposable elements occurs through the piRNA pathway which involves interactions of PIWI proteins with piRNA via Tudor domain-containing proteins (Beyret *et al*, 2012; Suh and Blelloch; 2011; Thomas and Lin, 2009). Tudor domain-containing proteins (TDRD1 and TDRD9) interact with PIWI proteins (MILI and MIWI2) in cytoplasmic chromatoid bodies to

silence transposon elements through the piRNA pathway (Shoji *et al,* 2009). piRNAs were found to be Immunoprecipitated with MILI from neonatal and adult mouse testes (Aravin*et al*, 2006; 2007).

RNF17 is a Tudor domain-containing protein and Immunoprecipitates with MIWI in adult mouse testis (Vagin *et al*, 2009) and with the ZILI zebrafish homologue of mouse MILI in zebrafish testis and ovary (Huang *et al*, 2011). The *D.melanogaster* Kumo protein homologue of mouse RNF17 interacts with nuage components, in germline cells of *Drosophila* egg, and this interaction is required for the localisation of piRNA pathway proteins to the perinuclear nuage for transposon repression (Anand and Kai, 2012). Microarray analysis identified that Rnf17, Tdrd7 and Piwil2/Mili are expressed in mouse germ cells at E15.5 and are involved in germ cell development. The study suggests a role of expressed genes in regulating DNA methylation and epigenetic modification in, a stage of *de novo* DNA methylation.

1.1.1 Aim of experiment

The aim of these experiments is to investigate the short and the long term effects of maternal LPD or HPD on the expression of Rnf17 mRNA and RNF17 protein in mouse embryos. For short term effects, mouse blastocysts at E3.5 were examined, whereas for long term effects the E17.5 mouse foetal testis were examined using RT-qPCR.

The second aim is to use the anti-RNF17 to detect whether maternal LPD or HPD alters the expression of RNF17 protein or changes its subcellular localisation in mouse E3.5 blastocysts and E17.5 testis.

1.2 Methods

5.2.1 Creating a standard curve for data normalization

Six reference genes (*Tuba1, 18S, Sdha, Mapk1, Canx* and *Tbp*) were selected, from the most commonly used housekeeping genes, for normalization of the examined genes in E17.5 foetal testis under maternal LPD or HPD compared to the control NPD. The efficiency of the designed primers for selected reference genes *Tuba1, 18S, Sdha* and *Tbp* was previously calculated by our laboratory (Lucas *et al*, 2011). The efficiencies of the designed primers for *Mapk1* and *Canx* were calculated by generating standard curves from reactions with serial dilutions of the previously prepared products from F9 cDNA (Fig 5.1 & Fig 5.2).

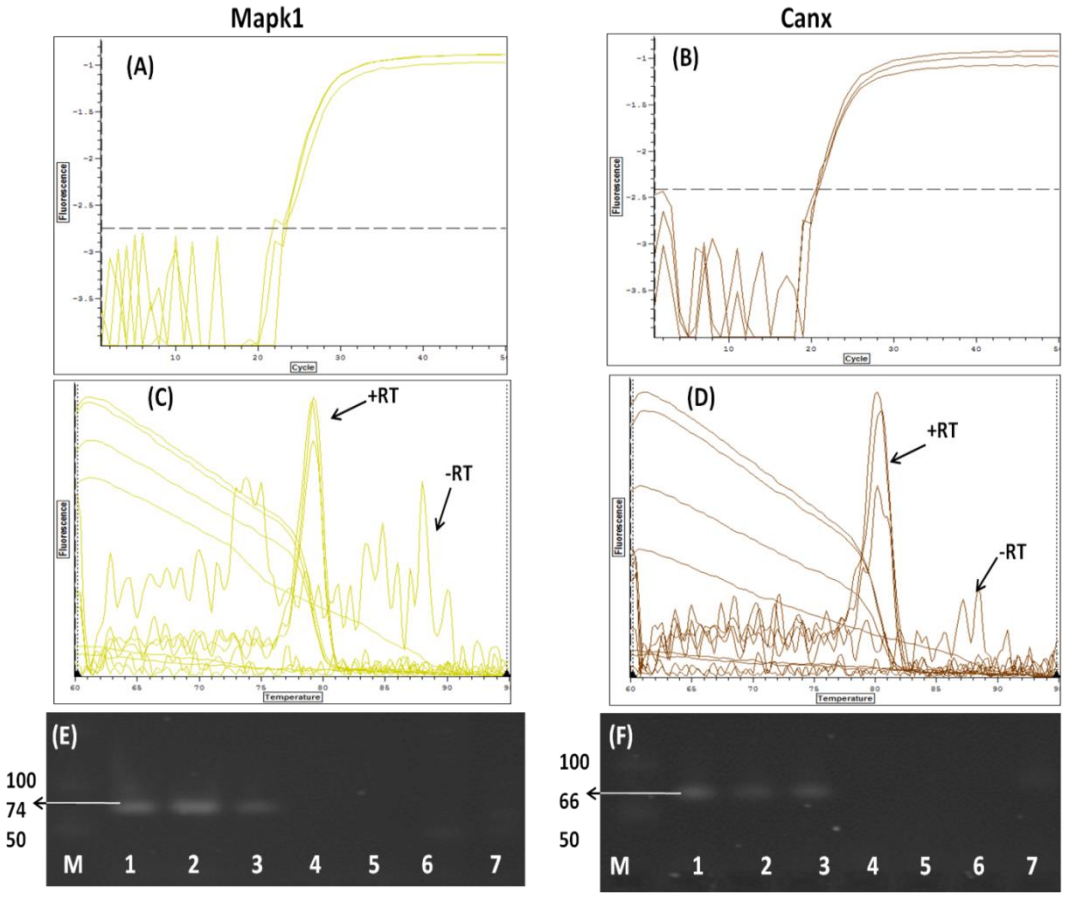

Fig 5.1: Primer specificity for Mapk1 and Canx. Primers for Mapk1 **(A, C, E)** and Canx **(B, D, F)** were tested using F9 cell cDNA. Ct plots (A, B), melting curve graphs (C, D) and product sizes (E, F) are shown from reactions. Expected sizes for the products are: MapK1 (74 bp) and Canx (66 bp)**.**

- **Lane 1-3:** mRNA treated with reverse transcriptase (RT)
- **Lane 4-6:** mRNA without RT
- **Lane 7:** no template control.

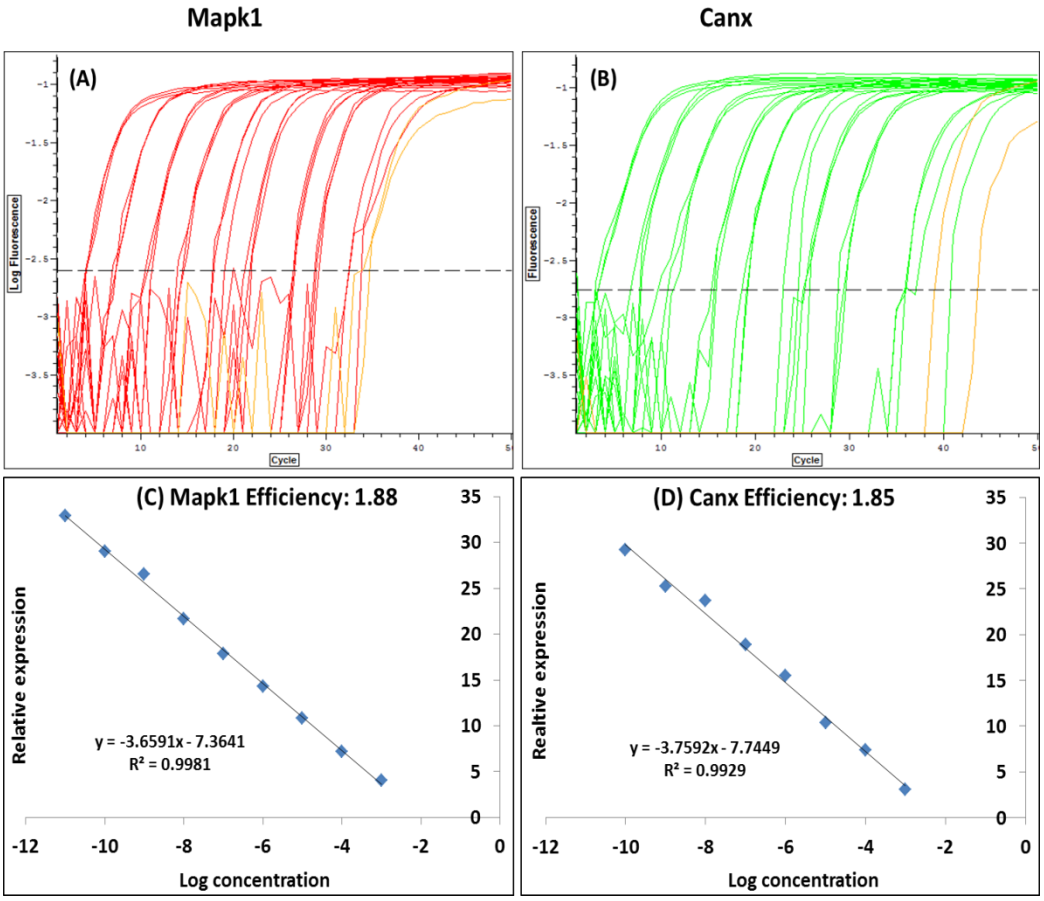

Fig 5.2: Determination of Efficiency for Mapk1 and Canx primers. Serial dilutions from (100 pg/µl) to (1 ag/µl) were generated from the products shown in (Fig 5.1) and used in reactions with Mapk1 primers **(A, C)** and Canx **(B, D).** The efficiency was determined by plotting the log concentration of the serially diluted DNA against the Ct value determined for each DNA dilution.

5.2.2 Determination of the most stable genes for data normalization in E17.5 foetal testes in response to maternal LPD, HPD and control NPD

RT-qPCR was run to assess the expression of selected 6 reference genes (*Tuba1, Mapk1, Canx, Tbp, Sdha,* and *18S)* in 8 samples from different mothers in each diet group; LPD, HPD or control NPD. Raw expression values were represented by mean Ct values of two biological replicates of each sample. Results showed a wide range of mRNA expression for the tested genes (Ct: between 13 and 23) (Fig 5.3) with no variations between diet treatments (LPD, HPD and control NPD). These results reflect the stability of tested reference genes under our experimental conditions.

Figure 5.4 shows the expression stability (*M)* of reference genes determined by GeNorm and NormFinder. Both softwares ranked *Mapk1* as the most stable gene with a lower *M* value (*M*= 1.049 for GeNorm and *M*= 0.156 for NormFinder) in E17.5 foetal testis in response to maternal NPD, LPD and HPD. The second most stable gene was *Tbp* (*M*= 1.110) ranked by GeNorm, whereas *18S* (*M*= 0.281) was ranked by NormFinder (Table 5.1). For data normalisation the geometric mean for *Mapk1* and *Tbp* was calculated and used as the normalisation factor to normalise the expression of the target genes.

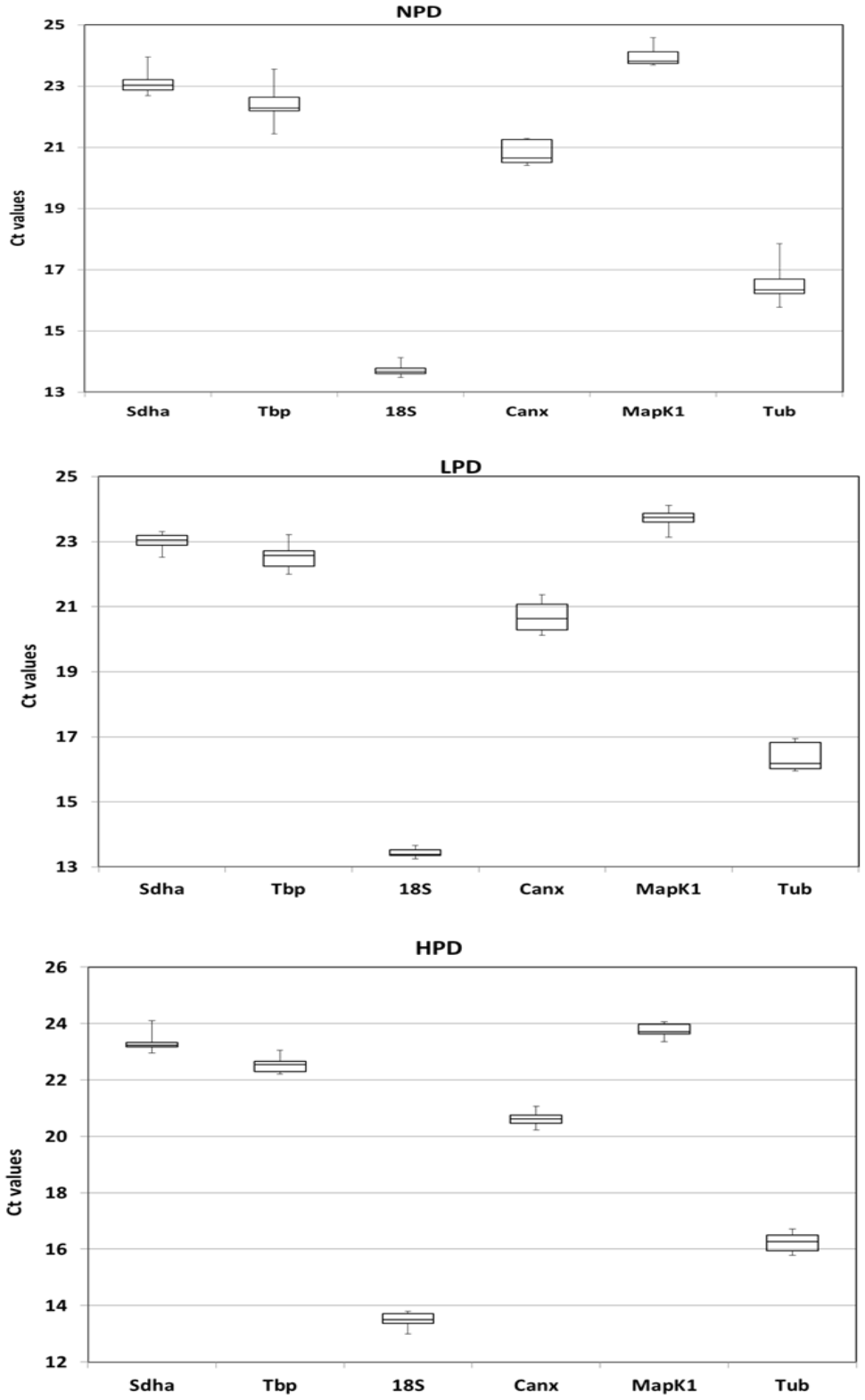

Fig 5.3 *(continued)*

Fig 5.3: Box plots representing mean Ct values for the 6 reference genes assayed in E17.5 foetal testis under maternal LPD, HPD and control NPD. Extracted RNA from diet foetal testes was subjected to RT-qPCR to examine stability of a number of reference genes under diet groups. Each box plot is based on the mean of biological duplicate Ct value for 8 samples per diet group. Boxes represent the lower and upper quartile ranges, the line between upper and lower boxes represent the median and whiskers indicate the maximum and the lower data value ranges.

Table 5.1: Ranking of the candidate reference genes according to their stability in tested samples of foetal testis in response to maternal diet.

Stability	**GeNorm**		**NormFinder**	
	Gene name	*M* values	Gene name	*M* values
Most stable	Mapk1	1.049	Mapk1	0.156
↓	Tbp	1.110	18S	0.281
↓	18S	1.214	Tbp	0.367
↓	Sdha	1.273	Sdha	0.488
↓	Canx	1.732	Canx	1.433
Least stable	Tuba1	2.246	Tuba1	2.515

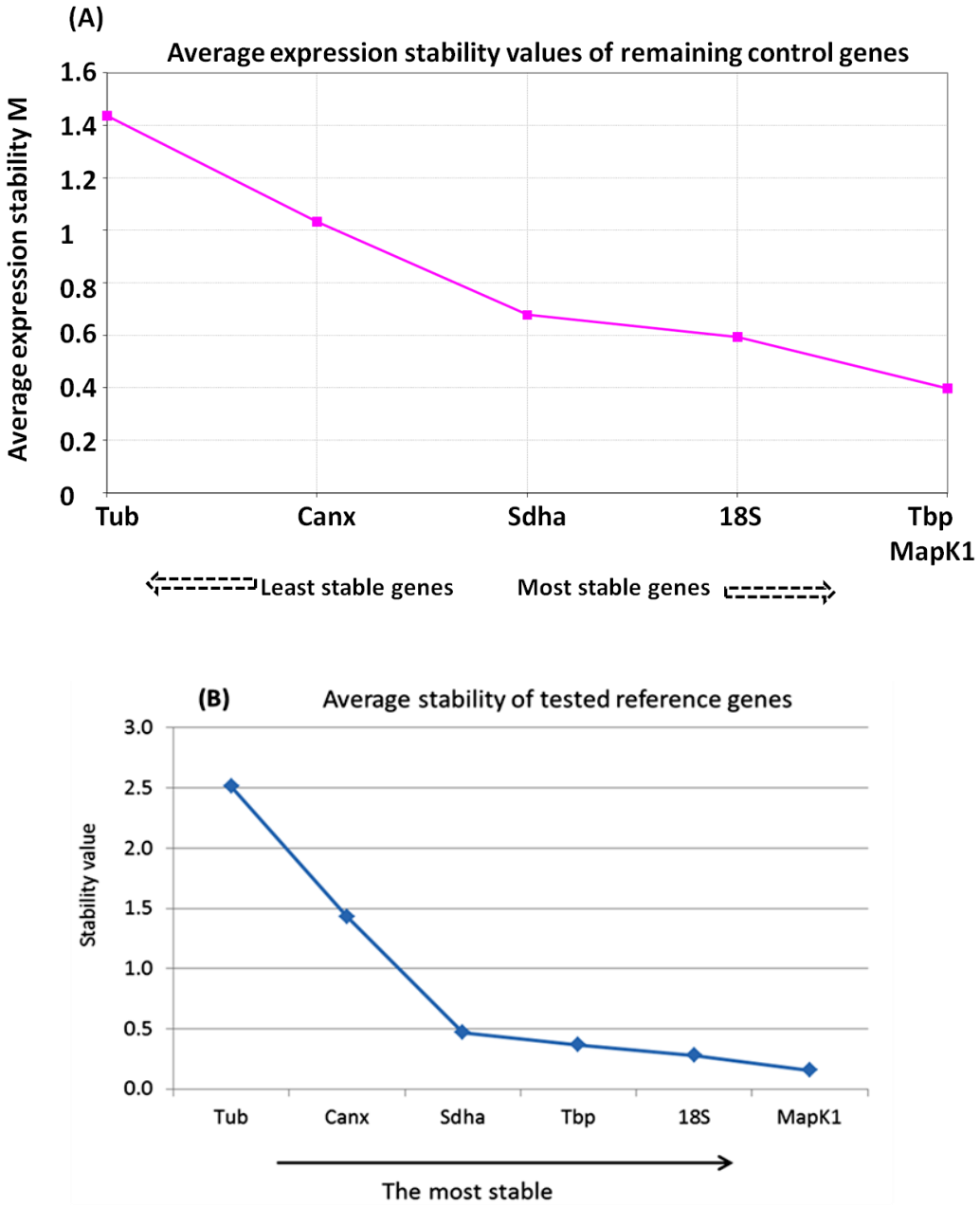

Fig 5.4: Stability values (*M*) for six reference genes tested in E17.5 foetal testis collected from different mothers fed LPD, HPD and control NPD. Average expression stability (*M)* values were ranked by **(A)** GeNorm and **(B)** NormFinder. High *M* values represent genes that have low stability; whereas low *M* values represent the most stable gene.

5.3 Results

5.3.1 Effect of maternal LPD or HPD on expression of Rnf17 and members of Myc/Max/Mxd network in mouse blastocyst

According to the results in Chapter 4, genes with early Ct values were tested using RNA extracted from single blastocysts, (Rnf17S, c-Myc and Lin-1) and genes that expressed late Ct values were tested using RNA extracted from a pool of five blastocysts (Rnf17L and Mxd3). The five pooled embryos were considered as a single embryo and were only collected from one mother. Single or pooled samples were analysed in duplicate and mean Ct values were normalised to the most stable reference genes (Tuba1 and Ppib) by calculating the geometric mean of selected reference genes. Table 5.2 shows the numbers (n) of statistically analysed embryos within each dietary group.

Table 5.2: Number of embryos analysed for RT-qPCR within each dietary group.

	NPD	LPD	HPD
	Single embryo		
Rnf17S	16 embryos from 9 mothers	16 embryos from 11 mothers	14 embryos from 10 mothers
c-Myc	16 embryos from 9 mothers	16 embryos from 11 mothers	14 embryos from 10 mothers
Line-1	8 embryos from 6 mothers	8 embryos from 5 mothers	7 embryos from 5 mothers
	Pooled embryos*		
Rnf17L	50 embryos from 8 mothers	45 embryos from 8 mothers	50 embryos from 10 mothers
Mxd3	40 embryos from 8 mothers	35 embryos from 7 mothers	40 embryos from 8 mothers

* Five embryos collected from same mother were pooled together and were considered as a single embryo per RT-qPCR.

The expression of Rnf17S, Rnf17L, c-Myc, and Mxd3 were not significantly different in mouse blastocysts from LPD or HPD maternal diet treatments compared to the control NPD. However, the expression of Rnf17L was decreased 40% in LPD blastocysts compared to HPD blastocysts (Fig 5.5).

The expression of Mxd3 was the lowest among the examined genes. Although Line-1 was not significantly different between the dietary groups, Line-1 was 20% lower in LPD blastocysts and 30% lower in HPD than control NPD (Fig 5.5).

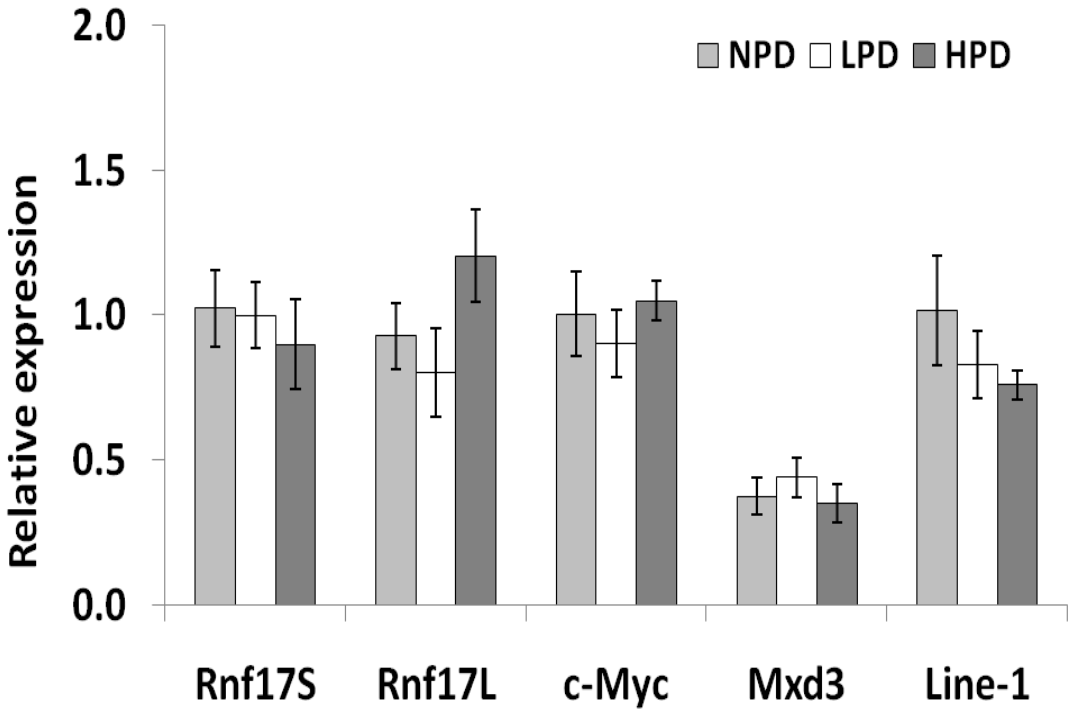

Fig 5.5: Expression profile of Rnf17, members of the Myc/Max/Mxd family and Line-1 in mouse blastocyst in response to maternal LPD, HPD and control NPD. Single blastocysts were analysed for Rnf17S, c-Myc and Lin-1, whereas a pool of five blastocysts were analysed for Rnf17L and Mxd3. Relative expression represents normalisation of examined gene to the geometric mean of two reference genes; Tuba-1-α and Ppib. Bar graphs show mean of examined embryos (Table 5.2) and error bars represent standard error of mean.

5.3.2 Effect of gender on expression of Rnf17 and members of Myc/Max/Mxd network in mouse blastocysts in response to maternal LPD, HPD and control NPD

Embryo sexing was applied through detection of *Sry* and *Zfy* genes on the Y chromosome. Male-specific fragments were represented by two bands amplified by primers for *Sry* (147 bp) and *Zfy* (217 bp) genes, whereas a single band was observed for *DXNds* (111 bp) fragments from both male and female (Fig 5.6). Samples not showing any amplified bands were excluded from the statistical analysis. The numbers of embryos examined are shown in Table 5.3.

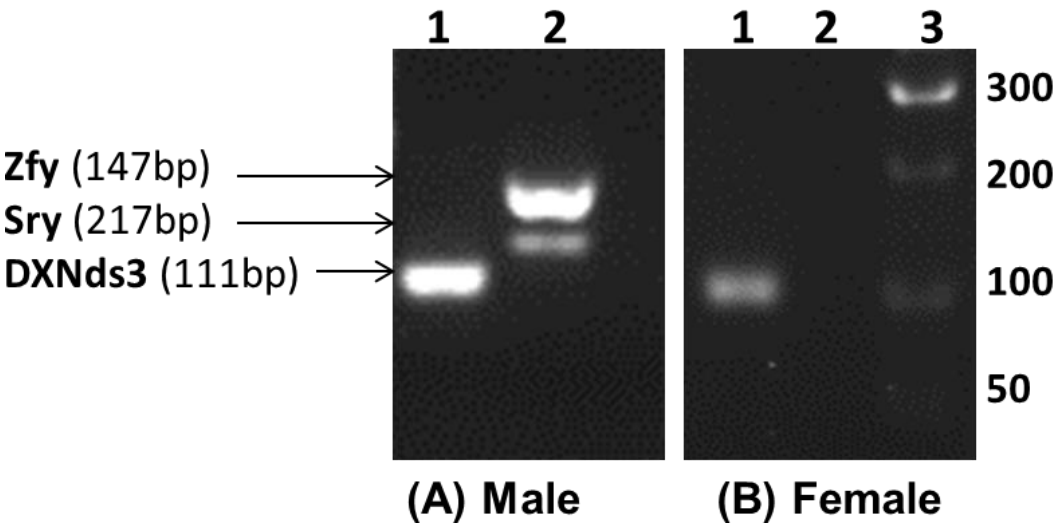

Fig 5.6: An example of blastocyst sex determination from single mouse embryo DNA. (A) Male embryo with Y-specific target sequences (Zfy and Sry) and a polymorphic microsatellite locus located on X chromosome (DXNds3). **(B)** Female embryo with DXNds3. Products of second-step PCR with DXNds3-specific primers **(Lane 1)** and with Zfy and Sry **(Lane 2).**

Table 5.3: Number of embryos examined for embryo sexing within each dietary group. The test was performed for Rnf17S and c-Myc from the same embryos.

Male	Female
•**NPD**	
5 embryos from 5 mothers	6 embryos from 4 mothers
•**LPD**	
5 embryos from 5 mothers	6 embryos from 4 mothers
•**HPD**	
2 embryos from 2 mothers	5 embryos from 5 mothers

As shown in Figure 5.7A, Rnf17S expression was increased in male blastocysts than female blastocysts derived from LPD and NPD groups.

The expression of c-Myc was analysed in individual blastocysts used for Rnf17S. The expression of c-Myc was more sensitive to maternal LPD in male blastocysts and was significantly reduced compared to female blastocysts ($P \leq 0.05$). c-Myc increased by 50% in HPD male blastocysts than in LPD blastocysts but did not reach significance, whereas female HPD blastocysts had greater levels than the control (Fig 5.7B).

It is important to mention here that embryo sexing results showed an unequal ratio of male to female in the HPD group. As shown in Table 5.3, two male embryos relative to 5 female embryos were analysed for Rnf17S or c-Myc expression.

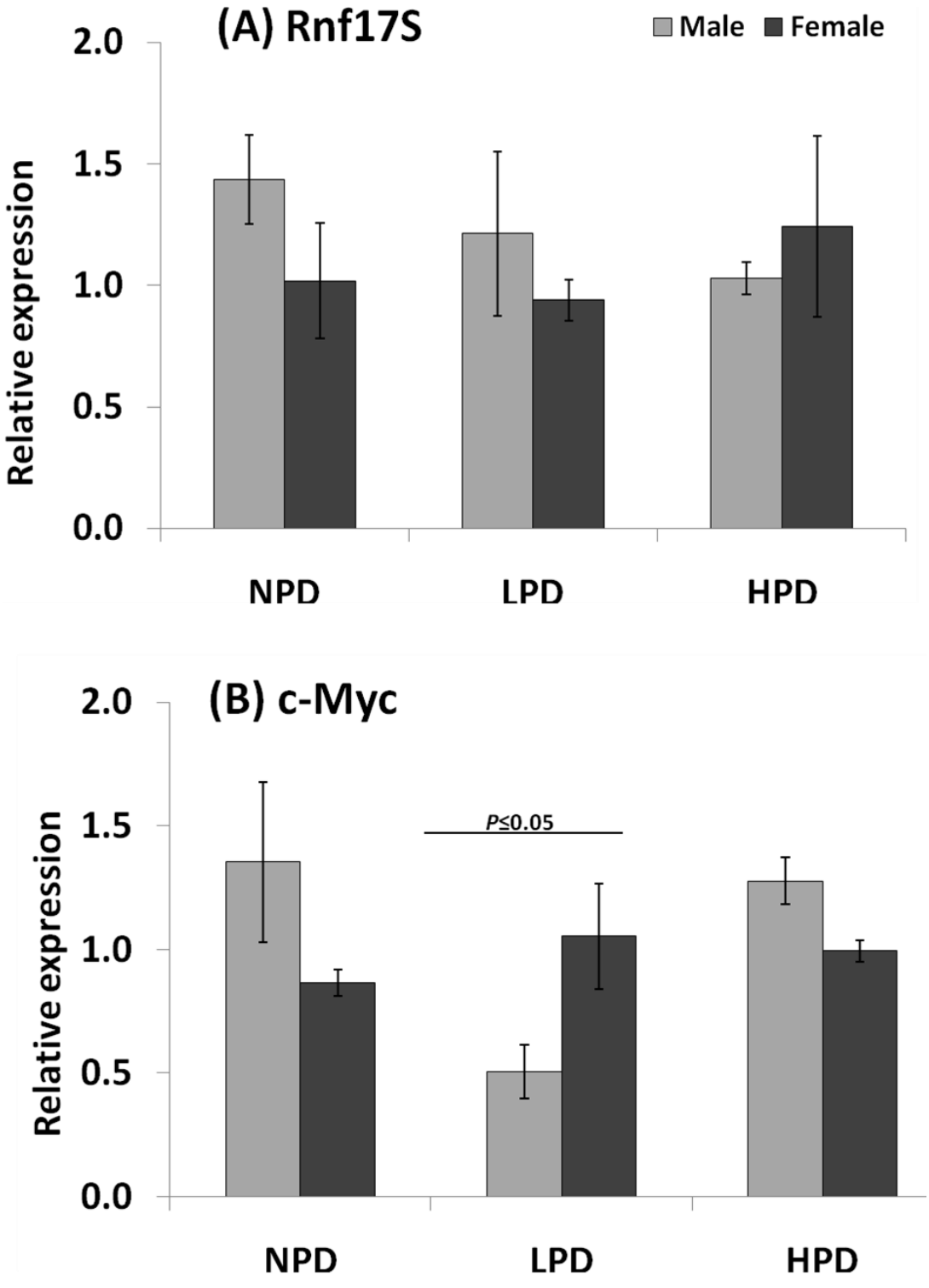

Fig 5.7 *(continued)*

Fig 5.7: Effect of gender on expression of Rnf17S and c-Myc in mouse blastocysts in response to maternal LPD, HPD and control NPD. Two-step PCR method were used to amplify sex-determining primers from single mouse blastocysts DNA to examine expression of **(A)** Rnf17S and **(B)** c-Myc. Relative expression represent normalisation of examined gene to the geometric mean of two reference genes; Tuba-1-α and Ppib. Bar graphs show the mean of examined embryos (Table5.3) and error bars represent standard error of mean.

5.3.3 Expression of Rnf17 and members of Myc/Max/Mxd network in mouse E17.5 foetal testes in response to maternal LPD, HPD and control NPD

Testes of foetuses derived from LPD mothers had a significantly increased expression of Rnf17S than control NPD ($P \leq 0.05$). The expression of c-Myc was significantly decreased in foetus testes from HPD mothers compared to LPD (Fig 5.8). The expression of the retro-transposable element Line-1 in foetal testis was investigated. Line-1 was 50% reduced in LPD or HPD testis relative to control NPD, and this change was significant ($P \leq 0.05$).

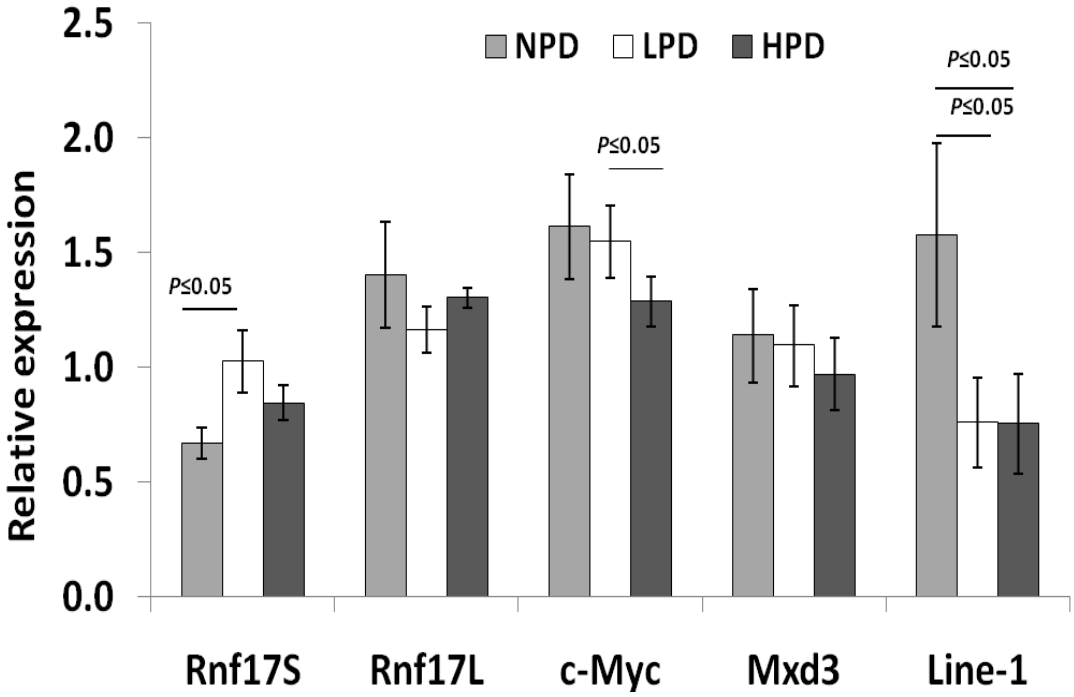

Fig 5.8: Expression profile of Rnf17, c-Myc, Mxd3 and Line-1 in mouse E17.5 foetal testis in response to maternal LPD, HPD and control NPD. Mouse testes were collected from mothers fed LPD, HPD or control NPD from day of plug E0.5 until day of dissection E17.5. Relative expression represent normalisation of examined gene to the geometric mean of two reference genes; Mapk1 and Tbp. Bar graphs show means of examined samples (n=9 foetal testes from 8 different mothers per dietary group), and error bars represent standard error of mean.

5.3.4 Effect of maternal LPD or HPD on subcellular localisation of RNF17 through preimplantation development

Mouse embryos were collected at 4-cell, 8-cell and blastocyst stages from mothers fed control, LPD or HPD from day of plug, immunolabelled with anti-RNF17 and the nuclei were stained with DAPI and examined with SP5 confocal microscopy. The numbers of examined embryos are shown in Table 5.4.

Figure 5.9 shows that RNF17 was prominently nuclear in all diet groups with no difference from the expression pattern shown in Chapter 4. RNF17 was exclusively nuclear and not present in the cytoplasm of 4-cell and 8-cell embryos derived from the maternal LPD group. 4-cell and 8-cell embryos derived from the maternal HPD group showed a very weak signal for RNF17 in the cytoplasm. However, nuclear RNF17 was more punctate in LPD embryos than in HPD embryos. It was noted that the signal obtained for anti-RNF17 was not consistent in embryos from LPD mothers compared to those from HPD mothers.

Table 5.4: Number of embryos immunostained per dietary group.

	LPD	HPD
4-cell	**4 embryos from 3 mother**	**4 embryos from 2 mothers**
8-cell	**8 embryos from 4 mothers**	**4 embryos from 3 mothers**
Blastocyst	**5 embryos from 3 mothers**	**7 embryos from 4 mothers**

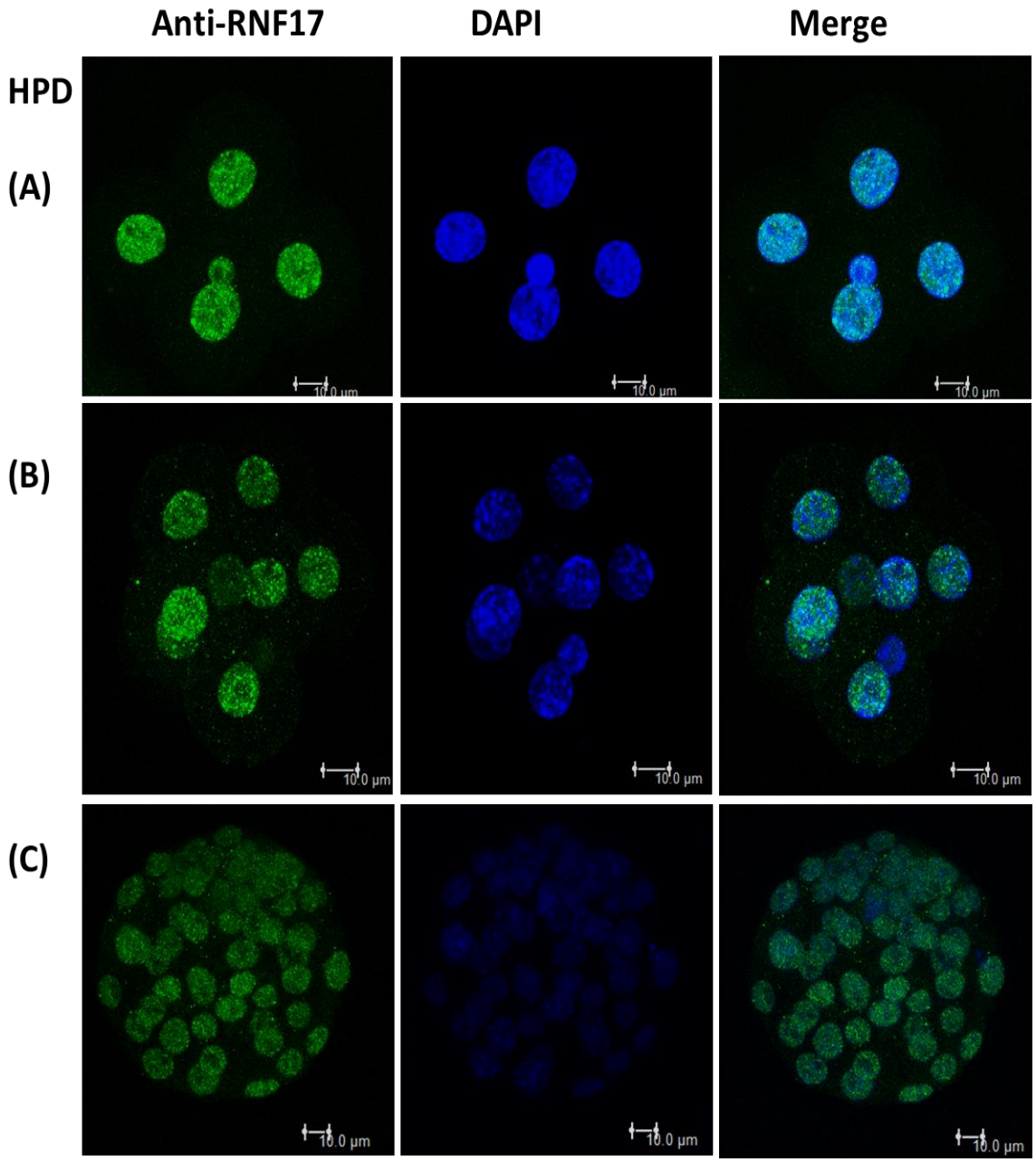

Fig 5.9 *(continued)*

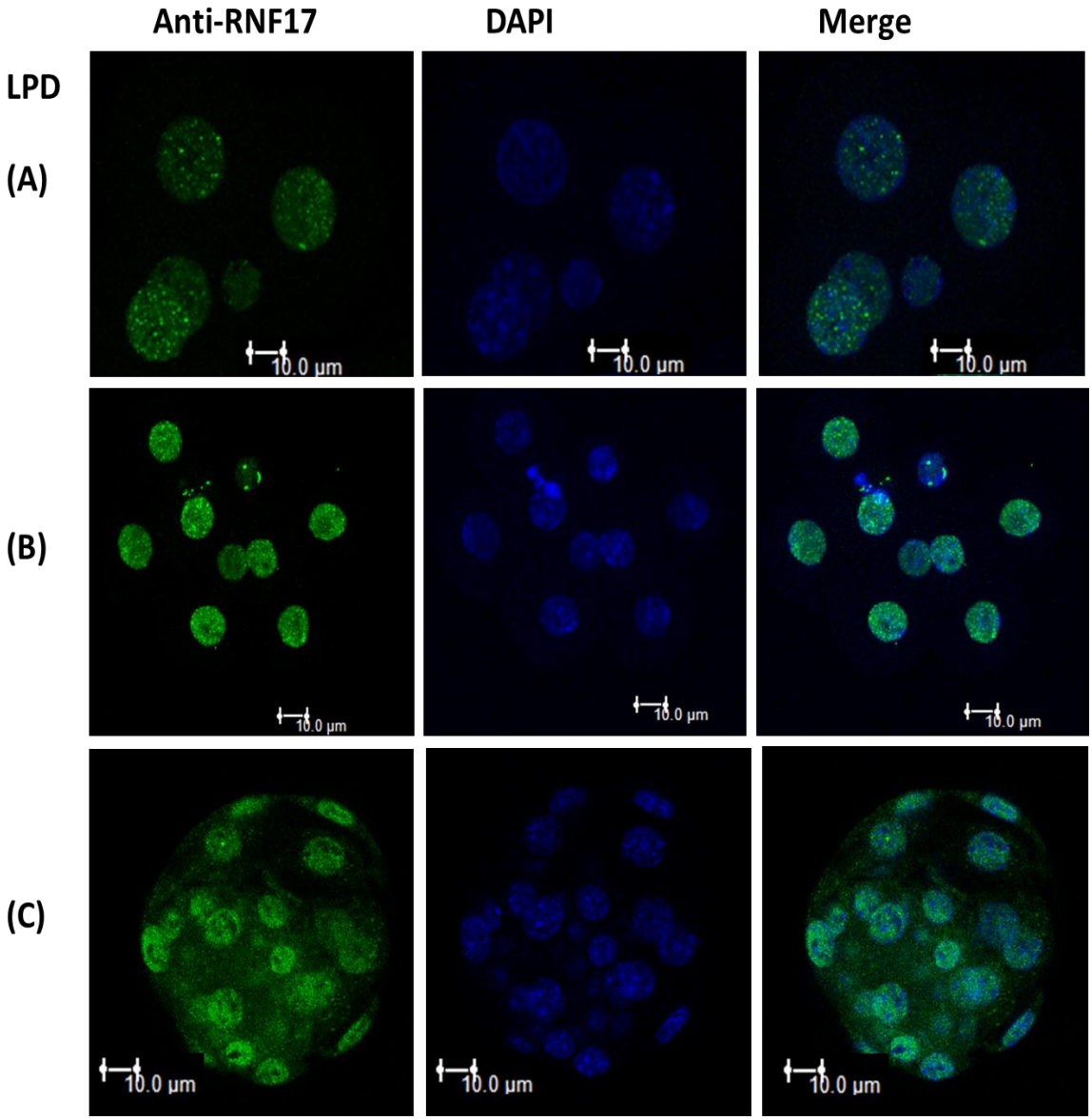

Fig 5.9: Comparison between subcellular localisation of RNF17 in cleavage stage embryos in response to maternal HPD or LPD. Mouse embryos from mothers fed HPD or LPD were collected at 4-cell, 8-cell, and blastocyst stages. Embryos were immunolabelled with anti-RNF17 and nuclei stained with DAPI. RNF17 is predominantly nuclear at all stages. RNF17 was seen in the cytoplasm of 4-cell and 8-cell HPD embryos but not LPD embryos. No differences were seen in RNF17 distribution in the nucleus or the cytoplasm of HPD or LPD embryos.

5.3.5 Effect of maternal LPD or HPD on subcellular localisation of RNF17 in E17.5 foetal testes

The morphology of E17.5 mouse foetal testis was identified by staining cryostat sections of foetal E17.5 dissected from mothers fed chow with Haematoxylin and Eosin (H & E) and compared to stained sections with anti-RNF17. Figure 5.10 shows that germ cells termed prospermatogonia at this stage were surrounded by Sertoli cells and formed the testis cord embedded within the interstitial tissue of the testis.

A very weak signal for RNF17 in the nuclei of prospermatogonia was observed. However, RNF17 was highly expressed in foci-like structures in the nuclei of somatic cells of Sertoli cells and epithelial cells of the interstitial tissues (Fig 5.11). This revealed no effect of maternal LPD or HPD on subcellular localization of RNF17 in E17.5 foetal testes compared to maternal control NPD.

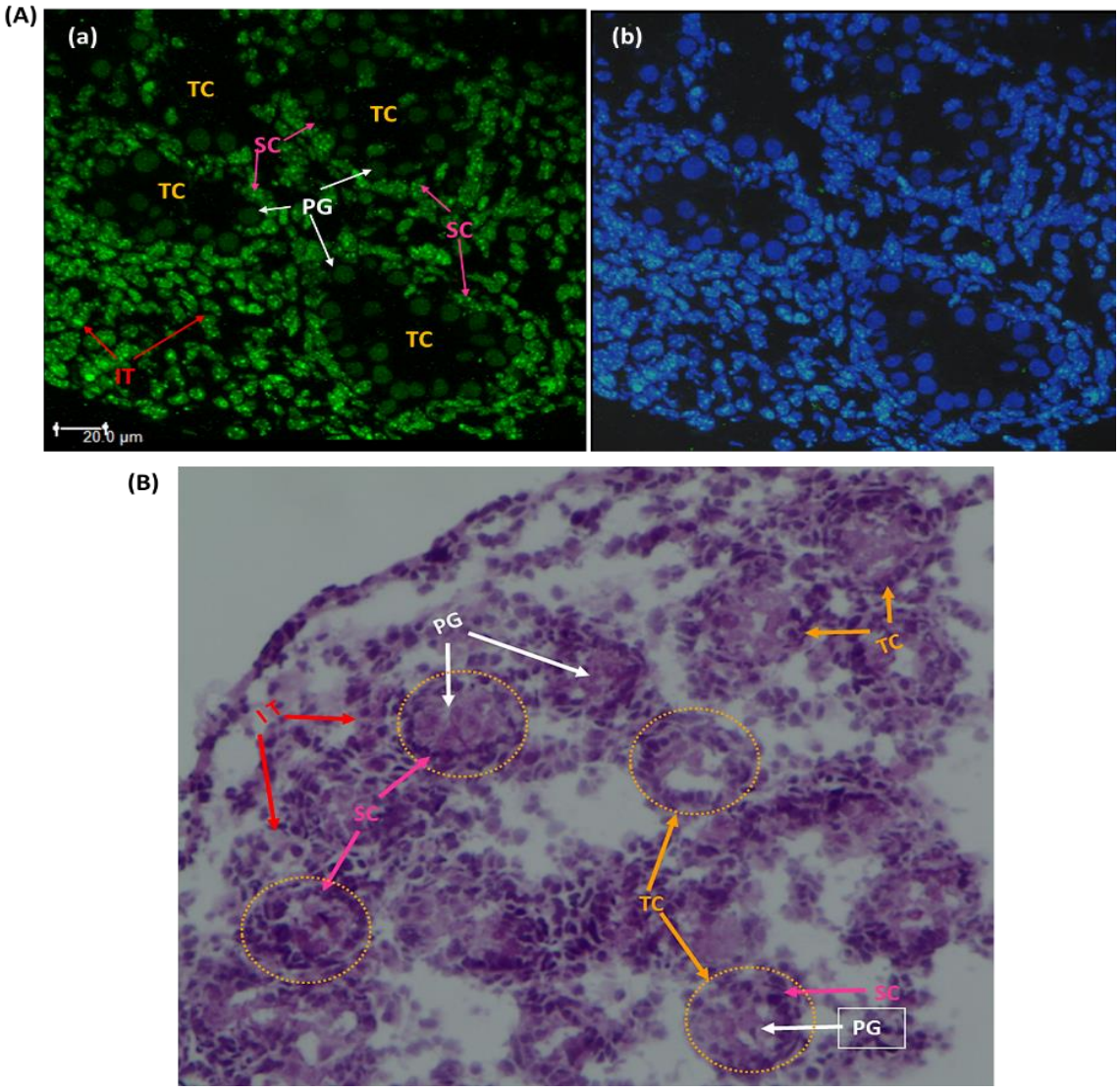

Fig 5.10: Foetal mouse testis morphology. Cryostat sections (6 µm) from mouse E17.5 testis collected from mothers fed chow from day of plug E3.5 until day of dissection E 17.5. The section shows a number of Prospermatogonia **(SG)** surrounded by Sertoli cells **(SC)** forming Testis cord **(TC)** into Interstitial tissue **(IT).** **(A)** Immunostaining localization of RNF17 in nuclei of Sertoli cells stained with **(a)** anti-RNF17 and **(b)** merged image of anti-RNF17 and DAPI. **(B)** H & E staining showing morphology of foetal testis displaying blue stain of nuclei with haematoxylin, and pink stain of the cytoplasm and extracellular matrix with eosin.

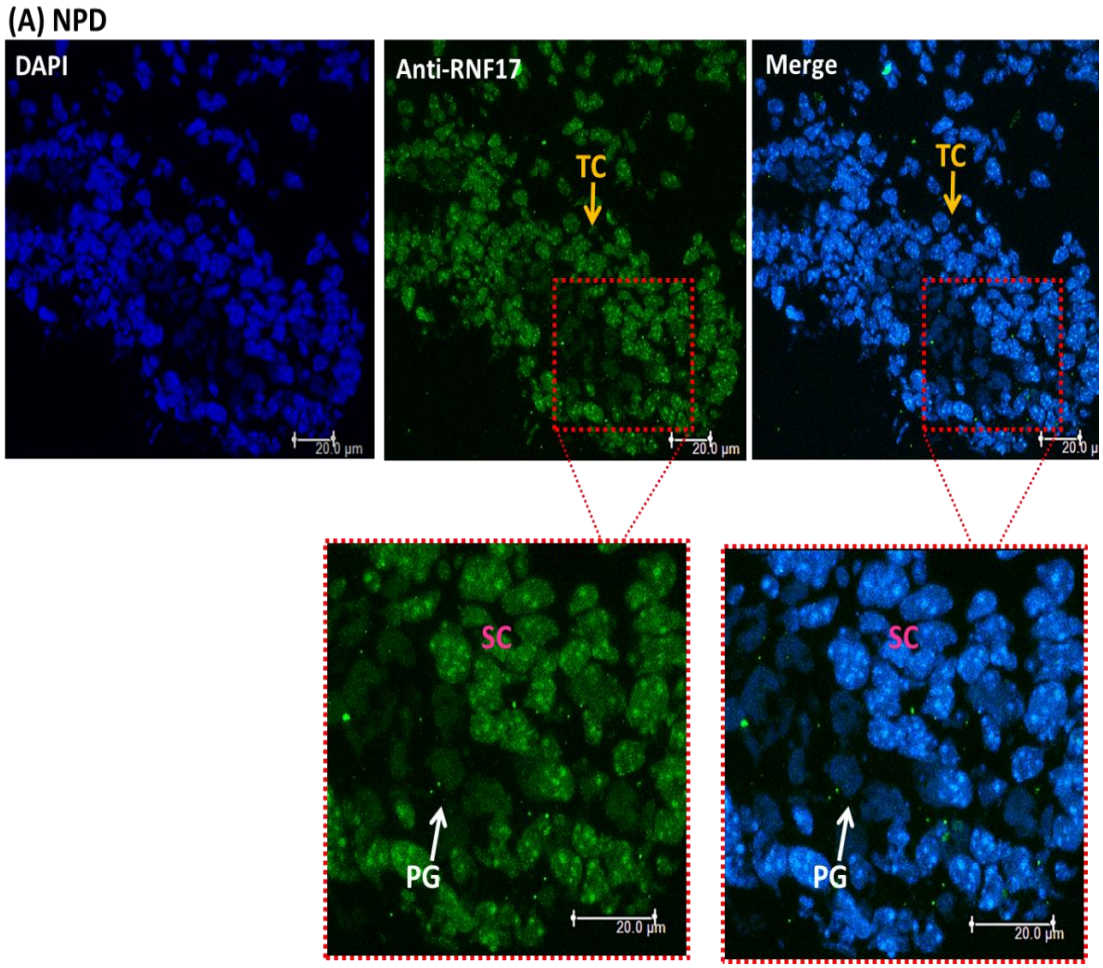

Fig 5.11 *(continued)*

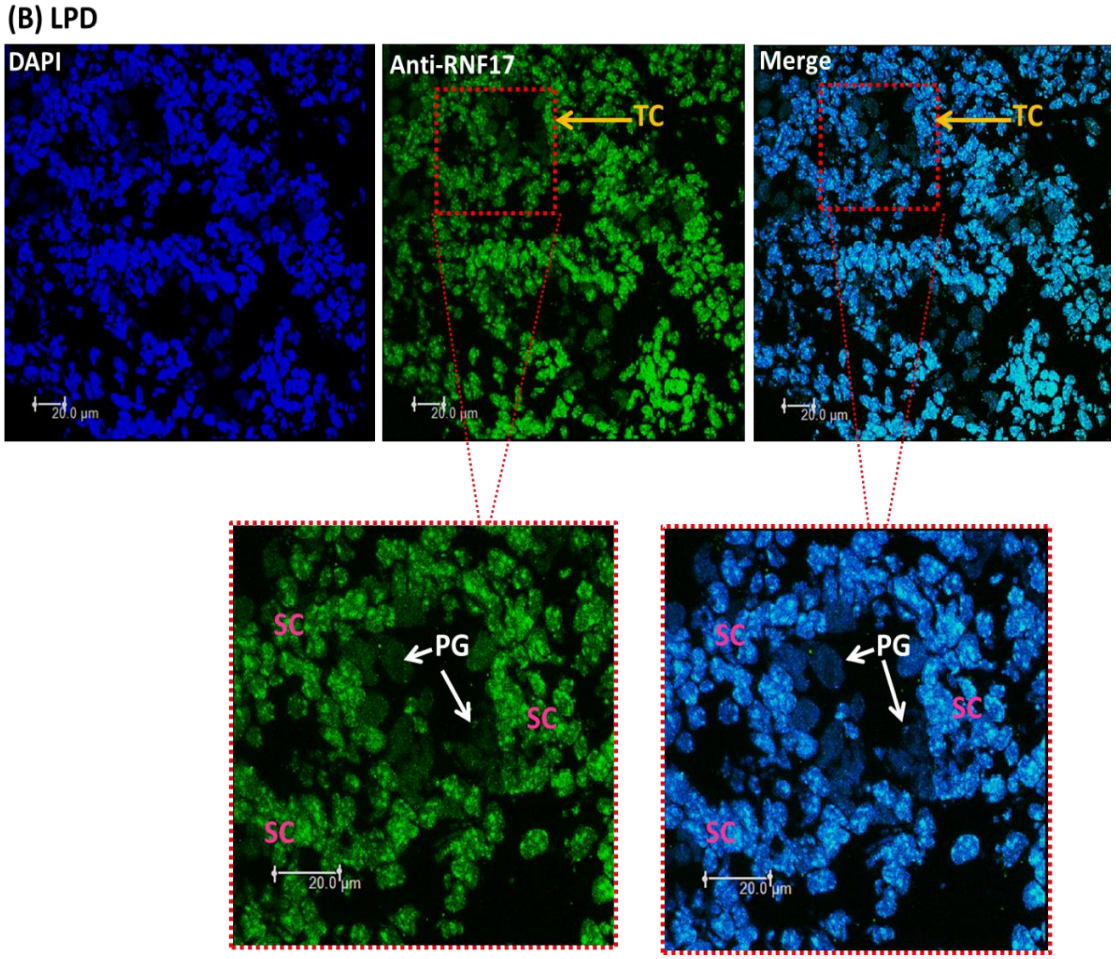

Fig 5.11 *(continued)*

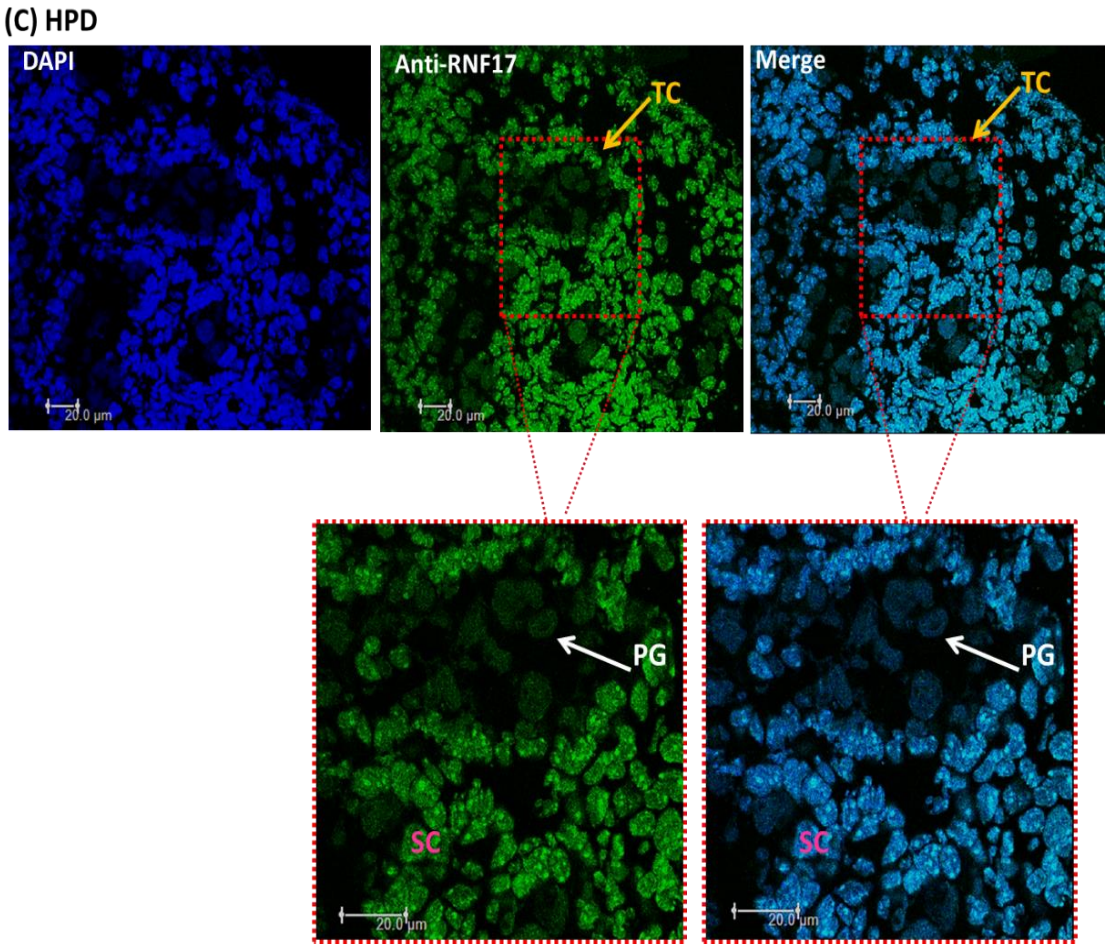

Fig 5.11: Subcellular localisation of RNF17 in E17.5 foetal testis in response to maternal LPD, HPD and control NPD. Cryostat sections (6 µm) of E17.5 mouse testis collected and stained with anti-RNF17 and nuclei stained with DAPI. No differences were seen in RNF17 localisation among diet groups (**A)** NPD control, **(B)** LPD and **(C)** HPD. Strong signal for RNF17 is evident in nuclei of Sertoli cells **(SC)** within foci-like structures, whereas Prospermatogonia **(PG)** gained a very weak signal for RNF17.

5.4 Discussion

In this Chapter, for the first time the expression of Rnf17 mRNA and RNF17 protein in mouse foetal testis was examined. In this chapter, also the effect of maternal protein diets on expression of Rnf17 mRNA and RNF17 protein were investigated in the preimplantation embryo and foetal testes. Although these results showed no significant effect of maternal LPD or HPD on the expression of Rnf17 mRNA in the blastocyst, the expression of Rnf17S mRNA was significantly increased in foetal E17.5 testes derived from mothers fed LPD compared to control NPD. There was no effect of maternal LPD or HPD on the expression or localisation of RNF17 proteins in blastocyst or foetal testes.

Using RT-qPCR, Figure 5.5 shows that expression of Rnf17S and Rnf17L was not significantly different in blastocysts between treatment groups of LPD and HPD relative to control NPD. No effect of maternal diets was seen in the expression and subcellular localisation of RNF17 in mouse blastocysts. Rnf17 is a male germ-specific gene (Pan *et al*, 2005), thus, embryo sexing was applied to find out whether the effect of maternal protein diets on the expression of Rnf17 is sex-dependent. Embryo sexing results (Fig 5.7) revealed that Rnf17S was more sensitive to maternal diet in male than in female blastocysts in the HPD group compared to LPD and control NPD groups. However, c-Myc expression was significantly reduced in male, compared to female, blastocysts derived from maternal LPD compared to HPD and control groups, indicating that c-Myc was more sensitive to maternal LPD in the male blastocyst. It is important to highlight here that the number of male blastocyst was not equal to female blastocysts in HPD group, thus no direct comparison can be made between sexes within this group.

Previous studies showed that male blastocysts develop faster than female blastocysts. The more quickly developing blastocyst is more sensitive to the

environment in terms of proliferation and they need to protect themselves against environmental changes in order to maintain their rate of proliferation (reviewed in Erickson, 1997). These findings are not consistent with our results which revealed decreased c-Myc mRNA, that heterodimerised with max to promote transcription and proliferation (Grandori *et al,* 2000). One explanation is that c-Myc mRNA is measuring the effect of maternal diets on the transcriptional level which indicates the changes in steady state level of mRNA. Thus, we need to measure protein levels to explain any contrary results, specifically that no differences between ICM and TE in expression and localisation of RNF17 protein was seen between the diet groups (Fig 5.9).

The sensitivity of the embryo to the environment has been explained by the DOHaD hypothesis, which proposes that changes in the embryo environment including, maternal diets or *in vitro* culture, may alter gene expression during embryo growth and affect adult later-life (Barker & Osmond, 1986; Barker,2000; Langley-Evans, 2006). It has been reported that there is a short-term effect on expression of Rnf17 in mouse blastocyst exposed to environmental changes including embryo culture (Giritharan *et al,* 2007) or maternal LPD (Papenbrock *et al,* unpublished data). However, our results implicated that there is no effect of maternal protein diets on expression of male germ-specific gene, specifically Rnf17.

The expression of Mxd3 was very low in the mouse blastocyst as explained in Chapter 4. Therefore, a five pooled blastocysts were considered as single embryo for each examined RT-qPCR cycle. Together, the low expression of Mxd3 with non-affected expression of Rnf17 and c-Myc, within the treatment and control diet groups, revealed the interplay between Mxd and Rnf17 in modulating c-Myc to regulate embryo proliferation and differentiation under restricted environmental conditions.

RT-qPCR showed that the expression of Rnf17 was induced in foetal testes in response to maternal protein diets, with a significant increase of Rnf17S in LPD group compared to control NPD. However, the expression of c-Myc was reduced in foetal testes from maternal LPD and HPD groups compared to control NPD (Fig 5.8). Maternal LPD has shown to induce adaptive responses in the blastocyst extra-embryonic region (extra-embryonic yolk sac) to protect foetal and postnatal growth (Watkins *et al*, 2008a). A significant increase in the expression of Rnf17S in the LPD group compared to the control NPD in E17.5 testes may implicate adaptive responses induced in primordial germ cells by maternal LPD to protect the differentiation and development of foetal gonads.

Immunostaining results in Figure 5.10 show that RNF17 was expressed in Sertoli cells with a very weak signal for RNF17 in prospermatogonia. No effect of maternal diets was seen in the expression and localisation of RNF17 protein in foetal testes. However, the expression of RNF17 protein detected in cytoplasmic nuage in the germ cells of mouse adult testis is stage dependent (Pan *et al,* 2005). The expression of RNF17 protein was described as stage dependent, of which RNF17L is expressed in spermatocyts, whereas RNF17S is expressed in spermatids. These findings suggest that the expression of RNF17 isoforms is not continued through germ cell development and differentiation and may explain why there is expression of RNF17 in foetal testis somatic cells but not in germ cells.

It is important to explain here, that although Rnf17 mRNA is expressed in foetal testis, the RT-qPCR was applied to the whole tissue of foetal testis including both somatic and germ cells. Therefore, it is important to examine Rnf17 mRNA expression in separated testis cells. This would give insight to the level of expression in each cell type as well as highlighting the function of Rnf17 in gonad development throughout foetal growth.

Another possibility to explain the expression pattern of RNF17 in foetal testes cells would relate to the cell cycle status of differentiated germ cells. After germ cell differentiation at E13.5, female germ cells enter meiosis, whereas male germ cells (spermatogonia) undergo mitotic arrest and resume meiosis after birth at round 10 days postpartum (Desjardins and Ewing, 1993). This is consistent with our results in Chapter 4 that RNF17 is not expressed in mitotic divided cells either in preimplantation embryos or in F9 cells. Therefore, as shown in our results, it is expected that RNF17 is not expressed in spermatogonia during mitotic arrest but resumed after birth (Pan *et al,* 2005).

Immunoprecipitation of RNF17 with MIWI in mouse adult testes (Vagin *et al*, 2009) suggested a role of Rnf17 in the silencing of transposons. However, the expression of RNF17 in Sertoli cells does not support this suggestion. Mutant Tdrd6 has no function in control transposons but has altered the expression of pre- and pri-forms of miRNAs (Vasileva *et al,* 2009). piRNAs were not detected in mouse testis somatic cells, including Sertoli cells (Beyret and Lin, 2011), but studies have shown the expression of miRNAs in Sertoli cells and that they are targets of Sox9 (SRY-box containing gene 9) in foetal and adult testes. For example, in foetal testes, pri-miR-202 is directly regulated by transcriptional factor Sox9 in the Sertoli cells of mouse foetal testes for male sex differentiation and testis development (Wainwright *et al*, 2013). miR-22 is involved in repressing oestrogen signalling within ovine foetal testes to induce testis differentiation (Torley *et al*, 2011). In postnatal mouse testes a number of miRNAs are expressed in Sertoli cells, and function in androgen signalling for germ cell differentiation and development during spermatogenesis (Panneerdoss *et al,* 2012).

Together with Pan's results, it is speculated that RNF17 has a different expression pattern within germ cell tissues through development. The expression of RNF17 in all germ cells in adult testes has a function in

spermiogenesis, whereas the expression of RNF17 in Sertoli cells of foetal testis may be associated with the nuclear transcription factor Sox9 (Nel-Themaat *et al*, 2009; reviewed in Park and Jameson, 2005). This suggests a role of Rnf17 through Sox9 and it may target a miRNA for testis development, or endocrine signalling for germ cell differentiation. Additionally, the significant reduction of Line-1 in diet foetal testis, with equivalent effects of LPD and HPD (50%) compared to the control NPD, indicates the effect of maternal diets, but not Rnf17, on the expression of line-1 in foetal testes.

In conclusion, our results revealed that there were no effects of maternal protein diets on the expression of Rnf17mRNA or RNF17 protein in mouse blastocyst or foetal testes. There was no interaction between maternal protein diets and sexes at the preimplantation stage in terms of Rnf17 expression. However, foetal testes were sensitive to maternal LPD that gave a significantly induced expression of Rnf17. Maternal LPD and HPD reduced the expression of c-Myc mRNA in foetal testes with early effect of maternal LPD on the male blastocyst. RNF17 protein is predominantly localised in the nuclei of foetal testes somatic cells. The RNF17 protein signal was weakly detected in mitotically arrested spermatogonia of foetal testes, confirming previous results in Chapter 4 that RNF17 is not expressed in mitotic cells.

Chapter 6

6. The Potential Function of Rnf17 in Mouse Blastocyst Development

6.1 Introduction

The function of Rnf17 has been studied in adult mouse testis but not in early embryo development. Over-expression of Rnf17 enhances Myc activities by sequestering Mxd in *in vitro* models (Yin *et al*, 1999). Pan *et al* (2005) showed that mutant Rnf17 mice (*Rnf17*$^{-/-}$) developed normally, however, *Rnf17*$^{-/-}$ males are infertile, but females exhibit normal fertility and produce normal litter sizes. In Chapter 3, the over-expression of Rnf17 plasmid induced Luciferase activity of c-Myc reporter gene in co-transfected F9 cells. Here, Rnf17 knockdown will be studied.

The application of RNA interference in mammals has the potential to allow the efficient knockdown of specific genes and enables phenotypic characterisation in the absence of gene function. RNA interference (RNAi) is a gene silencing mechanism through homologous short interfering RNA (siRNA), which elicits the destruction of corresponding mRNAs by the RNA-induced silencing complex (RISC). The siRNA expressing short hairpin RNAs (shRNA) can either be added to the cells exogenously or produced intracellularly from plasmid DNA templates (Agrawal e*t al*, 2003). In the RNAi reaction, the cellular RNase III enzyme, Dicer, cleaves the dsRNA into smaller multiple trigger molecules, siRNA, each of about 21–25 bps, that become incorporated into the RISC. This complex pairs, via Watson-Crick base pairing, with the homologous mRNA in a sequence-specific manner. This then leads to the degradation of the target mRNA and a subsequent decrease in the encoded protein (Agrawal e*t al*, 2003).

6.1.1 Aim of experiment

The aim of this experiment is to investigate the role of Rnf17 in modulating c-Myc and subsequently in cell proliferation. Rnf17 was down regulated by RNA interference (RNAi) technology in F9 cells using Rnf17-directed siRNA

expression plasmids. Results were measured by Luciferase activity of Rnf17-sensor plasmid (as explained in the methods) to determine the specificity of targeting Rnf17 in F9 cells.

The second aim is to examine the role of Rnf17 in cell proliferation and embryo development in the preimplantation period. Rnf17 was knocked down by a short interference (siRNA) oligonucleotide microinjection technique in mouse embryos at zygote or 2-cell stage. Embryo development was estimated by the percentage of Rnf17 knockdown by RT-qPCR and by evaluating embryo developmental stage on day-3 post microinjection.

6.2 Methods

6.2.1 RNA interference and cell transfection

An Rnf17-sensor was produced to be inserted into pGL3-control for the selected target sequence **AA<u>CTCAGATCTGCTCCTTCTC</u>**. Rnf17 wild type (Rnf17-RNAi-wt) or a non-targeting negative control for RNAi Rnf17 mutant (Rnf17-RNAi-mut) were prepared to be inserted into p*Silencer*™ 1.0 U6 vector. Prepared constructs were dose-dependent transfection into F9 cells or Raw 264.1 murine macrophage cells.

6.2.2 Production of expressing vectors for Rnf17-RNAi

Annealed sense and antisense for mutant or wild type RNAi oligonucleotides were ligated to linearised p*Silencer*™ 1.0 U6 (pSil) (Fig 6.1A). Following transformation, extracted DNA plasmids were single cut with *Bam*HI to confirm the insertion of the 60 bp RNAi template insert. There were two sites of *Bam*HI in the p*Silencer*™ 1.0 U6 of 376 bp in which the RNAi template was inserted. Figure 6.1B & C showed a dropped band of about 400 bp which represent the insertion of the RNAi oligonucleotides between the *Bam*HI sites.

A single cut with *Hin*dIII was also performed to confirm that the region between the *Apa*I and the *Eco*RI had been replaced by the Rnf17-RNAi inserts. Figure 6.2 showed that Rnf17-RNAi did not cut with *Hin*dII confirming its replacement with the RNAi insert.

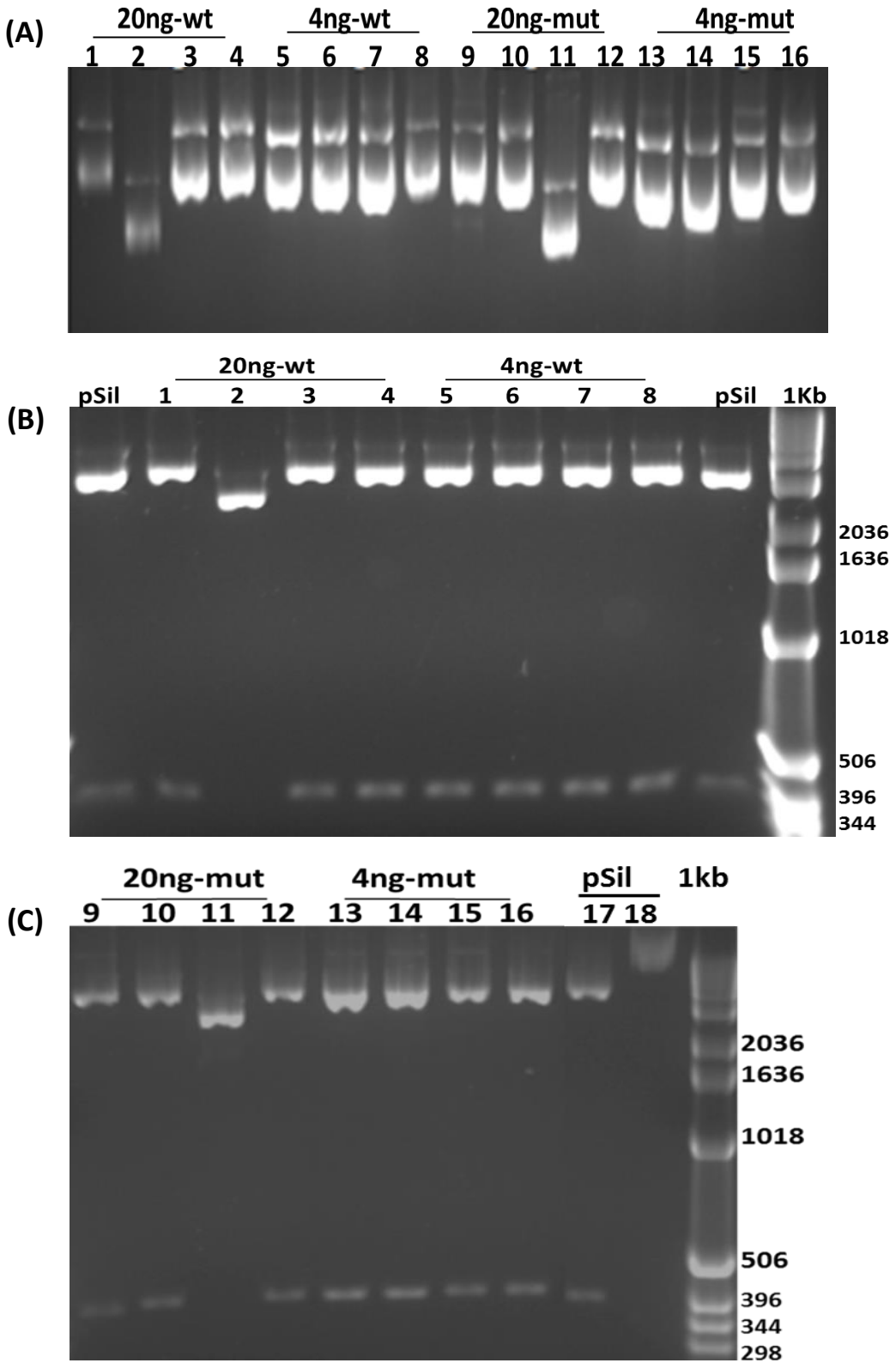

Fig 6.1 (*continued*)

Fig 6.1: Preparing of Rnf17-RNAi expressing constructs. Annealed oligonucleotides for wild type and mutant Rnf17-RNAi were diluted to 4 and 20 ng/µl and ligated into the linearised p*Silencer*™ 1.0 U6. The cut plasmids dropped a band of 400 bp represent the size between two sites of *Bam*HI in the pSilencer (376 bp) and the ligated insert (60 bp). Clones not drop a band confirm no template inserted.

(A) Uncut DNA plasmids of 4 clones of each dilution of Rnf17-RNAi-wt (Lane 1-8) and Rnf17-RNAi-mut (Lane 9-16) shows different sizes of plasmid. Clones number 2 and 11 were running faster suggesting no insert.
(B) Single cut with *Bam*HI for Rnf17-RNAi-wt (Lane 1-8) compared to a cut p*Silencer*™ 1.0 U6 (pSil).
(C) Single cut with *Bam*HI for Rnf17-RNAi-mut (Lane 9-16) compared to cut pSil (Lane 17) and uncut pSil (Lane 18).

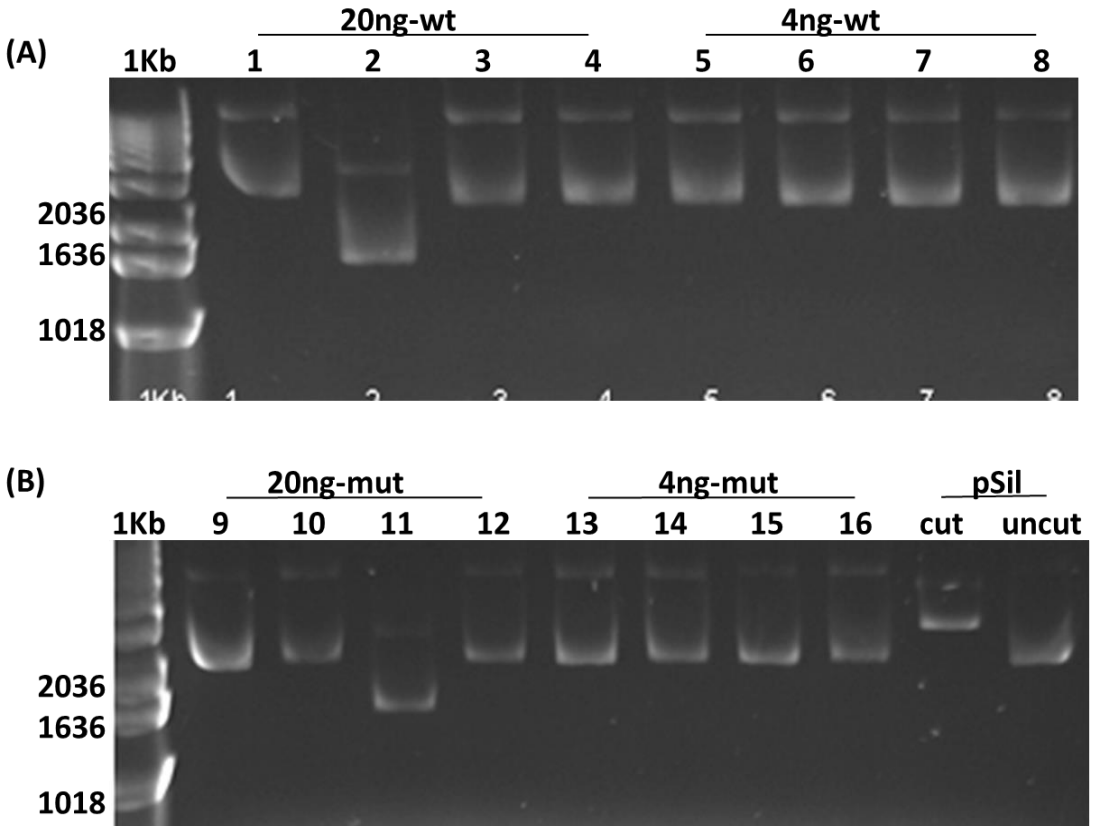

Fig 6.2: Single cut for Rnf17-RNAi expressing constructs with *Hin*dIII. DNA plasmids for **(A)** Rnf17-RNAi-wtand **(B)** Rnf17-RNAi-mut expressing plasmids shows no cut with *Hin*dIII, and confirming the insertion of Rnf17-RNAi templates between *Apa*I and *Eco*RI sites which include the *Hin*dIII site. The results were compared to cut and uncut pSil in (**B)**. Clones number 2 **(A)** and 11 **(B)** show different sizes compared to the pSil, and indicating no insertion of Rnf17-RNAi templates. **1kb:** DNA ladder (Invitrogen).

6.2.3 Production of Rnf17-sensor construct

Annealed sense and antisense oligonucleotides for Rnf17 sensor were ligated into linearisedpGL3-Control vector. Following transformation, extracted DNA plasmids were single cut with *Eco*RI or *Eco*RV to ensure the insertion of Rnf17-sensor template. The results showed a cut with *Eco*RI but not *Eco*RV, which is located upstream the *Pst*I (Fig 6.3).

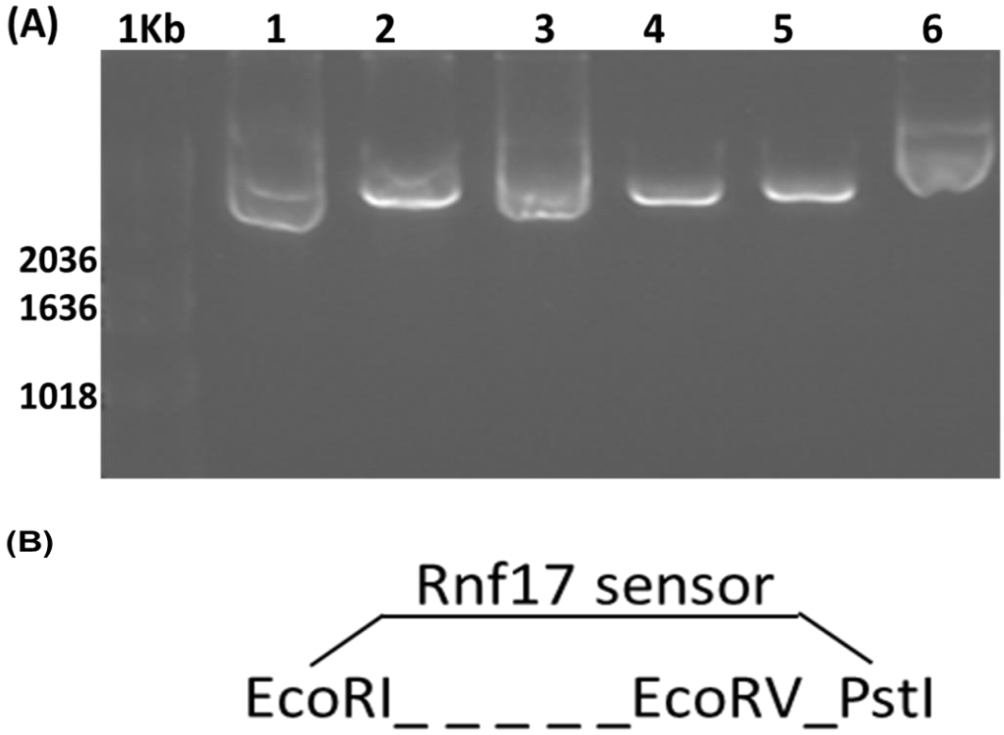

Fig 6.3: Rnf17-sensor construct. (A) Extracted DNA plasmids of Rnf17-sensor template were single cut with *Eco*RV or *Eco*RI to confirm the insertion. Rnf17-sensors construct was linearised with *Eco*RI but not *Eco*RV compared to single cut of pGL3-control with *Eco*RV or *Eco*RI. **(B)** Schematic diagram for restriction map of the modified pGL3-Control showing the insertion of the Rnf17-sensor.

- **Lane1:** Rnf17-sensor cut with *Eco*RV
- **Lane2:**Rnf17-sensor cut with *Eco*RI
- **Lane3:** uncut Rnf17-sensor
- **Lane4:** pGL3-control cut with *Eco*RV
- **Lane5:** pGL3-control cut with *Eco*RI
- **Lane6:**uncut pGL3-control
- **1kb:** DNA ladder (Invitrogen)

6.2.4 Microinjection of Rnf17_siRNA into mouse embryo

Microinjection was performed using oligonucleotide sequences for Rnf17 (Rnf17_siRNA) or a negative control siRNA sequence (AllStar_siRNA) designed by the manufacturer (QIAGEN, UK). Rnf17_siRNA were injected individually into embryos collected from superovulated female FVB/N mice. Rnf17 knockdown was determined in microinjected embryos by RT-qPCR. RNF17 protein expression following embryo microinjection was evaluated by immunostaining using anti-RNF17. Table 6.1 shows number of embryos examined by immunostaining.

6.2.5 Quantitative real-time PCR (RT-qPCR)

Microinjected embryos were examined by RT-qPCR. The level of knockdown was calculated by normalising the Ct value of siRNA-microinjected and siRNA-negative control embryos to the Ct value of the reference gene; Tuba-1-α (delta Ct; dCt). The dCt value of siRNA-microinjected was then normalised to the dCt of siRNA-negative control (delta delta Ct; dtdtCt) to calculate the change in the expression of the Rnf17_siRNA injected embryo compared to the negative control. Statistically, data collected are primary data and a significance test was not run. The experiment was performed with error bars representing the standard deviation of biological duplicate of Ct values of four embryos analysed within four RT-qPCR cycles at different times. Table 6.1 shows number of embryos examined by RT-qPCR.

Table 6.1: Number of embryos examined by RT-qPCR or Immunostaining following Rnf17_siRNA or control microinjection

	RT-qPCR	Immunostaining
AllStar_siRNA	4 embryos from 4 mothers	20 embryos from 4 mothers
Rnf17_siRNA_1	4 embryos from 4 mothers	10 embryos from 3 mothers
Rnf17_siRNA_2	4 embryos from 4 mothers	13 embryos from 3 mothers
Rnf17_siRNA_3	4 embryos from 4 mothers	7 embryos from 2 mothers
Rnf17_siRNA_4	4 embryos from 4 mothers	4 embryos from 2 mothers

6.3 Results

6.3.1 Rnf17-RNAi expressing constructs target Rnf17-sensor at low concentration in F9 cells

Rnf17-RNAi-wt or Rnf17-RNAi-mut were co-transfected together with a constant amount of Rnf17-sensors (0.5 µg) into Raw264.7 cells, as a control experiment, and F9 cells. The total amount of DNA was normalised to 2 µg with pUC plasmid (empty vector).

Figure 6.4A shows that in the Raw cells, Luciferase activity of the Rnf17-sensor significantly increased with 0.5 µg Rnf17-RNAi plasmid ($P \leq 0.05$) in response to the mutant RNAi expressing construct compared to the control untreated cells (0.0 µg Rnf17-RNAi). Increasing the concentration of the Rnf17-RNAi expressing plasmids (1.0 µg) significantly reduced ($P \leq 0.05$) Luciferase activity of the Rnf17-sensor 4-fold in response to Rnf17-RNAi-wt plasmid compared to the control.

Introducing Rnf17-RNAi expressing plasmids (wild and mutant types) into F9 cells at 0.5 µg concentration was not able to inhibit the Luciferase activity from the Rnf17-sensor. Luciferase activity for Rnf17-sensor was significantly increased 3-fold in response to Rnf17-RNAi-wt plasmid and 4-fold in response to Rnf17-RNAi-mut plasmid compared to the control ($P \leq 0.05$). Increasing the concentration of the Rnf17-RNAi expressing plasmids to 1.0 µg decreased Luciferase activity of the Rnf17-sensor in response to Rnf17-RNAi-wt and Rnf17-RNAi-mut plasmids compared to the 0.5 µg concentration, however Luciferase activity was still higher than the control 0.0 µg Rnf17-RNAi (Fig 6.4B).

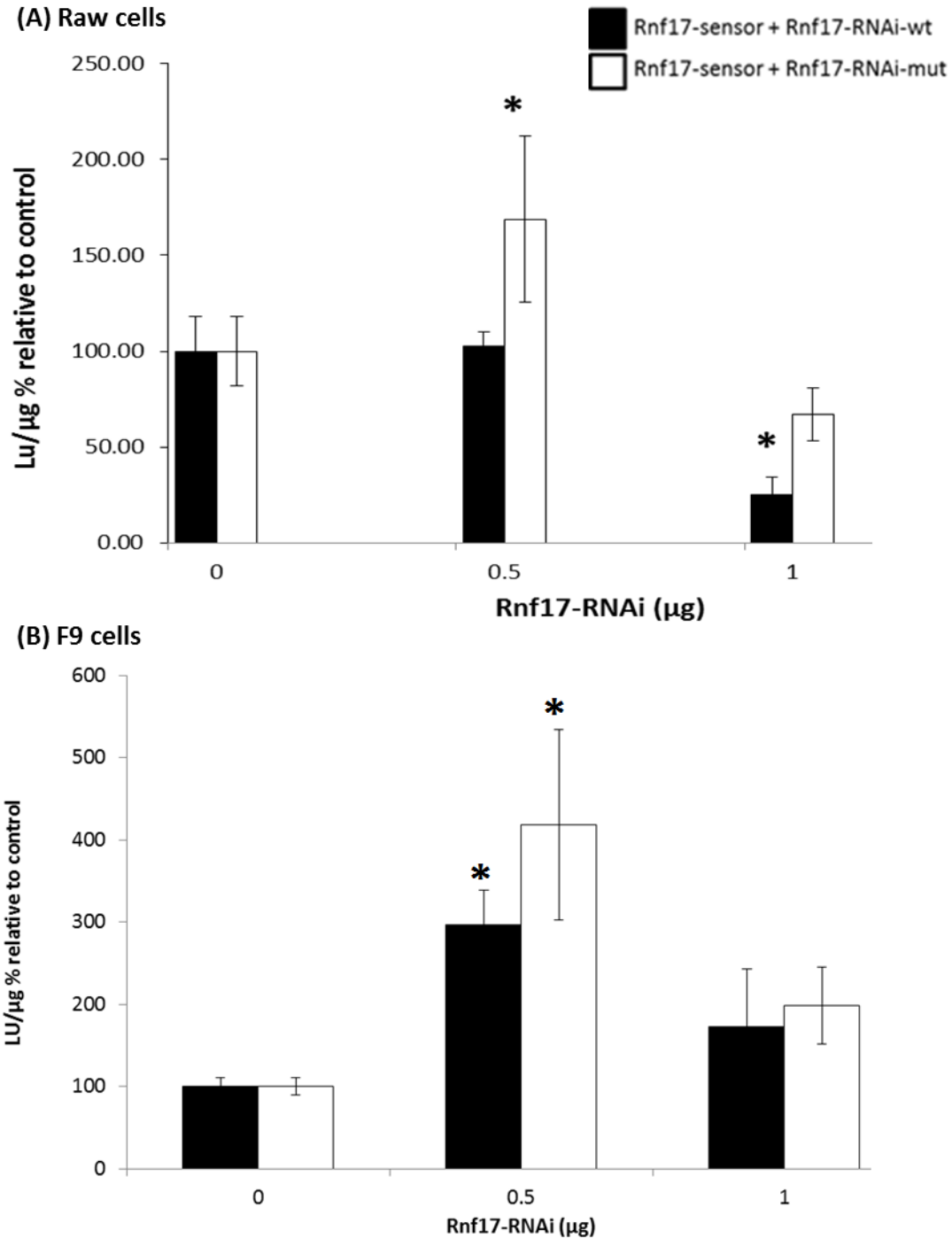

Fig 6.4 *(continued)*

Fig 6.4: Effect of Rnf17-RNAi expressing plasmids on Luciferase activity of the Rnf17-sensor in transfected cells. **(A)** Raw cells and **(B)** F9 cells were transfected with a constant amount of Rnf17-sensors (0.5 µg) together with 0.5 µg or 1.0 µg of Rnf17-RNAi-wt or Rnf17-RNAi-mut expressing plasmids. In Raw cells, Luciferase activity of Rnf17-sensors significantly induced at 0.5 µg concentration of Rnf17-RNAi-mut plasmids, whereas in F9 cells Luciferase activity is significantly induced at 0.5 µg of Rnf17-RNAi-wt and Rnf17-RNAi-mut (*; $P \leq 0.05$). Bar graphs show mean of three replicates and error bars represent standard deviation.

6.3.2 Efficiency level of Rnf17 knockdown in Rnf17_siRNA microinjected embryos.

Using RT-qPCR, the mean Ct values of two biological replicates for four replicate experiments of Rnf17_siRNA were normalised to the reference gene (Tuba-1-α) and then to the negative AllStar_siRNA. siRNA was injected into 2-cell stage embryos. The level of Rnf17 knockdown varied between the four Rnf17_siRNA oligonucleotides. Rnf17_siRNA_4 was about 80% efficient in knocking down Rnf17 expression in the mouse embryo compared to the negative control (AllStar_siRNA), whereas the efficiency of Rnf17_siRNA_1 and Rnf17_siRNA_3 were the lowest in knocking down Rnf17 and ranged between 48 to 50% (Fig 6.5).

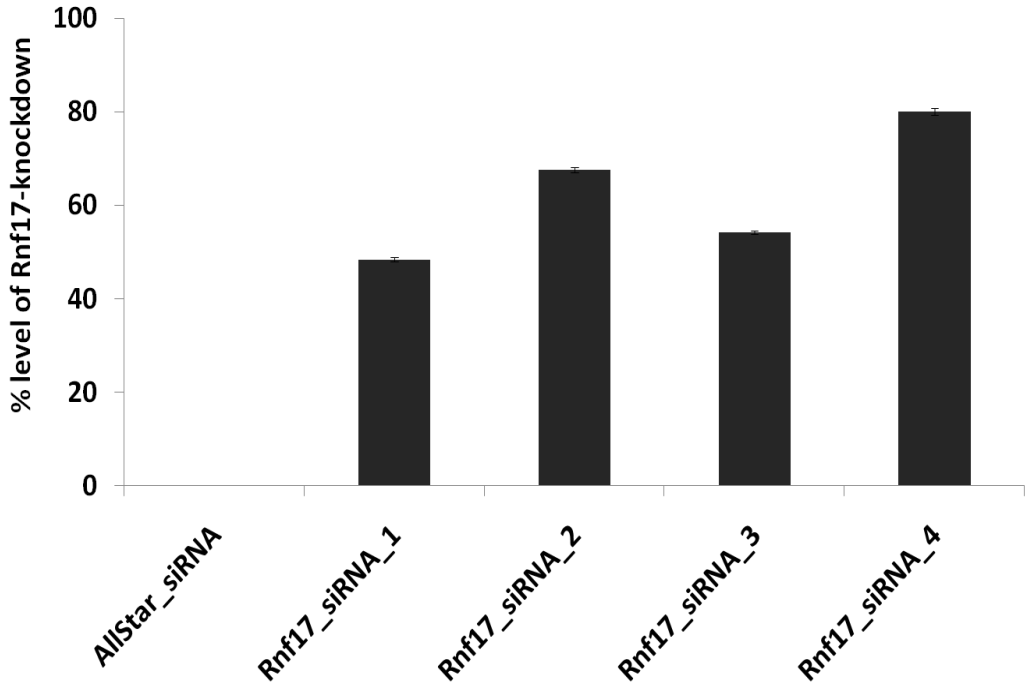

Fig 6.5: The efficiency of Rnf17_siRNA to knockdown Rnf17 in mouse blastocyst using RT-qPCR. 2-cell stage embryos were microinjected with different siRNA sequences targeting Rnf17 (Rnf17_siRNA_1 to _4). Injected embryos were *in vitro* cultured for 3 days before analysed for expression level of Rnf17. All Rnf17_siRNA were able to knockdown Rnf17 in mouse embryo with more than 80% efficiency for Rnf17_siRNA_4 sequence. Relative expression of Rnf17 was normalised to negative control injected embryos (dtdtCt). Bar graphs show mean of dtdtCt of examined embryos (Table 6.1) and error bars represent standard deviation.

6.3.3 RNF17 protein expression

Embryos of the 2-cell stage were microinjected and cultured *in vitro* for three days post-injection. RNF17 expression was reduced in Rnf17_siRNA compared to the negative control (AllStar_siRNA) microinjected embryos (Fig 6.6 A-E). Embryos microinjected with Rnf17_siRNA_4 (Fig 6.6E) displayed a weak RNF17 signal compared to the embryos injected with other Rnf17_siRNA. No effect of Rnf17 knockdown was seen in nuclear localisation of RNF17 in all injected embryos with different Rnf17_siRNA oligonucleotides (Fig 6.6).

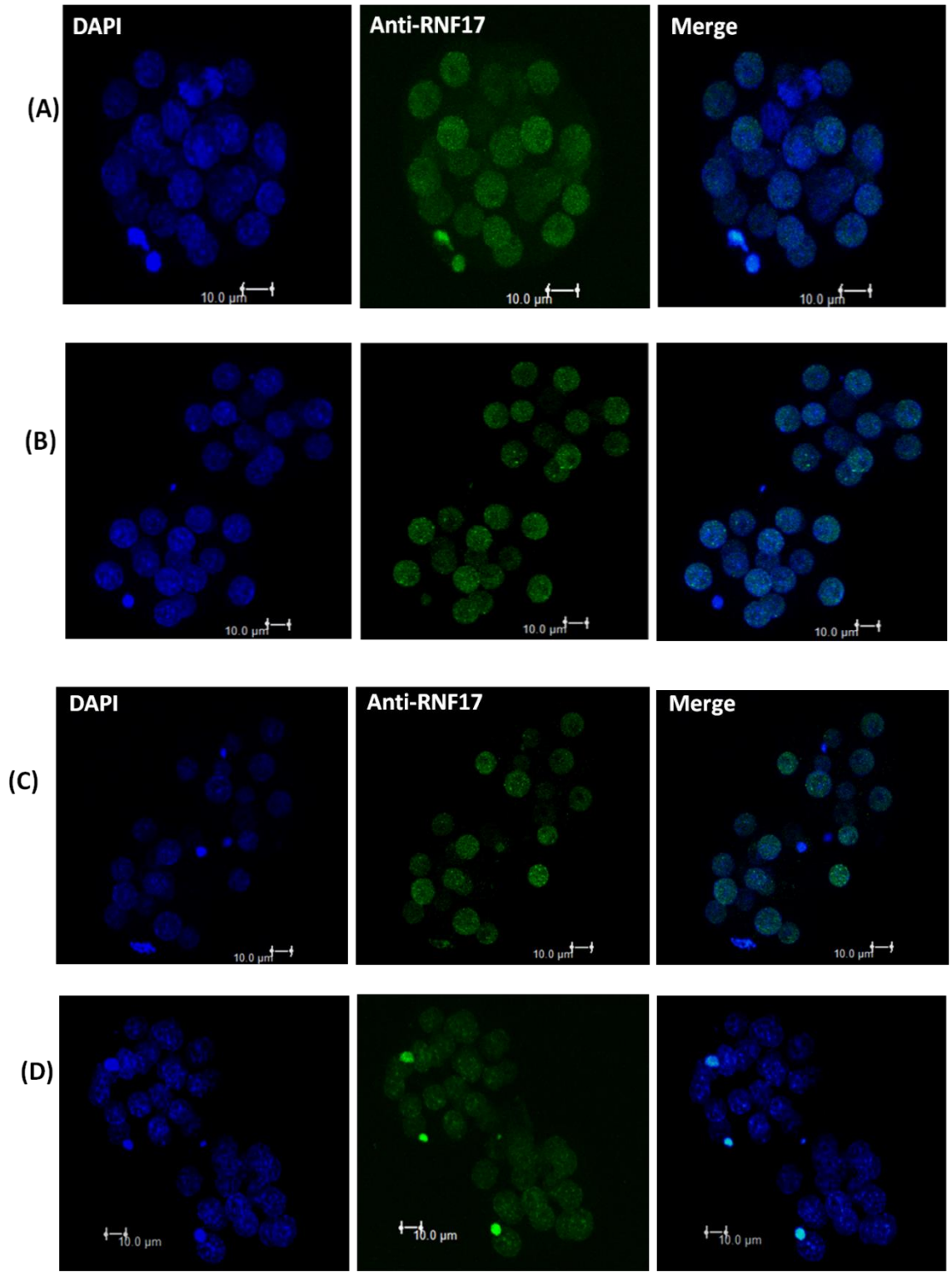

Fig 6.6 *(continued)*

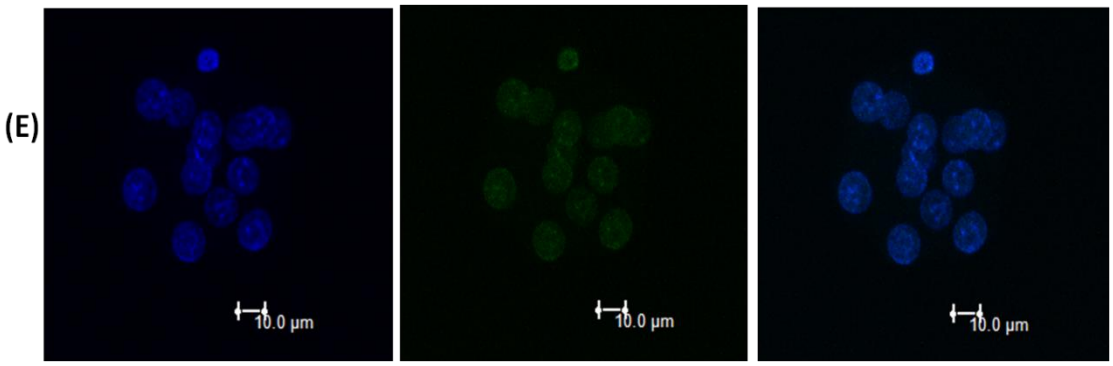

Fig 6.6: Expression and subcellular localisation of RNF17 in Rnf17 knockdown embryos. 2-cell stage embryos were microinjected with **(A)** AllStar_siRNA, **(B)** Rnf17_siRNA_1, **(C)** Rnf17_siRNA_2, **(D)** Rnf17_siRNA_3 or **(E)** Rnf17_siRNA_4. Injected embryos were *in vitro* cultured for 3 days before immunostained with anti-RNF17. Embryo injected with Rnf17_siRNA_4 display faint signal for RNF17 compared to other Rnf17_siRNA embryos.

- **Left panels:** staining of the nuclei with DAPI
- **Middle panels**: RNF17 signal
- **Right panels:** overlays (merge) of the two signals

6.3.4 Embryo development

Embryo development was assessed on day 3 post-injected embryos at the zygote and at the 2-cell stage. No significant differences were seen in embryo morphology within injected embryos. However, embryos injected at zygote stage were able to develop to blastocyst (cell number >30 cells), whereas embryos injected at 2-cell developed to the compacted stage of the morula (cell number <15 cells) or early blastocyst (>25 cells) on day 3 post-injection.

55% of embryos microinjected with Rnf17_siRNA_4 at the zygote stage were able to develop into blastocysts compared to 60% embryos injected with AllStar_siRNA or 65% non-injected embryos (Fig 6.7A). Embryos injected with Rnf17_siRNA_4 at 2-cell stage showed about 9% of embryos developing to blastocysts and 90% developing to morula compared to, 65% blastocyst and 35% morula with AllStar_siRNA, and 76% blastocyst and 23% morula for non-injected embryos (Fig 6.7B).

The cell number was counted, on day 3 post-injection of 2-cell embryos, by counting nuclei labelled with DAPI in immunostaining method. Embryos injected with Rnf17_siRNA_4 or AllStar_siRNA developed to the compacted morula stage, with cell a number of less than 15 cells. Those embryos had a reduced cell number compared to the morula stage of non-injected embryos. However, there were no significant differences between embryos injected with Rnf17_siRNA_4, which showed about 13 cells, and embryos injected with negative control AllStar_siRNA which showed about 15 cells (Fig 6.8).

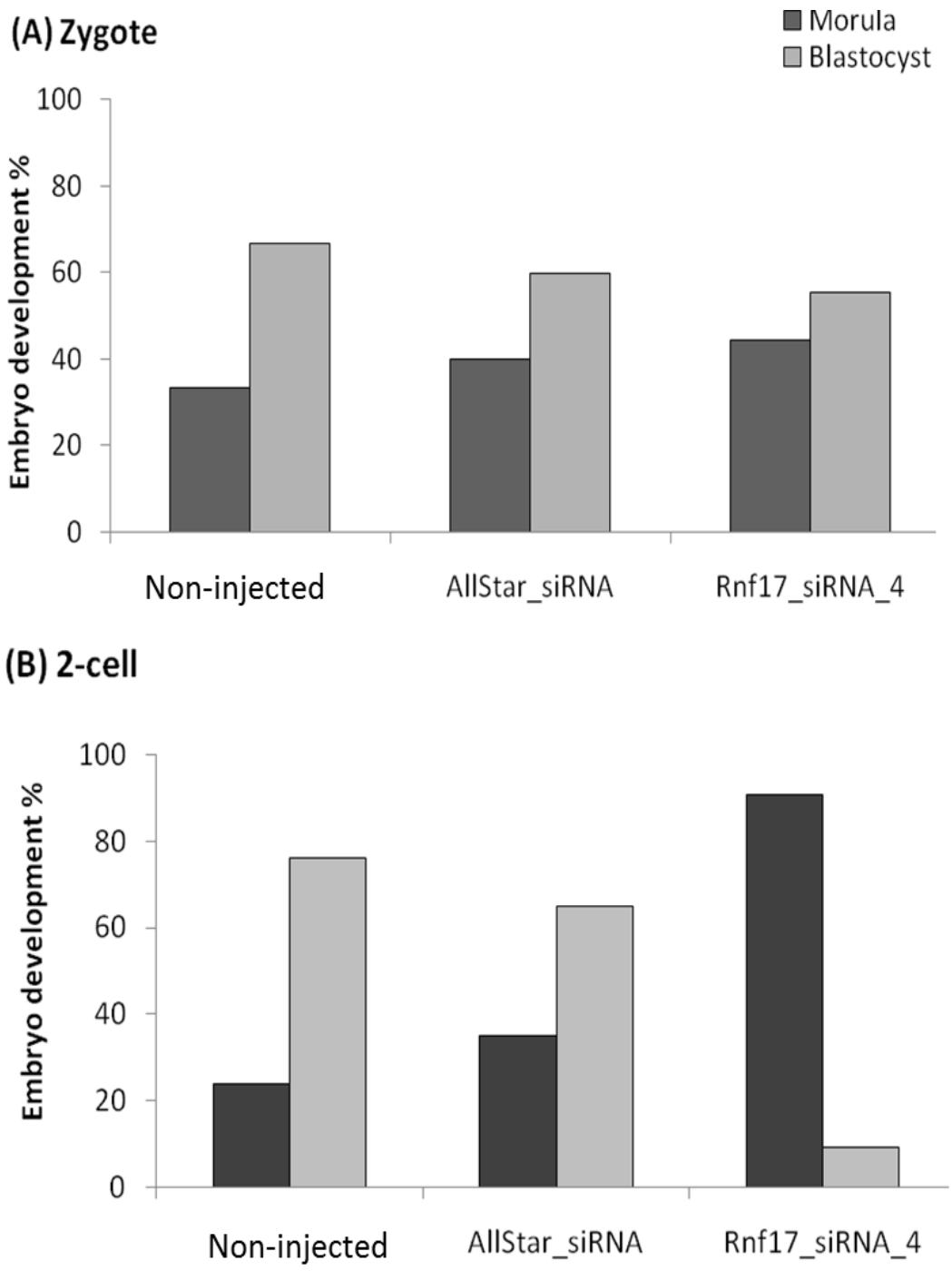

Fig 6.7 *(continued)*

Fig 6.7: Percentage of embryo development on day 3 post-microinjection with Rnf17_siRNA_4. Embryos microinjected with Rnf17_siRNA_4 or negative control AllStar_siRNA at **(A)** zygote or **(B)** 2-cell stage were *in vitro* cultured for three days. Non-injected embryos were *in vitro* cultured as negative control. Embryos injected at 2-cell stage with Rnf17_siRNA_4 delayed development to early blastocyst compared to those injected at zygote stage.

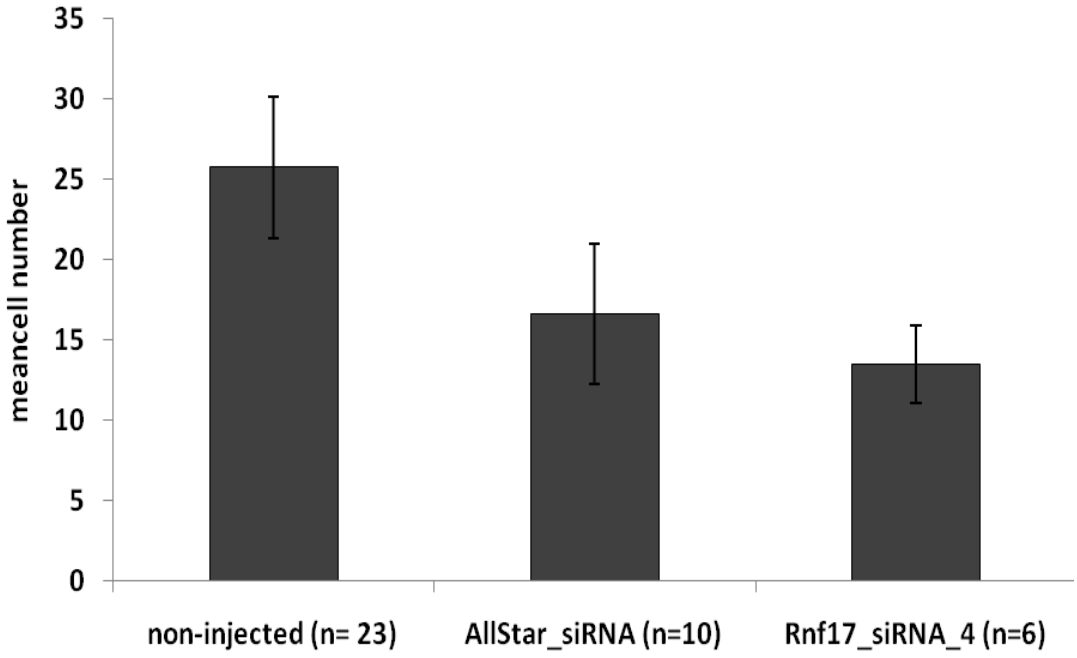

Fig 6.8: Rnf17 knockdown reduced embryo cell number. Microinjected 2-cell embryos with Rnf17_siRNA_4 or negative control AllStar_siRNA developed to compacted morula stage and were reduced cell number comparing to morula of non-injected embryos. Bar graphs show mean of cell number of microinjected embryos (n) and error bars represent standard deviation.

6.4 Discussion

In this chapter the potential function of Rnf17 in the development and growth of preimplantation embryos was investigated by RNA interference techniques. Our results revealed that Rnf17 knockdown reduced the embryo cell number and may have the potential to delay embryo development.

In Chapter 3 and 4 our results revealed that expression of Rnf17 in F9 cells and the preimplantation embryo were equivalent, and thus F9 cells provided a useful model for the study of expression and function of Rnf17 during embryo development. Here, F9 cells were transfected with a U6 promoter plasmid coding for an RNA composed of two identical 19-nucleotide sequence motifs in an inverted orientation, separated by a 9- base pair spacer to form a hairpin dsRNA (Elbashir *et al*, 2001) capable of mediating target Rnf17 inhibition. Transient transfected cells showed a decreased level of Luciferase activity of the Rnf17 sensor. Rnf17-RNAi expression plasmids were capable of inhibiting the Rnf17-sensor at high concentration (1.0 µg) in raw cells as a control experiment. However, this response was not seen within F9 cells. The Luciferase activity of the Rnf17-sensor increased on introducing the Rnf17-RNAi expressing plasmid in F9 cells. By increasing the dose of Rnf17-RNAi expressing plasmid, Luciferase activity of the Rnf17-sensor was reduced but not below the control level. Introducing a mutant sequence for Rnf17-RNAi induced Luciferase activity of the Rnf17-sensor, indicating that Rnf17-RNAi-mut is not compatible with the target sequence of the Rnf17-sensor.

In a biological experiment, Rnf17_siRNA oligonucleotides were microinjected into zygote or 2-cell embryos. Rnf17_siRNA effectively reduced levels of mRNA and protein RNF17 in microinjected embryos. Rnf17_siRNA microinjected into 2-cell embryos showed delayed embryo development, indicating a reduction in embryo proliferation. Rnf17 knockdown at 2-cell stage reduced the embryo cell number, although no significant reductions in

cell number were seen between the Rnf17_siRNA and negative control (AllStar_siRNA) microinjected embryos.

Injected embryos at zygote were 6-fold more developed to the early blastocyst than those injected at the 2-cell stage. This may suggest that Rnf17_siRNA would not target or perturb the potential involvement of maternal Rnf17 in blastocyst development, but would target transcribed Rnf17 mRNA from the embryonic genome (Hamatani *et al*, 2004). The delayed development of the blastocyst and reduced signal of RNF17 protein in Rnf17_siRNA injected embryos indicates that the reduction in Rnf17 mRNA was sufficient to inhibit the expression of RNF17 protein. This is consistent with the level of cells per embryo stained with anti-RNF17 as seen in Figure 6.6, which also indicates that not all cells within single embryos had Rnf17-knockdown. For Rnf17_siRNA_1 and Rnf17_siRNA_2, about 40% of cells per embryo were labelled with anti-RNF17. In the case of embryos injected with Rnf17_siRNA_3, about 60% of cells per embryo did not gain an anti-RNF17 signal, whereas those injected with Rnf17_siRNA_4 were completely (about 90%) without the anti-RNF17 signal.

Rnf17 knockdown further suggests that Rnf17 is required during the early embryonic stages following embryonic genome activation and suggests a role for Rnf17 in the development of mouse blastocysts. However, there is the possibility of the effect of experimental procedure on the expression of Rnf17, such as mouse superovulation or embryo culture. Microarray analysis revealed that Rnf17 is differentially regulated at large antral follicles isolated from superovulated female mice and cultured *in vitro* to meiotic competence (Pan *et al*, 2005). Also Rnf17 has been shown to be differentially regulated following *IVC* or *IVF* cultured mouse embryos compared to *in vivo* cultured (Giritharan *et al,* 2007). These findings may explain variabilities in the non-injected embryo development percentages in Figure 6.7

In c-Myc mutant mice, the complete loss of c-Myc function blocks the proliferation of isolated mouse embryonic fibroblasts (MEFs) at E9.5 (Trumpp *et al,* 2001). In the same study, for some organs (thymus, spleen, lymph nodes and bone marrow) the organ/body weight ratio was reduced and consequently had a decreased cell number in those organs (Trumpp *et al,* 2001). Our results showed that Rnf17 knockdown reduced the cell number in mouse embryos, therefore, it would be interesting to examine the expression of c-Myc in those embryos and also whether the knockdown of c-Myc compromises the expression level of Rnf17. In both experiments for Rnf17 knockdown, only the efficiency of Rnf17 knockdown was investigated in cells co-transfected with Rnf17-RNAi and mouse microinjected embryos with Rnf17_siRNA. Further studies would be important in quantifying the levels of mRNA and protein for Rnf17 and c-Myc in Rnf17 or in c-Myc knockdown embryos. This might give insight to the function of Rnf17 in embryo development and cell proliferation.

In summary, down regulation of Rnf17by siRNA technology decreased cell proliferation in the preimplantation embryo. However, no specific knockdown was a achieved in transfected F9 cells with Rnf17-RNAi plasmids. Further experiments to investigate cell proliferation and protein level are required to answer the question whether the endogenous Rnf17 in F9 cells might provide a sink to mop up the Rnf17-RNAi plasmids, so that it is not targeting the Rnf17-sensor. Our data also provide considerable results to suggest that Rnf17_siRNA could potentially be an experimental approach to identify a role for Rnf17 in cell proliferation and/or embryo development.

Chapter 7

7. General Discussion

The preimplantation period of embryo development is critical as stresses can effect embryo development and postnatal health. Alterations to the *in vitro* or *in vivo* embryo environment can influence blastocyst proliferation and differentiation, gene expression and embryo morphogenesis which may contribute to long-term health and adult-onset disease. The aim of this PhD was to study one particular gene: Rnf17 that contributes to the cell signalling network comprising Myc/Max/Mxd, and functions to regulate cell proliferation and differentiation.

The function of Rnf17 in embryo development is elusive; however, over-expression of Rnf17 in cell culture models enhances Myc activity by sequestering Mxd (Yin *et al*, 1999). Using RT-qPCR our results showed that Rnf17 is expressed in the preimplantation embryo and its expression is increased from the 2-cell to blastocyst stages, consistent with previous Microarray studies (Zeng *et al,* 2004). However, the expression level for Rnf17L was reduced compared with that from Rnf17S. Rnf17 mRNA and protein were detected during the cleavage stages of mouse embryos from 2-cell to blastocyst. Raw data for Ct values for RT-qPCR revealed increased expression of Rnf17S, Rnf17L and c-Myc throughout embryo development consistent with the database that detected Rnf17 in pre- and post-implantation embryo (Smith *et al*, 2012). The increased expression for Rnf17 and c-Myc during embryo cleavage implicates the possibility that Rnf17 modulates c-Myc activity in preimplantation embryos. This was shown *in vitro* in Chapter 3, that over-expression of Rnf17 expression construct induced Luciferase activity of c-Myc reporter construct in co-transfected F9 cells.

No significant effects of a maternal LPD or HPD were seen on the expression of Rnf17S, Rnf17L, c-Myc and Mxd3 in mouse blastocysts. Previous studies have revealed the effect of maternal LPD on embryo

growth regarding gene expression and signalling pathways, for example, the mTOR (mammalian target of rapamycin) and eukaryotic initiation factor 2 (eIF2) signalling pathways that control protein synthesis in response to nutrient availability. Degradation of MXD1 and inducing activity of c-Myc target genes (Zhu *et al*, 2008; Chou *et al*, 2009), suggest a role for E3 ligase via ubiquatinylation pathway downstream of the mTOR pathway for embryo proliferation and growth. Although expression of Mxd3 was very low in mouse blastocysts, the result revealed the interplay between Mxd and Rnf17 in modulating c-Myc at preimplantation stages, under environmental conditions which could influence embryo proliferation and differentiation.

The expression of Rnf17 is associated with the regulation of some of the genes which have been identified as c-Myc targets (Yin *et al*, 2001). Therefore, it is possible to suggest here that some of these target genes are subject to the same regulation by Rnf17 as they are by c-Myc. It is also possible to interpret that Rnf17 down regulates the expression of endogenous c-Myc as a means of compensating for its pro-apoptotic activity (Yin *et al*, 2001). However, over-expression of Rnf17 sequestering Mxd raises the possibility that Rnf17 may deplete the nucleus of Mxd proteins leaving other Mxd-interacting proteins free to interact with other nuclear partners. Therefore, it is expected that over-expression of Rnf17 induces cell proliferation and apoptosis, under appropriate conditions, as is expected for cells with over-expressed c-Myc (Yin *et al*, 2001).

RNF17 protein was identified in a yeast two-hybrid screen by its ability to interact with members of the MXD family, a transcriptional repressor of Myc target genes. The RNF17-MXD member interaction causes the loss of DNA binding by MXD-MAX heterodimers (Yin *et al,* 1999; 2001). Using the proteasome inhibitor MG132 and Western blotting RNF17 and MXD co-expression causes the loss of both factors via the ubiquitinylation pathway. MXD1 protein is also a target protein for the oncogene c-IAP (Xu *et al,* 2007).

However, serum induction in cultured cells induced MXD1 degradation by phosphorylation at Ser 145 by p90 ribosomal kinase (RSK) and by p70 S6 kinase (S6K) independent of c-IAP (Zhu *et al*, 2008). PI3/AKT is another kinase that phosphorylates MXD1 at Ser 145, which inhibits the repressor function of MXD1 by interfering with its DNA binding (Chou *et al*, 2009). Activation of RSK leads to the activation of mTORC1 and subsequently of S6K (Wang *et al*, 2001; Raught *et al,* 2004), whereas mutations that activate the PI3K pathways will stimulate the mTORC1–S6K pathway (Carriere *et al,* 2008; Roux *et al,* 2004). Both RNF17 and c-IAP proteins contain a RING motif and have the properties of a ubiquitin E3 ligase. The two proteins possess similar mechanisms of MXD protein degradation, suggesting a common means of promoting cell proliferation and controlling Myc/Max/Mxd network associations. However, it is possible to suggest that the RING finger domain of RNF17 may bind other targets, perhaps as part of a higher order complex, in association with MXD proteins within the RSK and S6K or PI3/Akt pathways.

It is also possible that the degradation of MXD1 in serum-induced cells (Zhu *et al,* 2008; Chou *et al*, 2009) is mediated by RNF17 and thus suggests induced RNF17 expression under serum-culture conditions. This supports our results in Chapter 5 that maternal diets do not interact with Rnf17 and thus that Rnf17 is differentially regulated by another mechanism *in utero* conditions or *in vitro* culture (Giritharan *et al*, 2007). Rhox5 is expressed in reproductive tissues such as those of the testis, ovary and placenta and plays a role in controlling the development of these organs. Rhox5 has been shown to be modified in mouse embryo cultured in KSOM media supplemented with foetal calf serum (FCS) (Fernandez-Gonzalez *et al,* 2009). Rhox5 has also been shown to be down regulated together with Rnf17 and other genes involved in germ cell development and fertility (including Dazl and Mvh) in Dppa4-deficient embryonic stem cells (Madan *et*

al, 2009). This may support our speculation that culture conditions differentially regulate Rnf17.

Early compensatory responses of the embryo to poor diet increase trophectoderm cell number and enhance embryo proliferation (Eckert *et al*, 2012). To be consistent with these findings, further experiments are required to investigate the expression of RNF17 protein in extended embryo growth, and whether RNF17 is related to embryo proliferation at this stage. However, maternal LPD has been shown to induce adaptive responses in the blastocyst extra-embryonic lineage (visceral yolk sac) to protect foetal and postnatal growth (Watkins *et al*, 2008a). RT-qPCR results, in Chapter 5, showed a significant increase in the expression of Rnf17S in E17.5 testes. Induced expression of Rnf17S in male germ gonadal tissues during *de novo* DNA methylation may implicate adaptive responses induced in primordial germ cells by maternal LPD to protect foetal gonad differentiation and development.

Immunostaining results in Chapter 3 and Chapter 4 revealed that the RNF17 protein is expressed in the preimplantation embryo and is predominantly nuclear with a low intensity level in the cytoplasm. Detected endogenous RNF17 in F9 cells displayed a similar pattern to that seen within the mouse embryo. The nuclear expression pattern of RNF17 in early embryo development or in F9 cells may suggest a role of RNF17 in the spliceosome complexes for pre-mRNA splicing. Proteomic analysis of nuclear complexes of Hela cells revealed an interaction between CDC5L and RNF17 (Lleres *et al*, 2010). CDC5L protein is required for the second catalytic step of pre-mRNA splicing, and its complex with PLRG1 interacts with hn-RNP-M to modulate both the 5' and 3' alternative splicing processes (Ajuh *et al,* 2000).

Interaction between Tudor domain-containing proteins and PIWI proteins is mediated by sDMA, which is brought about by protein arginine N-

methyltransferases such as PRMT5 (Arkov and Ramos, 2010). The nuclear expression of Prmt5 at early mouse embryonic stages (Tee *et al*, 2010) together with that of RNF17 raises the possibility of an interaction between RNF17 and PRMT5 via sDMA to promote biological activities such as chromatin remodelling or transposon silencing in the preimplantation embryo.

Another possibility for the nuclear expression of RNF17 protein is the presence of two bipartite NLS encoded within RNF17 isoforms (AceView) which revealed the ability of RNF17 to shuttle between the cytoplasm and the nucleus. The results showing that RNF17 exhibits a punctate distribution in the nucleus and in the cytoplasm is consistent with the tendency of other well characterised RING finger proteins to display related behaviours. For example, BRCA1 RING finger-containing is a tumour suppressor protein that associates with BARD1 to form a RING/RING heterodimer and functions as an ubiquitin E3 ligase. The Ub-conjugating enzyme UbcH5c binds only to the BRCA1 RING domain and not the BARD1 RING (Brzovic *et al,* 2003). Using immunostaining and proteasome inhibitor MG132 (Chapter 3), our results in Cos-1 cells revealed that RNF17 is shuttled between the cytoplasm and the nucleus in response to proteasome inhibition. BRCA1 also contains nuclear exporting (NES) and localising (NLS) signals which allow it to co-localise to nuclear foci following interaction with RAD51, where DNA repair occurs after treatment with DNA damaging reagents (Rodriguez *et al,* 2000; Thakur *et al,* 1997).

It is important to note here that no differences were found in the expression and distribution of RNF17 between the inner cell mass and the trophectoderm, suggesting that RNF17 is expressed in both embryonic and extra-embryonic tissues and may be involved in germline development and differentiation. This may support the immunostaining results that the expression of RNF17 in foetal E17.5 testes is expressed in the nuclei of Sertoli cells with weak signal in those of prospermatogonia. Previously,

Rnf17 was detected in mouse adult testes and localised to specific cytoplasmic structures, termed nuage, in all germ cells including spermatogonia, spermatocysts and spermatids (Pan *et al*, 2005). RNF17 can be Immunoprecipitated from adult testes with MIWI- a PIWI protein that is expressed after birth in mouse testes (Vagin *et al,* 2009; Beyret *et al*, 2012), although $Rnf17^{-/-}$ mice had no effect on the expression of Miwi (Pan *et al*, 2005). Additionally, the differentiation of somatic cells into germ cells from bone marrow (Nayernia *et al,* 2006) or embryonic stem cells (Lavagnolli *et al,* 2009) showed that Rnf17 is expressed as PGC marker (including fragilis, stella, Mvh and Oct4) but not those for spermatogonia or spermatogonial stem cells (such as Rbm, c-Kit, Tex18, Stra8, Mili, Dazl, Hsp90) (Nayernia *et al,* 2006), which supports our results that RNF17 is expressed in foetal Sertoli cells.

In male gonads, Sertoli cells are differentiated between E11.0 and E13.5 (Adams and McLaren, 2002; reviewed in Ross and Capel, 2005; McLaren, 2003) and coincides with proliferation of transcriptional factors such as *Sox9* localised in the nuclei of the Sertoli cells (Nel-Themaat *et al*, 2009; reviewed in Park and Jameson, 2005). Studies showed expression of miRNA in mouse and bovine foetal and adult Sertoli cells and that these are involved in endocrine signalling for male sex differentiation and testis development (Wainwright *et al*, 2013; Torley *et al*, 2011; Panneerdoss *et al,* 2012). This suggests that Rnf17 in foetal testes may function with transcriptional factors; such as Sox9, and with miRNA for endocrine signalling and testis development.

In Chapter 6, preliminary experiments showed Rnf17 knockdown by siRNA could delay preimplantation development, suggesting a role for Rnf17 in embryo proliferation, although more work is needed. Microinjection of mouse embryos with siRNA targeting Rnf17 reduced the cellular mRNA level of Rnf17 and the protein signal of RNF17 in mouse embryo blastocysts.

Knockdown of Rnf17 in 2-cell embryo, at the time of zygotic gene activation, has the potential to delay blastocyst development. However embryos were able to reach the blastocyst stage on day 3 post-injection which indicates that maternal Rnf17 mRNA and protein is not a storage pool for zygotic RNF17 involved in embryo growth.

Using Rnf17-RNAi construct, transfected F9 cells reduced the Luciferase activity of target construct for Rnf17 compared to the control. It is possible that higher dose of RNAi constructs is targeting endogenous Rnf17 within transfected F9 cells. Further investigation using Western blot to measure protein levels for RNF17 and c-Myc following stable transfection may assist in clearing up any ambiguities. This is may be consistent with embryo microinjection results that 20 µM, but not 10 µM, of siRNA oligonucleotide was able to knockdown Rnf17. Another possibility is that different proteins have different turnover rates in which stable proteins require a longer period of exposure to siRNAs to be knocked down (McManus and Sharp, 2002). Thus incubation of injected embryos with Rnf17_siRNA for 3 days reduced the expression of mRNA and protein signal for Rnf17. Further repeats of this experiment is recommended to identify the long-term effects on embryo development for Rnf17 knockdown.

In conclusion, our results for up- and down- regulation of Rnf17 support the role of Rnf17 in modulating c-Myc activity and, therefore, regulating the Myc/Max/Mxd signalling network in preimplantation embryos. The expected function of specific domains of RNF17 suggests that these domains are critical for cell proliferation and differentiation. Subcellular localisation results indicated that RNF17 is shuttled between the nucleus and the cytoplasm by means of NLS domains. In response to proteasomal activity RNF17 acts as a RING E3 ligase to degrade MXD via ubiquitinylation. RNF17 is a multi-Tudor-containing protein, which interacts via sDMA with target proteins for posttranscriptional activity or chromatin remodelling.

It is possible that Rnf17 expression creates a Mxd-null phenotype by MXD ubiquitinylation leading to its subsequent degradation and that Rnf17 modulates c-Myc in early development and contributes to embryo proliferation. Conversely, with the loss in function of Rnf17, by siRNA knockdown, a delayed development and reduced cell proliferation in embryos was observed; however more repeats are necessary to confirm these findings.

7.1 Future prospective

More studies are needed to fully understand the molecular function of RNF17 in embryo growth as well as in the oocyte and the testis. While structural studies of the RING and Tudor domains have greatly increased our knowledge of RNF17, its function is still elusive. Further experiments for co-transfection of RNF17 expression plasmids with mutant interacting residuals for MXD1-RNF17 into MG132-treated or untreated cultured cells is important to investigate the effect of MXD1-RNF17 interaction on cell proliferation and growth. The ability of RNF17 to shuttle between the nucleus and the cytoplasm could be examined in a transfection model for Rnf17 expression construct with mutant K/R residues to perturb NLS functioning. Studying the nuclear localisation property of RNF17 is vital in studying the role of Rnf17 in cell cycle. Therefore, experiments for mutation of cell cycle regulators (entry or exit) may point out the mechanism of disappearance of RNF17 during cell division.

Further investigations are required to investigate the function of Rnf17 in preimplantation development and whether RNF17 interacts with PIWI proteins at early stages for transposable element silencing. Using F9 cells, as a model for preimplantation embryo, Immunoprecipitation would be a useful experiment to find out the interaction between RNF17 and PIWI proteins, and whether this is related to transposable element silencing during embryo development. It would be interesting to apply the experiments to

examine mRNA and protein levels for Rnf17 and c-Myc expression within F9 cells or embryo following Rnf17 knockdown.

Further experiments are important to test whether the knockdown of endogenous Rnf17 may induce c-Myc activity in co-transfected F9 cells with Rnf17-RNAi. This would be useful by measuring the Luciferase activity of c-Myc reporter construct or examine the expression of c-Myc target genes by RT-qPCR. Investigations for expression of Line-1 in Rnf17 knockdown in F9 cells and embryos are required to answer the questions whether Rnf17 has a role in silencing transposon elements in early embryo stages and whether Line-1 influence embryo growth and development.

It is important to examine the level of RNF17 and c-MYC protein to point out their transcriptional level for cell proliferation in the early embryo, specifically since no differences were seen in the expression of RNF17 protein between ICM and TE. It is interesting to examine the effect of maternal LPD on the expression of RNF17 and c-MYC in ICM and TE and whether this is related to the migration and proliferation of the primordial germ cell from E9.0 to E13.5.

Finally, more repeats for experiments in this thesis are recommended to give insight whether of Rnf17 modulates Myc in the early embryo and to explain the mechanism of Rnf17 in creating a MXD-null phenotype.

Appendices

Appendix I: Media preparation for embryo

H6-BSA

Stock B (stored at 4-8°C for up to 2 weeks)

dH2O	10 ml
Sodium hydrogen carbonate ($NaHCO_3$)	0.216 g

Stock E (stored at 4-8°C for up to 3 months)

dH2O	50 ml
Hepes	2.9785 g

Stock F (stored at 4-8°C for up to 3 months)

Sodium chloride (NaCl)	4.720 g
Potassium chloride (KCl)	0.110 g
Sodiumdihydrogenorthophosphate ($NaH_2PO4.2H_2O$)	0.060 g
Magnesium chloride ($MgCl_2$)	0.100 g
D-glucose	1.000 g
DL-lacticacid	3.4 ml
dH2O	Made-up to 100 ml

Stock G (stored at 4-8°C for up to 2 weeks)

dH2O	10 ml
Pyruvic acid	0.0 30g
Penicillin	0.0 60g
streptomycin	0.0 50g

Stock H (stored at 4-8C for up to 3 months)

dH2O	10 ml
Calciumchloridedehydrate (CaCl2.2H2O)	0.260 g

20% sodium Chloride

dH2O	10 ml
Sodiumchloride (NaCl)	1.0 g

To prepare 100ml of H6-BSA

dH2O	78 ml
Stock B	1.6 ml
Stock E	8.4 ml
Stock F	10 ml
Stock G	1.0 ml
Stock H	1.0 ml
20% NaCl	0.6 ml
BSA (sigma, embryo culture tested, A3311)	0.4 g

PH adjusted to 7.4; osmolarilty adjusted to 270-280 mOsm; sterile filtered (0.22µm filter); aliquots and stored at 4°C

Appendix II: Reagents for western blotting

1. SDS/PAGE gel

10% Amps (ammonium persulphate (200µL)	0.02g Amps in 200µl dH2O
10% SDS	50g SDS in 50ml dH2O

Reagents	**Resolving gel buffer (3M Tris-HCl pH 8.85)**	**Stacking gel buffer (0.25M Tris-HCl pH 6.8)**
Tris	36.33g	3.028g
dH2O	80ml	80ml
Adjust pH with concentrated HCl	to 8.85	6.8

Make volume with dH2O up to 100ml

Gel preparation	**Resolving gel 8% (10 ml for 2 gels)**	**Stack gel 4% (5 ml for 2 gels)**
dH_2O	4.61ml	3.4ml
Acrylamide (Protogel) (30% stock)	2.66ml	0.625ml
TRIS Res	2.5ml	0.835ml
10% SDS	100µl	50µl
10% Amps*	100µl	50µl
Temed*	10 µl	5µl

*Amps and Temed must be added last as they cause polymerisation.

2. Reagent for blotting

5X SDS PAGE running buffer (1L) (0.125M Tris, 1.25M Glycine, 0.5% SDS)

Tris base	15.1g
Glycine	94g
10% SDS	50ml
dH2O	Make up to 1L

Use at 1x (0.025M Tris, 0.25M glycine, 0.1%SDS)

Transfer buffer (1L)

100% Methanol	50ml
1x SDS running buffer	200ml

3. Reagents for gel labelling

PBS (500ml)

5 tablets of phosphate buffer saline (Dulbecon) in 500ml dH_2O.
Autoclave

0.1% Tween-20 in PBS (0.1% PBS-T)

500µl tween-20 in 500ml PBS

10% Blocking solution

Powder dried milk	10g
0.1% PBS-T	100ml

5% Blocking solution

Powder dried milk	5g
0.1% PBS-T	100ml

Appendix III: Media and reagents for cloning

1. Growth media

LB media

Bacto-tryptone	10g
Bacto-yeast etract	5g
NaCl	10g
dH_2O	950 ml

Shake until the solutes have dissolved. Adjust volume to 1L with dH_2O. Autoclave.

LB agar

Dissolve 15g Agar into 1L LB media

IPTG (100mM)

238mg dissolved in 10ml dH_2O

X-gal

200mg X-gal dissolved in 10ml

2. Addition of 3' A overhang to PCR product (total volume 50µl)

5X *GoTaq*® Flexi Buffer	10µl
25 mM MgCl2	4µl
GoTaq® DNA Polymerase	0.5µl
25mM dNTP	0.5µl
PCR Product	35µl

3. TA cloning of 3´A overhangs PCR products(total volume 5µl)

Taq tailed PCR product	1µl
pGEM®-TEasy vector	0.5µl
Ligase 2X Rapid Buffer	2.5µl
T4 DNA Ligase	0.5µl
dH_2O	0.5 µl

Appendix IV

1. **End point PCR reaction (total volume 50µl) using Phusion® Hot Start**

	10µl
5X Phusion® HF Buffer	
50mM MgCl2	2µl
25mM dNTP	0.5µl
Forward Primer (100ng)	1µl
Reverse Primer (100ng)	1µl
Template (1:100diluted)	1µl
Phusion® Hot Start DNA polymerase	0.5µl
dH2O	34µl

2. **End point PCR reaction using *GoTaq* (total volume 1µl)**

5X *Go Taq*® Flexi Buffer	10µl
25mM MgCl2	4µl
25mM dNTP	0.5µl
Forward Primer (100ng)	1µl
Reverse Primer (100ng)	1µl
Template	1µl
GoTaq® DNA polymerase	0.25µl
dH2O	32.25µl

3. **Treatment of extracted RNA with DNaseI (total volume 25µl**)

RNA template	10µl
RNA inhibitor	0.5µl
Buffer	2.5µl
DNaseI	1µl

4. **cDNA synthesis (total volume20 µl)**

	4µl
5X RT reaction Buffer	
2mM dNTP	0.5µl
RNAs Inhibitor	0.5µl
Random primer	2µl
Reverse Transcriptase (RT)	1µl
cDNA	12µl

References

Adams, I. R. and McLaren, A. (2002) 'Sexually dimorphic development of mouse primordial germ cells: switching from oogenesis to spermatogenesis', *Development,* 129(5), 1155-1164.

Agrawal, N., Dasaradhi, P. V. N., Mohmmed, A., Malhotra, P., Bhatnagar, R. K. and Mukherjee, S. K. (2003) 'RNA interference: Biology, mechanism, and applications', *Microbiology and Molecular Biology Reviews,* 67(4), 657-685.

Ajuh, P., Kuster, B., Panov, K., Zomerdijk, J., Mann, M. and Lamond, A. I. (2000) 'Functional analysis of the human CDC5L complex and identification of its components by mass spectrometry', *Embo Journal,* 19(23), 6569-6581.

Anand, A. and Kai, T. (2012) 'The tudor domain protein Kumo is required to assemble the nuage and to generate germline piRNAs in Drosophila', *Embo Journal,* 31(4), 870-882.

Andersen, C. L., Jensen, J. L. and Orntoft, T. F. (2004) 'Normalization of real-time quantitative reverse transcription-PCR data: A model-based variance estimation approach to identify genes suited for normalization, applied to bladder and colon cancer data sets', *Cancer Research,* 64(15), 5245-5250.

Aravin, A., Gaidatzis, D., Pfeffer, S., Lagos-Quintana, M., Landgraf, P., Iovino, N., Morris, P., Brownstein, M. J., Kuramochi-Miyagawa, S., Nakano, T., Chien, M. C., Russo, J. J., Ju, J. Y., Sheridan, R., Sander, C., Zavolan, M. and Tuschl, T. (2006) 'A novel class of small RNAs bind to MILI protein in mouse testes', *Nature,* 442(7099), 203-207.

Aravin, A. A., Sachidanandam, R., Girard, A., Fejes-Toth, K. and Hannon, G. J. (2007) 'Developmentally regulated piRNA clusters implicate MILI in transposon control', *Science,* 316(5825), 744-747.

Arkov, A. L. and Ramos, A. (2010) 'Building RNA-protein granules: insight from the germline', *Trends in Cell Biology,* 20(8), 482-490.

Barker, D. J. P. (2000) 'In utero programming of cardiovascular disease', *Theriogenology,* 53(2), 555-574.

Barker, D. J. P. and Osmond, C. (1986) 'Infant-Mortality, Childhood Nutrition, and Ischemic-heart-Disease in England and Wales', *Lancet,* 1(8489), 1077-1081.

Beyret, E. and Lin, H. (2011) 'Pinpointing the expression of piRNAs and function of the PIWI protein subfamily during spermatogenesis in the mouse', *Developmental Biology,* 355(2), 215-226.

Beyret, E., Liu, N. and Lin, H. F. (2012) 'piRNA biogenesis during adult spermatogenesis in mice is independent of the ping-pong mechanism', *Cell Research,* 22(10), 1429-1439.

Brzovic, P. S., Keeffe, J. R., Nishikawa, H., Miyamoto, K., Fox, D., Fukuda, M., Ohta, T. and Klevit, R. (2003) 'Binding and recognition in the assembly of an active BRCA1 /BARD1 ubiquitin-ligase complex', *Proceedings of the National Academy of Sciences of the United States of America,* 100(10), 5646-5651.

Cahill, M. A., Ernst, W. H., Janknecht, R. and Nordheim, A. (1994) 'Regulatory Sequelching', *Febs Letters,* 344(2-3), 105-108.

Cano, F., Saavedra, D. M. and Lehner, P. J. (2010) 'RNA-binding E3 ubiquitin ligases: novel nucleic acid regulation', *Biochemical Society Transactions,* 38, 1621-1626.

Carriere, A., Cargnello, M., Julien, L.-A., Gao, H., Bonneil, E., Thibault, P. and Roux, P. P. (2008) 'Oncogenic MAPK signaling stimulates mTORC1 activity by promoting RSK-mediated Raptor phosphorylation', *Current Biology,* 18(17), 1269-1277.

Castiel, A., Danieli, M. M., David, A., Moshkovitz, S., Aplan, P. D., Kirsch, I. R., Brandeis, M., Kraemer, A. and Izraeli, S. (2011) 'The Stil protein regulates centrosome integrity and mitosis through suppression of Chfr', *Journal of Cell Science,* 124(4), 532-539.

Ceelen, M., van Weissenbruch, M. M., Vermeiden, J. P. W., van Leeuwen, F. E. and de Waal, H. A. D.-v. (2008) 'Cardiometabolic differences in children born after in vitro fertilization: Follow-up study', *Journal of Clinical Endocrinology & Metabolism,* 93(5), 1682-1688.

Chan, G. K. and Yen, T. J. (2003) 'The mitotic checkpoint: a signaling pathway that allows a single unattached kinetochore to inhibit mitotic exit', *Progress in cell cycle research,* 5, 431-9.

Chaturvedi, P., Sudakin, V., Bobiak, M. L., Fisher, P. W., Mattern, M. R., Jablonski, S. A., Hurle, M. R., Zhu, Y., Yen, T. J. and Zhou, B. B. S. (2002) 'Chfr regulates a mitotic stress pathway through its RING-finger domain with ubiquitin ligase activity', *Cancer Research,* 62(6), 1797-1801.

Chen, C., Jin, J., James, D. A., Adams-Cioaba, M. A., Park, J. G., Guo, Y., Tenaglia, E., Xu, C., Gish, G., Min, J. and Pawson, T. (2009) 'Mouse Piwi interactome identifies binding mechanism of Tdrkh Tudor domain to arginine methylated Miwi', *Proceedings of the National Academy of Sciences of the United States of America,* 106(48), 20336-20341.

Chen, C., Nott, T. J., Jin, J. and Pawson, T. (2011) 'Deciphering arginine methylation: Tudor tells the tale', *Nature Reviews Molecular Cell Biology,* 12(10), 629-642.

Chou, C.-K., Lee, D.-F., Sun, H.-L., Li, L.-Y., Lin, C.-Y., Huang, W.-C., Hsu, J.-M., Kuo, H.-P., Yamaguchi, H., Wang, Y.-N., Liu, M., Wu, H.-Y., Liao, P.-C., Yen, C.-J. and Hung, M.-C. (2009) 'The Suppression of MAD1 by AKT-Mediated Phosphorylation Activates MAD1 Target Genes Transcription', *Molecular Carcinogenesis,* 48(11), 1048-1058.

Cooney, C. A., Dave, A. A. and Wolff, G. L. (2002) 'Maternal methyl supplements in mice affect epigenetic variation and DNA methylation of offspring', *Journal of Nutrition,* 132(8), 2393S-2400S.

De Fazio, S., Bartonicek, N., Di Giacomo, M., Abreu-Goodger, C., Sankar, A., Funaya, C., Antony, C., Moreira, P. N., Enright, A. J. and O'Carroll, D. (2011) 'The endonuclease activity of Mili fuels piRNA amplification that silences LINE1 elements', *Nature,* 480(7376), 259-U148.

DeBaun, M. R., Niemitz, E. L. and Feinberg, A. P. (2003) 'Association of in vitro fertilization with Beckwith-Wiedemann syndrome and epigenetic alterations of LIT1 and H19', *American Journal of Human Genetics,* 72(1), 156-160.

Deshaies, R. J. and Joazeiro, C. A. P. (2009) 'RING Domain E3 Ubiquitin Ligases', *Annual Review of Biochemistry,* 78, 399-434.

Desjardins, C. and Ewing, L.L. (1993) 'Cell and Molecular Biology of Testis'. Oxford University Press, Oxford, UK

Doherty, A.S., Mann, M. R. W., Tremblay, K. D., Bartolomei, M. S. and Schultz, R. M. (2000) 'Differential effects of culture on imprinted H19 expression in the preimplantation mouse embryo', *Biology of Reproduction,* 62(6), 1526-1535.

Domashenko, A. D., Latham, K. E. and Hatton, K. S. (1997) 'Expression of myc-family, myc-interacting, and myc-target genes during preimplantation mouse development', *Molecular Reproduction and Development,* 47(1), 57-65.

Durban, M., Benet, J., Sarquella, J., Egozcue, J. and Navarro, J. (1998) 'Chromosome studies in first polar bodies from hamster and human oocytes', *Human Reproduction,* 13(3), 583-587.

Eberhardy, S. R., D'Cunha, C. A. and Farnham, P. J. (2000) 'Direct examination of histone acetylation on Myc target genes using chromatin immunoprecipitation', *Journal of Biological Chemistry,* 275(43), 33798-33805.

Eckert, J. J. and Fleming, T. P. (2008) 'Tight junction biogenesis during early development', *Biochimica Et Biophysica Acta-Biomembranes,* 1778(3), 717-728.

Eckert, J. J., Houghton, F. D., Hawkhead, J. A., Balen, A. H., Leese, H. J., Picton, H. M., Cameron, I. T. and Fleming, T. P. (2007) 'Human embryos developing in vitro are susceptible to impaired epithelial junction biogenesis correlating with abnormal metabolic activity', *Human Reproduction,* 22(8), 2214-2224.

Eckert, J. J., Porter, R., Watkins, A. J., Burt, E., Brooks, S., Leese, H. J., Humpherson, P. G., Cameron, I. T. and Fleming, T. P. (2012) 'Metabolic Induction and Early Responses of Mouse Blastocyst Developmental Programming following Maternal Low Protein Diet Affecting Life-Long Health', *Plos One,* 7(12).

Eisenman, R. N. (2001) 'Deconstructing Myc', *Genes & Development,* 15(16), 2023-2030.

Erickson, R. P. (1997) 'Does sex determination start at conception?'*Bioessays,* 19(11), 1027-1032.

Elbashir, S. M., Harborth, J., Lendeckel, W., Yalcin, A., Weber, K. and Tuschl, T. (2001) 'Duplexes of 21-nucleotide RNAs mediate RNA interference in cultured mammalian cells', *Nature,* 411(6836), 494-498.

Evsikov, S. V. and Evsikov, A. V. (1994) 'Preimplantation Development of Manipulated Mouse Zygotes Fused with the 2nd Polar Bodies- a Cytogenetic Study', *International Journal of Developmental Biology,* 38(4), 725-730.

Fang, G. W., Yu, H. T. and Kirschner, M. W. (1998) 'The checkpoint protein MAD2 and the mitotic regulator CDC20 form a ternary complex with the anaphase-promoting complex to control anaphase initiation', *Genes & Development,* 12(12), 1871-1883.

Fernandez-Gonzalez, R., de Dios Hourcade, J., Lopez-Vidriero, I., Benguria, A., Rodriguez De Fonseca, F. and Gutierrez-Adan, A. (2009) 'Analysis of gene transcription alterations at the blastocyst stage related to the long-term consequences of in vitro culture in mice', *Reproduction,* 137(2), 271-283.

Fleming, T. P., Kwong, W. Y., Porter, R., Ursell, E., Fesenko, I., Wilkins, A., Miller, D. J., Watkins, A. J. and Eckert, J. J. (2004) 'The embryo and its future', *Biology of Reproduction,* 71(4), 1046-1054.

Geraedts, J., Montag, M., Magli, M. C., Repping, S., Handyside, A., Staessen, C., Harper, J., Schmutzler, A., Collins, J., Goossens, V., van der Ven, H., Vesela, K. and Gianaroli, L. (2011) 'Polar body array CGH for prediction of the status of the corresponding oocyte. Part I: clinical results', *Human Reproduction,* 26(11), 3173-3180.

Ghassemifar, M. R., Eckert, J. J., Houghton, F. D., Picton, H. M., Leese, H. J. and Fleming, T. P. (2003) 'Gene expression regulating epithelial intercellular junction biogenesis during human blastocyst development in vitro', *Molecular Human Reproduction,* 9(5), 245-252.

Giritharan, G., Talbi, S., Donjacour, A., Di Sebastiano, F., Dobson, A. T. and Rinaudo, P. F. (2007) 'Effect of in vitro fertilization on gene expression and development of mouse preimplantation embryos', *Reproduction,* 134(1), 63-72.

Grandori, C., Cowley, S. M., James, L. P. and Eisenman, R. N. (2000) 'The Myc-Max-Mad network and the transcriptional control of cell behavior', *Annual Review of Cell and Developmental Biology,* 16, 653-699.

Guo, Y., Kim, C., Ahmad, S., Zhang, J. and Mao, Y. (2012) 'CENP-E-dependent BubR1 autophosphorylation enhances chromosome alignment and the mitotic checkpoint', *Journal of Cell Biology,* 198(2), 205-217.

Hamatani, T., Carter, M. G., Sharov, A. A.and Ko, M. S. H. (2004) 'Dynamics of global gene expression changes during mouse preimplantation development', *Developmental Cell,* 6(1), 117-131.

Hansen, M., Kurinczuk, J. J., Bower, C. and Webb, S. (2002) 'The risk of major birth defects after intracytoplasmic sperm injection and in vitro fertilization', *New England Journal of Medicine,* 346(10), 725-730.

Hawkins, S. M., Buchold, G. M. and Matzuk, M. M. (2011) 'Minireview: The Roles of Small RNA Pathways in Reproductive Medicine', *Molecular Endocrinology,* 25(8), 1257-1279.

Huang, H.-Y., Houwing, S., Kaaij, L. J. T., Meppelink, A., Redl, S., Gauci, S., Vos, H., Draper, B. W., Moens, C. B., Burgering, B. M., Ladurner, P., Krijgsveld, J., Berezikov, E. and Ketting, R. F. (2011) 'Tdrd1 acts as a molecular scaffold for Piwi proteins and piRNA targets in zebrafish', *Embo Journal,* 30(16), 3298-3308.

Huang, Y., Fang, J., Bedford, M. T., Zhang, Y. and Xu, R. M. (2006) 'Recognition of histone H3 lysine-4 methylation by the double tudor domain of JMJD2A', *Science,* 312(5774), 748-751.

Hultquist, A., Cetinkaya, C., Wu, S. Q., Castel, A., Erlandsson, A. and Larsson, L. G. (2004) 'Mad 1 inhibits cell growth and proliferation but does not promote differentiation or overall survival in human U-937 monoblasts', *Molecular Cancer Research,* 2(8), 464-476.

Hurlin, P. J., Queva, C. and Eisenman, R. N. (1997) 'Mnt, a novel Max-interacting protein is coexpressed with Myc in proliferating, rating cells and mediates repression at Myc binding sites', *Genes & Development,* 11(1), 44-58.

Hurlin, P. J., Steingrimsson, E., Copeland, N. G., Jenkins, N. A. and Eisenman, R. N. (1999) 'Mga, a dual-specificity transcription factor that interacts with Max and contains a T-domain DNA-binding motif', *Embo Journal,* 18(24), 7019-7028.

Igosheva, N., Abramov, A. Y., Poston, L., Eckert, J. J., Fleming, T. P., Duchen, M. R. and McConnell, J. (2010) 'Maternal Diet-Induced Obesity Alters Mitochondrial Activity and Redox Status in Mouse Oocytes and Zygotes', *Plos One,* 5(4).

Ke, L., Chen, C., Yahong, G., Lam, R., Chuanbing, B., Chao, X., Zhao, D. Y., Jing, J., MacKenzie, F., Pawson, T. and Jinrong, M. (2010) 'Structural basis for recognition of arginine methylated Piwi proteins by the extended Tudor domain', *Proceedings of the National Academy of Sciences of the United States of America,* 107(43).

Kim, J., Daniel, J., Espejo, A., Lake, A., Krishna, M., Xia, L., Zhang, Y. and Bedford, M. T. (2006) 'Tudor, MBT and chromo domains gauge the degree of lysine methylation', *Embo Reports,* 7(4), 397-403.

Kunieda, T., Xian, M. W., Kobayashi, E., Imamichi, T., Moriwaki, K. and Toyoda, Y. (1992) 'Sexing of Mouse Preimplantation Embryos by Detection of Y-chromosome-Specific Sequences using Polymerase Chain-Reaction', *Biology of Reproduction,* 46(4), 692-697.

Kwong, W. Y., Miller, D. J., Ursell, E., Wild, A. E., Wilkins, A. P., Osmond, C., Anthony, F. W. and Fleming, T. P. (2006) 'Imprinted gene expression in the rat embryo-fetal axis is altered in response to periconceptional maternal low protein diet', *Reproduction,* 132(2), 265-277.

Kwong, W. Y., Osmond, C. and Fleming, T. P. (2004) 'Support for Barker hypothesis upheld in rat model of maternal undernutrition during the preimplantation period: application of integrated 'random effects' statistical model', *Reproductive Biomedicine Online,* 8(5), 574-576.

Kwong, W. Y., Wild, A. E., Roberts, P., Willis, A. C.and Fleming, T. P. (2000) 'Maternal undernutrition during the preimplantation period of rat development causes blastocyst abnormalities and programming of postnatal hypertension', *Development,* 127(19), 4195-4202.

Lane, M. and Gardner, D. K. (2003) 'Ammonium induces aberrant blastocyst differentiation, metabolism, pH regulation, gene expression and subsequently alters fetal development in the mouse', *Biology of Reproduction,* 69(4), 1109-1117.

Langley-Evans, S. C. (2006) 'Developmental programming of health and disease', *Proceedings of the Nutrition Society,* 65(1), 97-105.

Lavagnolli, T. M. C., Fonseca, S. A. S., Serafim, R. C., Pereira, V. S., Santos, E. J. C., Abdelmassih, S., Kerkis, A. and Kerkis, I. (2009) 'Presumptive germ cells derived from mouse pluripotent somatic cell hybrids', *Differentiation,* 78(2-3), 124-130.

Li, X. M., Yang, Y. L. and Ashwell, J. D. (2002) 'TNF-RII and c-IAP1 mediate ubiquitination and degradation of TRAF2', *Nature,* 416(6878), 345-349.

Lleres, D., Denegri, M., Biggiogera, M., Ajuh, P. and Lamond, A. I. (2010) 'Direct interaction between hnRNP-M and CDC5L/PLRG1 proteins affects alternative splice site choice', *Embo Reports,* 11(6), 445-451.

Lucas, E. S., Watkins, A. J., Cox, A. L., Marfy-Smith, S. J., Smyth, N. and Fleming, T. P. (2011) 'Tissue-specific selection of reference genes is required for expression studies in the mouse model of maternal protein undernutrition', *Theriogenology,* 76(3), 558-569.

Madan, B., Madan, V., Weber, O., Tropel, P., Blum, C., Kieffer, E., Viville, S. and Fehling, H. J. (2009) 'The Pluripotency-Associated Gene Dppa4 Is Dispensable for Embryonic Stem Cell Identity and Germ Cell Development but Essential for Embryogenesis', *Molecular and Cellular Biology,* 29(11), 3186-3203.

Maher, E. R., Brueton, L. A., Bowdin, S. C., Luharia, A., Cooper, W., Cole, T. R., Macdonald, F., Sampson, J. R., Barratt, C. L., Reik, W.and Hawkins, M. M. (2003) 'Beckwith-Wiedemann syndrome and assisted reproduction technology (ART)', *Journal of Medical Genetics,* 40(1), 62-64.

Masaki, H., Nishida, T., Kitajima, S., Asahina, K. and Teraoka, H. (2007) 'Developmental pluripotency-associated 4 (DPPA4) localized in active chromatin inhibits mouse embryonic stem cell differentiation into a primitive ectoderm lineage', *Journal of Biological Chemistry,* 282(45), 33034-33042.

Masaki, H., Nishida, T., Sakasai, R. and Teraoka, H. (2010) 'DPPA4 modulates chromatin structure via association with DNA and core histone H3 in mouse embryonic stem cells', *Genes to Cells,* 15(4), 327-337.

McLaren, A. (2003) 'Primordial germ cells in the mouse', *Developmental Biology,* 262(1), 1-15.

McManus, M. T. and Sharp, P. A. (2002) 'Gene silencing in mammals by small interfering RNAs', *Nature Reviews Genetics,* 3(10), 737-747.

Mitchell, M., Schulz, S. L., Armstrong, D. T. and Lane, M. (2009) 'Metabolic and Mitochondrial Dysfunction in Early Mouse Embryos Following Maternal Dietary Protein Intervention', *Biology of Reproduction,* 80(4), 622-630.

Morgan, H. D., Sutherland, H. G. E., Martin, D. I. K. and Whitelaw, E. (1999) 'Epigenetic inheritance at the agouti locus in the mouse', *Nature Genetics,* 23(3), 314-318.

Morgenstern, B. and Atchley, W. R. (1999) 'Evolution of bHLH transcription factors: Modular evolution by domain shuffling?', *Molecular Biology and Evolution,* 16(12), 1654-1663.

Nel-Themaat, L., Vadakkan, T. J., Wang, Y., Dickinson, M. E., Akiyama, H. and Behringerl, R. R. (2009) 'Morphometric Analysis of Testis Cord Formation in Sox9-EGFP Mice', *Developmental Dynamics,* 238(5), 1100-1110.

Nagamatsu, G., Kosaka, T., Kawasumi, M., Kinoshita, T., Takubo, K., Akiyama, H., Sudo, T., Kobayashi, T., Oya, M. and Suda, T. (2011) 'A Germ Cell-specific Gene, Prmt5, Works in Somatic Cell Reprogramming', *Journal of Biological Chemistry,* 286(12), 10641-10648.

Nayernia, K., Lee, J. H., Drusenheimer, N., Nolte, J., Wulf, G., Dressel, R., Gromoll, J.and Engel, W. (2006) 'Derivation of male germ cells from bone marrow stem cells', *Laboratory Investigation,* 86(7), 654-663.

Nigg, E. A. (2001) 'Mitotic kinases as regulators of cell division and its checkpoints', *Nature Reviews Molecular Cell Biology,* 2(1), 21-32.

Ohnishi, Y., Totoki, Y., Toyoda, A., Watanabe, T., Yamamoto, Y., Tokunaga, K., Sakaki, Y., Sasaki, H. and Hohjoh, H. (2010) 'Small RNA class transition from siRNA/piRNA to miRNA during pre-implantation mouse development', *Nucleic Acids Research,* 38(15), 5141-5151.

Pan, H., O'Brien, M. J., Wigglesworth, K., Eppig, J. J. and Schultz, R. M.(2005) 'Transcript profiling during mouse oocyte development and the effect of gonadotropin priming and development in vitro', *Developmental Biology,* 286(2), 493-506.

Pan, J. Y., Goodheart, M., Chuma, S., Nakatsuji, N., Page, D. C.and Wang, P. J. (2005) 'RNF17, a component of the mammalian germ cell nuage, is essential for spermiogenesis', *Development,* 132(18), 4029-4039.

Panneerdoss, S., Chang, Y.-F., Buddavarapu, K. C., Chen, H.-I. H., Shetty, G., Wang, H., Chen, Y., Kumar, T. R. and Rao, M. K.(2012) 'Androgen-Responsive MicroRNAs in Mouse Sertoli Cells', *Plos One,* 7(7).

Park, S. Y. and Jameson, J. L. (2005) 'Minireview: Transcriptional regulation of gonadal development and differentiation', *Endocrinology,* 146(3), 1035-1042.

Peaston, A. E., Evsikov, A. V., Graber, J. H., de Vries, W. N., Holbrook, A. E., Solter, D. and Knowles, B. B. (2004) 'Retrotransposons regulate host genes in mouse oocytes and preimplantation embryos', *Developmental Cell,* 7(4), 597-606.

Pickart, C. M. (2001) 'Mechanisms underlying ubiquitination', *Annual Review of Biochemistry,* 70, 503-533.

Privette, L. M. and Petty, E. M. (2008) 'CHFR: A Novel Mitotic Checkpoint Protein and Regulator of Tumorigenesis', *Translational Oncology,* 1(2), 57-64.

Raught, B., Peiretti, F., Gingras, A. C., Livingstone, M., Shahbazian, D., Mayeur, G. L., Polakiewicz, R. D., Sonenberg, N. and Hershey, J. W. B. (2004) 'Phosphorylation of eucaryotic translation initiation factor 4B Ser422 is modulated by S6 kinases', *Embo Journal,* 23(8), 1761-1769.

Reik, W. and Maher, E. R. (1997) 'Imprinting in clusters: Lessons from Beckwith-Wiedemann syndrome', *Trends in Genetics,* 13(8), 330-334.

Rikin, A. and Evans, T. (2010) 'The Tbx/bHLH Transcription Factor mga Regulates gata4 and Organogenesis', *Developmental Dynamics,* 239(2), 535-547.

Rinaudo, P. F., Giritharan, G., Talbi, S., T Dobson, A. and Schultz, R. M.(2006) 'Effects of oxygen tension on gene expression in preimplantation mouse embryos', *Fertility and Sterility,* 86, 1252-1265.

Rodriguez, J. A. and Henderson, B. R. (2000) 'Identification of a functional nuclear export sequence in BRCA1', *Journal of Biological Chemistry,* 275(49), 38589-38596.

Ross, A. J.and Capel, B. (2005) 'Signaling at the crossroads of gonad development', *Trends in Endocrinology and Metabolism,* 16(1), 19-25.

Roux, P. P., Ballif, B. A., Anjum, R., Gygi, S. P. and Blenis, J. (2004) 'Tumor-promoting phorbol esters and activated Ras inactivate the tuberous sclerosis tumor suppressor complex via p90 ribosomal S6 kinase', *Proceedings of the National Academy of Sciences of the United States of America,* 101(37), 13489-13494.

Schultz, R. M.(2002) 'The molecular foundations of the maternal to zygotic transition in the preimplantation embryo', *Human Reproduction Update,* 8(4), 323-331.

Seto, A. G., Kingston, R. E. and Lau, N. C.(2007) 'The coming of age for Piwi proteins', *Molecular Cell,* 26(5), 603-609.

Shen-Li, H., O'Hagan, R. C., Hou, H., Jr., Horner, J. W., II, Lee, H.-W. and DePinho, R. A.(2000) 'Essential role for Max in early embryonic growth and development', *Genes and Development,* 14(1), 17-22.

Shoji, M., Tanaka, T., Hosokawa, M., Reuter, M., Stark, A., Kato, Y., Kondoh, G., Okawa, K., Chujo, T., Suzuki, T., Hata, K., Martin, S. L., Noce, T., Kuramochi-Miyagawa, S., Nakano, T., Sasaki, H., Pillai, R. S., Nakatsuji, N. and Chuma, S. (2009) 'The TDRD9-MIWI2 Complex Is Essential for piRNA-Mediated Retrotransposon Silencing in the Mouse Male Germline', *Developmental Cell,* 17(6), 775-787.

Siegel, D., Schuff, M., Oswald, F., Cao, Y. and Knoechel, W. (2009) 'Functional dissection of XDppa2/4 structural domains in Xenopus development', *Mechanisms of Development,* 126(11-12), 974-989.

Sinclair, K. D., Allegrucci, C., Singh, R., Gardner, D. S., Sebastian, S., Bispham, J., Thurston, A., Huntley, J. F., Rees, W. D., Maloney, C. A., Lea, R. G., Craigon, J., McEvoy, T. G. and Young, L. E. (2007) 'DNA methylation, insulin resistance, and blood pressure in offspring determined by maternal periconceptional B vitamin and methionine status', *Proceedings of the National Academy of Sciences of the United States of America,* 104(49), 19351-19356.

Sheth, B., R. L. Nowak, R. Anderson, W. Y. Kwong, T. Papenbrock and T. P. Fleming. (2008). "Tight junction protein ZO-2 expression and relative function of ZO-1 and ZO-2 during mouse blastocyst formation." *Experimental Cell Research* 314(18):3356-3368.

Smith, Z. D., Chan, M. M., Mikkelsen, T. S., Gu, H., Gnirke, A., Regev, A. and Meissner, A. (2012) 'A unique regulatory phase of DNA methylation in the early mammalian embryo', *Nature,* 484(7394), 339-U74.

Stephens, D. J. and Banting, G. (2000) 'The use of yeast two-hybrid screens in studies of protein: protein interactions involved in trafficking', *Traffic,* 1(10), 763-768.

Suh, N. and Blelloch, R. (2011) 'Small RNAs in early mammalian development: from gametes to gastrulation', *Development,* 138(9), 1653-1661.

Suzuki, T., Abe. K,, Inoue. A.and Aoki. F. 2009. “Expression of c-MYC in nuclear speckeles during mouse oocyte growth and preimplantation development.” Journal of Reproduction and Development 55 (No 5):491-495

Suzumori, N., Burns, K. H., Yan, W.and Matzuk, M. M. (2003) 'RFPL4 interacts with oocyte proteins of the ubiquitin-proteasome degradation pathway', *Proceedings of the National Academy of Sciences of the United States of America,* 100(2), 550-555.

Tee, W.-W., Pardo, M., Theunissen, T. W., Yu, L., Choudhary, J. S., Hajkova, P.and Surani, M. A.(2010) 'Prmt5 is essential for early mouse development and acts in the cytoplasm to maintain ES cell pluripotency', *Genes & Development,* 24(24), 2772-2777.

Thakur, S., Zhang, H. B., Peng, Y., Le, H., Carroll, B., Ward, T., Yao, J., Farid, L. M., Couch, F. J., Wilson, R. B. and Weber, B. L. (1997) 'Localization of BRCA1 and a splice variant identifies the nuclear localization signal', *Molecular and Cellular Biology,* 17(1), 444-452.

Thomson, T. and Lasko, P. (2005) 'Tudor and its domains: germ cell formation from a Tudor perspective', *Cell Research,* 15(4), 281-291.

Thomson, T. and Lin, H. F.(2009) 'The Biogenesis and Function of PIWI Proteins and piRNAs: Progress and Prospect', *Annual Review of Cell and Developmental Biology,* 25, 355-376.

Trumpp, A., Refaeli, Y., Oskarsson, T., Gasser, S., Murphy, M., Martin, G. R. and Bishop, J. M.(2001) 'c-Myc regulates mammalian body size by controlling cell number but not cell size', *Nature,* 414(6865), 768-773.

Vagin, V. V., Wohlschlegel, J., Qu, J., Jonsson, Z., Huang, X., Chuma, S., Girard, A., Sachidanandam, R., Hannon, G. J.and Aravin, A. A. (2009) 'Proteomic analysis of murine Piwi proteins reveals a role for arginine methylation in specifying interaction with Tudor family members', *Genes & Development,* 23(15), 1749-1762.

van Wijk, S. J. L., de Vries, S. J., Kemmeren, P., Huang, A., Boelens, R., Bonvin, A. M. J. J. and Timmers, H. T. M. (2009) 'A comprehensive framework of E2-RING E3 interactions of the human ubiquitin-proteasome system (vol 5, art no. 295, 2009)', *Molecular Systems Biology,* 5.

Vandesompele, J., De Preter, K., Pattyn, F., Poppe, B., Van Roy, N., De Paepe, A. and Speleman, F. (2002) 'Accurate normalization of real-time quantitative RT-PCR data by geometric averaging of multiple internal control genes', *Genome Biology,* 3(7).

Vasileva, A., Tiedau, D., Firooznia, A., Mueller-Reichert, T. and Jessberger, R. (2009) 'Tdrd6 Is Required for Spermiogenesis, Chromatoid Body Architecture, and Regulation of miRNA Expression', *Current Biology,* 19(8), 630-639.

Wainwright, E. N., Jorgensen, J. S., Kim, Y., Vy, T., Bagheri-Fam, S., Davidson, T., Svingen, T., Fernandez-Valverde, S. L., McClelland, K. S., Taft, R. J., Harley, V. R., Koopman, P. and Wilhelm, D. (2013) 'SOX9 Regulates MicroRNA miR-202-5p/3p Expression during Mouse Testis Differentiation', *Biology of Reproduction,* 89(2).

Wakayama, T. and Yanagimachi, R. (1998) 'The first polar body can be used for the production of normal offspring in mice', *Biology of Reproduction,* 59(1), 100-104.

Wang, P. J., McCarrey, J. R., Yang, F. and Page, D. C.(2001) 'An abundance of X-linked genes expressed in spermatogonia', *Nature Genetics,* 27(4), 422-426.

Wang, S., Kou, Z., Jing, Z., Zhang, Y., Guo, X., Dong, M., Wilmut, I. and Gao, S. (2010) 'Proteome of mouse oocytes at different developmental stages', *Proceedings of the National Academy of Sciences of the United States of America,* 107(41), 17639-17644.

Wang, X. M., Li, W., Williams, M., Terada, N., Alessi, D. R. and Proud, C. G. (2001) 'Regulation of elongation factor 2 kinase by p90(RSK1) and p70 S6 kinase', *Embo Journal,* 20(16), 4370-4379.

Wang, Y. E., Park, A., Lake, M., Pentecost, M., Torres, B., Yun, T. E., Wolf, M. C., Holbrook, M. R., Freiberg, A. N. and Lee, B. (2010) 'Ubiquitin-Regulated Nuclear-Cytoplasmic Trafficking of the Nipah Virus Matrix Protein Is Important for Viral Budding', *Plos Pathogens,* 6(11).

Waterland, R. A., Tahiliani, K. G., Rached, M. T. and Travisano, M. (2007) 'Diet-induced hypermethylation at viable yellow agouti is not inherited transgenerationally', *Faseb Journal,* 21(5), A291-A291.

Watkins, A. J., Platt, D., Papenbrock, T., Wilkins, A., Eckert, J. J., Kwong, W. Y., Osmond, C., Hanson, M. and Fleming, T. P.(2007) 'Mouse embryo culture induces changes in postnatal phenotype including raised systolic blood pressure', *Proceedings of the National Academy of Sciences of the United States of America,* 104(13), 5449-5454.

Watkins, A. J., Ursell, E., Panton, R., Papenbrock, T., Ollis, L. H., Cunningham, C., Wilkins, A., Perry, V. H., Sheth, B., Kwong, W. Y., Eckert, J. J., Wild, A. E., Hanson, M. A., Osmond, C. and Fleming, T. P. (2008a) 'Adaptive responses by mouse early embryos to maternal diet protect fetal growth but predispose to adult onset disease', *Biology of Reproduction,* 78(2), 299-306.

Watkins, A. J., Wilkins, A., Cunningham, C., Perry, V. H., Seet, M. J., Osmond, C., Eckert, J. J., Torrens, C., Cagampang, F. R. A., Cleal, J., Gray, W. P., Hanson, M. A. and Fleming, T. P.(2008b) 'Low protein diet fed exclusively during mouse oocyte maturation leads to behavioural and cardiovascular abnormalities in offspring', *Journal of Physiology-London,* 586(8), 2231-2244.

Wisborg, K., Ingerslev, H. J.and Henriksen, T. B.(2010) 'In vitro fertilization and preterm delivery, low birth weight, and admission to the neonatal intensive care unit: a prospective follow-up study', *Fertility and Sterility,* 94(6), 2102-2106.

Wolff, G. L., Kodell, R. L., Moore, S. R. and Cooney, C. A. (1998) 'Maternal epigenetics and methyl supplements affect agouti gene expression in A(vy)/a mice', *Faseb Journal,* 12(11), 949-957.

www.ambion.com 15-3-2012

www.ebi.ac.uk 16-8-11

http://www.ebi.ac.uk/arrayexpress/ 16-8-11

www.ensemble.org. 18-10-10

www.genecards.org 18-10-10

www.ncbi.nlm.nih.gov/bookshelf 16-8-11

http://www.ncbi.nlm.nih.gov/pubmed?term=Rnf17 16-8-11

http://medgen.ugent.be/genorm/ 4-1-2013

www.uniprot.org 5-3-2013

Xu, L., Zhu, J., Hu, X., Zhu, H., Kim, H. T., LaBaer, J., Goldberg, A. and Yuan, J. (2007) 'c-IAP1 cooperates with Myc by acting as a ubiquitin ligase for Mad1', *Molecular Cell,* 28(5), 914-922.

Yabuta, Y., Ohta, H., Abe, T., Kurimoto, K., Chuma, S. and Saitou, M. (2011) 'TDRD5 is required for retrotransposon silencing, chromatoid body assembly, and spermiogenesis in mice', *Journal of Cell Biology,* 192(5), 781-795.

Yin, X. Y., Grove, L. E. and Prochownik, E. V.(2001) 'Mmip-2/Rnf-17 enhances c-Myc function and regulates some target genes in common with glucocorticoid hormones', *Oncogene,* 20(23), 2908-2917.

Yin, X. Y., Gupta, K., Han, W. P., Levitan, E. S. and Prochownik, E. V. (1999) 'Mmip-2, a novel RING finger protein that interacts with mad members of the Myc oncoprotein network', *Oncogene,* 18(48), 6621-6634.

Young, L. E., Fernandes, K., McEvoy, T. G., Butterwith, S. C., Gutierrez, C. G., Carolan, C., Broadbent, P. J., Robinson, J. J., Wilmut, I. and Sinclair, K. D. (2001) 'Epigenetic change in IGF2R is associated with fetal overgrowth after sheep embryo culture', *Nature Genetics,* 27(2), 153-154.

Zeng, F. Y., Baldwin, D. A. and Schultz, R. M. (2004) 'Transcript profiling during preimplantation mouse development', *Developmental Biology,* 272(2), 483-496.

Zeng, F. Y. and Schultz, R. M. (2005) 'RNA transcript profiling during zygotic gene activation in the preimplantation mouse embryo', *Developmental Biology,* 283(1), 40-57.

Zhu, J., Blenis, J. and Yuan, J. (2008) 'Activation of PI3K/Akt and MAPK pathways regulates Myc-mediated transcription by phosphorylating and promoting the degradation of Mad1', *Proceedings of the National Academy of Sciences of the United States of America,* 105(18), 6584-6589.